Role of Tal1 in Murine Blood Vessel Development

Martin Fritzsche

Somerville College

University of Oxford

Trinity 2015

Supervisor: Dr Sarah De Val

A thesis submitted for the degree of

Doctor of Philosophy

Martin Fritzsche Doctor of Philosophy

Somerville College Trinity, 2015

Abstract

Role of Tal1 in Murine Blood Vessel Development

Detailed knowledge about the mechanisms involved in vascular establishment, differentiation and growth is essential to develop new therapies to treat blood vessel formation related conditions like cancer and blinding eye diseases. Although research has investigated the cellular mechanisms of vessel growth in great detail, a clear understanding of the integration of extracellular signals into the transcriptional programme regulating blood vessel formation still remains elusive.

In this thesis the role of the transcription factor Tal1 as a regulator of blood vessel formation and differentiation is investigated. Tal1 is a master regulator of embryonic haematopoiesis, adult megakaryopoiesis, and erythrocyte maturation. Tal1 depleted mice die at gestational day E9.5 due to a complete lack of blood. However, several lines of evidence also suggest an important function of Tal1 in blood vessel development.

I chose an inducible, endothelial-specific knock-out strategy to investigate the effects of Tal1 depletion in mice with a focus on vascular development. A distinct time window during embryogenesis, in which Tal1 is required for the proper formation of the primitive intra-embryonic vascular network and the dorsal aorta, was identified. In contrast, I demonstrate that there is no requirement of Tal1 for postnatal sprouting angiogenesis or blood vessel homeostasis. This suggests an important role in vasculogenesis rather than angiogenesis and is in line with recent findings which attribute the proper differentiation of endothelial cells to Tal1.

In addition, I have generated and characterised transgenic mouse lines in which Cre recombinase activity is controlled by a Dll4 promoter/enhancer construct. Thereby, Cre expression is specifically directed to the arterial endothelium. I believe that this model can be of great interest for angiogenesis research in general and especially for the understanding of induction and maintenance of arterial-venous identity.

Declaration

This thesis is submitted to the Department of Medical Science, University of Oxford, in fulfilment of the requirements for the degree of Doctor of Philosophy. This thesis is entirely my own work, and except where otherwise stated, describes my own research. It has not been submitted for a degree to any other university or similar institution.

Martin Fritzsche

Word count: 44,436

Acknowledgments

First and foremost I would like to thank Dr Sarah De Val for providing me the fascinating topic of this thesis. I am grateful for the constant advice and support for new experiments, the critical discussion of my results and the perusal of this thesis.

I would like to thank in particular Dr Leonid Nikitenko for countless stimulating discussions and scientific advice and Dr Natalia Sacilotto, who introduced me to a lot of experimental methods and helped me to cope with many challenging problems in the lab.

Furthermore, I would also like to thank Dr Ben Davies, Dr Ke Liu and Professor George Bou-Gharios for their help on generating transgenic mice and Dr Indrika Ratnayaka and Mark Shipman for the invaluable assistance on sectioning and microscopy.

For many interesting discussions, extensive help and especially for the pleasant and motivating working atmosphere I want to thank every past and present member of the De Val research group and especially Pijus Brazauskas and Zhe Zhao for making the last four years truly enjoyable, both in and outside the lab.

Special thanks are due to Diana Khoromskaia who constantly motivated and supported me in every situation and who was invaluable for the proofreading of this thesis.

Finally, I am greatly indebted to my parents to whom this thesis is dedicated. Thank you very much indeed for unconditionally supporting me through so many years and making this possible.

Abbreviations

4-OHT	4-hydroxytamoxifen
AF	AlexaFlour™
AGM	Aorta-gonad-mesonephros
al.	Others
BL-CFC	Blast colony forming cell
Bp	Base pair/s
ddH2O	Double distilled H_2O
DIC	Differential interference contrast microscopy
E	Embryonic day
EC	Endothelial cell
EDTA	Ethylenediaminetetraacetic acid
EPC	Endothelial progenitor cells
et	and
HE	Hemogenic endothelium
HSC	Haematopoietic stem cell
ID	Identification number
IF	Immunofluorescence
IHC	Immunohistochemistry
INR	Initiator region
Kb	Kilo base pair/s
KO	Knock-out
LCR	Locus control region
ON	Over night
ORF	Open reading frame
P	Postnatal day
PBS	Phosphate buffered solution
PCR	Polymerase chain reaction
PFA	Paraformaldehyde
PPE	Proximal promoter element
px	Pixel/s
RPE	Retinal pigment epithelium
rpm	Revolutions per minute
RT	Room temperature (i.e. 20-24 °C)
TF	Transcription factor
Tris	Tris(hydroxymethyl)aminomethane
TSS	Transcriptional start site
UTR	Untranslated region
v/v	Percent volume per volume
vSMC	Vascular smooth muscle cell
w/v	Percent weight per volume
WT	Wild type

Contents

Chapter 1:

Introduction

1.1 Transcriptional Control of Gene Expression

The main factors which determine the structure and the function of any cell are the kinds and amounts of proteins it contains. Therefore, understanding the regulation of genes, which encode the proteins, is of fundamental importance in molecular biology, as they control the development and maintenance of any living organism.

One of the many surprising discoveries made by the human genome project and its successors was the finding that the human genome contains a comparatively small number of genes. Early mathematical estimates were ranging up to 2 million genes (Kauffman, 1969) while the actual number of protein coding genes annotated in today's public databases such as UniProt (http://www.uniprot.org) is slightly over 20,000 (Magrane and Consortium, 2011). Since humans are more complex in morphology and behaviour than, for example, nematodes, which contain a similar number of genes, it is likely that this complexity arises from different parameters. Besides an increased number of protein modifications and splice-variants, differentially regulated gene expression has been associated with increased complexity (de Laat and Duboule, 2013).

Gene expression means that a protein that is encoded by a gene is produced through the molecular machinery of the cell. In an initial step, named transcription, an mRNA copy of a segment from the DNA strand is synthesised by the enzyme RNA polymerase. In eukaryotes the mRNA chain is then modified and exported out of the nucleus into the cytosol. Finally the mRNA sequence is translated into an amino acid string, the polypeptide. This polypeptide string now folds and gets further modified in order to form a functional protein.

All of the steps mentioned above are subject to regulation through the cell and lead to differential production of proteins depending on developmental programs or external influences. Here I will focus on the initial step of gene transcription and in particular on the initiation of transcription.

Before transcription of a particular gene can ensue, the RNA polymerase (polymerase II in eukaryotes for mRNA) has to recognise and bind a specific site on the DNA directly upstream of the gene, called promoter. In eukaryotes several proteins, called general or basal transcription factors (TFs), are necessary for this initial step. They include the factors TFIIA, TFIIB, TFIID, TFIIE, TFIIF, and TFIIH. These factors sequentially bind to specific DNA sequence motifs, called binding sites, within the promoter and to each other and then recruit the RNA polymerase II, forming the transcription initiation complex (Lodish et al., 2008).

The polymerase/transcription factor complex then melts the duplex DNA near the transcriptional start site (TSS) and forms the "transcriptional bubble". Then the polymerase begins to polymerise ribonucleotides (rNTPs) at the TSS and moves down the template DNA in 3' to 5' direction, adding more rNTPs to the RNA chain. However, for convenience the non-template strand or the newly formed RNA strand can be used as reference, which leads to transcription being described as occurring from 5' to 3'. When the polymerase arrives at a transcriptional stop site, the enzyme dissociates from the DNA and a series of adenines are added to its 3' end by a polyadenylation protein complex (Boeger et al., 2005).

Regulation of the initiation of transcription is fundamental for both the embryonic development of a multicellular organism and for the execution of physiological processes such as immune response, hormone homeostasis and cognitive activities.

1.1.1 Promoters

In eukaryotes the initiation of transcription is tightly regulated by various protein-binding DNA sequences. A lot of them cluster directly upstream of the regulated gene in the promoter region. Promoters vary in length from around 100 to 1000 base pairs (bp). The region in close proximity of the TSS is named core promoter and contains a conserved DNA sequence, called TATA box. The first step of assembling the transcription initiation complex is often described as binding of TFIID to the TATA box, although only around 24% of all human genes contain a

TATA box in their promoter regions. In contrast ~46% of all human promoters contain a different consensus sequence, named "initiator" (INR) (Yang et al., 2007), and additional elements such as "Downstream Promoter Element" (DPE), "Downstream Core Element" (DCE), "TFIIB-Recognition Element" (BRE), and "Motif Ten Element" (MTE) have been described, with none of them being essential for transcription (Juven-Gershon and Kadonaga, 2010).

Interestingly, around 60% of human promoters are positioned close to so called CpG islands (Venter et al., 2001). These are short stretches of DNA (~500 – 2000 bp), containing a high frequency of unmethylated C+G nucleotides compared to the genome wide average. In mammals around 70% of all CpG sequences display methylation, most likely in order to repress transcription. The CpG dinucleotide is therefore the least frequent dinucleotide in the genome because methylated cytosines tend to be deaminated to thymines. CpG islands at promoter regions are exempted from that rule and seem to be protected from methylation (Jabbari and Bernardi, 2004).

Finally, it is important to mention that the presence of the transcription initiation complex at a promoter is *in vitro* only sufficient for low levels of template transcription, referred to as basal transcription. Effective transcription often requires the presence of additional regulatory elements such as enhancers.

1.1.2 Enhancers and other *Cis*-Regulatory Elements

In addition to promoters, the eukaryotic genome contains another class of regulatory elements called enhancers. In contrast to promoters, enhancers are characterised as *cis*-regulatory DNA segments that are distal to the regulated gene and can enhance gene expression independently of their orientation towards the target gene (Banerji et al., 1981). Enhancers share functional and structural similarities with promoters, and enhancers which are positioned close to the core promoter are sometimes referred to as proximal promoter elements. However, it was demonstrated many years ago that promoters alone often have little control over

transcriptional regulation during development, and therefore most of the establishment of spatio-temporal gene expression patterns relies on enhancers (Banerji et al., 1981). Consequently, distant-acting transcriptional enhancers by far outnumber the amount of promoters in the mammalian genome, with over one million regulatory elements being predicted and over 80% of the genome estimated to have some regulatory potential (The ENCODE Project Consortium, 2012). However, those estimations, which are entirely based on biochemical properties of DNA segments such as chromatin state or binding events, have been harshly criticised for ignoring the fact that only 9% of the human genome show evidence for evolutionary selection, which renders such a large fraction of regulatory sequences unlikely (Doolittle, 2013; Graur et al., 2013).

Enhancers contain clusters of multiple TF binding sites or "motifs" that are required for the enhancer activity. These TF binding motifs are defined as short (~6-10 bp) and degenerate DNA sequence patterns that summarise the binding preference of one or more TFs. They can be represented as consensus sequences, which constitute the result of a multiple sequence alignment. It is therefore possible to computationally scan whole genomes for TF motifs in order to identify putative regulatory elements. A reverse approach is possible, although this is more effective when multiple different binding motifs are used in combination. For complex developmental processes, for instance the formation of the vascular system, where no single master regulator TF controls development single-handedly, complex processes are regulated by specific sets of TFs. Therefore, enhancers which control genes that play important roles in settings like vascular development are enriched for repeating motif signatures and consequently can be used to elucidate the underlying transcriptional networks (Randi et al., 2009; De Val and Black, 2009).

After TFs bind to their cognate DNA motifs, it is thought that they also interact with the "mediator", a co-activator protein complex that consists of ~30 subunits. This complex then connects the site specific TFs at the enhancer with the general transcriptional machinery at the promoter and activates transcription. To accomplish this, the enhancer region loops out of the

intervening DNA strand and comes in close spatial proximity to the promoter, thereby enabling distance independent function (Schoenfelder et al., 2010). These interactions are stabilised by the chromatin remodelling protein cohesin and the zinc-finger protein "CCCTC-binding factor" (CTCF).

Enhancers are able to act in a modular fashion. Most genes are regulated by several enhancers which control additively and partly redundantly the expression of the target gene (Sanyal et al., 2012). Secondary and remote enhancers with overlapping activities with the primary enhancer (or, more often, the enhancer discovered first) are also referred to as "shadow-enhancers" (Hong et al., 2008).

Recently a special subset of enhancers, termed "super enhancers" has been identified, proposed to have crucial functions in specification of cell identity. Super enhancers were described as large clusters of enhancers, spanning up to 50 kilo base pairs (kb) and being unusually enriched for mediator binding. Sets of genes located on the same topological domain as the super enhancers were found to be highly expressed and mainly involved in embryonic stem cell differentiation (Whyte et al., 2013). Notably, the differentiation of normal enhancers and super enhancers has been challenged due to lack of sufficient mechanistic differences between the two and the term has generated some controversy (Pott and Lieb, 2015).

In addition to enhancers and promoters, other *cis*-regulatory elements have been identified in eukaryotes. The counterpart to enhancers are silencers. These sequences bind repressive TFs and cause reduced expression of their target genes by blocking nearby enhancers, by interfering with the assembly of the general transcription factors or by inhibiting helicase activity. Overall they share many properties with enhancers by acting synergistically and independently of position and orientation, although a few orientation-dependent enhancers have been described. In order to allow specific regulation, the chromatin needs to contain barriers that shield genes from being affected by the regulatory elements of neighbouring genes. This function is carried out by insulators (also known as boundary elements) which are DNA sequences that partition the genome into discrete domains of specific regulation. They are

~0.5 – 3 kb in length and act in an orientation independent but position dependent manner (Maston et al., 2006). Insulator activity has been associated with CTCF binding, but the overall mechanisms of insulator activity are poorly understood (Mishiro et al., 2009). It has been suggested that insulators may spatially block looping of other regulatory elements and limit the linear spread of chromatin modifications (Capelson and Corces, 2004). A final class of *cis*-regulatory elements is the "locus control region" (LCR). Originally identified at the human β-globin locus, these are genomic regions that contain a cluster of elements which regulate multiple genes in tissue-specific fashion (Grosveld et al., 1987). By introducing an ectopic human LCR into a transgenic mouse it could be demonstrated that DNA regulatory elements can also act in *trans* and activate targets on different chromosomes (Noordermeer et al., 2011). The definition of the LCR somewhat overlaps with the characteristics of the aforementioned super enhancers and is now rarely used apart from studies about the regulation of the β-globin locus.

In summary, it can be said that in comparison with enhancers other *cis*-regulatory elements are less well studied and understood.

1.1.3 Chromatin Structure of Regulatory Elements

It is easy to recognise that the DNA in any cell has to be compacted because the total length of genomic DNA is around 100,000 times the cell's diameter. This task is accomplished by various abundant proteins that bind DNA and form a complex, termed chromatin. The fundamental structural packaging unit of chromatin is the nucleosome, a complex that contains ~146 bp DNA which is wrapped around eight highly alkaline proteins called histones. The nucleosomes are joined by linker DNA of around 20 bp, depending on species. This chain of nucleosomes folds into a "zig-zag ribbon" like structure of around 30 nm diameter. The 30 nm fibre is the predominant conformation of DNA which is not transcribed or replicated. Further folding and compaction is needed for cell division where the 30 nm fibre first forms loops of around 300

nm length which are then compressed into a fibre with a diameter of ~250 nm. Finally these fibres tightly coil into the 500 – 750 nm diameter chromatids which form the chromosomes observable in metaphase (Lodish et al., 2008).

It is now known that DNA must be accessible (or "open") to TFs and the transcriptional machinery. This "naked" DNA is especially sensitive to enzymatic cleavage by the endonuclease DNaseI. Therefore DNaseI digestion patterns can be used for identifying regulatory elements (The ENCODE Project Consortium, 2012). Moreover, active enhancers and promoters are depleted of nucleosomes and nucleosomes in the vicinity of active elements contain histones with characteristic modifications at their amino termini. Notably, these epigenetic modifications can be inherited during mitosis and therefore influence the gene expression profile of daughter cells. Methylation of histones, usually found on lysine or arginine amino acids, enables the binding of chromatin remodelling proteins which can render the DNA more or less accessible to TFs. In contrast, histone acetylation is only observed on lysines. Acetylation of lysine partially neutralises the positive (basic) N-terminal tail of the histone and therefore weakens the electrostatic interactions between the histone and the negatively charged DNA. This opens up the chromatin and makes it more accessible to TFs and polymerases (Bannister and Kouzarides, 2011).

Active enhancers usually display the flanking histone modifications histone H3 lysine 4 monomethylation (H3K4me1) and histone H3 lysine 27 monoacetylation (H3K27ac) while some active promoters are flanked by histones with H3K27ac and H3K4me3 modifications. Inactive enhancers are silenced by the polycomb-group protein associated repressive H3K27me3 mark. Interestingly, some closed or poised enhancers can carry both activating H3K27ac and repressive H3K27me3 histone modifications, while latent enhancers carry no modifications at all (Arnold et al., 2013; Bonn et al., 2012; Rada-Iglesias et al., 2011). Besides hypersensitivity to DNaseI digestion, the presence of histone modifications is used for genome wide identification of regulatory elements.

A brief overview of the spatial and epigenetic features of transcriptional regulatory elements in metazoans is given in Figure 1.

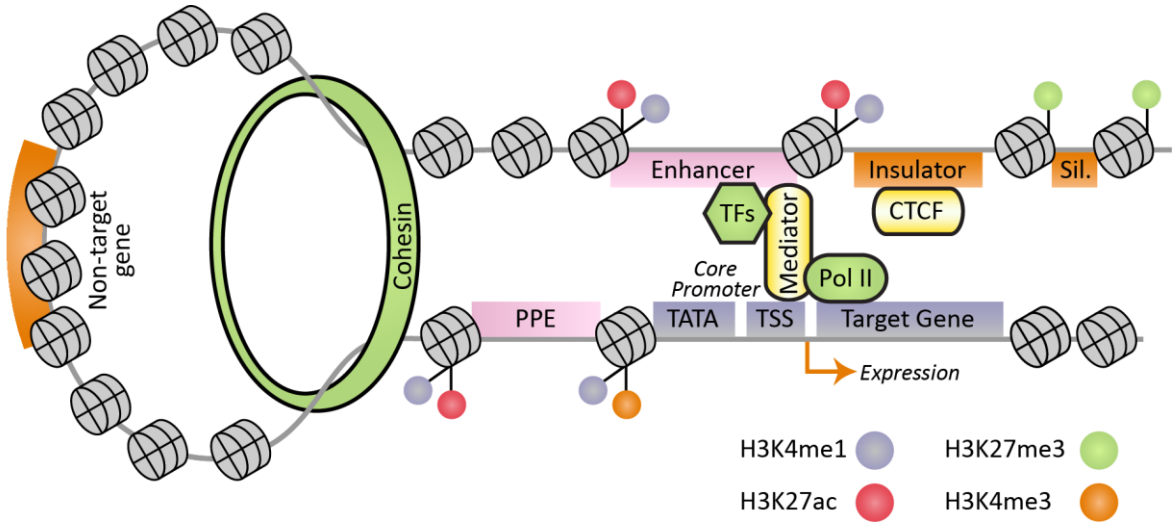

Figure 1 | Transcriptional regulatory elements

TFs: Activating transcription factors; **TSS:** Transcriptional start side; **Pol II:** RNA polymerase II; **PPE:** Proximal promoter element; **Sil.:** Silencer; **TATA:** TATA box; **H3K4me1:** histone H3 monomethylation at lysine 4; **H3K4me3:** histone H3 trimethylation at lysine 4; **H3K27me3**: histone H3 trimethylation at lysine 27; H3K27ac: histone H3 acetylation at lysine 27; *Adapted from* (Shlyueva et al., 2014)

1.2 The Vasculature

The complex bodies of vertebrates require an efficient delivery system for oxygen, nutrients, hormones and immune cells as well as for the removal of waste products. These needs are met by two different branched, tubular networks lined by the endothelium – the blood vessel system and the lymphatic system. The endothelium is formed by a single layer of endothelial cells (ECs), a population of squamous cells of mesodermal origin. They are in direct contact with the blood or lymph and generally align with the direction of flow within the vessel.

Specialised and hierarchically structured vessels (arteries, veins, arterioles, venules and capillaries) form a closed circulatory system that promotes the exchange of oxygen and carbon dioxide between the lungs and the oxygen consuming tissues, whereas the blind-ended lymphatic vessels provide distribution of immune cells and fluid. Besides ECs the mature vessels contain various other cell types that form additional layers such as smooth muscle cells, pericytes, nerves and mesenchymal cells.

The vertebrate blood vessel networks are formed by two main, highly evolutionarily conserved processes, vasculogenesis and angiogenesis.

1.2.1 Vasculogenesis

Vasculogenesis means the *de novo* formation of vascular structures through the assembly and subsequent tube formation of angioblasts. These mesoderm derived endothelial precursor cells are not yet fully differentiated and share some properties with stem cells. The first primitive vascular system, the honeycomb-like primary capillary plexus, which nourishes the embryonic tissues, is created through vasculogenesis and entirely derives from angioblasts. In the mouse embryo the first angioblasts can be identified as non-aggregated TAL1 (see 1.5.3) and VEGFR-2 (see 1.4.2) positive cells in the extraembryonic regions at embryonic stage 6.5 (E6.5) (Drake and Fleming, 2000). As reviewed by Ferguson et al. (Ferguson et al., 2005) these vascular

precursors first colonise the primitive yolk sac and aggregate with hematopoietic precursors to form the so-called blood islands. The close relationship between the haematopoietic and vascular cell lineages and the concept of the haemangioblast will be discussed in 1.3.2. The blood islands coalesce into a primary capillary plexus within the yolk sac at around E7.5.

The fusion of blood islands is accompanied by a differentiation of angioblasts into the more specialised ECs. This maturation, which starts around E8.0, is characterised by the upregulation of the surface molecule PECAM-1 (also known as CD31), CD34, TIE2 (see 1.4.7) and vascular endothelial (VE)-cadherin (also known as CDH5) (Drake and Fleming, 2000). At the same time Tal1 is reported to be downregulated, however there is also evidence for a later involvement of Tal1 in formation of the vasculature (see 1.5.1).

The primitive network then undergoes the process of lumenisation where the solid strings are transformed into hollow tubes of ECs. Extraembryonic vasculogenesis also occurs in parallel in the allantois, where the umbilical vessels connect the chorion with the embryo and thereby allow the formation of maternal-fetal circulation.

In addition to the primitive extraembryonic network of yolk sac and allantois, also the first major embryonic vessels including the dorsal aorta and posterior cardinal vein are directly formed by angioblasts. The same is true for the endocardium, the inner layer of ECs that lines the chambers of the heart, which in mammals originates from the presomitic cranial mesoderm. The primitive vascular plexus remodels into the endocardial tube, which at E7.3 is the first intraembryonic vascular structure in the mouse embryo. Later on at E8.0 the paired dorsal aortae and the cardinal veins can be observed (Drake and Fleming, 2000).

Although vasculogenesis is generally considered to be primarily an embryonic process, there are occurrences of *de novo* blood vessel formation in the adult organism. In 1997 Asahara *et al.* isolated cells from human peripheral blood which subsequently could be differentiated into ECs *in vitro* (Asahara et al., 1997). This cell population was named circulating endothelial progenitor cells (EPC) and it was shown that they originate from the bone marrow (Shi et al., 1998). It has been suggested that EPCs home to sites of neovascularisation such as in the

response to ischaemia, in case of endometriosis and during tumour growth (Asahara et al., 1997; Nolan et al., 2007; Schmidt et al., 2007). Although EPCs constitute promising targets for regenerative medicine, their definition remains under debate. The putative EPCs have been found to be members of the hematopoietic lineage and very rarely incorporate into functional endothelium (Yoder and Ingram, 2009).

1.2.2 Angiogenesis

In contrast to the *de novo* formation of structures during vasculogenesis, the term angiogenesis means the formation of new blood vessels from pre-existing ones. The primary vasculature is already functional as erythroblasts can be observed to enter the mouse embryo at E8.25 (McGrath et al., 2003). However, this network is not yet optimised and insufficient for supporting the increasingly complex tissues of the developing embryo. As the embryo grows, the primary vasculature therefore branches through the whole organism and gets remodelled into a hierarchical, arborescent network.

The mechanisms that control the development of ramified organs such as lung, kidney and the vascular system have fascinated scientists since Aristotle who compared the vascular network to irrigation systems in gardens (King, 2006). In modern times a lot of insight was gained through studies of the branching of the tubular airway system (trachea) in embryos of the fruit fly *Drosophila melanogaster*. A lot of concepts such as the differential functions of tip and stalk within a sprout and even the roles of key molecular pathways like fibroblast growth factor (FGF) and Notch signalling seem to be conserved from insects up to mammals (Metzger and Krasnow, 1999).

1.2.2.1 Sprouting Angiogenesis

Electron microscopy of cross sections from the cerebral cortex of rats first revealed that extending vascular cords have no lumen and are led by "tip cells" which extend "tentacles" into their surroundings (Mato and Ookawara, 1982). Later these tentacles were named filopodia and characterised as thin (diameter 0.1–0.3 μm) actin containing cytoplasmic projections that are formed by different kinds of migrating cells such as fibroblasts, neurons and of course ECs. They carry out various functions including probing the surroundings for signal molecules, forming adhesion sites with the microenvironment and in case of sprouting ECs, engaging in the fusion of sprouts (Mattila and Lappalainen, 2008).

By analysing induced vessel growth in the corneal pocket model in rabbits it was found that EC proliferation is mainly restricted to the stalk of a vessel sprout (Ausprunk and Folkman, 1977). This cell population, which elongates the growing sprout, was later named "stalk cells".

Recent studies, utilising the model system of the developing mouse retina (see 3.1.1) and *in vitro* approaches, have led to a highly sophisticated mechanistic model of vessel branching.

As a first step in sprouting angiogenesis, where ECs react to a pro-angiogenic signal, the basement membrane that envelops endothelial tubes must be proteolytically degraded by matrix-metalloproteases (MMPs). These enzymes, such as Mmp1, which are expressed preferentially by tip cells, enable EC migration and also release angiogenic cues stored within the matrix (Arroyo and Iruela-Arispe, 2010). The quiescent ECs that form the pre-existing vessel now reverse their apicobasal polarity and move along a gradient of pro-angiogenic signals.

In order to extend a new tube the ECs have to respond in a highly coordinated fashion. If all cells would move towards a stimulus at the same time, the vessel would disintegrate and if cells would all start to proliferate when sensing a pro-angiogenic cue, the vessel would just increase in diameter. Therefore a specific location on the pre-existing vessel must be chosen and only a few selected ECs should adopt a migratory or proliferating and tube forming behaviour (Gerhardt, 2008). Lateral inhibition by the Notch signalling pathway (discussed in 1.4.3.1)

serves this purpose and creates a dynamic but functional ratio between invasive tip and tube forming stalk cells.

To be functional, the new vessels have to develop a lumen that can support blood flow. Lumen formation can occur through different mechanisms and is the subject of ongoing studies. Investigations in zebrafish intersegmental vessels have demonstrated that a transcellular lumen can be established through fusion of intracellular vacuoles generated by pinocytosis (Kamei et al., 2006). For the developing aorta in mouse embryos and other larger vessels a different mechanism for lumen formation has been proposed. As a first step apicobasal polarity is re-established and the anti-adhesive sialomucins CD34 and PODXL are localised to the apical (luminal) EC-EC cell contacts, which leads to a repulsion of the cell surfaces from each other. Motor proteins subsequently open up the slit into the aortic lumen and finally the re-established polarity is stabilised by stalk cells which secrete extracellular matrix components (Strilić et al., 2009). A related process has recently been identified for vessel sprouts in mammalian vascular beds where two overlapping tip cells form a lumen via a tube hollowing mechanism (Pelton et al., 2014).

The dead end sprouts that are created by angiogenic sprouting finally have to fuse in order to connect to the existing

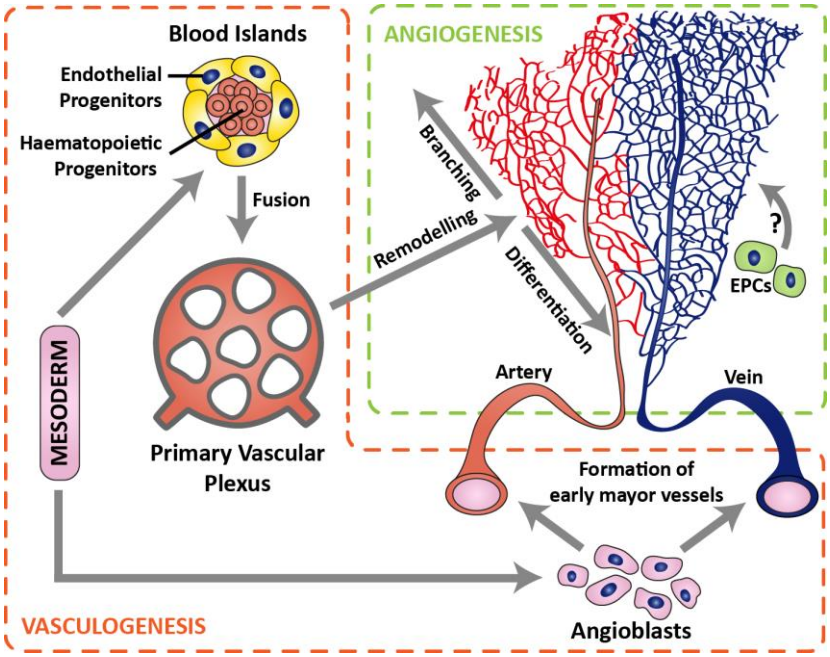

Figure 2 | Assembly of the vasculature
Orange box: During vasculogenesis mesodermal derived angioblasts form the primitive vascular plexus and the major vessels
Green box: After circulation is established the primitive plexus is remodelled into a hierarchical system of vessels with arteries and veins
EPCs: Endothelial precursor cells (contribution to vasculature remains under debate)
Adapted from (Adams and Alitalo, 2007)

network and to get perfused. This process is named anastomosis and is supported by the interaction of filopodia of neighbouring tip cells (Mato and Ookawara, 1982). It has been shown in zebrafish that inhibition of filopodia formation has only minor effects on EC migration and guidance. However anastomosis of intersomitic vessels was significantly reduced (Phng et al., 2013). In addition, the recruitment of macrophages to the sites of anastomosis has been shown to support the fusion process (Fantin et al., 2010).

Finally, after perfusion is established, the now available oxygen, nutrients and possibly blood-borne signalling molecules inactivate the sprouting signalling cascade and induce EC quiescence.

The mechanisms of vasculogenesis and angiogenesis are summarised in Figure 2.

1.2.2.2 Other Forms of Blood Vessel Formation:

Besides the already discussed processes of vasculogenesis and angiogenesis, tissue can also become vascularised by other, less understood mechanisms. One mechanism is the splitting of already existing vessels into daughter vessels named intussusception. Intussusception allows the branching of a functional network without interrupting blood flow and has been identified in lung and tumour angiogenesis (Mentzer and Konerding, 2014), as well as in tissue repair and formation of the lymphatic system and certain stages of embryonic development (Makanya et al., 2009). The process can be subdivided in three categories, intussusceptive microvascular growth, intussusceptive arborisation and intussusceptive branching remodelling. Intussusceptive microvascular growth means the process of a transluminal pillar forming inside the vessel and the resulting splitting of the vessel. In contrast, intussusceptive arborisation includes the formation of multiple pillars in a row and the resulting segregation of various primitive vessels into a tree-like arrangement. Finally, intussusceptive branching remodelling entails the optimisation of the existing network by insertion of transluminal pillars and the resulting modification of branching angles and vessel diameters (Makanya et al., 2009).

Other modes of blood vessel formation have been mainly described in cancer settings. Tumour cells can hijack pre-existing vasculature, known as vessel co-option or line normal vessels, known as vascular mimicry. Also the direct differentiation of cancer stem-like cells into ECs and the formation of a tumour endothelium has been described (Wang et al., 2010a). In addition, the contribution of the already discussed circulating EPCs to the tumour endothelium has been proposed but remains under controversial debate.

1.2.3 Vascular Remodelling and Maturation

Although the final shape of a mature vascular network with its countless branches and complex interconnections is not entirely encoded within the genome, it is far from being random. The tree-like structure of the network, where the diameter of the vessels decreases with increasing branch generation is created in a process of self-organisation, governed by universal patterning rules. Vessels that are non-functional need to be pruned and vessels that have high flow-through rates must be reinforced.

1.2.3.1 Haemodynamics

A critical factor for this kind of maturation are the forces that the fluids inside the vessel exert on the tube (Lucitti et al., 2007). These forces are called haemodynamic forces and can be divided into two categories. The flowing blood and plasma exerts a frictional force parallel to the surface of the blood vessel. This force results in a shear stress, which is proportional to the viscosity and the velocity of the fluid, and is inversely proportional to the radius of the vessel. Additionally, the blood pressure is the hydraulic pressure that results from the pumping of the heart. The pressure causes a force which is orthogonal to the vessel wall and induces a circumferential stress on the vessel wall (Hahn and Schwartz, 2009).

The general concept is that high shear stress stabilises vessels and induces their enlargement (Di Stefano et al., 1998), while low shear stress leads to vessel narrowing and can ultimately

lead to their regression which involves EC apoptosis (Meeson et al., 1996). As far as microvascular remodelling is concerned, the situation is less clear. One study surprisingly found that increased shear stress increases vascular remodelling but leads to reduced vascular density and that reverse intussusception (merging of two vessels) is inhibited by increasing levels of shear stress in the atrial plexus (Chouinard-Pelletier et al., 2013). However, this result could not be reproduced by a another study that showed *in vitro* that luminal and transmural shear stress above a certain threshold induces angiogenic sprouting (Galie et al., 2014). These contradicting results might hint to a necessary differentiation when comparing the remodelling of the immature vascular tree during development and the formation of new vascular beds through sprouting angiogenesis.

ECs must express sensors, called mechanotransducers, which convert these physical forces into biochemical signals. Among the many proposed mechanotransducers are ion channels, integrins, receptor tyrosin kinases, cilia, CD31, VE-cadherin and others (Hahn and Schwartz, 2009). It was proposed that the flow-induced transcription factor Krüppel-Like Factor 2 (KLF2) induces the EC specific microRNA *miR-126* which promotes angiogenesis by inhibiting a VEGF repressor. This would constitute a possible way in which mechanosensoric stimuli are integrated with signalling molecules (Nicoli et al., 2010). Moreover, it was recently found that Notch1 expression can be modulated by blood flow (Jahnsen et al., 2015). Importantly, chronic exposure to disturbed blood flow (low flow, turbulences, reversed flow, etc.) leads to increased expression of inflammatory mediators and to vascular diseases such as atherosclerosis.

1.2.3.2 Mural Cells

As mentioned before, blood vessels do not only consist of ECs but incorporate other cell types as well. Two prominent types, pericytes and vascular smooth muscle cells (vSMCs) fall under the umbrella term of “mural cells”. Already during angiogenesis pericytes are recruited to the sprouts and loosely attach to the endothelium, with which they then produce a common basement membrane. Pericytes enwrap the sprouts, suppress EC proliferation and secrete EC

survival signals. Thereby they promote vessel maturation and stabilisation. ECs (preferentially tip cells) release "platelet-derived growth factor B" (PDGFB) which leads to the recruitment of PDGF receptor beta (PDGFR-β) expressing pericytes (Armulik et al., 2010; Gaengel et al., 2009). Mice deficient for Pdgfb (Lindahl et al., 1997) or Pdgfr-β (Hellström et al., 2001) display failed pericyte coverage leading to micro-aneurysm, haemorrhages and blood brain barrier defects.

In contrast to pericytes, vSMCs are recruited later during vessel maturation and form a closed layer around vessels of larger diameter. They are separated from the endothelium and due to their contractile properties and deposition of elastic fibres provide mechanical stability to the pulsating vessel (Adams and Alitalo, 2007). Similar to pericytes, vSMC recruitment depends on PDGF, angiopoietin and TGF-β signalling. In addition, Notch3 signalling has been associated with vSMC maturation (see 1.4.3.2).

The complex ontology of mural cells is subject of ongoing research. Depending on the vascular bed and the developmental stage, various different origins have been identified for both pericytes (Berthod et al., 2012) and smooth muscle cells (Majesky et al., 2011). Therefore, it seems likely that this binary classification of mural cells is an oversimplification and sub-types of these cells follow unique recruitment mechanisms. Moreover, the phenotypes of pericytes and vSMCs are possibly interconvertible and until now no molecular marker that exclusively labels one or the other cell type has been identified (Armulik et al., 2010).

Mural cell recruitment and signalling pathways during vessel maturation are illustrated in Figure 3.

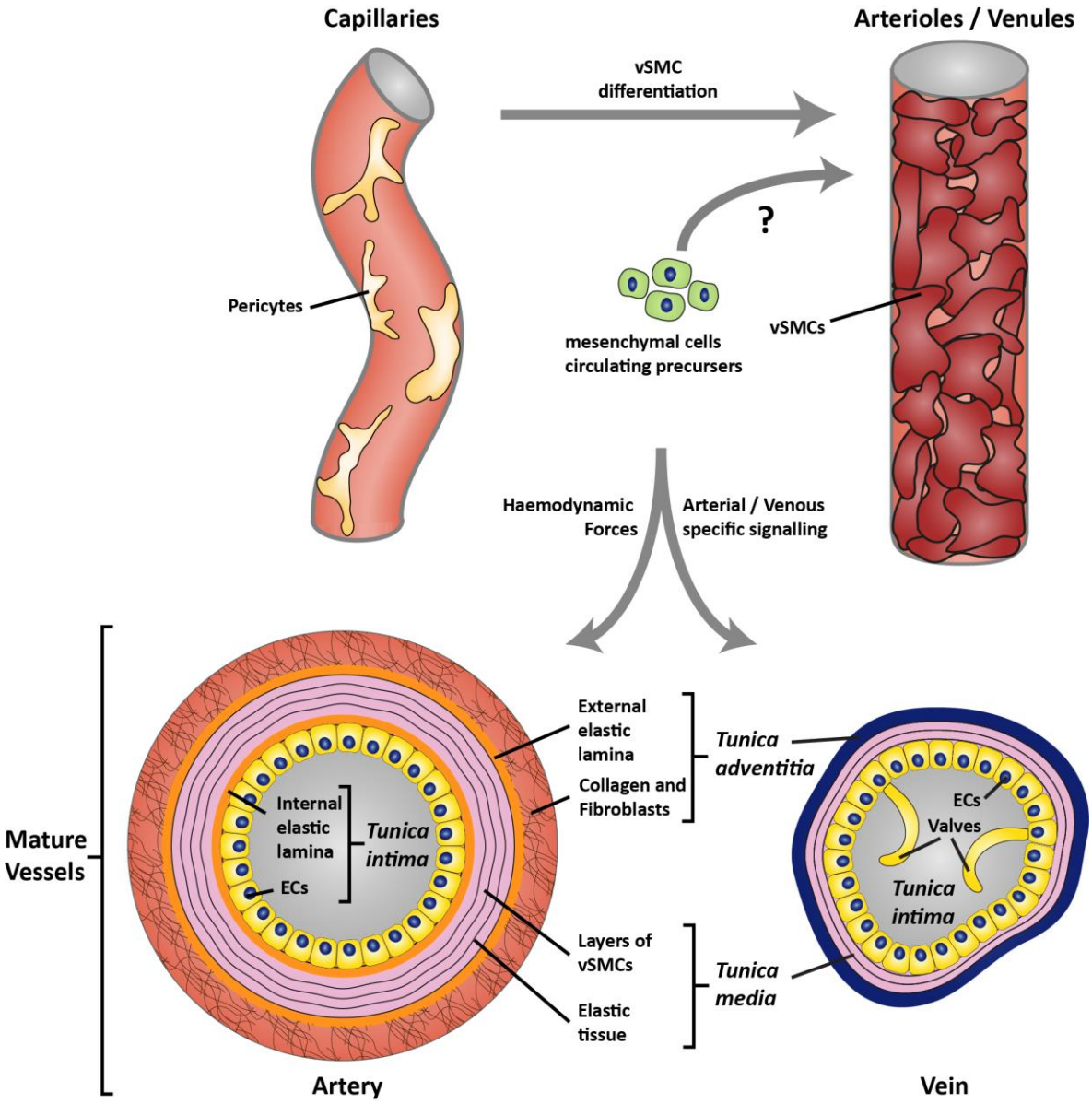

Figure 3 | Mural cell recruitment and arteriovenous differentiation

At the beginning capillaries are only loosely covered by pericytes which stabilise the vessels and control angiogenesis. During maturation of the vascular tree the capillaries differentiate into arterioles and venules and get populated by more mural cells (vascular smooth muscle cells [vSMCs] and pericytes). These mural cells are derived from mesenchymal and possibly circulating progenitors. Haemodynamic and morphogenic signals drive further arteriovenous differentiation, which is accompanied by changes in EC and vSMC morphology. Large mature arteries need to resist high pressure and have the ability to contract in order to control blood pressure. They are composed of the inner tunica intima (ECs and elastic lamina), the central tunica media with several alternating layers of vSMCs and elastic tissue (mainly matrix), and the outermost tunica adventitia, which is rich in collagen and fibroblasts. Major veins display less extensive vSMC coverage, have thinner walls and additionally contain valves to prevent backflow.

Adapted from (Adams and Alitalo, 2007) and (Potente et al., 2011)

1.2.4 Arteriovenous Differentiation

As outlined in the previous paragraphs, in the developing organism various haemodynamic properties arise within individual parts of the blood vessel network. The arteries carry blood away from the heart to the capillaries. Therefore, blood pressure and shear stress are elevated which requires an enlargement of diameter and mechanical enforcement. Arteries are supported by many layers of vSMCs (up to 50 on major arteries in humans) and a specialised matrix containing elastic fibres (Gaengel et al., 2009). In contrast, the veins carry lower oxygenated, lower pressure blood back to the heart. Veins contain flap-like structures, called valves. By opening unidirectionally, they prevent backflow of the blood, especially within the legs where the blood has to be transported against gravitational pull. Veins are enveloped by vSMCs as well, however the vSMC layer is thin compared to arteries, as veins do not primarily function in a contractile manner (Gaengel et al., 2009).

The process of the formation of arteries and veins from the primitive capillary plexus is called arteriovenous differentiation. Although the existence of two distinct vessel types has been known for more than 2,000 years, science just started to elucidate the cellular and molecular differences between arteries and veins in recent years. Originally it was thought that the different features of arteries and veins develop entirely due to the influence of haemodynamic forces (Atkins et al., 2011). However, in a landmark study it was shown that the arterial and venous endothelium of the mouse embryo differentially express the markers EphrinB2 and Ephb4 (see 1.4.4) before the initiation of circulation flow at E8.75 (Wang et al., 1998). In a similar fashion it has later been shown in zebrafish that the bHLH transcription factor Gridlock (GRL) guides arterial-venous decision of angioblasts (Zhong et al., 2001).

Besides the genetic pre-determination of precursor cells to arterial or venous fate, environmental factors such as haemodynamic forces and oxygenation play a role in the specification and maintenance of vessel identity as well. In the avian embryo ligation of arterial branches to the venous plexus result in the switch from arterial to venous specific markers (le Noble et al., 2004). And in both humans and aged rats veins lose their identity when grafted

into an arterial environment (Kudo et al., 2007). Moreover, the de-differentiation of sprouting venous ECs during invasion of the myocardium and re-differentiation into coronary arteries has been reported (Red-Horse et al., 2010)

Similarly, it has been demonstrated that oxygen levels are an instructive signal for artery and vein specification as forming retinal arteries fail to express the artery-specific markers Dll4 and EphrinB2 in hypoxic conditions (Claxton and Fruttiger, 2005). Conversely, hyperoxia in the developing retina leads to vaso-obliteration, especially along arteries. This has been explained with the downregulation of VEGF-A as a response to elevated oxygen levels and a consequent lack of EC survival signalling (Claxton and Fruttiger, 2003).

1.2.5 Vascular Beds and Vascular Heterogeneity

As outlined previously, ECs build up highly diverse structures such as arteries, veins and lymphatic vessels and display a great variety of molecular features depending on the identity of the respective vessel. However, the heterogeneity of ECs does not end there. The vascular system penetrates all organs and almost all tissues of the vertebrate body. Considering that different structures fulfil different and sometimes opposed roles, it seems natural that ECs accommodate the needs of their respective environments. Therefore, the vasculature can be subdivided in various “vascular beds” that are named after their respective environment, such as the pulmonary or retinal vascular bed.

A striking example of EC heterogeneity is the comparison of the microvascular beds of the brain and the kidney. In order to protect the sensitive brain tissues, ECs in brain capillaries form a restrictive barrier that limits the passage of substances and cells between the peripheral circulatory system and the central nervous system, the so called blood-brain barrier (BBB). The ECs in the BBB are connected via tight junctions, exhibit a limited set of cellular trafficking processes and are especially dependent on pericyte coverage (Armulik et al., 2010). On the other end of the functional spectrum lie the ECs in the capillaries of kidney glomeruli. The

kidney filters waste products from the blood and for that reason these vessels are highly fenestrated (Herzlinger and Hurtado, 2014).

Besides the adaptation to tissue specific requirements, another function of the vasculature makes EC diversification necessary. It has recently become evident that ECs not only form the passive wall of a blood flow conduit but also actively produce "angiocrine" factors. These are paracrine-trophic signal molecules that are involved in the regulation of organ specific physiological processes like pancreatic differentiation, reconstitution of haematopoietic stem cells and expansion of neuronal precursors (Carmeliet and Jain, 2011). Moreover, it has been suggested that aberrant angiocrine signalling can even support tumour growth (Butler et al., 2010) and recently it was found that the bone vasculature contains ECs specialised to support bone maturation and regeneration (Ramasamy et al., 2014). Although EC heterogeneity is widely acknowledged, the molecular signatures of ECs in different vascular beds remain poorly understood. Using intravital labelling and flow sorting Nolan *et al.* isolated mouse ECs from various tissues and conducted transcriptional profiling (Nolan et al., 2013). They found that the most closely related ECs were from the heart and muscle ($R^2 = 0.98$), whereas the least similar pair was the lung and bone marrow ($R^2 = 0.80$).

It is important to note that the concept of vascular heterogeneity is not only limited to the characteristics of the fully developed vessel network but also encompasses angiogenesis and vasculogenesis. Every tissue has its own specific architecture and creates an individual environment for growing blood vessels in terms of available guidance cues and also mechanical resistance. A lot of the knowledge about the mechanisms of vascular development that I have presented in the previous paragraphs was gained through the use of selected *in vivo* and *in vitro* models. It needs to be considered that those mechanisms differ considerably in other environments.

1.3 The Related Ontogeny of Blood and Vasculature

During embryogenesis the development of blood vessels and the blood itself have to occur in parallel to ensure both that all the tissues get nourished and oxygenated and that the circulatory system is shaped according to local tissue demands. It is therefore not surprising that the developmental origins of blood and vasculature, although not yet entirely clear, are tightly interlinked. In the following I give a short overview of the current concepts about their shared ontogeny. These concepts are essential for understanding the functions of the main subject of this thesis, the transcription factor Tal1.

1.3.1 Embryonic Haematopoiesis

As outlined in 1.2.1, the primitive vasculature is assembled by stem cell like precursor cells named angioblasts. In a different but related fashion, all cellular components of the blood including erythrocytes, thrombocytes and the cells of the immune system emerge from one multipotent, self-renewing progenitor cell type – the hematopoietic stem cell (HSC). These bone marrow derived cells provide a life-time supply of blood cells through a process named haematopoiesis, which during development is established in several waves.

In mouse the first blood cells emerge at E7.0 - E7.25 from blood islands within the yolk sac (Maximow, 1924). These blood cells are not yet enucleated and are termed “primitive”. The second wave of multi-lineage haematopoiesis is called “definitive” because the progenitors produced in this process can reconstitute the entire haematopoietic system of an irradiated mouse. Definitive haematopoiesis begins at around E10.5 in a distinct mesodermal region, the aorta-gonad-mesonephros (AGM) (Müller et al., 1994). The yolk sac (Samokhvalov et al., 2007) and placenta (Gekas et al., 2005) as possible earlier sites of definitive haematopoiesis remain under debate.

Subsequently, haematopoiesis is established in the fetal liver (E11.5), thymus and spleen (E12.5) and eventually shortly before birth in the bone marrow. The fetal liver is also the first site of haematopoietic differentiation, giving rise to mature erythrocytes (Golub and Cumano, 2013). From here, the lineage relationships between blood forming cells from different stages of development are still not clearly agreed upon in the literature. In particular, the question of at which stage and location truly definitive haematopoiesis occurs remains under debate. Similarly, it is still not clear if initial yolk sac derived progenitors eventually die out or if they contribute to the adult population of HSCs (Golub and Cumano, 2013).

1.3.2 The Hemangioblast

A first hint that ECs and HSCs share a common ancestral progenitor came from the close spatial association of both cell types in the developing avian embryo, where haematopoietic precursors are formed in the vasculature of the yolk sac and within the ventral wall of the dorsal aorta (Murray, 1932; Sabine, 1920). This hypothetical bi-potential haematopoietic precursor cell, which originates within the primitive streak, was called the hemangioblast. Later it was found that isolated and cultured VEGFR-2 positive embryonic stem cells, so called "blast-colony-forming cells" (BL-CFCs) can produce colonies that contain both endothelial and haematopoietic progenitor cells when treated with VEGF-A and BMP-4 (Choi et al., 1998; Kennedy et al., 1997; Lu et al., 2007). Despite this molecular and cell biological evidence, the final *in vivo* proof of the hemangioblast is still lacking, although cell labelling experiments in zebrafish demonstrated that certain cell populations commit to both the haematopoietic and vascular lineage (Vogeli et al., 2006). Nevertheless this study also showed that just a minority of cells had a bipotential progenitor and most of the haematopoietic and vascular cells arose from independent sources. In addition, close re-examination of the blast-colony experiments reveals that these cells were not strictly bipotential and also produced smooth muscle cells

(Huber et al., 2004). Although several signalling pathways such as Bmp-4, Vegf-A, Ihh, Shh, Lycat, Hhex, and Mixl1 have been shown to be essential for hemangioblast formation in mouse embryo, the precise details of hemangioblast formation and the existence of a possible master regulator remain currently unknown (Xiong, 2008).

1.3.3 Hemogenic Endothelium

While the concept of the hemangioblast was introduced almost a century ago the competing idea of the hemogenic endothelium (HE) is just as old (Jordan, 1917). In this model differentiated ECs give rise to HSCs by trans-differentiation or asymmetric cell division. At the moment the collective weight of scientific evidence supports this concept, suggesting that, at least in later stages of blood formation, progenitor cells arise from specialised vascular cells (Antas et al., 2013; Hirschi, 2012). For example, ECs positive for VE-cadherin within the AGM, the placenta and the yolk sac give rise to HSCs that populate the fetal liver and later the embryonic and even adult bone marrow (Zovein et al., 2008). Similar findings supporting the concept of HE were obtained in murine cell culture (Goldie et al., 2008) and zebrafish (Boisset et al., 2010) experiments. Morphologically, the HE is presented as groups of haematopoietic cells, called intra-aortic or aorta-associated cluster, which extend from the vessel wall into the lumen. Aorta-associated clusters are best described in the dorsal aorta where they can be found from E9.5. (Yokomizo and Dzierzak, 2010).

The concept of HE does not need to be restricted to embryonic haematopoiesis. For instance it is known that HSCs in the adult bone marrow are in close physical association with ECs (Kiel et al., 2005). However, the idea of ECs producing HSCs within the adult bone marrow remains highly controversial and is not supported by strong experimental evidence at the moment. In particular the observation that the adult HSC pool can be exhausted in the course of transplantation contradicts this idea (Harrison et al., 1978).

In summary, it should be noted that the concepts of hemangioblast and HE are not mutually exclusive, and hybrid models, in which that hemangioblasts can give rise to blood cells via a HE intermediate have been proposed. This theory is supported by several studies that showed that mouse embryos contain VEGFR-2(+) cells that, when cultured as BL-CFCs, give rise to VEGFR-2(+), VE-Cadherin(+), C-KIT(+), TIE2(high) and CD41(-), CD45(-) endothelial cell populations. Subsequently, the generation of free-floating haematopoietic cells from adherent ECs can be observed (Eilken et al., 2009; Lancrin et al., 2009). The transcription factor TAL1 is critical for this transition from hemangioblast to HE populations (Lancrin et al., 2009).

1.4 Major Signalling Pathways in Vascular Development

The complex mechanisms of cell migration, differentiation and proliferation necessary for the establishment of hierarchically structured vessel networks have to be orchestrated by well-balanced cell-cell communication. Different guidance cues for the developing vasculature that are secreted by the surrounding tissues and act in endo-, para-, and autocrine fashion have been identified. In the following I will give a short overview about the most important regulatory pathways and outline their function in angiogenesis. A graphical summary is given in Figure 4.

1.4.1 Hedgehog Signalling

The hedgehog (HH) proteins constitute a family of secreted signalling molecules which display an extremely deep evolutionary conservation and play a central role in the embryonic development of metazoans. Amnoites (reptiles, birds and mammals) have three Hedgehog homologues, Desert Hedgehog (Dhh), Indian Hedgehog (Ihh) and Sonic Hedgehog (Shh), which is the best studied Hedgehog member in vascular development. (Ingham et al., 2011).

Signal receiving cell expresses the receptor Patched (PTCH) which inhibits the co-receptor Smoothened (SMO). HH binding inhibits PTCH and thereby releases SMO which leads to the

activation of the transcription factor glioma-associated oncogene family zinc finger 1 (GLI1) that accumulates within the nucleus and binds to its target genes (Nagase et al., 2008).

$Shh^{-/-}$ mice die between E14.5 and birth dependent on the respective genetic background due to failed organogenesis and limb development (Chiang et al., 1996). In vascular development, Shh has been implicated in various contexts. It has been shown in zebrafish that Shh signalling derived from the notochord stimulates the formation of the dorsal aorta by inducing Vegf-A expression in the somatic tissue and consequent upregulation of the Notch pathway in the aorta (Lawson et al., 2002). Subsequently it was shown that Smo mutant zebrafish lack the dorsal aorta (Gering and Patient, 2005) and the mechanistic explanation proposed that HH signalling represses venous fate in angioblast populations (Williams et al., 2010).

Similar defects can be observed in Smo deficient mice which display a defective dorsal aorta and die at E9.5. However, the authors of this study suggested that HH mediates arterial assembly independently of VEGF (Vokes et al., 2004). Later in development Shh is necessary for coronary vessel growth (Lavine et al., 2006) and for the transition of vasculogenesis to remodelling angiogenesis (at ~E9.0) in mouse embryo yolk sac vascularisation (Nagase et al., 2006).

In addition to its widespread functions during embryonic development, Shh signalling also plays a role during postnatal angiogenesis (Surace et al., 2006) and wound healing (Pola et al., 2001).

In summary, it appears clear that the hedgehog family of morphogens plays a role in vascularisation due to the interplay with several other pathways. Nevertheless, mechanistic details like the question if HH signalling has a direct or indirect effect on ECs still remain to be elucidated.

1.4.2 VEGF Signalling

One of the most potent modulators in blood vessel development is Vascular Endothelial Growth Factor A (Vegf-A). Together with its six homologues Vegf B-F and placental growth factor (Plgf) it forms the family of Vegfs. VEGF-A binds to VEGF receptor 1 (VEGFR-1, also known as FLT-1) and VEGFR-2 (also known as FLK-1 or KDR). VEGF-C and VEGF-D bind to VEGFR-3 (also known as FLT-4). By contrast VEGF-B and PlGF are bound by VEGFR-2. All three VEGF receptors are expressed on ECs and belong to the family of receptor tyrosine kinases. These receptors dimerise in the course of ligand binding, autophosphorylate on various tyrosine residues and induce various downstream signalling cascades (Moens et al., 2014).

The crucial roles of Vegf signalling for blood vessel development are highlighted by the severe vascular defects observed in mouse embryos lacking just one Vegf-A allele or both Vegfr-2 alleles. Heterozygosity for an inactivated Vegf-A allele is lethal at around E10.5. The embryos show an abnormal development of the dorsal aorta and disorganised intra- and extra-embryonic vasculature. In complete Vegf-A knockouts the effects are even more severe with the dorsal aorta completely missing at E8.5 (Carmeliet et al., 1996). Embryos homozygous for a disruption in the Vegfr-2 gene die between E8.5 and E9.5 due to a lack of blood island formation and consequently no formation of organised vasculature, suggesting a role in initial vascular progenitor formation (Shalaby et al., 1995).

The main initial pro-angiogenic signal is tissue hypoxia. The organism tries to compensate the local lack of oxygen by developing new blood vessels within the hypoxic area. The hypoxic tissues upregulate and secrete VEGF-A which induces angiogenesis and attracts blood vessels in the surroundings. Thereby a key molecule in sensing hypoxia is the transcription factor hypoxia-inducible factor (HIF)1α which is stabilised under low-oxygen conditions and activates the transcription of several genes by binding HIF-responsive elements (HREs) in their promoters, including Vegf-A.

The effects of Vegf-A on angiogenic processes depend on its splicing variants, which have different molecular properties and carry out different functions. These isoforms differ in affinity to VEGF receptors, ability to diffuse and length (amino acid number is depicted in subscript). In humans the isoforms are $VEGF_{121}$, $VEGF_{145}$, $VEGF_{165}$, $VEGF_{189}$, and $VEGF_{206}$. The murine orthologues each contain one amino acid less.

Although VEGFR-1 and VEGFR-2 are both high affinity receptors for VEGF-A, the weak kinase activity of VEGFR-1 is expendable for VEGF-A mediated signal transduction. Moreover, VEGFR-1 also exists in a soluble, secreted form (also known as sVEGFR-1) that binds VEGF, prevents its binding to VEGFR2 and as a result limits VEGF signalling. This led to the assumption that VEGFR-1 acts as a decoy receptor and regulates signalling through VEGFR-2 by sequestering excess VEGF-A (Park et al., 1994). This model is supported by the knockout experiments. Loss of Vegfr-1 is embryonic lethal at E8.5 due to vessel overgrowth and disorganisation (Kearney et al., 2004). In addition mice homozygous for a Vegfr-1 tyrosine kinase deficient but ligand binding variant survive with normal vasculature (Hiratsuka et al., 1998).

In addition to angiogenesis the VEGF signalling pathway is also involved in embryonic lymphatic development. It has been demonstrated that VEGF-C (and to a minor degree VEGF-D) promote migration, proliferation and survival of lymphatic ECs (LECs) by signalling through VEGFR-3 (Karkkainen et al., 2004). Moreover, VEGFR-3 is also essential for postnatal lymphangiogenesis and lymphatic vessel maintenance.

VEGF signalling not only influences the development on the microvascular level but also induces the differentiation of major blood vessels. During development Vegf is upregulated in the somites bordering the inner cell mass in response to Shh. The secretion of VEGF creates a gradient of high concentration at the developing dorsal aorta to low concentration at the developing posterior cardinal vein. Also later in development, increased Vegf expression results in upregulation of arterial markers such as Ephrin-B2 and Neuropilin 1 (Nrp1) and elevated arterial/venous ratio (Lanner et al., 2007). The exact mechanism of how Vegf induces arterial fate still remains elusive, especially due to the fact that the main VEGF-A receptor Vegfr-2 is

expressed in both arterial and venous ECs. A possible explanation is provided by the differential expression of Neuropilin (Nrp) receptors which act as VEGFR-2/VEGFR-3 co-receptors (Soker et al., 1998). Nrp1 is expressed in arteries and Nrp2 in veins and lymphatic vessels (Gu et al., 2003). The two receptors bind to different splice variants of VEGF and therefore might trigger different signalling cascades that lead to arterial or venous fate.

Vegf also fulfils many of its functions by acting upstream and in feedback loops with the Notch pathway (Lawson et al., 2003), which is discussed in the section below.

1.4.3 Notch Signalling

The Notch pathway participates in many processes of cell differentiation and is highly conserved in metazoans. Its main functions are to mediate lateral inhibition, keep cells in undifferentiated states or to ensure that adjacent and developmentally similar cells obtain different fates. Both Notch receptors and its ligands are type I single-pass transmembrane proteins. In mammals the four Notch receptors (Notch1, Notch2, Notch3 and Notch4) are bound by three "delta-like" (DLL1, DLL3, DLL4) and two "jagged" (JAG1 and JAG2) ligands. Together the ligands form the family of Delta/Serrate/LAG-2) proteins (D'Souza et al., 2010).

Notch can bind to one of its ligands on an adjacent cell, leading to Notch transactivation. The interaction leads to proteolytic cleavage by disintegrin and metalloproteinase domain-containing protein 10 (ADAM10) and subsequently by the Presenilin/γ-secretase complex. The cleaved-off Notch intracellular domain (NICD) is translocated to the nucleus, interacts with its co-activator mastermind-like protein 1 (MAML-1) and activates the otherwise inhibitory transcription factor Recombining Binding Protein J kappa (RBP-J_κ), also known as CSL and CBF-1 (Guruharsha et al., 2012). The best studied target genes of the activated RBP-J_κ complex in ECS are the basic-helix-loop-helix (bHLH) transcription factor families hairy and enhancer of split" (HES) and hes-related family bHLH transcription factor with YRPW motif (HEY). Hey1

and Hey2 seem to be partially functionally redundant since only a double KO of both of them leads to similar defects (death at E9.5) as a homozygous Notch KO (Fischer et al., 2004).

Notch signalling plays various roles in vascular patterning and homeostasis.

1.4.3.1 Notch in Angiogenic Sprouting

As discussed in 1.2.2, angiogenic sprouts are led by endothelial tip cells that protrude filopodia and migrate towards angiogenic cues. They are followed by the dividing and tube forming stalk cell population. Inactivation or pharmacological inhibition of Notch1 or Dll4 in the mouse retina and in zebrafish leads to a characteristic hypersprouting phenotype with an increased number of tip cells and filopodia, elevated EC proliferation and an immature appearance of the vascular plexus. Conversely, the artificial activation of Notch signalling leads to sprouting inhibition and a sparser network (Hellström et al., 2007; Leslie et al., 2007; Siekmann and Lawson, 2007). Together with the finding that tip cells display high expression levels of Vegfr-2 and Vegfr-3, a model was established where VEGF-A and VEGF-C induce Dll4 expression in tip cells, which then activate Notch signalling and transcription of Notch target genes such as Hey1, Hey2 and Nrarp (see 1.4.5) in the adjacent stalk cell (Tammela et al., 2011). As a consequence, the Notch signal receiving stalk cell downregulates Vegfr-2 and Vegfr-3 and upregulates the decoy receptor Vegfr-1, creating a local VEGF-A sink. By this tightly regulated and dose dependent interplay between VEGF and Notch signalling, the tip/stalk cell phenotypes get established. However, these phenotypes show high plasticity with tip and stalk cells interchanging positions within hours. In embryonic body assays it was shown that ECs with reduced levels of VEGFR-2 have a cell-autonomous decreased probability of assuming tip cell identity and position whereas reduced levels of VEGFR-1 lead to the opposite effect. Similar EC shuffling could be observed *in vivo* in the brain vasculature of the zebrafish. It is hypothesised that the reason for this constant position shuffling is to ensure that the leading tip cell has the optimal VEGF receptor configuration for detecting the direction of the VEGF-A gradient and other environmental clues (Jakobsson et al., 2010).

The detailed implications of the interplay of Vegfr-2, Vegfr-3 and Notch still remain under discussion. In 2011 it was shown that endothelial loss of Vegfr-3 leads to hypersprouting due to failed Notch activation (Tammela et al., 2011). This result was in contrast to previous findings where VEGFR-3 blocking antibodies suppressed angiogenesis (Tammela et al., 2008). Later in 2012 Benedito *et al.* published the surprising result that DLL4 expression in retinal tip cells seems to be only weakly modulated by VEGFR-2 but dependent on ligand independent VEGFR-3 signalling (Benedito et al., 2012). These findings are challenged by a recent study that showed that Notch inhibition promotes sprouting in the absence of VEGFR-3 but not in the absence of VEGFR-2 (Zarkada et al., 2015).

In contrast to Dll4, the loss of Notch ligand Jag1, which is mainly expressed in stalk cells, leads to decreased Notch signalling and the resulting hyposprouting phenotype (Benedito et al., 2009). This surprising result is explained by a model where Jag1 is glycosylated by enzymes of the Fringe family, especially by lunatic fringe (LFNG). These proteins add N-acetylglucosamine sugars to the extracellular domains of the Notch receptor and thereby enhance the signalling abilities of Delta-like family ligands but reduce signalling through Jagged family ligands (Hicks et al., 2000). Therefore, if Jag1 and Dll4 are expressed in the same cell, Jag1 acts as a competitive antagonist, preventing Notch signalling in neighbouring cells and thus stabilising the tip/stalk cell distinction (Benedito et al., 2009). Previously it was found that endothelial specific Jag1 KO mouse embryos also show deficits in vSMC development (High et al., 2008) which might contribute to the phenotype.

1.4.3.2 Notch in Specification of Arteriovenous Identity

In addition to a role in angiogenic sprouting, the Notch pathway is also a crucial determinant for arterial identity. Blockage of Notch signalling in zebrafish (Lawson et al., 2001) and in mice (Krebs et al., 2010) enhances venous specification at the expense of arterial formation. These defects phenocopy the malformations seen in EphrinB2 and EPHB4 mutants (see 1.4.4). Together with the finding that Notch overexpression can rescue arterial specification in VEGF

deficient zebrafish (Lawson et al., 2002), and that arterial-specific EphrinB2 is a direct Notch target (Grego-Bessa et al., 2007), this led to the model that SHH induced activation of VEGFR-2 in angioblasts leads to Dll4/Notch signalling and the downstream expression of EphrinB2.

Detailed studies of mutants of components of the Notch pathway have revealed that almost all of them are necessary for proper arterial specification. Besides the Notch receptors Notch 1 and 4, Notch ligands DLL4, JAG1 and JAG2 are also expressed in arterial endothelium (Shutter et al., 2000; Villa et al., 2001). While JAG1$^{-/-}$ mice die between E10.5 and E11.5 from vascular defects in yolk sac and embryonic vasculature (Xue et al., 1999), deficits in vSMCs might underlie these defects, as Notch activation in ECs and arterial-venous differentiation appear normal (High et al., 2008). In humans the autosomal dominant disease Alagille syndrome (ALGS), which manifests among other symptoms in pulmonary artery defects, is caused by mutations in JAG1 and very rarely NOTCH2 (Kamath et al., 2012).

In contrast to deletions of Notch receptors and Jag ligands, loss of just one Dll4 allele leads to embryonic lethality at E9.5 with remodelling defects in the primitive vascular plexus and failed arterial lineage specification, suggesting a critical, dosage-sensitive requirement for DLL4 (Duarte et al., 2004; Gale et al., 2004; Krebs et al., 2004). Additionally, Dll4 mRNA can be detected in the forming dorsal aortae at E8.0, preceding all other canonical markers and its receptors Notch1/4 (Chong et al., 2011).

As outlined in 1.4.8.2 it has been established that the transcription factor Sox17 bridges Wnt and Notch for coordinated signalling in arterial specification.

1.4.4 EphrinB2 and EphB4 Signalling

The EPH receptors (receptor tyrosine kinases) and their ligands, the Ephrins, are both transmembrane proteins, meaning that binding and activation of Eph/Ephrin intracellular signalling pathways can only occur upon cell-cell contact. Of the eight Ephrins and fourteen EPH receptors identified in humans, only the receptor EPHB4 and its ligand with the highest affinity

Ephrin-B2 have a known role in vascular development. An unusual feature of Eph/Ephrin interaction is that it can generate bidirectional signals. This means that upon Eph/Ephrin interaction the downstream signalling cascade can also be initiated in the Ephrin (ligand) expressing cell, termed reverse signalling.

EphrinB2 is one of the most prominent arterial EC markers whereas EPHB4 marks venous endothelium, although weak expression on arteries has been reported (Gerety et al., 1999). In zebrafish the first embryonic artery (dorsal aorta) and vein (cardinal vein) arise by selective sprouting of progenitor cells from a common precursor vessel. The mutually exclusive expression of EphrinB2 and EphB4, which is regulated by VEGF-A, was uncovered to prevent intermingling of progenitors and allow arterial-venous segregation (Herbert et al., 2009; Wang et al., 1998).

Mutant mice lacking EphrinB2 (Wang et al., 1998) or EphB4 (Gerety et al., 1999) die before E11.0 and display similar cardiovascular defects with dilated major vessels and an almost complete abolition of angiogenesis. In the postnatal retina it was demonstrated that mice with a mutated version of EphrinB2 incapable of reverse signalling exhibit a reduced number of tip cells. Mechanistically it was shown that reverse signalling by EphrinB2 in tip cells reduces VEGFR-2 internalisation which is necessary for VEGF-induced tip-cell filopodial extension (Sawamiphak et al., 2010a).

Figure 4 | Interacting signalling pathways in tip and stalk cells

In response to VEGF stimulation, ECs get selected into tip and stalk cells which display characteristic surface receptor settings and transcriptional programs. The guidance cue sensing tip cells upregulate Vegfr-2/3 and the co-receptors Efnb2 and Nrp1 while stalk cells downregulate these proteins and upregulate the decoy receptor Vegfr-1 through Notch signalling. Tip cells express Mmp1 and PdgfB in order to migrate and interact with pericytes.

Lateral inhibition between tip and stalk cells is mediated by Notch signalling. Tip cells express Dll4 which induces the formation of NICD in the stalk cell via the Notch1 receptor which gets glycosylated by LFNG. Notch-Target genes such as Hey1/2 and Nrarp stabilise the non-motile, dividing stalk cell phenotype. In contrast, stalk cells express the Notch ligand Jag1 that competes with Dll4 and thereby limits Notch signalling in the tip cell.

TGF-β and BMP9 signalling via ALK1 and ALK5 activates SMAD2/3 which supports the transcription of Notch target genes in the stalk cell.

The proliferate potential of stalk cells is supported by induction of the cell-cycle checkpoint molecule CyclinD1 through Wnt-signalling. Upon binding of Wnt signal molecules to receptors of the Fzd family and Lrp co-receptors, β-catenin is stabilised and acts together with TCF/LEF as a transcriptional activator.

Nrarp was suggested to act as mediator between Notch and Wnt signalling, as it limits its own expression through interference with Notch transcription factor RBPJ and stimulates expression of Wnt target genes.

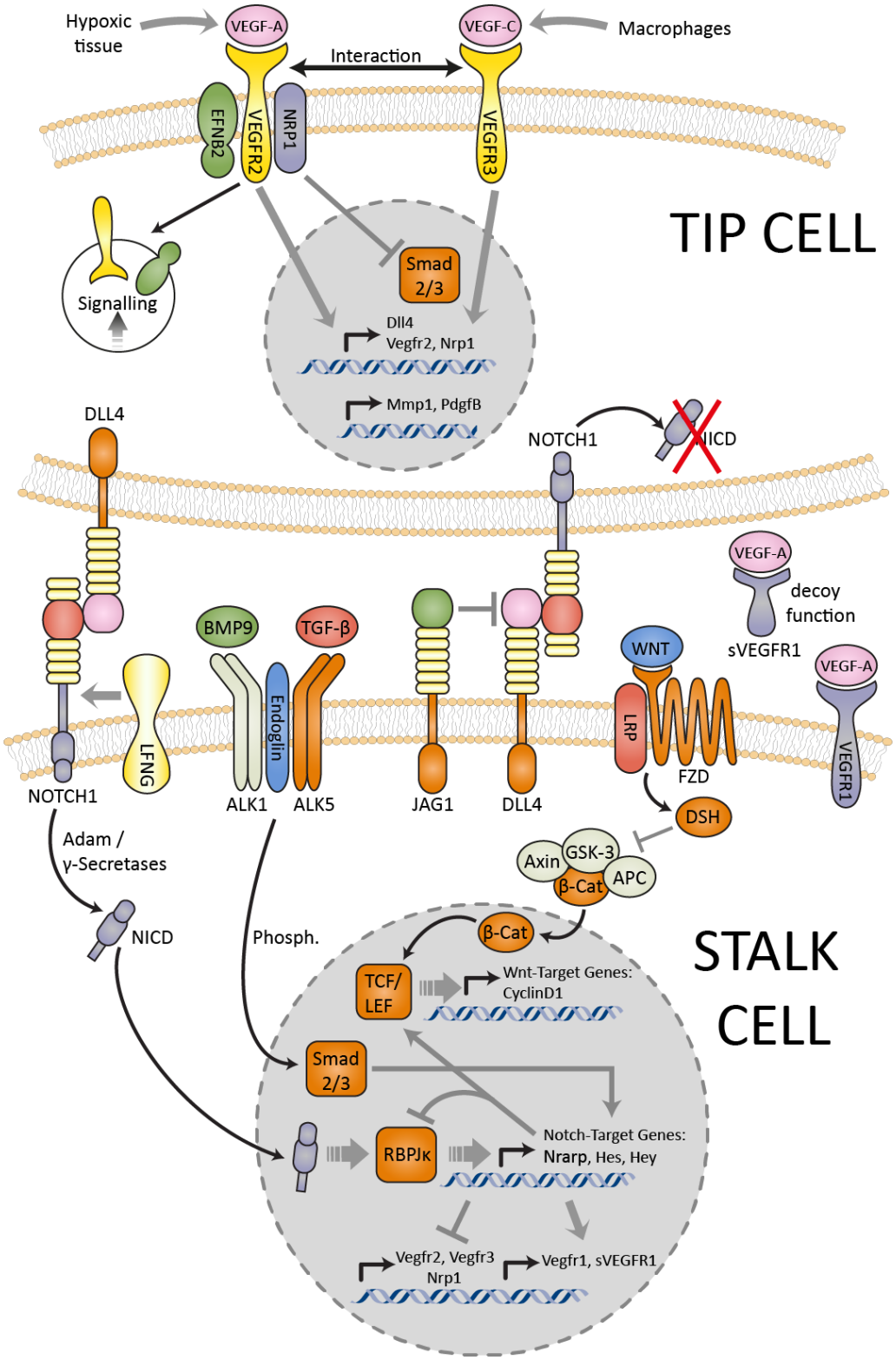
Hypoxic tissue
VEGF-A
VEGF-C
Macrophages
Interaction
EFNB2
VEGFR2
NRP1
VEGFR3
TIP CELL
Signalling
Smad 2/3
Dll4
Vegfr2, Nrp1
Mmp1, PdgfB
DLL4
NOTCH1
NICD
VEGF-A
decoy function
sVEGFR1
BMP9
TGF-β
WNT
LFNG
Endoglin
LRP
VEGF-A
VEGFR1
NOTCH1
ALK1
ALK5
JAG1
DLL4
FZD
DSH
Adam / γ-Secretases
Axin
GSK-3
β-Cat
APC
NICD
Phosph.
β-Cat
STALK CELL
TCF/ LEF
Wnt-Target Genes: CyclinD1
Smad 2/3
RBPJκ
Notch-Target Genes: Nrarp, Hes, Hey
Vegfr2, Vegfr3 Nrp1
Vegfr1, sVEGFR1

1.4.5 WNT Signalling

The activation of the Wnt pathway controls numerous developmental processes such as brain development, limb patterning, bone formation and is also crucial for the angiogenic process.

Wnt proteins signal through a heterodimeric complex of cell-surface receptors: Frizzled (FZD) and co-receptor lipoprotein receptor-related protein (LRP). The main intracellular signal transduction molecule of canonical Wnt signalling is β-catenin, which can function as a membrane-cytoskeleton linker and transcriptional activator.

In the absence of Wnt-ligands, β-catenin is degraded by a multi-protein complex which dissociates upon binding of Wnt ligands to the Frizzled/LRP-receptor complex. Hereafter β-catenin is stabilised, translocates into the nucleus where it interacts with transcription factors from the TCF/LEF family and initiates the transcription of target genes including Myc, CyclinD1 and Axin (Dejana, 2010).

During development ECs express Wnt receptors, ligands and β-catenin, suggesting the possibility of autocrine signalling (Goodwin et al., 2006). Both gain- and loss-of-function mutations of components of the Wnt pathway lead to early embryonic lethality due to defects in vascular organisation and remodelling (Ye et al., 2009). Of special interest is the finding that β-catenin stabilisation in venous ECs leads to upregulation of arterial markers and loss of venous identity, which is characteristic for EC specific Notch GOF. In addition, other findings, including the upregulation of Dll4 upon Wnt induction (Corada et al., 2010) and the formation of a NICD/RBPJ-κ/β-catenin transcription complex (Yamamizu et al., 2010), suggest that Wnt and Notch signalling act in concert. Indeed, it has been found that the "Notch-regulated ankyrin repeat protein" (Nrarp) is induced by Notch signalling in stalk cells, where it limits Notch signalling and promotes canonical Wnt signalling through interaction with LEF1 (Phng et al., 2009).

1.4.6 TGF-β Signalling

The Transforming Growth Factor β (TGF-β) superfamily includes a number of related extracellular molecule families such as TGF-β itself, BMPs, AMH, GDF, Activin/Inhibin, Nodal and others. Upon binding of TGF-β to one of several TGF-β receptor, a receptor-complex is recruited, autophosphorylates and releases an inhibited kinase activity. Subsequently intracellular proteins from the SMAD class get phosphorylated and translocated into the nucleus where they act as transcription factors (Massagué, 2012).

The dominant genetic disorder hereditary haemorrhagic telangiectasia (HHT) is in more than 80% caused by mutations in either endoglin, a TGF-β co-receptor, or activin-receptor-like kinase-1 (ALK1), an EC-specific TGF-β receptor. The disease is characterised by arteriovenous malformations and local haemorrhage. Knockout studies in mice have shown that the lack of TGFβ1, TGF-β receptor-2 (Tgfbr2), Alk1, Alk5, endoglin or Smad5 all lead to severe vascular defects reminiscent of those seen in HHT patients (Pardali et al., 2010).

Virtually all mammalian cells secrete at least one TGF-β isoform and most express TGF-β on their surface. Therefore, it is not surprising that the function of TGF-β appears to be highly context specific, with both pro- (Castañares et al., 2007) and anti- (Wiley et al., 2011) angiogenic effects attributed to this signalling pathway; possibly downstream of different TGF-β type-1 receptors (Goumans et al., 2002). In addition to the pro- and anti-angiogenic effects of TGF-β signalling, it was also found that TGF-β induces the differentiation, proliferation and migration of mural cells, and the vessel fragility observed in mice with deficient TGF-β signalling can partially be attributed to the impaired mural cell development (Pardali et al., 2010).

Recently a study integrated Notch-, VEGF- and TGF-β-signalling within tip/stalk cell specification. It was found that in tip cells Nrp1 inhibits Smad2/3 phosphorylation by Tgf- β /Alk5 and Bmp9/Alk1. In stalk cells Notch activation decreases Nrp1 levels which leads to an increase of phosphorylated Smad2/3 levels which drive stalk cell behaviour by activating Notch

downstream target genes Hey1 and Hey2. However, the exact mechanism how Nrp1 inhibits Smad2/3 signalling remains elusive (Aspalter et al., 2015; Morikawa et al., 2011).

1.4.7 Tie2 and Angiopoietin Signalling

Another class of receptor tyrosine kinases that play an important role in blood vessel remodelling and maturation are the Tyr kinase with Ig and epidermal growth factor homology domains (TIE) receptors. In humans two receptors TIE-1 and TIE-2 (also known as TEK) and three secreted angiopoietin ligands ANG-1, ANG-2 and ANG-4 (mouse orthologue is Ang-3) have been described (Carmeliet and Jain, 2011).

ANG-1 acts as a TIE-2 agonist, whereas ANG-2 induces weaker TIE-2 activation and therefore acts in a context dependent manner as a competitive antagonist (Maisonpierre et al., 1997) or agonist (Daly et al., 2013).

Ang-1 is expressed by mural cells whereas tip cells and tumour vessels express Ang-2 and the Tie receptors. In the presence of ANG-1, TIE-2 is translocated to cell-cell junctions where the ANG-1/TIE-2 complex mediates *in trans* EC quiescence (Saharinen et al., 2008). Furthermore ANG-1 increases pericyte coverage and vessel stabilisation. In contrast, upon angiogenic induction ECs secrete ANG-2 which leads to pericyte dropout and enables EC sprouting (Hammes et al., 2004).

Loss-of-function studies have highlighted that mice deficiencies for Tie-2, Tie-1 and Ang-1 are all embryonic lethal with embryos dying from compromised blood vascular development and integrity (Eklund and Saharinen, 2013). Overexpression of Ang-2 in mouse embryos phenocopied Ang-1 and Tie-2 null embryos, corroborating the antagonistic role of Ang-2 in development (Maisonpierre et al., 1997). Depending on the genetic background Ang-2 deficient mice die within the first two weeks after birth due to lymphatic defects with blood vessel defects mainly limited to the retinal vasculature (Gale et al., 2002).

1.4.8 Transcription Factor Families in Vascular Regulation

As outlined in the paragraphs above, during the formation of the vascular system different populations of progenitor cells have to commit to specific developmental lineages and subsequently form a complex organ that permeates through the whole organism. This process depends on the precise orchestration of many genes that need to be regulated in a temporally and spatially specific manner (De Val and Black, 2009). In the following I will introduce the most important TFs that regulate endothelial gene expression and highlight a few aspects of the complex interplay. A schematic overview of the TFs involved in vascular differentiation is given in Figure 5.

1.4.8.1 Gata Factors

The transcription factors of the Gata family (Gata1 – Gata6) share a dual zinc finger domain that allows them to bind the consensus motif 5'-(A/T)GATA(A/G)-3' (Ko and Engel, 1993). They are involved in the differentiation of diverse tissues and play roles both as oncogenes and tumour-suppressor genes (Zheng and Blobel, 2010).

Of the six Gata factors, Gata2 has been most studied in vascular settings. It is highly expressed in ECs (Lee et al., 1991) and early hematopoietic cells (Tsai and Orkin, 1997). Gata2 deficient embryos die between E9.5 and E11.5 due to impaired primitive and failed definitive haematopoiesis (Tsai et al., 1994). Together with the transcription factor Tal1, Gata2 has later been implicated in the formation of haematopoietic stem cells (see 1.3.1). However, the finding that regulatory elements of several key EC genes contain GATA motifs also suggests an involvement of Gata2 in vessel development. A regulatory role of Gata2 was reported for endomucin, matrix metalloproteinase-2, endothelin-1, Vegfr-2 and VE-cadherin (Han et al., 2003; Kanki et al., 2011; Lee et al., 1991; Park et al., 2013). Intriguingly, a more recent study found that induced, EC-specific loss of Gata2 leads to embryonic death at E16.5 due to defective lymphatic development rather than impaired angiogenesis (Lim et al., 2012). Nevertheless, it is

possible that other Gata factors compensate for Gata2 loss and prevent a visible blood vessel phenotype.

Other Gata factors are expressed in the endothelium and have potential involvement in vascular development, although their actual function still remains to be fully established. For example Gata3 is highly expressed in large human blood vessels and interacts with the ETS factor ELF1 to regulate Tie2/Ang1 signalling (Song et al., 2009), while Gata4 is involved in cardiac development (Schachterle et al., 2012).

1.4.8.2 SOX Factors

The "Sry-related HMG box" (SOX) gene family encodes a large group of transcription factors with approximately 30 members. Sox transcription factors play important roles in many developmental processes such as sex determination and neurogenesis (Kamachi and Kondoh, 2013). The Sox members Sox7, Sox17 and Sox18 form the SoxF group and have been implicated in connecting several signalling pathways during vascular development. SoxF factors show overlapping expression patterns in ECs with primarily arterial expression (Matsui et al., 2006). Only combined loss of SoxF factors in zebrafish results in arterial identity loss and arteriovenous shunts (Cermenati et al., 2008; Herpers et al., 2008; Pendeville et al., 2008). EC-specific KO of Sox17 results in mouse embryonic lethality at mid-gestation due to failed arterial development and vascular remodelling, proposed to be downstream of canonical Wnt and upstream of Dll4/Notch signalling (Corada et al., 2013). In accordance with these results Sacilotto *et al.* demonstrated that arterial expression of Dll4 requires the combinatorial binding of both NICD and SoxF transcription factors to an arterial specific enhancer upstream of the Dll4 locus (Sacilotto et al., 2013).

1.4.8.3 FOX Factors

Forkhead box (FOX) transcription factor proteins are characterised by a conserved DNA-binding domain, that recognises the 5'-TTGTTAC-3' consensus motif and play essential roles during embryonic development. FOXO and FOXC sub-family members have both been implicated in EC generation and blood vessel formation (Park et al., 2013; De Val, 2011). FOXO1 is highly expressed in embryonic ECs and FOXO1 deficient mice die at E10.5 because of defective vascular remodelling (Furuyama et al., 2004; Kume et al., 2001). While FOXO factors generally can act as both transcriptional activators and repressors, the expression of gap junction α-4 (GJA4) and GJA5 (also known as connexin 37 and 40) have been shown to be dependent on FOXO1 (Furuyama et al., 2004).

The members of the forkhead C sub-family FOXC1 and FOXC2 are important for arterial and lymphatic EC specification, and compound FOXC1/2 deletion leads to embryonic death between E9.0 and E11.5 (Kume et al., 2001). Although EC specification is detectable in compound and double KOs, the expression of arterial markers is impaired and *in vitro* studies suggest that FOXC1 and FOXC2 act upstream of Notch in arterial specification (Hayashi and Kume, 2008; Seo et al., 2006). Additionally it was shown that FOXC2 interacts with ETV2 (see 1.4.8.4) to synergistically bind a FOX:ETS composite DNA motif which is found in enhancers of many endothelial genes (De Val et al., 2008).

1.4.8.4 ETS Factors

The E26 transformation-specific (ETS) transcription factors are a family of at least 27 known proteins with more than a dozen members expressed in the endothelium during different stages of vascular development. Almost all known endothelial *cis*-regulatory elements contain multiple ETS binding motifs, highlighting their critical roles in vasculogenesis and angiogenesis (De Val et al., 2008). All ETS factors bind to the 5'-GGA(A/T)-3' consensus sequence through the highly conserved ETS binding domain (Hollenhorst et al., 2004; Liu and Patient, 2008).

The ETS factor friend leukaemia integration 1 (FLI1) is one of the developmentally earliest TFs involved in EC and haematopoietic cell specification. In zebrafish and *Xenopus laevis* embryos a loss of FLI1 function leads to an absence of hemangioblasts, and FLI1 overexpression leads to induction of key EC specification genes such as TAL1, LMO2, GATA2, ETSRP, and VEGFR-2 (Liu et al., 2008). In contrast Fli1$^{-/-}$ mouse embryos die comparatively late around E11.5 due to loss of vascular integrity (Spyropoulos et al., 2000). The differing results may be explained through the redundant function of other ETS factors in mice, especially ERG binds similar target sites (De Val, 2011). Recently it was found that FLI1 forms a feed-forward loop downstream of another ETS factor, ETV2 (also known as ER71). After FLI1 is activated by ETV2 it sustains its own expression and binds to regulatory elements of other ETV2-regulated endothelial genes (Abedin et al., 2014). Unlike with Flk1, loss of ETV2 function in mice leads to embryonic lethality at E9.0 due to the abolishment of EC specification and the resulting complete absence of vascularisation (Lee et al., 2008). Similar results were

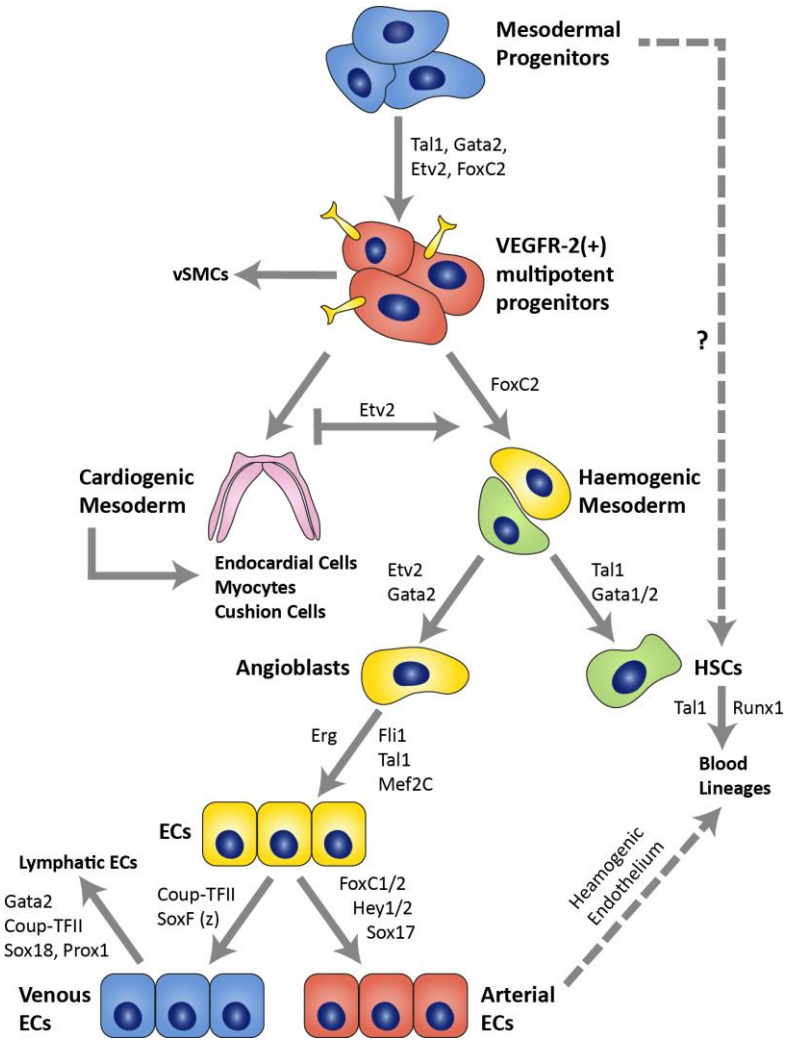

Figure 5 | Progenitor differentiation during early vascular development with transcription factors likely required for individual steps
Transcriptional hierarchies and regulatory networks are not included in the diagram. Speculative models of embryonic haematopoiesis are shown as broken lines. (z): SoxF TFs could only be shown to facilitate venous EC differentiation in zebrafish. For a detailed description of the depicted TFs, please refer to the main text. vSMCs: vascular smooth muscle cells; HSCs: haematopoietic stem cells
After De Val et al., 2011 and Park et al., 2013

obtained in zebrafish with the ETV2 orthologue ETSRP (Sumanas and Lin, 2006). As blood vessels mature, ETV2 is rapidly downregulated, suggesting an early role as master regulator of EC specification downstream of BMP, Notch and Wnt signalling (Lee et al., 2008) and a partial replacement by FLI1 (Abedin et al., 2014). Similar to the GATA factors, ETV2 has been shown to transcriptionally regulate the specification of mesodermal progenitor cells into endothelial or haematopoietic lineages (Ferdous et al., 2009), see also 1.3.2, and recently it was reported that GATA2 actually serves as a co-factor for ETV2 (Shi et al., 2014).

In contrast to ETV2, the ETS factor erythroblast transformation- specific (ERG) is expressed in ECs throughout development, which facilitates the use of ERG expression as an EC-specific nuclear marker. A recent study elucidated that EC-specific KO of Erg, leads to disrupted cranial vessels, disorganised intersomitic vessels and embryonic lethality between E10.5 and E11.5. In the same study induced EC-specific KO in the retina results in reduction of vessel outgrowth, vessel density and sprouting. Mechanistically the authors explain the phenotype trough ERG dependent control of canonical Wnt/β-catenin signalling by regulating FZD4 and VE-cadherin levels (Birdsey et al., 2015).

Other ETS factors such as ETV6 (also known as Tel), ETS1 and ELF1 also display endothelial expression and bind to enhancers of endothelial genes (De Val, 2011). However, their highly variable expression patterns and partially lacking vascular KO-phenotypes make it hard to ascribe specific vascular functions to them (Park et al., 2013).

1.4.8.5 Important Individual Transcription Factors

Coup-TFII

As already introduced, the identity of veins and arteries is established early on before the onset of circulation. An important regulator for venous differentiation is chicken ovalbumin upstream transcription factor II (Coup-TFII) (also known as Nr2f2). Coup-TFII is a nuclear orphan receptor that is expressed in venous and lymphatic ECs from E8.5 until the vasculature is matured (Pereira et al., 1999). Endothelial specific deletion of Coup-TFII in mice results in

embryonic lethality at around E12.0 and is accompanied by a loss of venous identity as evident by expression of the arterial markers Jag1, Notch1, EphrinB2 and Nrp1 in mutant veins (You et al., 2005). Further, EC-specific double knock-out of Coup-TFII and Rbpj-κ partially rescued the loss of venous identity (Srinivasan et al., 2010). These findings suggest a regulation of Notch through Coup-TFII, however no direct transcriptional target of COUP-TFII in veins has been found yet. Coup-TFII is also essential for lymphatic specification and identity, through its interaction with the transcription factor Prox1 (Lee et al., 2009).

Mef2C

Out of the four "myocyte enhancer factor 2" (Mef2) transcription factors that can be found in vertebrates (Mef2A – Mef2D), Mef2C, which is expressed in both ECs and vSMCs, has been specifically implicated in vascular development. In mice, MEF2C can first be detected in yolk sac blood islands and remains in the vasculature throughout development. Mef2c deficient mouse embryos die at around E9.5 with detectable expression of early vascular markers but failed assembly of functional vasculature and cardiac defects (Bi et al., 1999; Lin et al., 1998). This phenotype is reminiscent of Vegfr-2 or Vegf KO mice and indeed later it was found *in vitro* that VEGF activates Mef2C transcription and thereby induces cell migration (Maiti et al., 2008). Mef2C is enriched at the angiogenic sprout during retinal angiogenesis, yet has also been implicated as an inhibitor of angiogenic sprouting downstream of hypoxia (Sturtzel et al., 2014).

1.5 Tal1

The basic-helix-loop-helix (bHLH) transcription factor Tal1 (T-cell acute lymphocytic leukaemia protein 1, also referred to as Scl and Tcl5, is required for both hematopoiesis and correct vascular formation. Tal1 was originally identified in a translocation event between chromosome 1 and 14, which is common in human leukaemia cells. As a result Tal1 mRNA is up-regulated in the leukaemic cells (Begley et al., 1989). Later it was found that Tal1 actively induces leukaemia by repression of the transcriptional activity of the bHLH TFs E47 and HEB (O'Neil et al., 2004). Tal1 is upregulated in 60% of T-cell acute lymphoblastic leukemia (T-ALL) cases and thereby is also an indicator of poor prognosis (Ferrando et al., 2002). In addition, Tal1 is expressed in ECs during tumour associated angiogenesis and even stronger during lymphangiogenesis (Tang et al., 2006).

Similar to many members of the bHLH transcription factor family, TAL1 binds DNA as an obligate heterodimer and forms complexes with members of the E-protein family which recognise the E-box consensus DNA binding motif (CANNTG). Following a common principle in eukaryotic gene regulation, widely expressed TFs like Tal1 interact with numerous other molecules to achieve temporal and spatial specificity of downstream gene expression. A short overview of the most important binding partners of TAL1 is given in Table 1. Dependent on its interaction partners, TAL1 can fulfil activating or repressing functions.

1.5.1 Tal1 Expression

TAL1 protein is detected first at E7.5 in embryonic and extraembryonic mesoderm and later at E8.5 in both endothelial and haematopoietic cells of yolk sac blood islands. Later on Tal1 is expressed in haematopoietic cells within the fetal liver with a peak of expression between E10.5 and 14.5 and in the spleen at E15.5. Expression of Tal1 has been reported in the ECs lining small blood vessels of various organs between E9.5 and 17.5, including ECs making up the dorsal aorta between E10.5 and 13.5, and in lung ECs at E15.5. Further, Tal1 is expressed in primitive

erythrocytes from E9.5 to E11.5, and transiently in the first definitive erythrocytes. In adult mice, TAL1 protein has been detected in erythroblast, macrophages and, neonatally, also in vSMCs of aorta and bladder (Elefanty et al., 1999; Kallianpur et al., 1994).

TAL1 Interaction Partner	Function
E47 (E12/E47; E2A)	VE-Cadherin induction, angiogenesis
LDB1	Bridging molecule
LMO1/2 (RBTN1/2)	Haematopoiesis, angiogenesis
LYL1	Haematopoiesis, angiogenesis
ETO2	Co-repressor, initiates onset of red blood cells
GATA1	E-Box/GATA composite motif recognition, Haematopoiesis
E2-2	Repressor of angiogenesis, inactivated by Tal1 (and Id-1)

Table 1 | Overview of the major binding partners of TAL1
1-3 constitute the "core complex" of active TAL1, additional binding of GATA1 initiates the "pentameric" complex that binds E-Box/GATA composite motifs (Deleuze et al., 2007; Goardon et al., 2006; Pirot et al., 2010; Tanaka et al., 2009, 2010; Wadman et al., 1997)

In summary, it is apparent that expression of Tal1 follows the spatial and temporal patterns of embryonic haematopoiesis outlined before. Moreover, Tal1 expression is also found in parts of the central nervous system like the midbrain and superior colliculi from E11.5.

In addition to its embryonic expression, Tal1 has also been reported to be upregulated in the non-resting adult vasculature. Transient Tal1 expression has been detected during uterine angiogenesis, wound healing, and tumour angiogenesis (Tang et al., 2006). Analysis of adult human tissues widely corroborated the findings in mice. Besides erythroblasts and megakaryocytes, TAL1 is found in vascular ECs of the thymus, spleen and the tonsils. Moreover, smooth muscle cells in the uterus are labelled (Pulford et al., 1995).

The haematopoietic and endothelial expression patterns of Tal1 appear to be evolutionary conserved. It was shown in *Xenopus* embryos that Tal1 is expressed early on in development in the ventral mesoderm and later in ventral blood islands, haematopoietic stem cells and spinal neurons (Mead et al., 1998). Similar results could be obtained in avian embryos. Tal1 is

expressed in both quail and chicken mesodermal precursor cells that, the authors suggest, are most likely angioblasts. Further, Tal1 is also detected in the ECs of the microvasculature and dorsal aorta (Drake et al., 1997). In zebrafish embryos it was initially shown that the orthologue of Tal1 is co-expressed with markers for haematopoietic, endothelial and pronephric duct progenitors in the lateral mesoderm (Gering et al., 1998). More recently, *in vivo* imaging of Tal1-GFP transgenic zebrafish revealed that GFP labels clusters of haematopoietic cells that are associated to the dorsal aorta and GFP positive cells give rise to both primitive macrophages and blood vessels (Zhang and Rodaway, 2007). These clusters are anatomically equivalent to clusters of haematopoietic stem cells that associate with the ventral wall of the dorsal aorta in mice and are considered critical for the concepts of the haemangioblast and hemogenic endothelium (see 1.3.2 and 1.3.3).

1.5.2 Role of Tal1 in Haematopoiesis

Gene ablation studies showed that mice homozygously lacking Tal1 ($Tal1^{-/-}$) display growth and turning retardation at E9.0 and die at E9.5 due to absolute anaemia (Robb et al., 1995; Shivdasani et al., 1995). Other mesodermal derived tissues such as somites, myocardium, and primitive blood vessels are present. Mice heterozygous for Tal1 ($Tal^{+/-}$) do not have observable defects and are born in Mendelian numbers. The $Tal1^{-/-}$ phenotype is reminiscent of mice deficient for Tal1 binding partners Lmo2 (Warren et al., 1994) or Gata1 (Weiss et al., 1994). Later it was found that HSCs deficient for Tal1 do not differentiate into any haematopoietic lineage both in chimeric mice and *in vitro* cell cultures (Porcher et al., 1996; Robb et al., 1996). Taken together these results established Tal1 as an essential, cell-autonomous regulator for the generation of both primitive and definitive hematopoietic cells from mesodermal precursors. In adult mice Tal1 is required for differentiation of haematopoietic progenitors into erythrocytes (Hall et al., 2005) and megakaryocytes (Chagraoui et al., 2011) but seems to be dispensable for the self-renewal of long-term HSCs (Curtis et al., 2004).

Similar to the expression pattern, the functions of Tal1 may be evolutionary conserved as well. Ectopic expression of Tal1 in zebrafish embryos expands haematopoietic and endothelial tissues at the expense of the somitic paraxial mesoderm (Gering et al., 1998), and co-expression of Tal1 binding partner Lmo2 extends this effect to head, heart, pronephros and pronephric duct mesoderm (Gering et al., 2003). A related effect can be observed in *Xenopus* embryos where combined overexpression of Tal1, Lmo2 and Gata1 leads to the expansion of ventral mesoderm derivatives, such as blood, at the expense of dorsal structures such as muscle and notochord. However, forced expression of either factor alone does not result in the described effect, suggesting synergistic action of all three proteins (Mead et al., 2001). By contrast, Morpholino (antisense nucleic acid analogues) mediated knock-down of Tal1 in zebrafish recapitulates the mouse knock-out phenotype and ablates both primitive and definitive haematopoiesis. Due to the fact that the early haematopoietic genes Gata2, Lmo2 and Fli1 are unaffected by Tal1 depletion, it was suggested that mesodermal cells can commit to a haematopoietic fate in the absence of Tal1, but are unable to further differentiate (Dooley et al., 2005; Patterson et al., 2005).

Interestingly, it has been shown in zebrafish (Porcher et al., 1999) and mice (Kassouf et al., 2008) that Tal1 can act as a crucial inducer of haematopoietic progenitor specification and definite haematopoiesis independently of its DNA-binding activity. In contrast, embryonic and adult erythrocyte maturation is mediated through direct DNA binding of Tal1. Mice that are homozygous for a Tal1 mutant with abolished DNA-binding activity ($Tal^{RER/RER}$) contain functional BL-CFCs but still display an embryonic lethality of around 80% due to failed erythrocyte maturation. No vascular abnormalities were described in $Tal1^{RER/RER}$ animals and extracted BL-CFCs formed adherent EC layers *in vitro* (Kassouf et al., 2008). Recent studies have also demonstrated that Tal1 is essential for the establishment of the HE, both by activating transcription factors required for HSC emergence, and by repressing cardiomyogenesis (Van Handel et al., 2012; Schumacher et al., 2013). These results and their possible implications for the role of Tal1 in vascular development are further discussed in 6.2.

1.5.3 Role of Tal1 in Vascular Development

Besides its essential and non-redundant role in primitive and definitive haematopoiesis, Tal1 may also play a role in embryonic blood vessel formation. As already mentioned, the close relationship between the formation of haematopoietic and endothelial cells, for example in blood islands, has led to the suggestion that both lineages derive from a common precursor, either the hemangioblast or HE. Due to its expression pattern and KO phenotype, it was speculated early on that Tal1 was essential for the formation of these progenitors (Elefanty et al., 1999). More recent *in vitro* studies confirmed that Tal1 and Vegfr-2 are both determinants of BF-CFCs. However it is not entirely clear if Tal1 is necessary for the formation of the hemangioblast (Chung et al., 2002) or just for its differentiation into haematopoietic and endothelial lineages (D'Souza et al., 2005). Transcriptionally, Fli1 has been positioned upstream of Tal1 in hemangioblast formation. Loss of Fli1 in zebrafish and *Xenopus* embryos leads to an absence of putative haemangioblasts and a constitutively active Fli1 transgene is sufficient to induce the expression of Tal1 and other key hemangioblast factors, such as Lmo2, Gata2, Etv2, and Vegfr-2 (Liu et al., 2008).

The early lethality of Tal1 KO mice precluded detailed studies on blood vessel development. However, when the hematopoietic defects in $Tal1^{-/-}$ mice were partially rescued by expression of Tal1 under the control of its binding partner Gata1, the mutant embryos still died at E9.5, this time with notable vascular defects, including the lack of vitelline vessels (Visvader et al., 1998). Endothelial specific deletion of Tal1 using Tie2-Cre mice ($Tie2^{Cre/+}$; $Tal1^{flox/flox}$) also resulted in embryonic lethality, although somewhat later at (E13.5-E14.5), with systemic edema and haemorrhage, all potential symptoms of defective vasculature. Although Tie-2 Cre is also expressed in hematopeoitic cells, and the vascular defect in these mice was poorly described, the yolk sac vasculature was reported to be abnormal, despite the fact that the Tie2-mediated deletion do not disrupt the generation or maintenance of the HSC pool (Schlaeger et al., 2005). The finding that Tal1 is also upregulated in the non-resting adult vasculature, for

example during uterine angiogenesis and wound healing, supports the assumption that its role in vascular development might not be confined to embryonic settings (Tang et al., 2006).

As previously discussed, the effects of Tal1 deficiency in mice are largely phenocopied in zebrafish. However, compared to mice, morpholino induced Tal1 knockdown in zebrafish generates earlier and more severe vasculogenic defects including failure of dorsal aorta formation and heavily disorganised intersomitic vessels. Thereby, the unaltered presence of Lmo2 positive cells suggests that not the formation of angioblasts, but the subsequent coalescence into functional vessels is affected by Tal1 knockdown (Dooley et al., 2005; Patterson et al., 2005). A possible explanation for the observed differences could arise from a different epistatic hierarchy of Vegfr-2 and Tal1 in mice and zebrafish. Vegfr-2 expression is lost in Tal1 deficient zebrafish, whereas it appears unaltered in $Tal1^{-/-}$ mouse embryos (Elefanty et al., 1999; Visvader et al., 1998). Moreover, Vegfr-2 expression precedes Tal1 expression in mouse embryos (Chung et al., 2002), while the opposite is true for zebrafish (Liao et al., 1998). Therefore, it is likely that in zebrafish Tal1 adopts an earlier role in vascular development than in mice where VEGF signalling is the prerequisite for any blood vessel formation.

In addition to mouse deletion studies, there is also some *in vitro* evidence suggesting a role for Tal1 in the vasculature. The knock-down of TAL1 or its obligate binding partners E47 and LMO2 in human umbilical vein ECs (HUVECs) leads to reduced expression of VE-cadherin and therefore impairing vessel formation (Deleuze et al., 2007). In a follow-up study the same authors found that in HUVECs and human lymphatic ECs ANG-2 is transcriptionally regulated by a complex consisting of TAL1, LYL1, LMO2 and GATA2 (Deleuze et al., 2012). Conversely, it was demonstrated that overexpression of Tal1 induces cell migration and capillary formation *in vitro* (Lazrak et al., 2004). More recently, reporter gene experiments revealed that Tal1 can bind the bHLH transcription factor E2-2 and reverse its inhibitory function on VEGFR-2 expression. It was demonstrated that unbound E2-2 inhibits endothelial migration, proliferation and network formation. This hints towards a more indirect role of Tal1 in angiogenesis (Tanaka et al., 2009, 2010).

Altogether these data suggest that additional to the closely related field of haematopoiesis, Tal1 could have a novel role in the blood vessel development. However, due to the early lethality of the Tal1$^{-/-}$ embryos, the lack of specificity of Tie2-Cre mediated deletions, and its complex interactions with other factors, this role is far less understood.

1.6 Aims of this Thesis

Part 1: "Role of Tal1 in murine blood vessel development"

The goal of my main project is to elucidate the role of the transcription factor Tal1 (Scl) in blood vessel formation and differentiation in the mouse model. Tal1 depleted mice die at gestational day E9.5 due to failure in haematopoiesis. However, the observation of both major defects in the yolk sac vasculature in $Tal1^{-/-}$ mice even after the hematopoietic defect has been rescued, and vascular defects in $Tie2^{Cre/+}$; $Tal1^{flox/flox}$ mice suggest a role in blood vessel development. Moreover, several vascular genes, including Vegfr-2 and Esam1 are downregulated in $Tal1^{-/-}$ endothelial cells. Although the involvement of Tal1 in embryonic and adult blood formation is well studied, the mechanistic details of its role in blood vessel development remain elusive. Using a variety of recently developed immunohistochemistry (IHC) markers in combination with several new transgenic mouse models, this project aims to investigate how Tal1 influences intra-embryonic vascular development as well as postnatal angiogenesis.

Part 2: "Development of arterial specific Cre mouse models"

My research into the role of Tal1 in the vasculature involves the use of different endothelial-specific Cre and inducible Cre mouse lines. However, the variety of transgenic Cre mice currently available does not cover all aspects of vascular research in a sufficient way. In particular, there is currently no way to specifically ablate gene expression from either the venous or arterial endothelial cell compartment from early on in development. Therefore, I have created a constitutive Cre and an inducible Cre pan-arterial specific mouse line to investigate the possible role of Tal1 in arterial development. Moreover, I have used the Cre lines in combination with the R26R-LacZ reporter line to map the fate of endothelial cells throughout embryonic and postnatal vascular development. To generate arterial specific Cre lines I used the novel Dll4 intron 3 enhancer (Dll4 i3). It was identified by our lab and was shown to direct reporter gene expression specifically to arteries from very early in development.

Chapter 2:

Materials and Methods

2.1 Mouse Work

Mice were bred and housed in ventilated cages in the Functional Genomics Facility in the Henry Wellcome Building of Genomic Medicine Oxford. All animal procedures were supervised under local ethical review and approved by the Home Office of the UK (PPL 30/2783).

2.1.1 Transgenic Mouse Lines

Dll4-in3smP-Cre and Dll4-in3smP-CreERT2 mouse lines were generated on a mixed CBA x C57BL/6 background by Ke Liu (Institute of Ageing and Chronic Diseases, University of Liverpool) via pronuclear injection as previously described in (Ittner and Götz, 2007). In brief, linearised DNA was injected into the pronucleus of zygotes from female donor mice and re-implanted into the oviduct of a pseudo-pregnant surrogate female that had previously been mated with a vasectomised male mouse.

$Tal1^{flox}$ mice were a kind gift from Catherine Porcher (The Weatherall Institute of Molecular Medicine, University of Oxford) and were previously described in (Chagraoui et al., 2011).

$Tal1^{LacZ/WT}$ mice were a kind gift from Bertie Göttgens (Cambridge Stem Cell Institute, University of Cambridge) and were previously described in (Elefanty et al., 1998).

ROSA26R-LacZ mice were a kind gift from George Bou-Gharios (Institute of Ageing and Chronic Diseases, University of Liverpool) and were previously described in (Soriano, 1999).

ROSA26R-EYFP were a kind gift from Xin Lu (Ludwig Institute for Cancer Research, University of Oxford) and were previously described in (Srinivas et al., 2001).

Cdh5(PAC)-CreERT2 (referred to as VE-Cadherin-CreERT2) mice were a kind gift from Ralf Adams (Max Planck Institute for Molecular Biomedicine, Münster) and were previously described in (Sörensen et al., 2009; Wang et al., 2010b).

2.1.2 Breeding Strategies

The different mouse breeding pairs that had to be set up in order to achieve the desired genotype combinations are listed in Table 2.

	Generation			Project Description
	P	F1	F2	
X	VE-CadCreERT2	VE-CadCreERT2 Tal1$^{flox/WT}$	VE-Cad-CreERT2 Tal1$^{flox/flox}$	Inducible, EC-specific KO of Tal1 in mouse embryos, neonatal and adult mice
	Tal1$^{flox/flox}$	Tal1$^{flox/flox}$	-	
X	Tie2-Cre (♂)	Tie2-Cre (♂) Tal1$^{flox/WT}$	Tie2-Cre Tal1$^{flox/flox}$	EC-specific KO of Tal1 in mouse embryos
	Tal1$^{flox/flox}$	Tal1$^{flox/+}$	-	
X	Tal1-LacZ/WT	Tal1-LacZ/WT	-	Expression studies of Tal1
	WT	Tal1-LacZ/WT	-	
X	R26R-LacZ/R26R-LacZ	R26R-LacZ/WT Dll4-in3Cre	R26R-LacZ/R26R-LacZ Dll4-in3Cre	Test of Dll4-in3Cre mouse lines
	Dll4-in3Cre	R26R-LacZ/WT Dll4-in3Cre	-	
X	R26R-EYFP/R26R-EYFP	R26R-EYFP/WT Dll4-in3Cre	R26R-EYFP/R26R-EYFP Dll4-in3Cre	Test of Dll4-in3Cre mouse lines
	Dll4-in3Cre	R26R-EYFP/WT Dll4-in3Cre	-	
X	R26R-LacZ/R26R-LacZ	R26R-LacZ/WT Dll4-in3CreERT2	R26R-LacZ/R26R-LacZ Dll4-in3CreERT2	Test of Dll4-in3CreERT2 mouse lines
	Dll4-in3CreERT2	R26R-LacZ/WT Dll4-in3CreERT2	-	
X	R26R-EYFP/R26R-EYFP	R26R-EYFP/WT Dll4-in3CreERT2	R26R-EYFP/R26R-EYFP Dll4-in3CreERT2	Test of Dll4-in3CreERT2 mouse line
	Dll4-in3CreERT2	R26R-EYFP/WT Dll4-in3CreERT2	-	

Table 2 | Overview of mouse breeding strategies

Note: The Tie2-Cre allele had to be delivered from a male breeding partner (♂) as it has been demonstrated that the Tie2 promoter exhibits activity in the germline, which could lead to the non-tissue specific inactivation of the Tal1 gene in the F2 generation. X: Crossing

2.1.3 Tamoxifen Administration for Cre Induction

In order to create sophisticated animal models that recapitulate human diseases and to study the individual function of genes it is often necessary to modify specific DNA sites *in vivo* in a tissue or time dependent manner.

One of the most versatile genetic modification tools relies on the use of the virus derived site-specific recombinase "causes recombination" (Cre) that catalyses the recombination between two 34 bp DNA recognition sites called "locus of crossing over of bacteriophage P1" (loxP). In order to manipulate the genome of the target organism, two loxP are inserted by homologous recombination. The loxP sites flank an essential exon of a gene that is supposed to be inactivated or flank another site of interest that shall be cut out. The second part of the system requires the Cre recombinase to be active in the cell. Therefore, the mice containing the loxP flanked allele are crossed with other mice that carry the Cre transgene. If cells contain the loxP flanked allele and express Cre at the same time, a recombination event occurs between the loxP sites. Cre cuts the DNA at both loxP sites and the strands are re-joined by DNA ligases. Depending on the orientation of the loxP sites, the result is an inversion or deletion of the interjacent DNA. Because the activity of the engineered Cre transgene is usually controlled by custom regulatory elements, the recombination event can be targeted to a specific cell type or tissue. In contrast to global gene knock-outs, which are often lethal and preclude detailed analysis of phenotypes, this approach circumvents these problems and allows to elucidate gene function in specific settings (Feil et al., 2009).

With the intention of adding temporal specificity to the spatially specific Cre/loxP recombinase system, ligand dependent Cre fusion proteins have been created (Feil et al., 1996). Fusing the Cre with the mutated binding domain of the human oestrogen receptor (ER) renders the recombinase inactive. This so-called CreER recombinase can then be activated by the synthetic oestrogen receptor ligand 4-hydroxytamoxifen (4-OHT), therefore allowing external temporal control of Cre activity. In mice CreER activation can be achieved by administration of tamoxifen which gets metabolised into 4-OHT. The $CreER^{T2}$ recombinase is a modern version of the

inducible Cre. It contains a triple mutation which renders it insensitive towards the natural ER ligand 17β-oestradiol and thereby less sensitive towards spurious activation of the recombinase (Indra et al., 1999). Inducible Cre/loxP systems allow cell lineage tracing and also reduce ectopic Cre expression due to background promoter activity and avoid the cytotoxic effects of prolonged Cre expression (Loonstra et al., 2001).

2.1.3.1 Tamoxifen Induction in Mouse Embryos

Pregnant females received intraperitoneal injections of 200 µl 10 mg/ml tamoxifen (MP Biomedicals, 156738) dissolved in peanut oil (Sigma, P2144) and 10% (v/v) ethanol on two consecutive days (in total 2 mg each day). The first day of injection is regarded as the first day of CreERT2 induction. For injection 1 ml syringes (Appleton Woods, GS572) and sterile 27 gauge × ½″ hypodermic needles (BD Becton Dickinson, 300635) were used. If tamoxifen was injected prior to E14.5, 150 µl 10 mg/ml progesterone (Sigma, P0130) dissolved in peanut oil and 10% (v/v) ethanol was intraperitoneally injected in parallel into the contralateral side of the abdomen. Co-administration of progesterone counteracts the oestrogen agonist side effects of tamoxifen and reduces the chance of foetal abortion.

Induction of Cre recombinase via oral administration (gavage) has been tested as well. For that a 22 gauge curved ball tip feeding needle (18061-22, Fine Science Tools) has been used. In order to calm the mice and induce them to swallow, the feeding needle was pre-coated in 1 g/mL sucrose solution (S7903, Sigma) prior to the procedure. In parallel to intraperitoneal injection of progesterone, 200 µl 10 mg/ml tamoxifen in peanut oil and 10% (v/v) ethanol have been administered on two consecutive days. However, this alternative administration route was not continued because no benefits in terms of transgene activation strength could be detected and stress levels in animals seemed to be elevated compared to intraperitoneal injection.

2.1.3.2 Tamoxifen Induction in Postnatal Mice

For tamoxifen induced Cre activation in the neonatal retina and adult spinotrapezius muscle, mice were injected with tamoxifen as described in (Pitulescu et al., 2010). In brief, neonatal pups were injected with 50 – 500 µl of 1 mg/ml tamoxifen dissolved in 2.5% ethanol (v/v) for three to five consecutive days depending on the age of the animals. For injection of neonatal mice 1 ml syringes (Appleton Woods, GS572) and sterile 30 gauge × ½″ hypodermic needles (BD Becton Dickinson, 304000) were used. Due to the small size of neonatal mice younger than P10, it is very difficult to perform intraperitoneal injections in a reproducible fashion. Therefore, tamoxifen was injected directly into the stomach of the pups, which is easy to identify through the presence of the white milk spot.

For all Cre-induction experiments injected littermates that did not carry the relevant transgene served as negative controls and animals that displayed clear growth retardation were excluded from analysis. In each experiment tamoxifen administrations were carried out the same way and approximately at the same hour of the day (late afternoon) to obtain reproducible results. All solutions were thoroughly vortexed immediately before injection since the oil and ethanol emulsion tends to slowly unmix.

2.1.4 Vaginal Plug Check

In order to perform timed analysis of embryonic development, the first day of pregnancy had to be precisely determined. This was achieved by checking the females in the morning for the presence of vaginal plugs after the male and the female(s) had been placed together on the previous evening. The vaginal plug resembles a whitish mass that can be found between the lips of the vulva and its presence indicates that sexual activity has occurred, albeit this does not guarantee pregnancy. If no plug was found, the male and the females were left together and the procedure was repeated every morning for two consecutive weeks. If a plug was found, the next day was considered the first day of gestation.

2.1.5 Genotyping

For genotyping, genomic DNA was isolated from ear notch biopsies collected from the auricles of living adult mice, *post mortem* from the tip of the tail of pups or *post mortem* from yolk sac biopsies collected from mouse embryos.

Ear, tail and yolk sac biopsies were digested ON at 55 °C in 100-500 µl GNT buffer + 2-10 µl proteinase K (10 mg/ml). After the digestion was finished, samples were vortexed vigorously and incubated 30 min at 95 °C to inactivate proteinase K. Immediately before using the digestion product for PCR (Primer sequences are listed under 2.7.4), the samples were centrifuged in a benchtop centrifuge for 1 min at 16.000 rcf in order to precipitate undissolved tissue residues. 2 µl of clear digestion product (cooled to RT) were used in one PCR reaction, using the Promega GoTaq Green master mix [Promega, M712]. Subsequently 18 µl PCR product were analysed on a 1.5 % [w/v] agarose gel by gel electrophoresis at 200 V.

The composition of GNT buffer can be found in Table 4 and the genotyping PCR mix in Table 3.

PCR cycling conditions are listed in Table 5 and primer combinations together with expected PCR products in the paragraph below.

GNT Buffer (250 ml)	
12.5 ml (50 mM)	1 M KCl
375 µl (1.5 mM)	1 M $MgCl_2$
2.5 ml (10 mM)	1 M Tris pH 8.5
25 mg	Gelatin
1.125 ml	NP-40
1.125 ml	Tween 20
added to 250 ml	ddH_2O

Table 4 | Recipe for GNT Buffer

Genotyping PCR Mix	
10 µl	Go Taq Green [Promega, M712]
2 µl	10 µM Primer 1
2 µl	10 µM Primer 2
2 µl	*Optional* 10 µM Primer 3
2 µl	*Optional* 10 µM Primer 4
2 µl	digested biopsy
added to 20 µl	ddH_2O

Table 3 | Recipe for general genotyping PCR mix

Transgene	Initial Denaturation	Denaturation	Primer Annealing	Elongation	Final Elongation	Hold
LacZ		34 cycles				
	3 min 95 °C	30 s 95 °C	30 s 58 °C	30 s 72 °C	5 min 72 °C	12°C
R26R-LacZ		35 cycles				
	3 min 95 °C	30 s 95 °C	1 min 65 °C	1 min 72 °C	2 min 72 °C	12°C
R26R-EYFP		35 cycles				
	3 min 95 °C	30 s 95 °C	1 min 58 °C	1 min 72 °C	2 min 72 °C	12°C
Cre		29 cycles				
	3 min 95 °C	30 s 95 °C	1 min 60 °C	30 s 72 °C	2 min 72 °C	12°C
Tal1-flox		30 cycles				
	3 min 95 °C	30 s 95 °C	30 s 50 °C	1 min 72 °C	5 min 72 °C	12°C

Table 5 | PCR cycling conditions for genotyping

LacZ:

Primers: #35 (Forward) #36 (Reverse)

Expected PCR Products: Mutant → 308 bp

Assay does not distinguish hemizygous from homozygous samples.

R26R-LacZ:

Primers: #29 (Mutant Reverse) #30 (Common Forward)
#31 (Wild type Reverse)

Expected PCR Products: Mutant → 340 bp
Heterozygote → 340 bp and 650 bp, shadow band at 700 bp
Wild type → 650 bp

Rosa26R-EYFP:

Primers:	#66 (Mutant Forward)	#67 (Common Reverse)
	#68 (Wild type Forward)	
Expected PCR Products:	Mutant	→ 320 bp
	Heterozygote	→ 320 bp and 600 bp, shadow band at 650 bp
	Wild type	→ 600 bp

Generic Cre:

Primers:	#25 (Cre Forward)	#26 (Cre Reverse)
	#27 (Actin Forward)	#28 (Actin Reverse)
Expected PCR Products:	Cre	→ 308 bp
	Actin (control)	→ 754 bp
	Shadow band	→ 600 bp

Assay does not distinguish hemizygous from homozygous samples.

Tal1-flox:

Primers:	#20 (Excised Forward)	#21 (Wild type Forward)
	#22 (Common Reverse)	
Expected PCR Products:	Wild type	→ 220 bp
	Floxed	→ 254 bp
	Heterozygous	→ 220 bp and 254 bp, shadow band at 300 bp
	Excised	→ 500 bp

2.2 Histology

2.2.1 Fixing and X-Gal Staining of Mouse Embryos

Pregnant mice were sacrificed by cervical dislocation, uteri were removed with forceps and immediately rinsed in ice-cold PBS. Subsequently, embryos, yolk sacs, and occasionally other internal organs were dissected and rinsed in PBS. Embryos were then fixed in fixing solution, containing 2% (w/v) PFA and 0.2% (v/v) Glutaraldehyde in PBS, at 4 °C and further processed according to Table 6.

Age	Fixation time	Further processing
E7.5-8.5	10 min	Embryos were rinsed twice in 1x PBS, then incubated in PBS for 30 min at 4 °C.
E8.5-9.0	20 min	
E9.5	30 min	
E10-11.5	60 min	
E12.5	1.5 h	Embryos were rinsed twice in 1x PBS, then incubated 2x30 min in Rinse Solution on rotor at 4 °C, the abdomen was opened for better perfusion, embryos older than E15.5 were skinned.
E13.5	2 h	
E14.5	2.5 h	
E15.5	3 h	
E16.5-17.5	4 h	

Table 6 | Fixation times for embryos of different developmental stages

Embryos were stained in Stain Solution (Table 8) + 1 mg/ml X-Gal in N,N-Dimethylformamide for 24 h or 48 h (depending on staining intensity) at RT while slowly rotating. Subsequently they were rinsed in PBS and then fixed overnight in 4 % PFA at 4 °C. Embryos were then rinsed 2x 10 min in PBS and further processed or stored at 4 °C.

Rinse Solution (500 ml)	
50 ml	10x PBS
1 ml	1 M $MgCl_2$
500 mg	Sodium Deoxycholate
1 ml	NP-40 substitute
added to 500 ml	ddH_2O

Table 7 | Recipe for Rinse Solution

Stain Solution (500 ml)	
500 ml	Rinse Solution
825 mg	Potassium Ferricyanide
920 mg	Potassium

Table 8 | Recipe for Stain Solution

2.2.2 X-Gal Staining of Mouse Retinas

After mouse retinas were dissected as described in section 2.2.8, the retinal cups were fixed in 2% (w/v) PFA in PBS fix solution for 1 h at RT. Subsequently, retinas were rinsed 2x 20 min in rinse solution at RT and then incubated ON in staining solution + 1 mg/ml X-Gal in N,N-Dimethylformamide at 37 °C in a microbiological incubator. 500 µl staining solution were used per retina. The next day the staining buffer was removed and the retinas were washed 2x 5 min in rinse solution and then 3x 5 min in PBS. If required by subsequent co-staining, retinas were post fixed in 4% PFA in PBS for 1 h at RT. Dissected hindbrains and spinotrapezius muscles were X-Gal stained according to the same protocol.

2.2.3 Clearing of X-Gal Stained Embryos and Organs

Due to the increasing size and decreasing transparency of whole-mount preparations of X-Gal stained embryos older than E15.5, only superficial structures can be imaged through stereo microscopy. Deeper structures either appear blurred or are not visible at all. Therefore, I increased the transparency of large whole-mount embryos and dissected organs through a clearing procedure that renders soft tissues translucent. The protocol was adapted from (Schatz et al., 2005). Fixed and X-Gal stained embryos were rinsed 3x10 min in ddH20 and were then incubated in a series of clearing solutions consisting of glycerol and 1% (w/v) KOH. The glycerol ratio of the solutions was increased in steps from 20% to 50%, 80%, and finally 100% glycerol. Specimens were incubated in each solution for 4 days at 37 °C and, after the transparency seemed sufficient, imaged submerged in 100% glycerol under a stereomicroscope. Although the clearing procedure also improves transparency in younger embryos, due to the time consuming protocol, it was only applied when absolutely necessary.

2.2.4 Paraffin Embedding and Sectioning

In order to allow fine sectioning, whole embryos and embryo limbs were embedded in paraffin wax. The procedure outlined below was used to process X-Gal stained and unstained embryos for *in situ* hybridisation, immunohistochemistry or immunofluorescence.

For automated dehydration and paraffin infiltration an Excelsior AS [Thermo Scientific, A82300001] tissue processor was used. The dehydration series consisted of sequential incubation in 70%, 80%, 90%, and 100% (twice) ethanol in water for 1 h each. Dehydrated material was incubated twice in xylene for 1h each and twice in liquid paraffin (at 56 – 58 °C) for 1.5 h each. The paraffin infused samples were then oriented and embedded in paraffin blocks using a HistoStar Embedding Workstation [Thermo Scientific, A81000002] and left on a cold plate to solidify. Sectioning of the blocks was performed on a HM 355S Automatic Microtome [Thermo Scientific, 905200] in collaboration with Sarah De Val and Indrika Ratnayaka (Ludwig Institute for Cancer Research, Oxford). Sections were mounted on standard polysine adhesion slides [VWR, 631-0107].

2.2.5 Processing of Paraffin Embedded Sections

The sectioned samples were deparaffinised and rehydrated through the following solution series: 2x 5 min Histo-clear II [National Diagnostics, HS-202], 2x 3 min 100% ethanol, 1 min 90% ethanol, 1 min 70% ethanol, 1 min in ddH_2O. For counterstaining of X-Gal stained samples, the slides were submerged in Nuclear Fast Red [Electron Microscopy science, Cat 26356-02] for 1 min and then rinsed 30 s in ddH_2O. Dehydration of counterstained samples was achieved through a reverse hydration series: 30 s 70% ethanol, 1 min 90% ethanol, 2x 3 min 100% ethanol, 2x 5 min Histo-clear II. Subsequently, the samples were mounted with Vectashield HardSet mounting medium [Vetorlabs, H-1004] and left to dry for about 1 h at RT.

2.2.6 Immunohistochemistry and Immunofluorescence

Immunohistochemistry (IHC) is the process of localising specific antigens such as proteins or other structures in tissues or individual cells by exploiting the binding of labelled antibodies. Visualisation of bound antibodies can be achieved through enzymatic reactions that yield coloured products, colloidal gold or fluorescent molecules. In the latter case the procedure is referred to as immunofluorescence (IF). As in this thesis both techniques were often used in parallel, they are sometimes jointly referred to as "immunostaining".

2.2.6.1 IHC and IF on Paraffin Embedded Sections

After sections of paraffin-embedded tissues were rehydrated as described earlier, an optional antigen retrieval protocol was performed in order to retrieve epitopes that were masked during PFA fixation. Sections were submerged in one out of three antigen retrieval buffers (Table 9), depending on the primary antibody, and boiled in a commercial pressure cooker for 1 – 5 minutes and afterwards left to cool in the buffer for another 5 min. Subsequently slides were rinsed for 5 min in PBS. If an antibody visualisation technique based on horseradish peroxidase (HRP) was about to be performed, slides were submerged for 30 min in a solution of 1.5% (v/v) H_2O_2 in PBS to block endogenous peroxidase activity. Following this slides were rinsed for 5 min in PBS again. Blocking of unspecific antibody binding sites was accomplished by incubating the slides for 1 h at RT in a blocking solution consisting of 5% (v/v) normal donkey serum [Sigma, D9663] and 0.1% (v/v) TritonX [Sigma, X-100] in PBS.

Primary antibodies (Table 10) were diluted in washing solution (0.1 – 0.5% (v/v) TritonX in PBS, adjusted to pH 7.4) and applied to sections (100 µl per section) which were then covered with cover slips and incubated ON at 4 °C. On the next day the sections were washed in 3x 5 min in washing solution and incubated with secondary antibodies (Table 11) diluted in washing solution for 2 h at RT. After secondary antibody incubation, slides were washed 3x 5 min in washing solution and 2x 5 min in PBS.

If a signal intensity amplification of a biotinylated secondary antibody was required, the Elite ABC kit [Vectorlabs, PK-6100] was now used according to manufacturer's instructions. Subsequently the now horseradish peroxidase conjugated antibodies were visualised by using the DAB peroxidase substrate kit [Vectorlabs, SK-4100] for IHC or the tyramide signal amplification kit [LifeTechnologies, T20922, T20924].

After the detection protocols were finished, the slides were washed 2x 10 min in PBS. DAB stained sections were dehydrated and mounted as described in 2.2.5 and fluorescently labelled sections were mounted using Vectashield anti-fade mounting medium for fluorescence [Vector Laboratories, H-1200] and stored in the dark at 4 °C.

Sodium Citrate Buffer (10 mM) pH 6.0		**EDTA Buffer (1 mM) pH 8.0**		**Tris (10 mM) – EDTA (1 mM) Buffer pH 9.0**	
2.96 g	Tri-sodium citrate	0.37 g	EDTA	1.21 g	Tris
Adjust to pH 6.0	1N HCl	Adjust to pH 8.0	1N Sodium hydroxide	0.37 g	EDTA
0.5 ml	Tween 20	0.5 ml	Tween 20	0.5 ml	Tween 20
1000 ml	ddH_2O	1000 ml	ddH_2O	1000 ml	ddH_2O

Table 9 | Recipe for antigen retrieval (AR) buffers

2.2.6.2 IHC and IF on Whole-Mounted Tissues

After mouse retinas, spinotrapezius muscles, and hindbrains were dissected as described in section 2.2.8**,** 2.2.9**,** and 2.2.10, they were moved to 1.5 ml Eppendorf tubes and fixed in 2 – 4 % PFA in PBS for 1 – 2 h on ice or at RT or ON at 4 °C. The appropriate fixation duration and temperature was dependent on the antibodies that were about to be used in IHC or IF. Usually no general blocking steps were performed on whole-mounted tissues, since no difference in staining specificity could be observed. Incubation with primary and secondary antibodies followed the same protocols described in the section above with the individual washing steps extended to 5 x 10 min.

2.2.7 Antibodies

Primary and secondary antibodies (and lectins) that were used for IHC and IF are listed in Table 10 and Table 11.

Target	Host	Manufacturer	Catalogue No.	Dilution
Beta-Galactosidase	Rabbit	Life Technologies	A11132	1:100
CD31 (PECAM-1)	Rat	Dianova	DIA-310	1:300
Collagen IV	Rabbit	AbD Serotec	2150-1470	1:100
Dll4	Goat	R&D Systems	AF1389	1:50
Endomucin	Rat	Santa Cruz	sc-65495	1:300
EYFP	Rabbit	Abcam	Ab290	1:100
Isolectin B4 - Biotinylated	-	Vector Laboratories	B-1205	1:100
Neurofilament 200	Rabbit	Sigma-Aldrich	N4142	1:200
Neuropilin 1	Rabbit	Abcam	ab81321	1:100
Tal1	Mouse	R&D Systems	MAB3360	1:200
Tal1	Rabbit	Abcam	75739	1:200
VE-Cadherin (CD144)	Rat	Affymetrix	14-1441	1:50
Vegfr-2 (Flk1)	Rat	BD Pharmingen	550549	1:100
α-SMA (ACTA2)	Mouse	Sigma-Aldrich	A5228	1:100

Table 10 | Primary antibodies used in IHC and IF (Isolectin B4 is technically not an antibody)

Target	Host	Conjugate	Manufacturer	Catalogue No.	Dilution
Isolectin B4	-	DyLight 594	Vector Laboratories	DL-1207	1:50
Mouse	Donkey	AlexaFlour 488	Thermo Scientific	A-21202	1:300
Mouse	Donkey	AlexaFlour 546	Thermo Scientific	A-10036	1:300
Rabbit	Donkey	AlexaFlour 488	Thermo Scientific	A-21206	1:300
Rabbit	Donkey	AlexaFlour 546	Thermo Scientific	A-10040	1:300
Rabbit	Goat	Biotin	Vector Laboratories	BA-1000	1:300
Rat	Donkey	AlexaFlour 488	Thermo Scientific	A-21208	1:300
Rat	Donkey	AlexaFlour 594	Thermo Scientific	A-21209	1:300
Rat	Goat	Biotin	Vector Laboratories	BA-9400	1:300
Streptavidin	-	DyLight 488	Vector Laboratories	SA-5488-1	1:300

Table 11 | Secondary antibodies used in IHC and IF (Isolectin and Streptavidin are technically not antibodies)

2.2.8 Preparation of Whole-Retina Flat-Mounts

Due to several factors such as decreased metabolic rate and increased resistance to damage by hypoxia, neonatal mice (younger than P10) are resistant to the effects of CO_2. Therefore, these mice were sacrificed directly by cervical dislocation. The eyes were enucleated with forceps by grabbing and pulling the optic nerve behind the eye. When eyes were prepared from stages younger than P13, eyelids were still closed and therefore cut off before enucleation. The freshly enucleated eyes were fixed in PFA (1%, 2% or 4% [w/v]) dissolved in 1x PBS under various conditions (shaking at ambient temperature, at 4 °C or on ice) and periods of time, depending on the staining protocol used. After fixation the eyes were either directly processed or stored up to 3 month in 100% methanol at -20 °C. The fixed eyeballs were washed twice in 1x PBS and transferred into a PBS-filled Petri dish. To reduce eye pressure the cornea was poked with spring scissors. Beginning from the puncture in the cornea, the eye was opened with radial cuts up to the ora serrata. Using fine forceps, the cornea was removed and retina pigment epithelium (RPE) and sclera were peeled away towards the optic nerve, which was subsequently cut directly beneath the optic disc. Next the lens with the adjacent vitreous was pulled out of the retinal cup. After cleaning the retina from possible remainders of RPE, the hyaloid vessels were carefully removed. Finally the retina was transferred into a 1.5 ml micro centrifuge tube using a clipped off pipette tip. Subsequent to the IHC or IF staining (see 2.2.6.2) the retina was separated into 4-5 sectors by 4-5 cuts perpendicular to the corneal plane. Each of the sectors was pulled to the bottom of a microscopy slide to flatten the retina to a structure resembling a 4-5 foil cloverleaf (see Figure 6). After removing remaining liquid from the slide

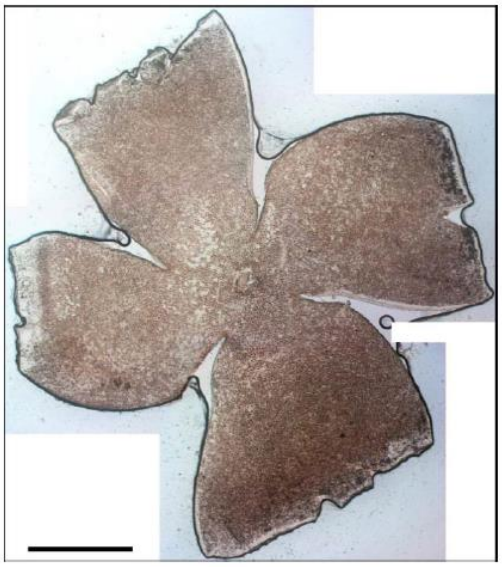

Figure 6 | Transmitted light image of whole-retina flat-mount of P7 WT mouse
Scale bar is 1 mm

the retina was covered with two drops mounting medium [Vector Laboratories, H-1200] and coated carefully with a cover slip.

2.2.9 Preparation of Spinotrapezius Flat-Mounts

Dissection of the spinotrapezius muscle was conducted after the mouse was euthanised by exposure to CO_2 gas in rising concentration. Cervical dislocation was avoided as it can cause damage to the neck area, which complicates dissection. After the death of the animal was confirmed, the back and neck of the animal was shaved with an electric shaver. Dissection had to ensue immediately in order to avoid complications by rigor mortis. Using iris scissors and fine forceps the skin was released from the upper torso and reflected laterally on both sides. Adipose tissue and fascia overlying the muscle was removed using forceps and spring scissors while the dissection site was kept hydrated with PBS. Subsequently blunt dissection was used to separate the spinotrapezius muscle from the underlying fat pad in cranial to caudal direction. In order to finally excise the spinotrapezius muscle, it was first cut transversely at its cranial end then along the spine in sagittal plane. The dissection was repeated for the contralateral spinotrapezius muscle.

After dissection, spinotrapezius muscles were immediately rinsed in ice-cold PBS, then fixed for 1 h at RT in 2 % PFA and washed 2x 10 min in PBS. Subsequently IHC or IF staining was performed as described in 2.2.6.2. Stained spinotrapezius muscles were flat-mounted on microscopy slides on which two layers of electrical tape have been affixed to serve as spacers. The specimen was placed into a rectangular pocket that has been cut out of the electrical tape, covered with one drop of mounting medium [Vector Laboratories, H-1200], coated with a cover slip and finally sealed with nail polish.

2.2.10 Preparation of Embryonic Hindbrain Flat-Mounts

The mouse embryonic hindbrain as a model for angiogenesis has been described previously (Fantin et al., 2013). Dissection of the embryonic hindbrain was conducted directly after dissecting the embryos out of the uterus without prior fixation under a stereomicroscope. The embryo has been submerged in PBS and by squeezing with forceps the head was first separated from the body and then the front of the head was removed. Subsequently the roof-plate overlying the hindbrain was opened, pulled laterally towards both sides of the head and removed by blunt dissection. Then the specimen was turned over and the pial membrane underneath the hindbrain was carefully peeled away, making sure no major blood vessels were left attached to the hindbrain. As a last step the midbrain and the remainders of the spinal cord were removed and the now unfurled hindbrain was transferred into an Eppendorf tube filled with PBS.

Hindbrains were fixed in 2% PFA for 1-4 h (depending on following protocol) at RT in 2 % PFA and subsequently washed 2x 10 min in PBS. IHC and IF staining was performed as described previously. After the staining procedure hindbrains were flat-mounted on microscopy slides in a similar way as spinotrapezius muscle whole-mounts (see 2.2.9).

2.2.11 Quantification of Morphometric Retinal Parameters

From every sacrificed animal only one eye was used for quantification to cover maximal natural variance. Each used mouse was genotyped, either from tail or ear notch biopsies (see 2.1.5). Because the genotype was not obvious from the appearance of the retinas, a blind analysis could be performed where specimens were numbered and associated with the results of the genotyping experiment only after the morphometric analysis had been finished. Data collection and calculation of the parameters were performed with a standard Excel (Microsoft) spread sheet.

The image processing techniques used to quantify the different morphometric parameters are illustrated in Figure 7.

2.2.11.1 Outgrowth Length

To evaluate the outcomes of induced EC-specific Tal1 KO in mice I have quantified the radial outgrowth length of the superficial retinal blood vessel plexus. The length of vascular outgrowth is informative on the velocity of endothelial migration. Therefore 4-6 overlapping confocal fluorescence microscopy pictures (50x magnification) of a retinal flatmount with IB4 stained blood vessels were automatically stitched together in Photoshop CS6 (Adobe), employing the "Photomerge" function. Subsequently, radial length measurements of the distance from the edge of the plexus, to the optical disc were performed with help of the "Ruler Tool" and a custom measurement scale (1058.6 pixel equal 1000 µm). Thereby the measurement line was placed in the middle of each leaf and the blood vessel plexus borderline was defined by eye.

Each leaf of the flatmount was measured separately and the results were averaged for each animal used for statistical analysis. Only animals with three or more measurable leaves were included into the analysis.

2.2.11.2 Vascular Coverage

For measuring the area within the primary retinal blood vessel plexus, which is covered by ECs and to gain insight into the degree of vascular proliferation, the vascular coverage within a 472.33 x 472.33 µm frame square was quantified.

Therefore, four confocal fluorescence microscopy pictures (120x magnification) from four different regions of the angiogenic front were taken, converted into tif files in ZEN (Zeiss) and loaded into Photoshop. With the help of the rectangular marquee tool a 2000 x 2000 (representing 472.33 x 472.33 µm) pixel square was defined in every image. The precise definition of the area of measurement is crucial for ensuring the reproducibility of data. The square was defined randomly but set adjacent below the borderline of the vascular plexus without touching it. Only regions without visible preparation-induced damage like holes or scars in the vasculature were used for quantification. Regions dominated by major blood vessels or regions with elevated macrophage coverage were also avoided. As a next step the brightness and contrast of the image were set to maximum and the vasculature was selected with help of Photoshop's "Magic Wand" tool (3x3 average; Tolerance 60; anti-alias; contiguous). The selection was then refined by excluding all

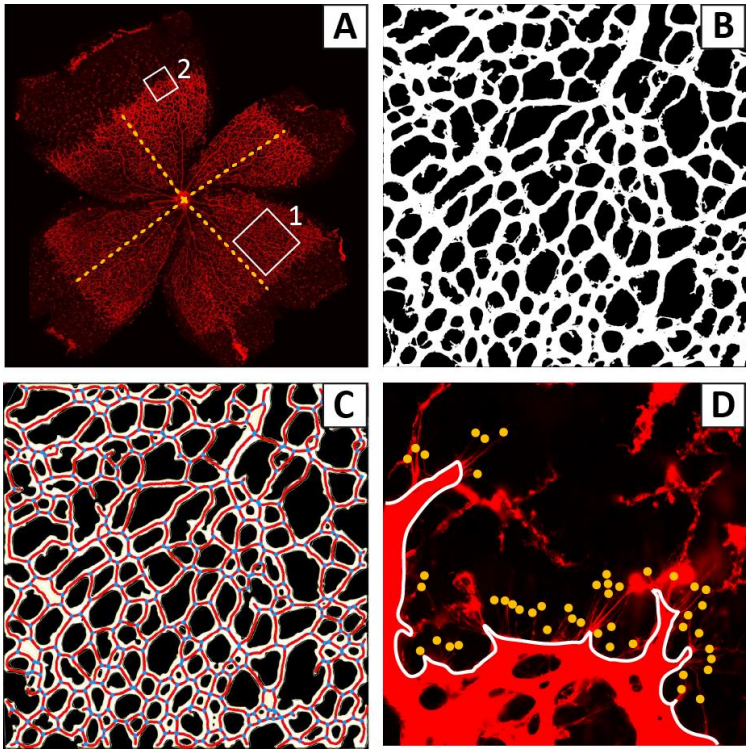

Figure 7 | Quantification of morphometric parameters in P5 mouse retina
Blood vessels were stained with IB4-594
A: Outgrowth length, yellow dashed lines indicate distances from optical disc to angiogenic front, white box #1 and #2 indicate typical measurement sectors for vascular coverage and filopodia; **B:** Vascular coverage, white area indicates area defined as covered with ECs; **C:** Branch points per area, automated skeletisation of EC covered area, branch points are shown as blue dots; **D:** Filopodia at the vascular front, yellow dots indicate single filopodia, white line indicates measured distance of vascular front

unspecifically stained objects like macrophages or dust. Subsequently, the number of selected pixels was measured in the "Histogram" panel (Cash Level: 1) and the resulting vascular density within the square was calculated according to the following equation.

$$Vascular\ Coverage\ (\%) = \ a * \frac{100}{2000^2}$$

a = Number of pixels measured within 2000 x 2000 pixel square

For each retina the average of the four individual measurement results was calculated and used for statistical analysis.

2.2.11.3 Branch Points per Area

In order to quantify a parameter which mirrors the level of complexity of the vascular plexus and is informative about sprouting behaviour, the number of branch points was quantified within the same 472.33 x 472.33 µm square used for measuring the vascular coverage (see previous section).

The vascular coverage selection was further modified in Photoshop by smoothing the selection (radius: 10 pixel) and filling it with 100% white. The image was then converted to greyscale, saved as a jpeg file, and opened in AngioTool 0.5a (Zudaire et al., 2011). In AngioTool a network analysis was run with the following settings: vessel diameter: 40, intensity: 15, no removal of holes or particles.

For each retina the average of the four individual measurement results was calculated and used for statistical analysis.

2.2.11.4 Filopodia at the Vascular Front

For gaining insight into the number of tip cells and thereby the sprouting behaviour I have quantified the tip cells at the vascular front. For that purpose I captured four confocal fluorescence microscopy pictures.

For quantifying filopodia I used four confocal fluorescence microscopy pictures (400x magnification) from the vascular front of each retinal flatmount. The pictures taken were non-overlapping and randomly selected from different regions of the vascular front. For proper visualisation of the thin filopodia, a strong overexposure of the adjacent vasculature was necessary. Using the "Counting Tool" in Photoshop I counted the number of filopodia per picture and measured the length of the measured area in ImageJ 1.50b (Wayne Rasband, National Institutes of Health, USA) with a custom measurement scale (847 pixels equal 100 µm).

2.2.12 Microscopy

The microscopy equipment used for this thesis is listed in Table 12.

Application	Microscope	Camera	Imaging Software
Confocal Fluorescence Microscopy	LSM 710 inverted laser scanning confocal microscope (Zeiss)	Built-in photomultiplier	ZEN system (Zeiss)
Stereo Microscopy	Upright stereo microscope (Leica, M165C	ProGres CF Scan (Jenoptik)	ProgRes CapturePro (Jenoptik)
Transmission Microscopy	Axioplan 2 upright microscope (Zeiss)	ProgRes C5 (Jenoptik)	ProgRes CapturePro (Jenoptik)

Table 12 | Microscopy equipment and their application

2.3 Statistical Analysis

Statistical data analysis and plot design were performed with the help of GraphPad Prism 6.0 (GraphPad Software). For pairwise comparison of means the two-tailed Student's *t*-test for independent samples with previous D'Agostino & Pearson omnibus test for normality was used. All pairwise tested variables displayed a sufficient normal distribution, being a prerequisite for a meaningful *t*-test. Only *p*-values below the significance level $\alpha=0.05$ were considered as statistically significant.

The power calculation for the estimation of the required sample size for the measurement of morphometric retinal parameters after induced, EC specific KO of Tal1 was performed in G*Power 3.1.4 (Faul et al., 2009).

2.4 Image Processing

Image processing was performed in ZEN Black Edition (Zeiss), Photoshop CS6 (Adobe) and ImageJ 1.50b (Wayne Rasband, National Institutes of Health, USA) according to the guidelines described by (Cromey, 2010). False colour rendering of X-Gal staining confocal microscopy images was performed with a custom ImageJ macro that has been developed with the help of Mark Shipman (Ludwig Insitute for Cancer Research, University of Oxford). The macro unmixes the blue component of the X-Gal dye from colour transmission images and generates a new image channel based on this information.

2.5 Illustrations

All figures were created on my own in Adobe Photoshop and Adobe Illustrator. If existing illustrations have served as inspiration, the authors are credited. For vector maps the freeware ApE v2.0.47 (Wayne Davis) was used to determine the proportions of the vector elements.

2.6 Tissue Culture

Primary R26R-LacZ MEFs were kindly provided by George Bou-Gharios (Institute of Ageing and Chronic Diseases, University of Liverpool) and used to test the pCRII-in3smP-Cre and pCRII-in3smP-CreERT2 constructs in tissue culture.

Tissue culture conditions:

Cells were cultured for three passages in supplemented MEF medium (DMEM [high glucose] + 10% FCS + 1x NEAA + 1x Sodium pyruvate + 1x L-Glutamine + 1% Penicillin/Streptomycin) at 37 °C in a humidified incubator with 5% CO_2.

Electroporation:

At ~60% confluency cells were harvested and ~7 x 10^7 cells per sample were electroporated with 2 µg of Maxi-prepped DNA (respective constructs and transfection control pSUPER-Tomato) or ddH_2O as negative control in 100 µl Opti-MEM I medium. Electroporation was performed with a Nucleofector II [Lonza] electroporation system using the program A-023, after which cells were cultured for 24 h in MEF medium.

Tamoxifen Induction:

100 nM (Z)-4-Hydroxytamoxifen [Sigma, H7904] in MEF medium was added to pCRII-in3smP-CreERT2 samples and respective controls and cells were cultured for 48 hours.

X-Gal staining (48 h after electroporation / tamoxifen induction):

Cells were fixed in ice cold 4% PFA/0.5% glutaraldehyde in PBS for 4 minutes in at RT, then rinsed 2x in PBS at RT. They were then stained in stain solution + 1 mg/ml X-Gal in N,N-Dimethylformamide for 24 h at 37 °C in a humidified incubator with 5% CO2, after which the staining solution was removed, cells were rinsed in PBS and photographed under a stereomicroscope.

2.7 Molecular Cloning

For a schematic overview of the designed and generated vectors see Figure 9 and Figure 8.

2.7.1 Construction of Dll4-In3-mP/smP-Beta Gal Vectors

As a first step of assembling the Dll4-in3Cre and Dll4-in3CreERT2 constructs, the Dll4 intron 3 (in3) fragment was amplified from an existing vector template via PCR (Primer: #3/#4), thereby 5' *SacII* and 3' *NotI* restriction sites were added to the fragment. Then the in3 fragment was restriction cloned into the pAUG-βGal reporter vector, using the restriction enzymes *SacII* [NEB, R0157S] and *NotI* [NEB, R0189L]. Thereby, the pAUG-in3- βGal intermediate vector was created.

Next, I amplified the putative Dll4 long (mP) and short (smP) promoter fragments by PCR (Primer: #1/#2/#11) from a BAC containing the murine Dll4 locus, thereby adding 5' *SpeI* and 3' *BamHI* restriction sides. Subsequently, both fragments were sub-cloned into the pCRII-TOPO vector by TOPO-TA cloning, using the pCRII-TOPO Cloning Kit [Life Technologies, KNM4600-01]. Thereby, the intermediate pCRII-mP and pCRII-smP vectors were generated.

Finally, both the smP and mP fragments were restriction cloned into the pAUG-in3-βGal vector, using the restriction enzymes *BamHI-HF* [NEB, R3136L] and *SpeI* [NEB, R0133L], resulting in the pAUG-in3-mP-βGal and pAUG-in3-smP-βGal vectors. These vectors were linearized and used for pronuclear injection.

2.7.2 Construction of Dll4-in3-smP-Cre/CreERT2 Vectors

In order to generate the Dll4-in3-smP-Cre/CreERT2 vectors, the Cre-ORF/polyA fragment was amplified from the pCAG-Cre vector and the CreERT2-ORF/polyA fragment was amplified from the pCAG-CreERT2 (both kindly provided by Rasmus Freter) vector via PCR (Primer: #32/#33),

thereby adding 5' *XmaI* and 3' *SalI* restriction sides. Subsequently, the fragments were sub-cloned into the pCRII-TOPO vector by TOPO-TA cloning. Thereby, the intermediate pCRII-Cre and pCRII-CreERT2 vectors were created.

As a final step, the Cre-ORF/polyA and CreERT2-ORF/polyA fragments were cloned into the pAUG-in3-smP-βGal vector by restriction cloning, using the restriction enzymes *SacI* [NEB, R0156L] and *XmaI* [NEB, R0180L], thereby replacing the β-Galactosidase reporter gene. This resulted in the generation of the pAUG-in3-smP-Cre and pAUG-in3-smP-CreERT2 vectors that were linearized and used for pronuclear injection.

2.7.3 Cloning Techniques

PCR

For amplifying fragments for cloning the Expand High Fidelity [Roche, 11732650001] polymerase was used according to manufacturer's instructions.

TOPO-Cloning

TOPO-TA cloning is based on the principle that a topoisomerase, which is conjugated to the TOPO vector, ligates 3' adenine overhangs of a PCR products to unpaired 5' thymine residues on the linear TOPO vector. The result of the TOPO reaction is a circular "Entry" vector. TOPO cloning was performed according to manufacturer's instructions, with the exception that 0.5 µl TOPO vector were used instead of 2 µl. Usually 4 µl PCR product were used for one TOPO reaction.

Restriction Digest

Restriction digest was carried out following the standard (double) digest protocol from NEB. For restriction cloning, both vector and insert were run on an agarose gel and bands of appropriate size were excised and purified using the QIAquick gel extraction kit (Qiagen, 28704). Subsequently, vector and insert were ligated using T4 DNA ligase (NEB, M0202) for 1 h at 37 °C and at molar vector/insert ratio of 1:3.

Transformation

Following restriction or TOPO cloning, the resulting vectors were used for bacterial transformation. For this, 2 µl of the reaction were carefully mixed with 50 µl chemically competent *E. coli* on ice and incubated for a further 30 minutes. The mixture was heat-shocked in a water bath at 42 ºC for 30 s and immediately cooled on ice. 250 µl S.O.C medium were added to the mixture which was then incubated for 1 h at 37ºC in a shaking incubator. Afterwards, 20 – 200 µl bacteria were plated on pre-warmed LB agar plates (1% Tryptone, 0.5% Yeast Extract, 1.0% Sodium Chloride, 1.5% agar) containing the appropriate antibiotic to select for successfully transformed bacteria. Plates were incubated at 37ºC overnight, after which single bacterial colonies were picked and cultured in a shaking incubator at 37ºC overnight in 4 ml LB medium (1% Tryptone, 0.5% Yeast Extract, 1.0% Sodium Chloride) containing the appropriate antibiotic.

Plasmid DNA Extraction

Extractions of plasmid DNA from bacterial cultures (4 – 100 ml) through mini-, midi- and maxi-preps were performed according to the manufacturer's instructions (Qiagen, 27106). Concentration of purified plasmid DNA was measured using a Nanodrop spectrophotometer followed by restriction digest and agarose gel electrophoresis on 1% (w/v) agarose gels in TBE, ran at 200V, to check correct insertion and orientation of the PCR product into the vector prior to sequencing.

Sequencing

After every cloning step involving restriction or TOPO cloning or PCR the DNA sequence fidelity and correct fragment orientation was validated by automated Sanger sequencing. All sequencing primers are listed under 2.7.5.

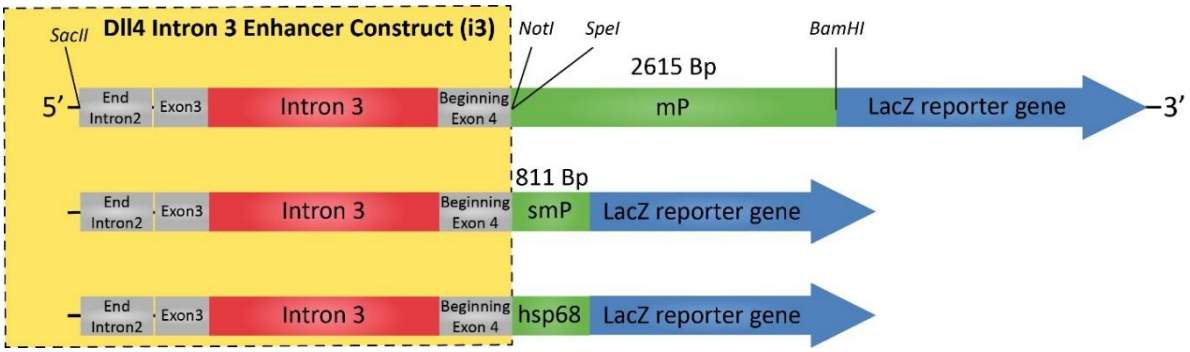

Figure 9 | Overview of Dll4 minimal promoter/enhancer reporter constructs
Hsp68 promoter containing plasmid was designed and generated by Natalia Sacilotto; Vector backbone is pAUG
mP-minimal promoter; smP – short minimal promoter

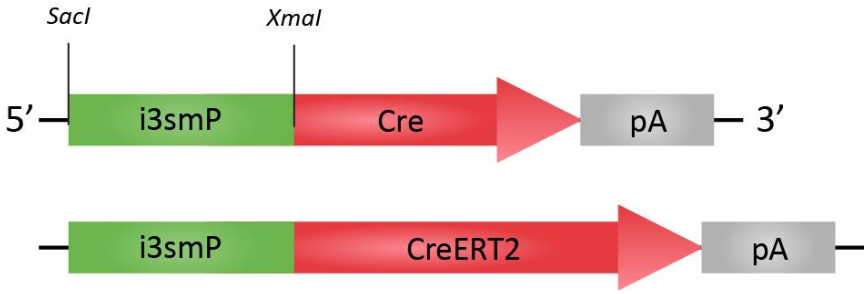

Figure 8 | Overview of the generated Dll4 minimal promoter/enhancer Cre and CreERT2 constructs
pA- polyadenylation sequence

2.7.4 Sequence of Dll4-In3smP Promoter/Enhancer Construct

CTGCTGATATCGCTATCTCTAATGTCCCCCACCCCCCCTTTTGCTTCCCAGGGAACCTTCTCACTC
AACATCCAAGCTTGGCACACACCGGGAGACGACCTGCGGCCAGGTGAGTATCTAACTTCTCGGCCA
CAGGGGGGCGACATCACACAGCGCCGAAAGAGTTAACCAGTTATAGGCGGGGGTGGGGGTTGGGGA
CGCAGGCTTGGGGGGTGGGGGCCAGGACGCTTAGCTTGGCCGGAGCTGCGCCCCGCGCTGGACGCT
CGGATTCCGCTCGCTGCCTGGACTCAGAGCACAATTGCGTTTCCTGCGGGTTATTTTTGGCGTGGG
AACGCGGGGAGCACGGCGGTGAGAAAGGCCGAGGCTGCCAGCGCCGCTGACGGGCCTCTTCCTGTA
TTTTACACCTTTTGCGAATTCCGCTCCTTTGGAAAGGGAATAATGGCTTTGGGATGTTGTTCTGAC
ACAGAGGAAAAGGATATTTCACCAGCACAACAATTCTCACTTTGAAAAGGAAAAAGAAAAACCATT
ACCTACGTCTAGAACAGAACCCCTTGCTCCCAGTTCTCGAACCAGAAAACTTCCCCCTTTAAATTT
TTTCTTTTTTTCCATTTTGACCTCTTTTCCTCTTTCCCCTCCGTATCTGCCTCCACAACCCTAGGA
TATCTTAACATCCGTCCATTGTACCCTTTTTTGAATGCTATCAAGCCCCCTGCACATGCACACACC
CAGGGAGACTAAGTAGCAAGATTCTGGGACCCTCTGGCCTGTGCTTACTTGCAGGTAGAGTTAATC
TAGATAATTAGAGTGTGAACTGACCACCATAGTCACAACTAAAGAGAGAGTTGGCAGCAGTCAACT
CTCTCTGAATCAGGTTGGCTTTCTGAATCAGGTTCTCTGACCAAAGCCTCTTTCTGCAGAGACTTC
GCCAGGAAACTCTGCGGCCGCTCTAGAACTAGTCTGGAAAGGAAAGGGAGATCCAAATCCCCTGGT
CCTGCTTTTTGCTTTCCTAGTTTAAGCTTTCCCCACCTGCTAGAGGACTGTAGGTATCTAATGCCT
GGATCAGGTGCACCGCCTACGGGGACCCCTTAGAGTTTCCACCCCCTGGACCATTCGGGAACCACC
TCACCTCCCGCCGCATCACTGGGCTACCCTCCTATCCTCTGGTGGCGAGGGTCTCAGCCTTTAAGC
AGACGATCTCTAAGGACTGCTCGCCGGGCACGCGCAGAGCTGGAAGCCCAGAAGTTGGAAGAGGGG
CGGGGACCTGCGCCCTACTGGCTGGCTGACAGGGGGAGCGGCGGGGGCGGAGGCCCCCTCCGGTGG
GTGCTGGGACTGTAGCCACTAGAGGCCTGGAGGGGAGGGGAGAGTGACCGTGAGTCTGTCTGACTG
ACAGGCTGCGAAGAGCAGCCAATATATATAAGAAAGGCTCTGGAGCAAGCAGGTTTCAGTAGCGGC
GCTGCTCGCAGGCTAGGAACCCGAGGCCAAGAGCTGCAGCCAAAGTCACTTGGGTGCAGTGTACTC
CCTCACTAGCCCGCTCGAGACCCTAGGATTTGCTCCAGGACACGTACTTAGAGCAGCCACCGCCCA
GTCGCCCTCACCTGGATTACCTACCGAGGCATCGAGCAGCGGAGTTTTTGAGAAGGCGACAAGGGA
GCAGCGTCCCGAGGGGAATCAGCTTTTCAGGAACTCGGCTGGCAGACGGGACTTGCGGGAGAGCGA
CATCCCTAACAAGCAGATTCGGAGTCCCGGAGTGGAGAGGACACCCCAAGGG

Dll4 Intron 3 Enhancer (i3) **Multiple Cloning Site** **Dll4 minimal promoter (smP)**

Putative transcriptional start side (TSS)

2.7.5 Primers

Primer ID	Sequence	Description
1	CCTAGACTAGTGGGTAAAGATTGATACCAG	Cloning Dll4-mP promoter
2	ATAATGGATCCCCCTTGGGGTGTCCTCTC	Cloning Dll4-mP promoter
3	ATATCCGCGGCTGCTGATATCGCTATCTC	Cloning Dll4-in3 enhancer
4	ATATGCGGCCGCAGAGTTTCCTGGCGAAGT	Cloning Dll4-in3 enhancer
5	GCTATGACCATGATTACGCCAAG	Seq. of Dll4 intron 3 fragment
6	CAAGGGGTTCTGTTCTAGACGTA	Seq. of Dll4 intron 3 fragment
7	CACCTTTTGCGAATTCCG	Seq. of Dll4 intron 3 fragment
8	GCTTTAGCAGGCTCTTTCGAT	Seq. of Dll4 intron 3 fragment
9	TCGGCTTGCCCATAACCTAC	Seq. of Dll4-mP fragment
10	AGTGGCCCAAGGAAATTCTG	Seq. of Dll4-mP fragment
11	AGTAGACTAGTCTGGAAAGGAAAGGGAGATC	Cloning Dll4-smP promoter
12	AGATCGCACTCCAGCCAGCT	Seq. of pAUG-mP/smP-BetaGal
16	GACGGTGGGAGAATGTTAATC	Seq. of pCRII-Cre
17	TACTGACCAACCTGGCAGAC	Seq. of pCRII-CreERT2
18	GCTCTACTTCATCGCATTCC	Seq. of pCRII-CreERT2
19	CTAGGATTTGCTCCAGGACAC	Seq. of pAUG-i3mP-Cre
20	TGGACCCAGACATTACTAGAA	Genotype Tal1-floxed
21	CAAACAGAGTGAAGTAGTAGG	Genotype Tal1-floxed
22	TTGAACAGAAGCTGCCACAAA	Genotype Tal1-floxed
25	CATTTGGGCCAGCTAAACAT	Genotype Generic Cre
26	ATTCTCCCACCGTCAGTACG	Genotype Generic Cre
27	GGTGTCATGGTAGGTATGGGT	Genotype Generic Cre
28	CGCACAATCTCACGTTCAG	Genotype Generic Cre
30	GCGAAGAGTTTGTCCTCAACC	Genotype Rosa26R-LacZ
31	AAAGTCGCTCTGAGTTGTTAT	Genotype Rosa26R-LacZ
32	GGAGCGGGAGAAATGGATATG	Genotype Rosa26R-LacZ
32	AGTTCACCCGGGATGTCCAATTTACTGACCGT	Cloning Cre and CreERT2
33	GAATCTGTCGACAATACGCAAACCGCCTCTC	Cloning Cre and CreERT2
35	GTCGTTTTACAACGTCGTGACT	Genotype General LacZ
36	GATGGGCGCATCGTAACCGTGC	Genotype General LacZ
37	GCAGGCAGCTCACAAAGGAACAAT	Genotype VE-Cadherin-Cre
38	TGTCCTTGCTGAGTGACAGTGGAA	Genotype VE-Cadherin-Cre
39	ATCACTCGTTGCATCGACCGGTAA	Genotype VE-Cadherin-Cre

Chapter 3:

Role of Tal1 in Postnatal Angiogenesis

3.1 Tal1 in the Mouse Retina

As outlined in the introduction (see 1.5.3), several lines of evidence suggest a role for Tal1 in embryonic vascularisation. TAL1 protein and mRNA have been detected in vascular ECs both during embryogenesis and in adulthood and endothelial specific depletion of Tal1 leads to severe vascular defects and embryonic lethality in mice and fish (Drake et al., 1997; Kallianpur et al., 1994; Schlaeger et al., 2005). Moreover, *in vitro* experiments suggest a role of Tal1 in EC migration and proliferation, possibly due to interaction with the VEGF pathway (Deleuze et al., 2007, 2012; Lazrak et al., 2004).

However, the mechanistic details remain elusive and very little is known about possible involvement of Tal1 in postnatal blood vessel development, since the EC-specific Tie2-Cre dependent KO of Tal1 results in embryonic lethality at around E13.5 and precludes further analysis. Postnatal expression of Tal1 during angiogenesis was reported during wound healing, uterine angiogenesis and in tumour vasculature (Tang et al., 2006), leading to the supposition that Tal1 may play an important role in postnatal angiogenesis. However, it is difficult to gain substantial insight into the function of a gene on the basis of expression studies alone and no functional studies in the postnatal vasculature have been performed yet. Moreover, the highly diverse nature of the aforementioned vascular beds and the irregular structure of their blood vessel networks complicate meaningful comparisons in KO studies. To investigate Tal1 in postnatal angiogenesis apart from these systems I chose the mouse retina as a suitable model (see Figure 10) for analysing both vascular Tal1 expression patterns and the effects of induced, EC-specific Tal1 deficiency on the vasculature.

3.1.1 The Mouse Retina as a Model for Angiogenesis

As in all rodents, the development of the mouse retinal vasculature occurs postnatally and in a highly stereotypic manner, meaning that arteries, veins, and capillaries sprout and mature in regular patterns. This developing vasculature is not covered by many layers of tissue and

therefore easily accessible for immunostaining and microscopy. Additionally, the morphological structure of the growing and maturing retinal vascular tree allows simultaneous imaging of different stages of vascular development in three dimensions. These characteristics allow a detailed quantitative analysis of genetic or chemical interference with retinal angiogenesis (Stahl et al., 2010). On these grounds I hoped to discern even subtle effects of Tal1 deficiency on angiogenesis. In the following I will briefly describe the development of the retinal vasculature, since an understanding of the chronology of angiogenic processes is necessary to interpret the effects of temporal genetic interference.

3.1.2 Development of the Retinal Vascular System

Due to the very energy consuming visual process, the retina is the vertebrate tissue with one of the highest demand for oxygen per weight (Warburg, 1927). The oxygen supply is covered by two different vascular networks: The choroidal vasculature is localised between retina pigment epithelium (RPE) and sclera, supplying the RPE and the photoreceptor layer. The inner portion of the retina with the neuronal network is nourished by the retinal vasculature, which is used as a model system for angiogenesis. The retinal vascular network is comprised of three parallel and interconnected layers. Within the superficial or primary layer, the primary arteries and veins extend radially from the origin of the optic nerve at the optical disc to the retinal periphery. Initially the retina is avascular and ECs enter the eye through the optical disc and form sprouts which grow out above the vitreal surface of the developing retina and form the superficial plexus. At around postnatal day 9 (P9) the superficial plexus reaches the retinal periphery. From this superficial vascular network, vertical sprouts emerge and penetrate the retina. Subsequently, horizontal sprouting occurs also in those deeper layers and the intra-retinal capillary beds of the tertiary and later the secondary plexus are formed. After several subsequent steps of outgrowth of the secondary and tertiary plexus and extensive remodelling, the mouse retina is completely vascularised at ~P25 (Ye et al., 2010). The development of the retinal vasculature is schematically illustrated in Figure 10.

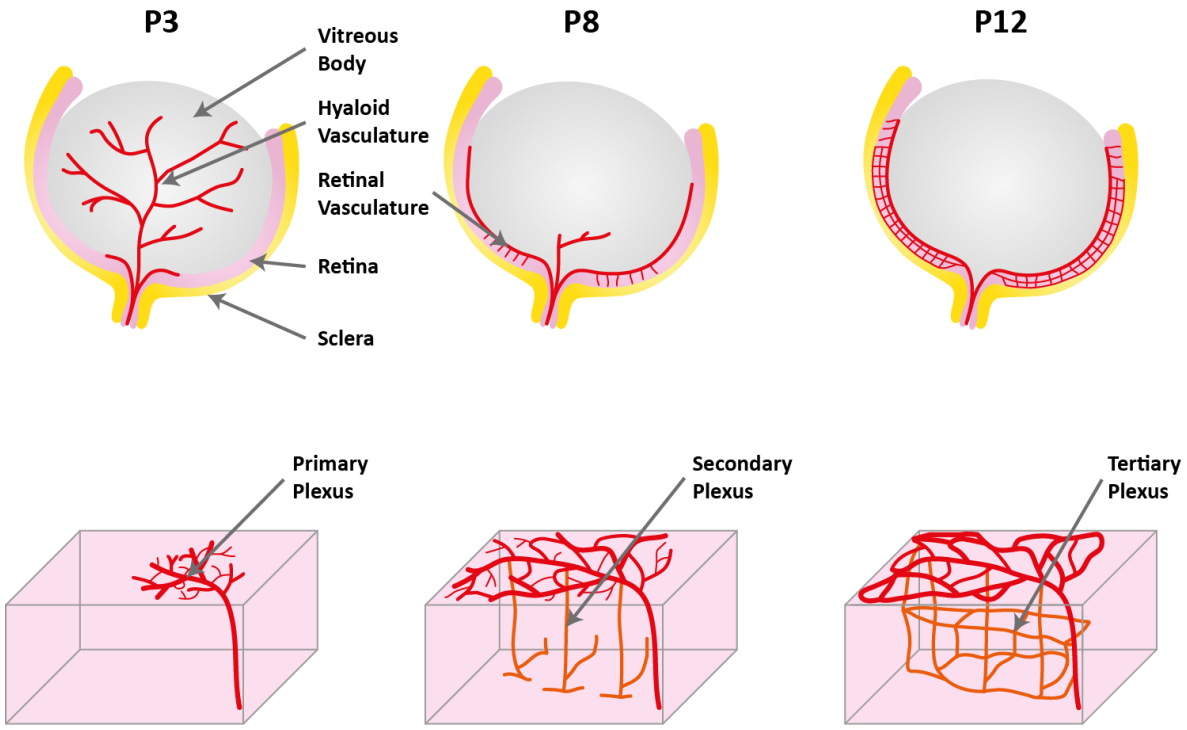

Figure 10 | Illustration of the development of the murine retinal vasculature
Three successive stages of retinal vascularisation and hyaloid vessel regression in mice are shown from left to right. Endothelial sprouts enter the eye, migrate towards the periphery on the surface of the retina and form the primary plexus. Subsequently sprouts turn perpendicularly downwards and form the deeper layers. Branching and remodelling occurs in all layers which get interconnected to form a functional vascular network.
Adapted from (Ye et al., 2010)

3.2 Expression of Tal1 in the Mouse Retina

In order to investigate a possible role of Tal1 in postnatal angiogenesis, I chose the mouse retina as a model system for immunostaining against TAL1 protein and Isolectin-B4 (IB4) as a blood vessel marker. IB4 is a lectin that specifically binds terminal α-galactosyl residues expressed by various cell types and especially in the basement membrane of ECs (Laitinen, 1987).

Unfortunately, the antibodies used in the original expression studies (Drake et al., 1997; Kallianpur et al., 1994; Tang et al., 2006) were custom made and not available to me. Therefore, I have tested a set of commercially available antibodies. I have based my selection of antibodies on the availability of IHC and IF related references and tried to exclude antibodies from the analysis that bind to the same epitope as an already tested antibody. However, commercial antibody distributors do not always disclose detailed information about the epitope which the antibody binds to. Of the four antibodies I have tested on P6 retinas, only two produced a detectable IF signal which was not present in negative controls.

In addition to the immunostaining approach I have also made use of the $Tal1^{lacZ/WT}$ reporter gene mouse line (see 4.1 for a detailed description of this mouse model). I have performed X-Gal staining on the retinal vasculature of $Tal1^{lacZ/WT}$ animals at P5, P8 and P10. However, I could not detect reporter gene activity in any case. Similarly, a staining approach by *in situ* hybridisation on retina whole-mounts was not successful due to extremely high background signals.

Antibody A (R&D, MAB-3360)

With antibody A I detected no TAL1 in the sprouting (at the vascular front and vertical sprouts), remodelling (area tailing the vascular front) or maturing (central areas of vascular plexus) vasculature at P7 (Figure 11, A-H). Furthermore, TAL1 was not detectable in the mature vasculature of P20 retinas (data not shown). Instead TAL1 antibody A stained tubular structures on the vitreal surface of the retina, proceeding radially from the edge towards the optical disc. Moreover, individual stains positive for TAL1 antibody, not associated with the

vasculature were visible all over the retinal plexus. These TAL1 positive speckles most likely represent macrophages, megakaryocytes or other lymphocytes. Lymphocytes in general are prone to give false positive immunostaining results due to their possession of immunoglobins. This phenomenon may be enhanced through the fact that the TAL1 antibody was generated in mouse. The cells co-stained for IB4 and TAL1 are most likely macrophages, as IB4 is known to label macrophage subpopulations and TAL1 protein already has been described in macrophages (Kallianpur et al., 1994). I suspected the TAL1 positive tubular structures to be retinal ganglion axons which transmit the optical information generated in the photoreceptor layer through the optical nerve. To test this hypothesis I co-stained against the heavy chain subunit (200 kDa) of neurofilament (NF), a specific marker for neuronal projections and against TAL1. TAL1 co-located with the retinal ganglion axons, whereas the staining intensity decreased from the optical disc towards the edge of the retina. Individual nerve fibres were stained completely for TAL1 and in comparison with NF, which marked the axon cytoskeleton, the staining appeared to be located closer to the surface of the axon. Deeper neuronal networks, which innervate horizontal, amacrin and bipolar cells, were not TAL1 positive.

Antibody B (Abcam, 75739)

Staining with antibody B resulted in a very faint signal that required several signal amplification techniques (Figure 11, J-I). However, the staining co-localised with ECs in small capillaries within the periphery of the vascular plexus. The elongated shape of the stained foci within the vessels is characteristic for EC nuclei, which corroborates the assumption that antibody B detects TAL1 in the vasculature. The staining pattern within the vasculature appeared random and only a minority of the vascular plexus could be stained. TAL1 protein could not be detected neither in major vessels nor at the angiogenic front.

The results of the immunostaining against TAL1 in the retina are summarised in Figure 11.

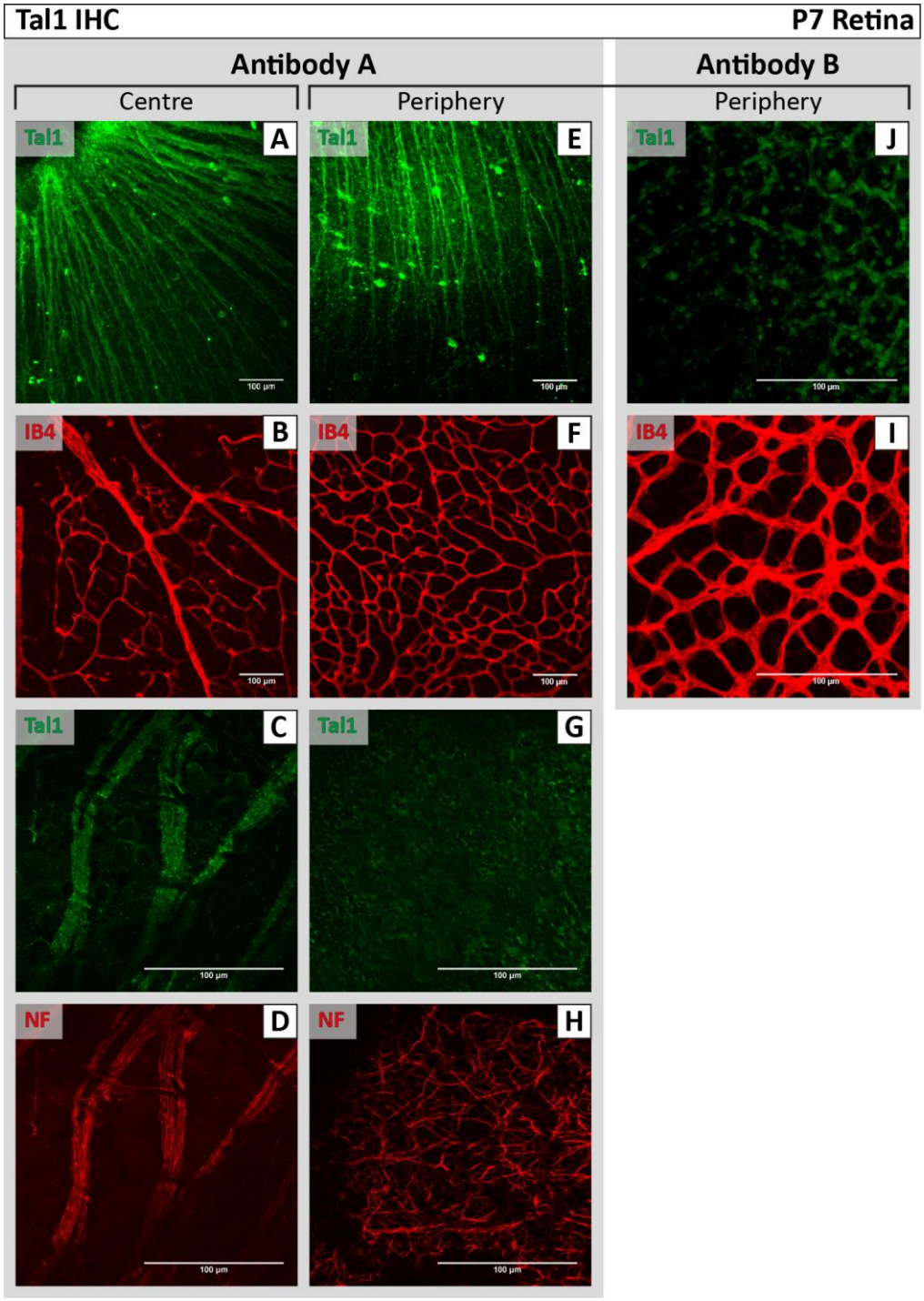

Figure 11 | Immunostaining for TAL1 in P7 retina with two different antibodies (A and B)
A/B: Central vasculature, TAL1 antibody A staining in long tubular structures that radially extend from the optical disc to the periphery of the retina and do not co-localise with vascular marker IB4
C/D: Magnified view on tubular structures that co-localise with neuronal marker neurofilament (NF)
E/F: TAL1 staining in tubular structures fades out towards the periphery
G/H: TAL1 staining is not present in the deeper neuronal layers of the retina
I/J: Diffuse staining of anti-TAL1 antibody B that partially co-localises with ECs of the peripheral retina capillary system

3.3 Endothelial Specific Ablation of Tal1 in the Retina

Although the results of the immunohistochemical and reporter gene analysis of Tal1 expression in the retina remained ambiguous, I could not rule out that TAL1 protein is present in the vasculature of the postnatal retina and influences angiogenesis. Transcription factors like Tal1 often tend to be expressed at very low levels (Beck et al., 2014) and in addition are hard to detect through immunostaining due to their location inside the nucleus that makes it harder for antibodies to reach their epitopes. Possible explanations why analysis of the $Tal1^{lacZ/WT}$ reporter gene knock-in mouse line did not reveal any Tal1 expression are discussed in detail in 3.4.1. Most likely, the single LacZ allele of the knock-in mice produces a weaker signal than the numerous integrated copies of enhancer-reporter constructs. Indeed, the vascular reporter gene expression in the original $Tal1^{lacZ/WT}$ study (Elefanty et al., 1999) appears much weaker to the results of later studies that used various Tal1 enhancer constructs (Göttgens et al., 2010; Sinclair et al., 1999). Only an induced KO of Tal1 can prove or disprove the functional involvement of Tal1 in postnatal angiogenesis. Therefore, I decided to deplete Tal1 in the endothelium of neonatal mice and analyse the effects.

Schlaeger *et al*. made use of the Tie2-Cre mouse line to specifically delete Tal1 in the endothelium. However, the analysis was limited to embryonic vascular development because Tie2-Cre/$Tal^{flox/flox}$ mice die at ~E13.5, at least partly due to hematopoietic defects (Schlaeger et al., 2005). Moreover, although strong vascular defects are referenced as results in this study, they remain poorly described and very little data supporting that claim is shown. No follow-up study on that matter has been published so far.

In the Tie2-Cre mouse line the recombinase activity is controlled by a fusion construct comprised of the Tie2 promoter and the Tie2 intron 1 enhancer (Kisanuki et al., 2001). In the publication which first presented the Tie2-Cre transgenic mouse line, the authors stress that Cre expression is observed in E8.5 yolk sac blood islands but not in haematopoietic cells. However, at E11.5 they detect circulating cells that are positive for Tie2-Cre dependent LacZ reporter gene activity. Further, this analysis was limited to X-Gal staining of embryos that carry

LacZ-reporter transgenes and no further IHC or cell sorting analysis is performed. Given the close relationship of endothelial and haematopoietic lineages in blood islands (see 1.3), an involvement of the Tie2 enhancer/promoter in early haematopoietic cell seems likely. Indeed it was previously shown that HSCs in the murine fetal liver express Tie2 (Hsu et al., 2000) and in a recent study the Kisanuki Tie2-Cre line was actually used to induce an overexpression of Notch1 in the haematopoietic linage (Cortegano et al., 2014). Another factor that confounds experiments involving the Tie2-Cre line is that, in addition to the Kisanuki line, at least another four Tie2-Cre mouse lines were independently created (Kano et al., 2003; Koni et al., 2001; Proctor et al., 2005; Theis et al., 2001). Most likely they differ in location, copy number and orientation of the integrated transgene and therefore also in their respective Cre expression pattern and endothelial specificity. In the literature it is often not clearly stated which mouse line is used, leading to conflicting results.

Collectively these lines of evidence indicate that the Tie2-Cre line directs Cre activity to both endothelial and haematopoietic lineages, this transgenic mouse line can be considered less than ideal when studying the vasculature. Due to fact that Tie2-Cre mediated Tal1 KO is not inducible and leads to embryonic lethality, it also precludes the investigation of later developmental stages.

Therefore, I decided to instead use the relatively new Cdh5(PAC)-CreERT2 (hereinafter referred to as VE-CadherinCreERT2) mouse line, where the Cre transgene is under control of the VE-Cadherin locus (Sörensen et al., 2009). This Cre line, first published in 2009, has already been used in more than 60 publications and shown to specifically direct inducible Cre activity to endothelial and endocardial tissues in mouse embryos from E15.5 up to adulthood. In particular, it has been used extensively to delete genes specifically in retinal ECs during post-natal angiogenesis (Sörensen et al., 2009; Zarkada et al., 2015).

The stereotypic development of the retinal vasculature allows to study various aspects of angiogenesis. As Tal1 could possibly play a role in all of them, I designed a three-part experiment for the tamoxifen induced EC specific KO. An overview over the different time

points of injection and subsequent harvest of the retinas together with the respective angiogenic process of interest is given in Table 13.

Age Injection	Age Euthanasia	Tamoxifen Injected	Process Analysed
P2 – P4	P5	50 µl (1 mg/ml) each	Sprouting angiogenesis
P5 – P8	P9	100 µl (1 mg/ml) each	Vessel remodelling / maturation
> 8 weeks 5 consecutive days	3 weeks later	500 µl (1 mg/ml) each	Vascular homeostasis

Table 13 | Overview of postnatal tamoxifen injection procedures according to age of injection and process of interest
Procedures were adapted and modified from (Pitulescu et al., 2010).

3.3.1 Positive Control for Inducible EC-Specific KO in P5 Retina

In order to perform meaningful induced, EC-specific KO experiments it was absolutely necessary to show that Cre recombinase is actually active in the retinal endothelium by adequate control experiments. Therefore, I crossed the VE-CadherinCreERT2 line with the Rosa26R-LacZ reporter line to monitor Cre activity. In this reporter mouse line the activity of the LacZ transgene is controlled by the ubiquitously active endogenous ROSAβ-geo26 locus which is silenced through a loxP flanked transcriptional stop sequence. When the Cre recombinase is active in a cell that carries the Rosa26R-LacZ allele, the stop sequence is excised and the LacZ transgene is turned on and remains active in all daughter cells (Soriano, 1999).

The control experiments mirrored the injection and sacrificing scheme of the KO experiments. LacZ reporter gene activity was visualised via X-Gal staining on retina whole-mounts. In a similar experiment, a previous study has proved, albeit using a different inducible Cre line, that LacZ expression can be detected as early as 12 h after induction (Tammela et al., 2011). Therefore, it is reasonable to assume that the reporter gene distribution accurately reflects the activity of the Cre recombinase. However, a certain lag between the recombination event and

the accumulation of detectable amounts of β-galactosidase that leads to a slight underrepresentation of actual recombination has to be borne in mind.

I could show that tamoxifen injection effectively and specifically induces Cre-dependent recombination in ECs of the P5 retina (Figure 12, A-B). Detailed examination revealed that all relevant EC types such as phalanx, tip and stalk cells displayed LacZ expression (Figure 12, C-E). It is important to note that the distribution of X-Gal positive ECs was not homogenous across the retinal blood vessel network. The transgene expression appears to be scattered in patches of local clusters across the entirety of the plexus. The distribution of patches is semi-random with a maximum of intensity approximately midway between the optical disc and the vascular edge. Especially larger vessels seem to display extended stretches of positive ECs. Except ECs, no other X-Gal positive cells could be found in the retina. The observed mosaicism is a known characteristic of inducible Cre-loxP systems, since gene inactivation does not occur abruptly but in a gradual fashion. Different cells activate the Cre gene at slightly different time points and with different efficiencies.

Overall, the positive control experiment demonstrates that I could effectively induce Cre mediated recombination specifically in ECs. This is in line with several previous studies in which the VE-CadherinCreERT2 mouse line and similar injection schemes were used to delete target genes in the retinal vasculature (Birdsey et al., 2015; Wang et al., 2010b; Zarkada et al., 2015).

The results of the positive control experiments in P5 retina are summarised in Figure 12.

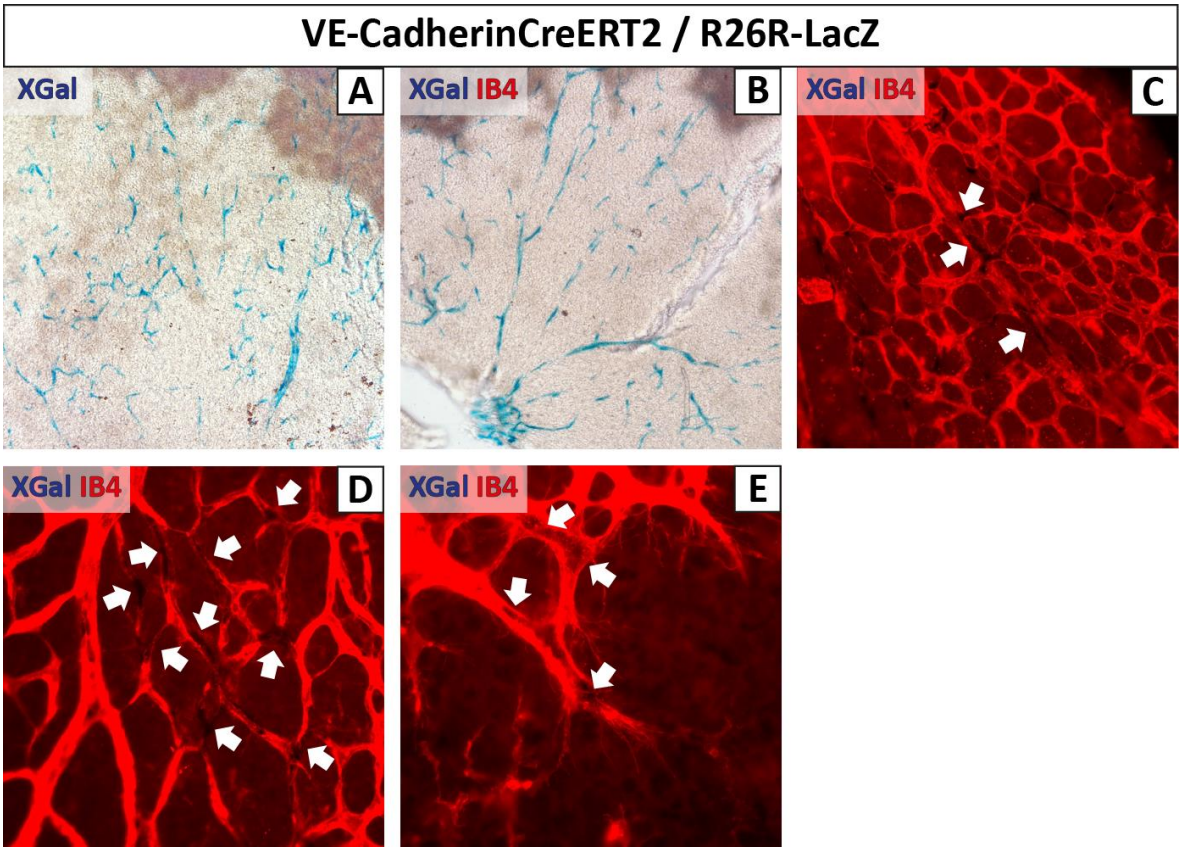

Figure 12 | Positive control for inducible EC specific KO in P5 retina
Pups received a daily injection of 50 µg tamoxifen at P1, P2 and P3, white arrows indicate X-Gal positive ECs
A: Overview X-Gal staining of retinal periphery, X-Gal positive areas appear blue in transmission image
B: Overview X-Gal staining of central vasculature with positive major vessels and microvasculature
C-E: Representative images of X-Gal positive phalanx (C), stalk (D) and tip (E) ECs, X-Gal positive areas appear black in confocal fluorescence image due to blocked IB4 binding

3.3.2 Power Calculation for Inducible Tal1 KO Experiment

In order to comply with the guidelines of animal research set out by the Home Office, which include ethical, scientific, legal, and economic reasoning, it is paramount that animals are used in minimum numbers while still obtaining the required amount of information. Therefore, I have performed a power calculation to determine the required scale of the induced EC specific Tal1 KO morphometric analysis experiment.

Type of power analysis: A priori, the test is performed before any experiment has started.

Test category: One-tailed unpaired Student's *t*-test

If induced EC specific KO of Tal1 has an effect on retinal vasculature, it is highly probable that it will be inhibitory as it has already been demonstrated that Tal1 deficiency disrupts vessel formation (Deleuze et al., 2007; Schlaeger et al., 2005). Therefore, a one-tailed test is sufficient.

Unit of measurement: An arbitrary unit of morphometric analysis of retinal vascularisation (vascular outgrowth, vascular coverage, branch points, filopodia per area)

Assumed standard deviation: $\delta = 20$ % The reference for this assumption is Figure 1 in (Zuercher et al., 2012) where a similar analysis was performed.

Assumed means for groups: Negative controls: $\mu 1 = 100$ % Tal1 deficient mice: $\mu 2 = 60$ %

Effect size: $d = \frac{|\mu 2 - \mu 1|}{\delta} = \frac{|0.6 - 1|}{0.2} = 2.0$

Calculation input parameters		**Calculation output parameters:**	
Significance level	$\alpha = 0.05$	*Actual power:*	$1-\beta = 0.94$
Allocation ratio n2/n1	1	*Sample size group 1*	n1 = 6
Effect size	d = 2.0	*Sample size group 2*	n2 = 6
Statistical power	$1-\beta = 0.9$	***Total sample size:***	**n = 12**

The calculation shows that with a total amount of 12 injected animals (6 KO and 6 WT) it should be possible to detect an effect of induced Tal1 deficiency on retinal vascularisation with a statistical power of 90 %. As it is improbable that pups are born in perfect Mendelian ratios (50% transgenic mice / 50% negative controls), a slightly higher number of animals was injected with tamoxifen.

3.3.3 Effects of EC Specific Tal1 Deletion in the P5 Retina

At first I performed a detailed morphometric analysis of four important parameters that are commonly used to characterise a vascular network: vascular coverage, outgrowth length, branch points per area and filopodia at the vascular front (see 2.2.11 for details concerning the image processing techniques that were utilised). Additionally, I have performed a linear regression analysis to model the relationship between branch per area and vascular coverage. This analysis is informative because it is possible that the two parameters influence each other. A highly ramified network with thinner vessels will display similar vascular coverage to a more sparsely ramified network with thicker vessels and *vice versa*. A linear correlation between the two parameters would indicate a comparable overall network structure in KO and control group.

In total, I have performed tamoxifen injection in 17 P5 pups, of which 8 were positively genotyped for the presence of the VE-CadherinCreERT2 allele. All injected pups were homozygous for the $Tal1^{flox}$ allele. The results of the morphometric analysis are summarised in Figure 13.

The analysis of morphometric parameters in the P5 retina did not reveal any significant difference between VE-CadherinCreERT2/WT;$Tal1^{flox/flox}$ (CKO) and VE-CadherinWT/WT;$Tal1^{flox/flox}$ (WT) animals. For all four parameters a performed *t*-test analysis resulted in p-values larger than $\alpha = 0.05$. In two KO animals the vascular outgrowth length was unusually low but the other parameters indicated a normal structure of the vascular network. Therefore, it is likely that these two animals experienced a developmental delay, possibly due to the injections, which is within the margins of natural variance. The number of branch points and the vascular coverage showed good linear correlation which indicates a comparable network composition in all analysed retinas.

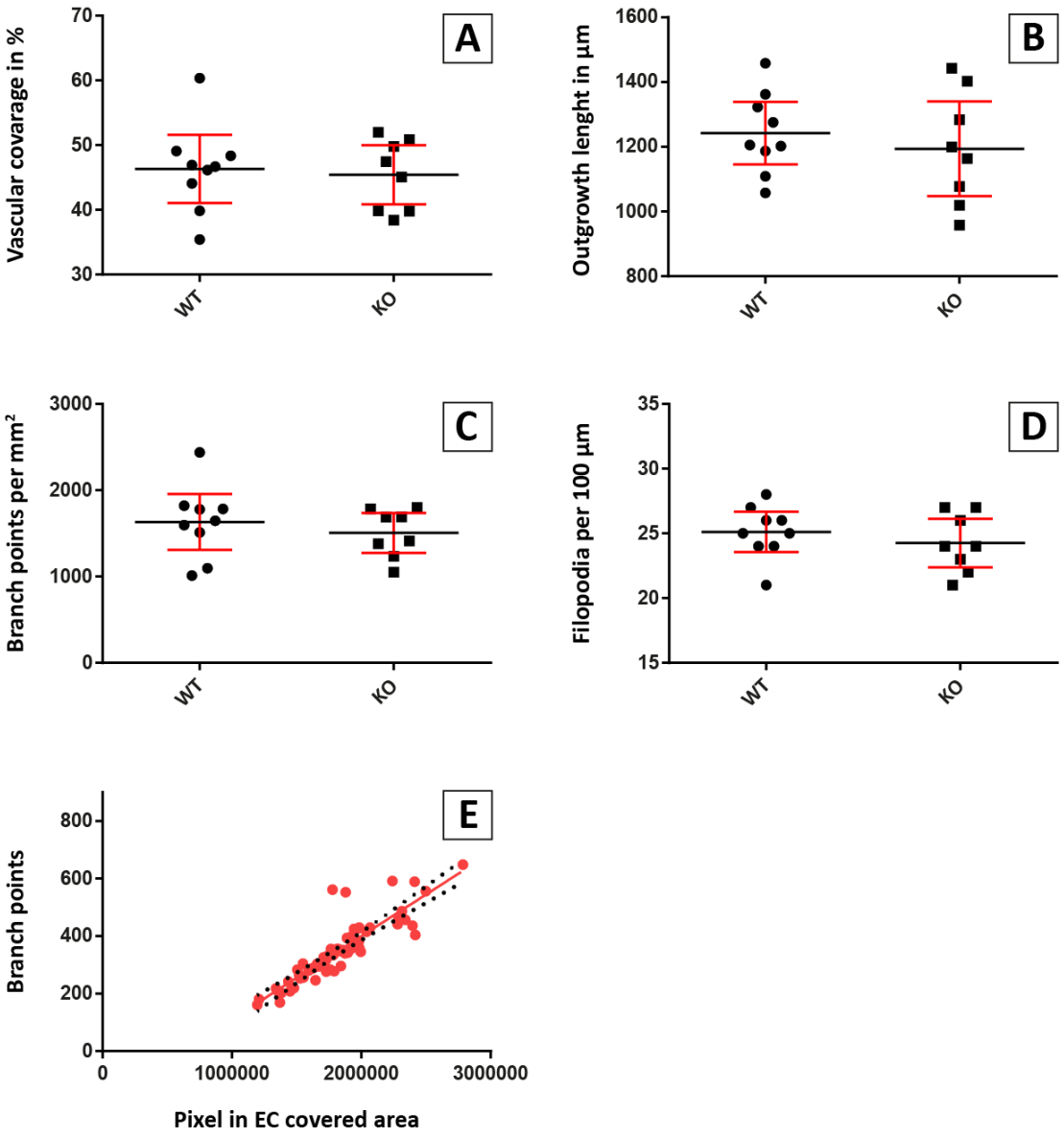

Figure 13 | Morphometric analysis of the effects of induced EC-specific KO of Tal1 in P5 mouse retina
Pups received a daily injection of 50 µg tamoxifen at P2, P3 and P4
A: Vascular coverage, p=0.56
B: Outgrowth length, p=0.37
C: Branch points, p=0.29
D: Filopodia at the angiogenic front, p=0.76
E: Regression analysis between the number of branch points and vascular coverage, red dots represent individual measurements from both KO and WT animals, red line represents fitted slope, dashed black line represents 95% CI, $r^2 = 0.7768$
n WT: 9, n KO: 8, Error bars are 95% CI, Black horizontal lines are the arithmetical mean

3.3.4 Positive Control for Inducible EC-Specific KO in P9 Retina

The results of the positive control experiment in P9 retinas widely corroborated that the VE-CadherinCreERT2 mouse line effectively drives EC specific Cre expression in the neonatal retina. Overall, an even greater amount of ECs appeared to have activated the LacZ transgene. It became apparent in the P9 retinas that that LacZ expression was not homogenous but that certain areas show high expression levels with nearly all ECs being X-Gal positive while a few areas are almost entirely negative (Figure 14, E). The transitions between these two types of areas appeared to be sudden and did not follow any recognisable pattern. X-Gal positive ECs could be detected in both major vessels and smaller capillaries and in all three vascular plexuses (Figure 14, C-D).

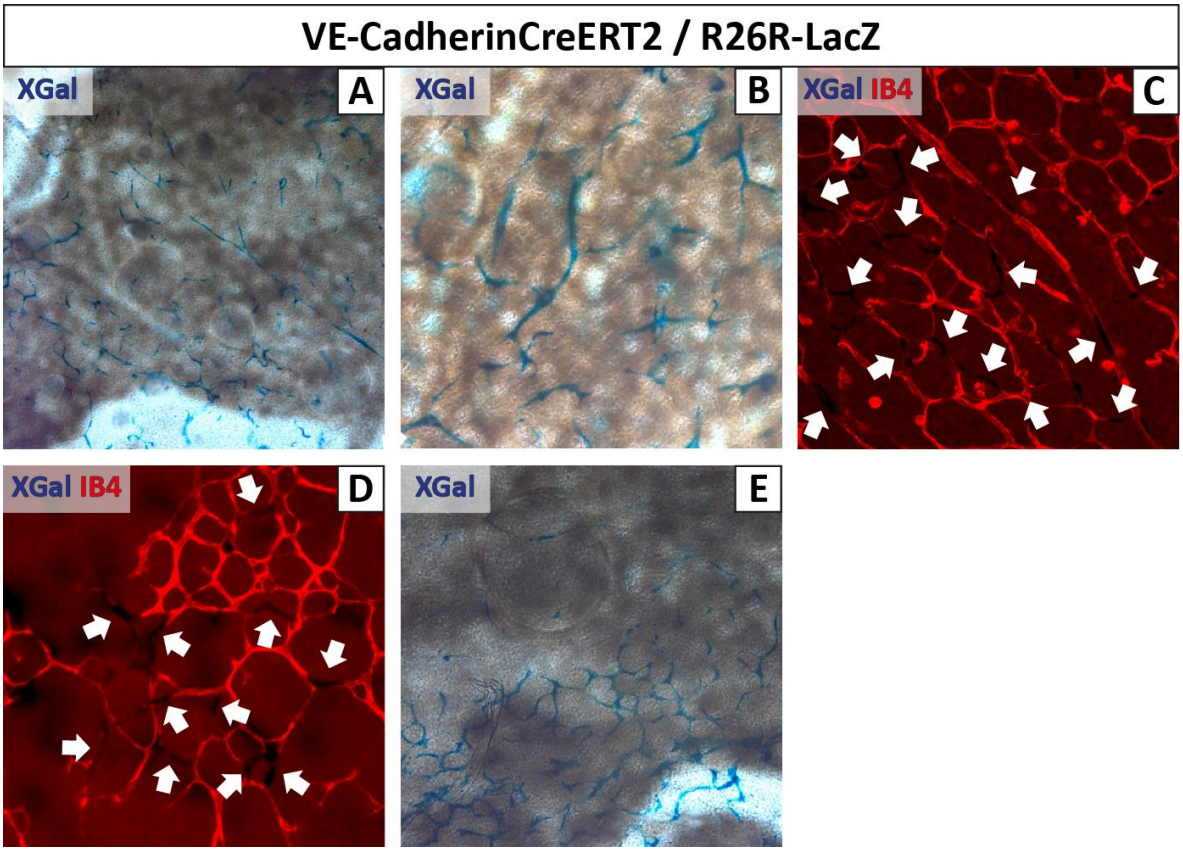

Figure 14 | Positive Control for Inducible EC Specific KO in P9 retina
Pups received a daily injection of 100 µg tamoxifen at P5, P6, P7 and P8, white arrows indicate X-Gal positive ECs
A: Overview X-Gal staining with positively stained artery and microvasculature
B: Magnified view on X-Gal(+) microvasculature
C-D: Representative image of superficial (C) and secondary (D) vascular plexuses, X-Gal (black) and IB4 (red) co-staining
E: Representative image of a sudden transition between regions of high and low ratios of X-Gal positive ECs

3.3.5 Effects of EC Specific Tal1 Depletion in the P9 Retina

After the primitive vascular network has covered the entire surface of the retina through angiogenesis, it needs to be optimised to meet the high metabolic needs of the retina while remaining transparent enough for light to pass through. Therefore, superfluous vessels are pruned and useful vessels get reinforced. It had been demonstrated that widespread CreERT2-dependent recombination can be detected in the retinal vasculature 12 h after tamoxifen induction (Tammela et al., 2011). The half-life of TAL1 protein has been reported to be ~4h (Lazrak et al., 2004) and the half-life of Tal1 mRNA is not published. However, the half-lives of mammalian transcription factor mRNAs are usually even shorter than protein half-lives (Schwanhäusser et al., 2011). I assume Tal1 depletion to reach effective levels between P6 and P7. To investigate if vascular remodelling is affected by the depletion of Tal1, I co-stained P9 retinas with the network forming collagen variant collagen IV (ColIV), which is a major component of the basal lamina in ECs, and IB4. Empty and obliterated blood vessel sleeves exhibit a basement membrane that is positive for IB4 but negative for ColIV staining (Baluk et al., 2003). Therefore, vessel regression can be visualised by co-staining for both surface markers. Through quantification of remodelling events I found that Tal1 KO pups showed vascular remodelling in a similar degree as WT pups (Figure 15, C-D).

Another aspect of vascular maturation is the progressive coverage of larger vessels with vascular smooth muscle cells (vSMCs). In particular, arteries acquire thick layers of vSMCs which form the tunica media. Disrupted vSMC coverage can hint towards a loss of arterial identity. Therefore, I co-stained the P9 retinas with the vSMC marker α-smooth muscle actin (αSMA) and IB4. As expected, arteries displayed strong αSMA staining while in veins the staining was absent or very weak. Arteries and veins could be distinguished morphologically as arteries appear straighter and are surrounded by larger avascular areas than veins. No apparent difference could be detected between Tal1 KO and WT animals (Figure 15, A-B). Finally I investigated the formation of deeper vascular layers in the retina (see Figure 10). Although poorly understood, the vertical turning of angiogenic sprouts is an important event

during network formation (Stefater et al., 2011; Zuercher et al., 2012). Through confocal microscopy and 3D reconstruction I could demonstrate that both secondary and tertiary plexuses are present and interconnected in both Tal1 KO and WT retinas (Figure 15, G-D).

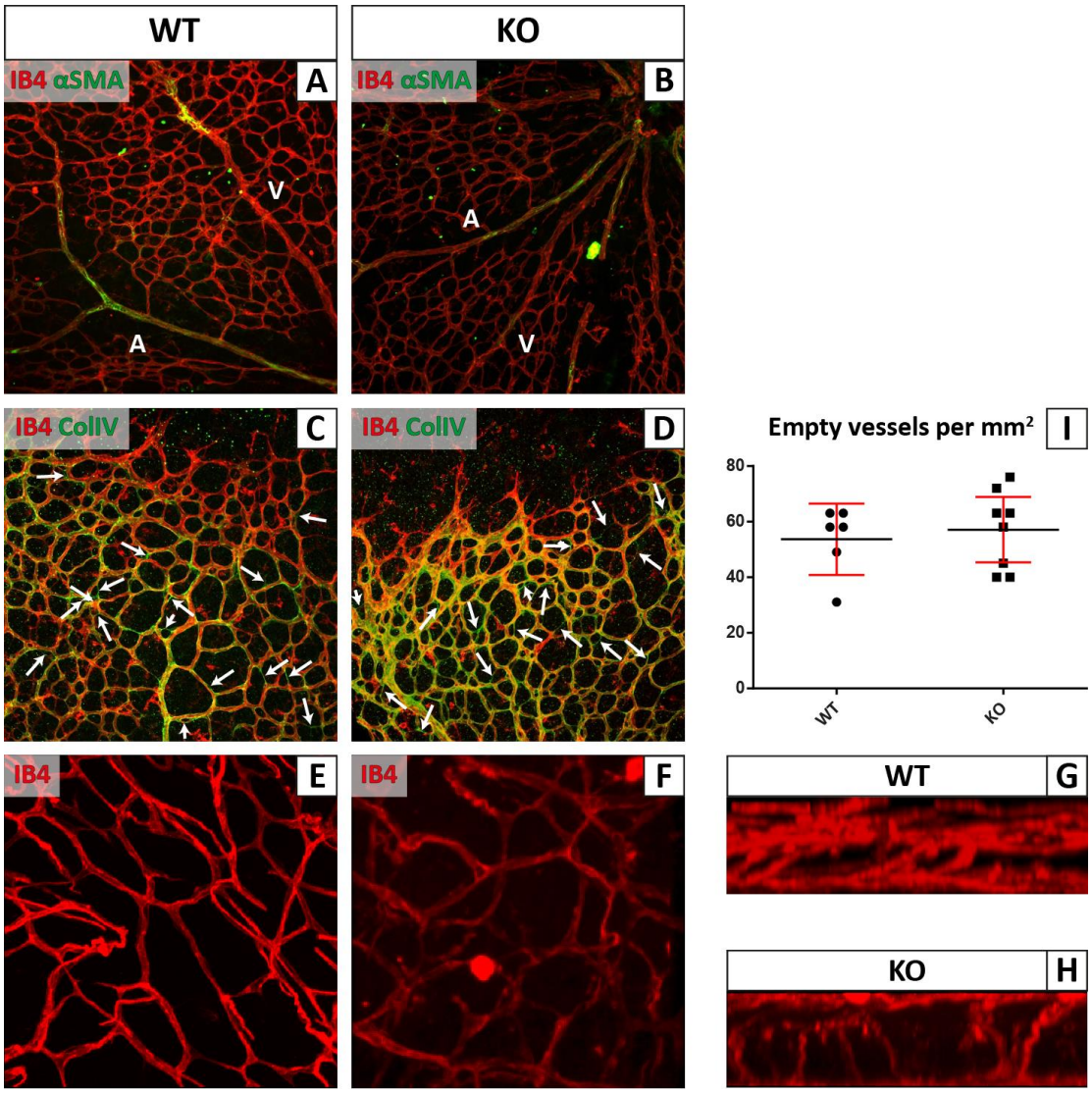

Figure 15 | Effects of induced EC-specific KO of Tal1 in the P9 mouse retina
Pups received a daily injection of 100 µg tamoxifen at P5, P6, P7 and P8
A/B: Visualisation of vSMC coverage through co-staining of IB4 and α-smooth muscle actin (αSMA)
C/D: Visualisation of vascular remodelling through co-staining of IB4 and collagen IV (ColIV), white arrows indicate empty ColIV(+) / IB4(-) vessel sleeves that represent remodelling events
E/F: Z-stack maximum intensity projections of secondary vascular plexus
G/H: Reconstructed orthogonal views of z-stack maximum intensity projections shown in E-F, interconnecting tertiary plexus is visible between primary (top) and secondary (bottom) plexus
I: Quantification of remodelling events, p=0.64, n WT: 6, n KO: 8, Error bars are 95% CI,

3.3.6 Effects of EC Specific Tal1 KO on Vascular Maintenance

Similar to any other tissue, the vascular system has to maintain its consistency in order to function properly. Dead cells need to be replaced to keep the system stable and in the case of the cardiovascular system, also a certain plasticity has to be ensured in order to be able to adapt to changes in environmental needs, for example tissue growth due to physical exercise. A phalanx-like morphology and quiescent behaviour of the endothelium is assured by autocrine signalling of Vegf, Tie2/Ang-1, Fgf and Notch and involves complex interplay with mural cells. Failed vascular maintenance can be causative for diseases like stroke, myocardial infarction, inflammatory disorders and cancer (Carmeliet and Jain, 2011).

To investigate if EC specific Tal1 depletion has an impact on vascular maintenance I induced endothelial specific Tal1 knockout in 16 weeks old mice and investigated the effects on the retinal vasculature and the vasculature of the caudal half of the spinotrapezius muscle three weeks later. The retinal vasculature has

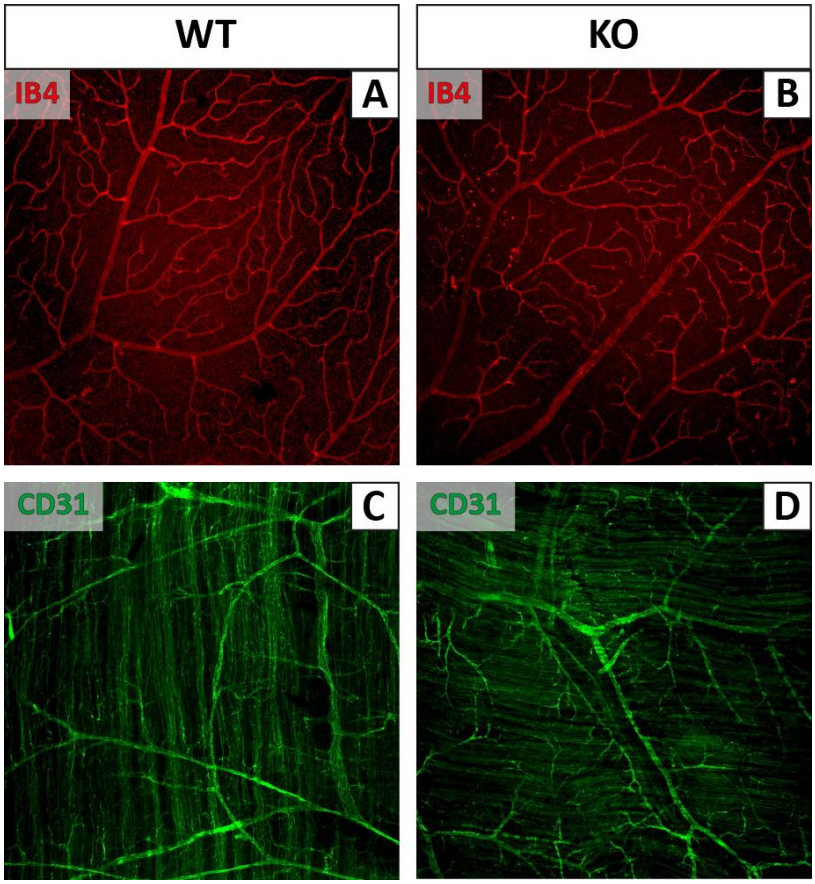

Figure 16 | Effects of induced EC-specific KO of on vascular maintenance
Adult animals (16 weeks) received a daily injection of 500 µg tamoxifen on five consecutive days and were sacrificed three weeks later
A/B: Representative images of superficial retinal vascular plexus in adult WT and KO animals
C/D: Representative images of vasculature in spinotrapezius muscle flat-mounts visualised with anti-CD31 staining (IB4 staining appeared to be not optimal for spinotrapezius staining)
n WT: 2 n KO: 6

certain features that distinguish it from other vascular beds and by referring to it as the only model for vascular development, the effects of Tal1 depletion in other tissues might be overlooked. To avoid this scenario I chose the spinotrapezius muscle as an additional vascular bed for analysis. This model is not as commonly used as the murine retina but has been described before (Moraes et al., 2013).

The finding in the retina were corroborated by the results of the analysis in the spinotrapezius muscle. Although the irregular structure of the blood vessel network makes comparison more difficult, a well-organised vascular network with distinguishable arteries and veins and interconnected capillaries was present in both WT and KO animals (Figure 16). No haemorrhages, which would indicate leaky blood vessels, or new sprouts, which would be signs of neo-angiogenesis, were visible.

3.4 Conclusions

The transcription factor Tal1 is essential for correct embryonic vascularisation in mice and it was suggested that the same may be true for later angiogenesis. Tal1 was reported to be expressed in the non-resting vasculature during adulthood and to be a pro-angiogenic factor in *in vitro* models of angiogenesis. Therefore, I tested the hypothesis that Tal1 plays a crucial role in angiogenic sprouting first by investigating its expression patterns in the developing vasculature of the murine retina and subsequently by analysing the effects of genetic interference with its expression in the retinal endothelium.

3.4.1 Expression of Tal1

No reporter gene activity could be detected at various stages of retinal vascularisation in $Tal1^{LacZ/+}$ animals. Two possible explanations are that Tal1 is not being expressed in the vasculature or that the reporter gene is too weak for detection. By review of the literature it becomes apparent that studies using the $Tal1^{LacZ/+}$ reporter line only find relatively faint expression of Tal1 in the endothelium (Elefanty et al., 1999) while studies that use different enhancer/reporter constructs to investigate Tal1 expression patterns, report much stronger signals (Göttgens et al., 2010; Sinclair et al., 1999). It is a known issue that the single reporter gene allele present in knock-in mouse lines often tends to underrepresent the true expression of the gene of interest. Studies on the Lyl1 gene, which displays an expression pattern comparable to Tal1, also showed discrepancies between *in situ* hybridisation and results obtained from a $Lyl^{LacZ/WT}$ reporter line, with LacZ expression pattern being both faint and not as widespread as the expression of the endogenous gene (Giroux et al., 2007). In contrast, the many integrated copies of *cis*-regulatory element/reporter transgenes, generated by pronuclear injection, result in much stronger reporter gene signals, although in these cases it is unclear whether the result is an amplified reporter gene signal or ectopic expression caused by abnormal accumulations of transcription factor binding sites. Which approach is more suited

to mimic the endogenous expression of the gene of interest remains a debatable point. Another possible explanation is that the insertion of the LacZ reporter gene itself caused deletion of enhancer sequences that are necessary for vascular expression of Tal1. The Tal1-LacZ targeting vector replaced the genomic region between exon III and exon VI of the endogenous Tal1 gene (Elefanty et al., 1998), thereby deleting 3 introns that potentially could contain regulatory elements as well.

For the interpretation of the negative results of the $Tal1^{LacZ/WT}$ reporter gene experiments in the retina, one has to keep in mind that I also could not detect LacZ expression in embryonic tissues that are known to express Tal1 and that are clearly affected after Tal1 deletion (see 4.6.1). Therefore, it is still reasonable to assume that Tal1 may be expressed in the retinal vasculature.

The results of the immunostaining experiment investigating Tal1 expression in postnatal retinal vasculature unfortunately also remain ambiguous, with one anti-Tal1 antibody producing a faint vascular signal, and a second antibody producing a neuronal staining. If the unexpected result of Tal1 being detected in the retinal ganglion cell axons could be confirmed, it would constitute a puzzling finding. Intriguingly, Tal1 is expressed in parts of the adult central nervous system that are involved in processing of auditory and visual stimuli including the superficial grey layer which is targeted by retinal axons. Moreover, mice deficient for Tal1 in neurons display altered behaviour, possibly due to increased light sensitivity (Bradley et al., 2006). However, a global expression of Tal1 in the whole axon body seems quite unlikely, considering the well-established function of Tal1 as a transcription factor that acts within the nucleus. On the other hand, DNA-binding independent activity of Tal1 (Kassouf et al., 2008) may be a pointer to undisclosed mechanisms of action.

Besides the explanation that Tal1 is not expressed in the sprouting postnatal vasculature, which would be in conflict with previous studies that found TAL1 in the non-resting vasculature (Pulford et al., 1995; Tang et al., 2006), Tal1 expression might be too weak to be detected by immunostaining. Transcription factors are known to be of quite low abundance, with only ~10,000 – 30,000 molecules per nucleus (Biggin, 2011), which makes them difficult to detect.

For the already known sites of postnatal microvascular Tal1 expression, the uterus and the ovary, it was reported that Tal1 is only expressed in a minority of ECs (Tang et al., 2006). Both anti-Tal1 antibodies used in this thesis produced a relatively high background staining, preventing detection of subtle signals. Published attempts of immunostaining for Tal1 have been riddled with poor signal to noise ratios as well (Kallianpur et al., 1994).

3.4.2 Endothelial Specific Deletion of Tal1

By choosing the developing mouse retina and the spinotrapezius muscle as model systems, I investigated the effects of induced Tal1 deletion in the endothelium on various aspects of sprouting angiogenesis, vessel maturation, and vascular homeostasis. Thereby, I used the relatively new but already well established VE-CadherinCreERT2 transgenic mouse line to direct Cre recombinase activity specifically to ECs. After establishing that the inducible Cre line is sufficiently active in the retinal vasculature, I analysed the effects of conditional Tal1 KO by quantifying various morphometric network parameters like density and outgrowth length and investigated if smooth muscle cell coverage and vascular remodelling were affected. Moreover, I have used the spinotrapezius muscle as an alternative vascular bed for analysis of the effects of Tal1 depletion on vascular homeostasis in adult mice. I could not find any significant differences between conditional KO and WT animals on any of the mentioned aspects of vascular development.

One considerable explanation for negative results is always the possibility that the chosen experimental set-up failed or was unsuitable for the posed scientific question. Since an *a priori* power analysis suggested that the number of mice I have analysed was sufficient to detect differences between WT and KO animals, I assume that my assay was saturated. The use of inducible KO systems has resulted in conflicting reports in the literature before. In 2012 Benedito *et al.* showed that Notch inhibition promotes hypersprouting in the retinal vasculature independently of VEGFR-2, but is suppressed by inhibition of VEGFR-3 (Benedito

et al., 2012). In contrast, a more recent study claimed that Notch inhibition promotes sprouting in the absence of VEGFR-3 but not in the absence of VEGFR-2 (Zarkada et al., 2015). Both studies made use of the same VE-CadherinCreERT2 line, which was also employed for the KO experiments in this thesis, to delete genes in the retina. Notably, Zarkada *et al.* also reported a variable efficiency in tamoxifen induced recombination, similar to what I have observed during embryonic development in crosses of VE-CadherinCreERT2 with the R26R-LacZ reporter line.

Despite these possible limitations of the experimental design, the retina vasculature model system has the unique advantage of allowing us to analyse the effects of genetic interference in a very controlled, stereotypical and two-dimensional system, permitting a very detailed analysis in which we can detect even subtle disturbances of normal development. Hence, I believe that I would have detected vascular defects if Tal1 had a critical role in retinal angiogenesis, vascular maturation or vessel homeostasis, regardless of variability in Cre efficacy. I therefore feel able to conclude that Tal1 does not play a critical role in postnatal sprouting angiogenesis, despite previous studies, which relied on *in vitro* (Deleuze et al., 2007, 2012) and matrigel models (Lazrak et al., 2004), suggesting otherwise. Moreover, Tal1 deficiency had no effect on the coverage of vessels with vSMCs, although previous *in vitro* experiments suggested that loss of Tal1 promotes smooth muscle cell differentiation (Ema et al., 2003). This conclusion does not exclude a possible involvement in postnatal vasculogenesis, as observed for example in tumour vascul arisation.

Chapter 4:

Role of Tal1 in Embryonic Vascular Development

4.1 Re-Examination of Tal1-LacZ Mouse Line

In 1998 the first Tal1 reporter mouse line was created by replacing one Tal1 allele with the β-galactosidase encoding gene LacZ from *Escherichia coli*, thereby putting it under control of the Tal1 *cis*-regulatory elements (Elefanty et al., 1998). The $Tal1^{lacZ/WT}$ knock-in mouse line has been used to characterise Tal1 expression in different haematopoietic progenitors and neuronal tissues (Elefanty et al., 1998, 1999). However, the vascular expression pattern remains relatively poorly described, especially regarding to embryos after mid-gestation.

With a special focus on vascular development in embryos older than E10.5, I re-examined the $Tal1^{lacZ/WT}$ reporter mouse line. A particular interest was to establish whether the expression pattern supported the idea of more widespread expression of Tal1 in the vasculature, as suggested by some reports that utilised Tal1 enhancer/reporter constructs (Deleuze et al., 2012; Göttgens et al., 2010; Sinclair et al., 1999; Tang et al., 2006) or that of a more limited expression pattern, restricted to very early stages of development (Elefanty et al., 1998, 1999).

An overview of the LacZ expression in embryos of various developmental stages, as detected by X-Gal blue staining, is given in Figure 17.

As reported previously, X-Gal staining was present in the ventral neural tube and developing midbrain of E11.5, E13.5 and E16.5 embryos. At E11.5 X-Gal staining in the brain could be detected in whole-mount embryo specimens but not in sections. This is most likely due to the fact that the Tal1 expressing tissue at the very dorsal end of the embryo was lost during sectioning. Very little endothelial expression of Tal1 within the embryos of the different stages could be observed. These observations are in direct conflict with Elefanty *et al*., 1999 and Göttgens *et al*., 2010, who reported strong global arterial X-Gal staining in E11.5 and E13.5 embryos. In addition, I could not detect Tal1 in the fetal liver or aortic wall clusters of E11.5 embryos, again in contrast to reports describing a peak in definite haematopoiesis within the fetal liver at E11.5. At E13.5 individual X-Gal positive erythrocytes and megakaryocytes were visible within the liver, again expression strength was considerably weaker than previously

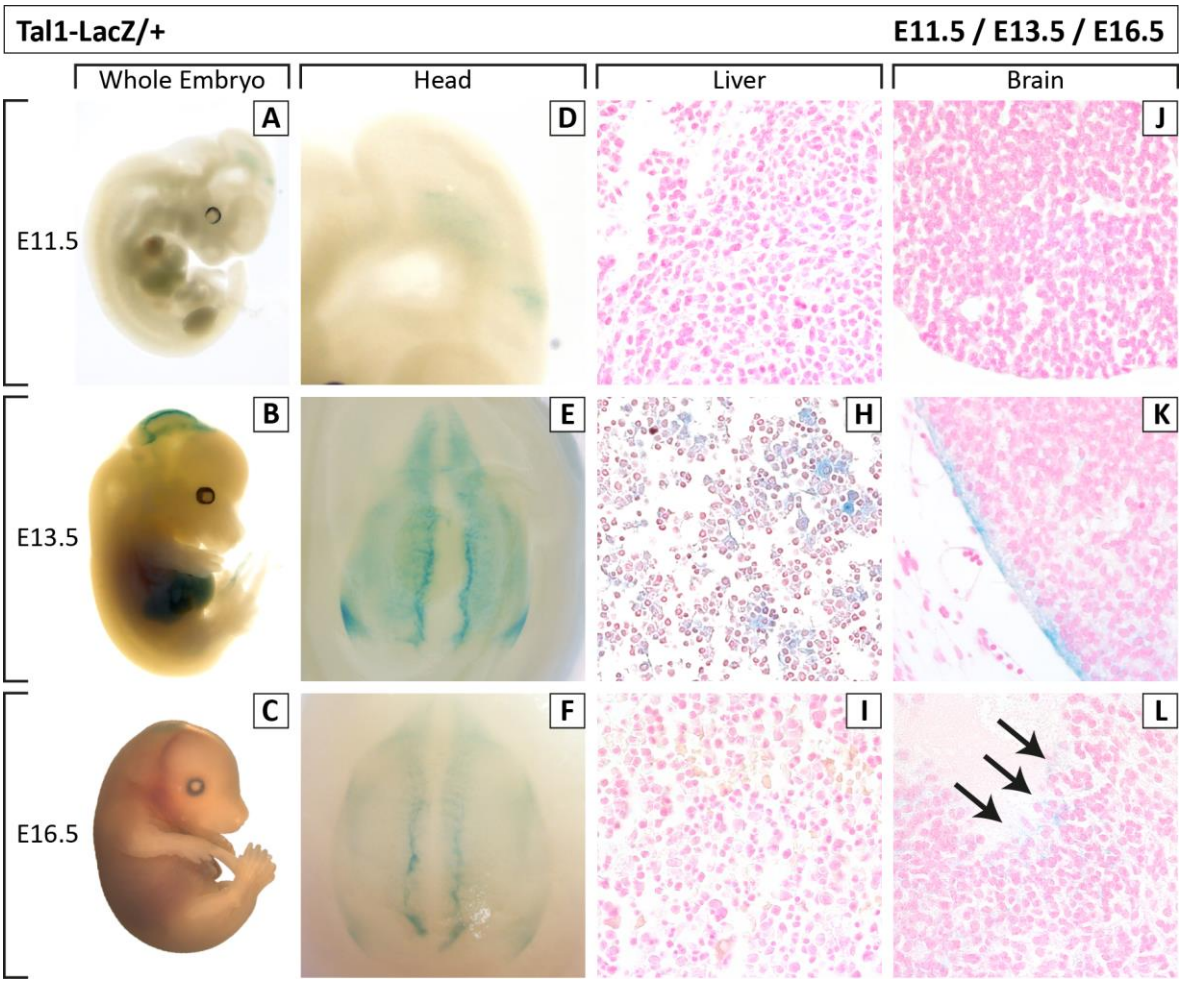

Figure 17 | Analysis of Tal1$^{LacZ/WT}$ reporter gene expression during different stages of embryonic development
A-C: Representative overview of X-Gal stained whole-mounts at E11.5, E13.5 and E16.5, showing faint expression, largely restricted to head areas and in E13.5 embryos to the abdomen
D-F: Magnified dorsal (in C lateral) view on heads showing X-Gal staining at E11.5, E13.5 and E16.5
D-F: Transverse section through liver showing individual X-Gal(+) in E13.5 embryos
J-L: Transverse sections through brain showing neuronal reporter gene expression in individual neurons in E13.5 and E16.5 embryos

reported. In the whole-mount sample of one E13.5 embryo a weak X-Gal staining in the umbilical vein vessel was visible. However, I was not able to detect any staining in the umbilical vein on sections. A possible explanation could be that the staining originated from Tal1 positive blood components within the vein which were lost during the embedding process.

Overall, the re-examination of Tal$^{LacZ/WT}$ reporter mice did not hint towards a strong expression of Tal1 in the embryonic vasculature, although the fact that X-gal staining was not detected in other known Tal1 expression domains suggested that further analysis was warranted.

4.2 Immunostaining of Tal1 in Embryonic Vasculature

Reporter gene based mouse models have the disadvantage that they can obscure the real dynamics of protein expression, especially if the protein of interest is a tightly regulated transcription factor. In mammalian cells β-galactosidase has a half-life of ~30 h whereas the half-life of TAL1 protein is just 4 h (Lazrak et al., 2004) and mRNA half-life is probably even shorter (Schwanhäusser et al., 2011). However, in case of $Tal1^{LacZ/WT}$ a more relevant limitation was the fact that I could not breed the reporter to homozygosity, since this would result in embryonic lethality. As already mentioned in 3.4.1 and further explained in 4.6.1 the single reporter allele most likely does not reveal all expression domains of Tal1. Another example of this phenomenon is the Tal1 binding partner and regulator of embryonic angiogenesis Lmo2, where, in contrast to studies using enhancer/reporter constructs (Landry et al., 2009), the knock-in reporter line (Yamada et al., 2002) does not reveal endocardial expression. To address this problem, I additionally performed immunostaining for Tal1 in embryos.

As previously mentioned (see 3.2), most of the antibodies used in previous publications (Drake and Fleming, 2000; Kallianpur et al., 1994) were not available to me. Therefore, my goal was to establish an anti-Tal1 immunohistochemical staining on paraffin sections with commercially available antibodies. At first I tried the anti-Tal1 antibody ab75739 [Abcam] which resulted in a faint endothelial staining in the postnatal retina and has been already published (Tsunoda et al., 2010). After several unsuccessful attempts with varying experimental conditions and helpful correspondence with the authors of the study, I established an anti-Tal1 IHC staining protocol by using the antibody MAB3360 [R&D Systems]. The use of this antibody resulted in neuronal staining in the retina. For my immunostaining conditions see 2.2.6.

My findings widely agreed with the results of the previously mentioned expression studies. At E8.5 heterogeneous staining could be detected in peripheral cells which are most likely ECs as well as in single rounded cells within the embryo which could represent first hematopoietic cells (Figure 18, A/B). Later at E11.5 Tal1 could be detected in the developing neural tube, blood cells and surprisingly just very faintly in the liver (data not shown). In respect of the

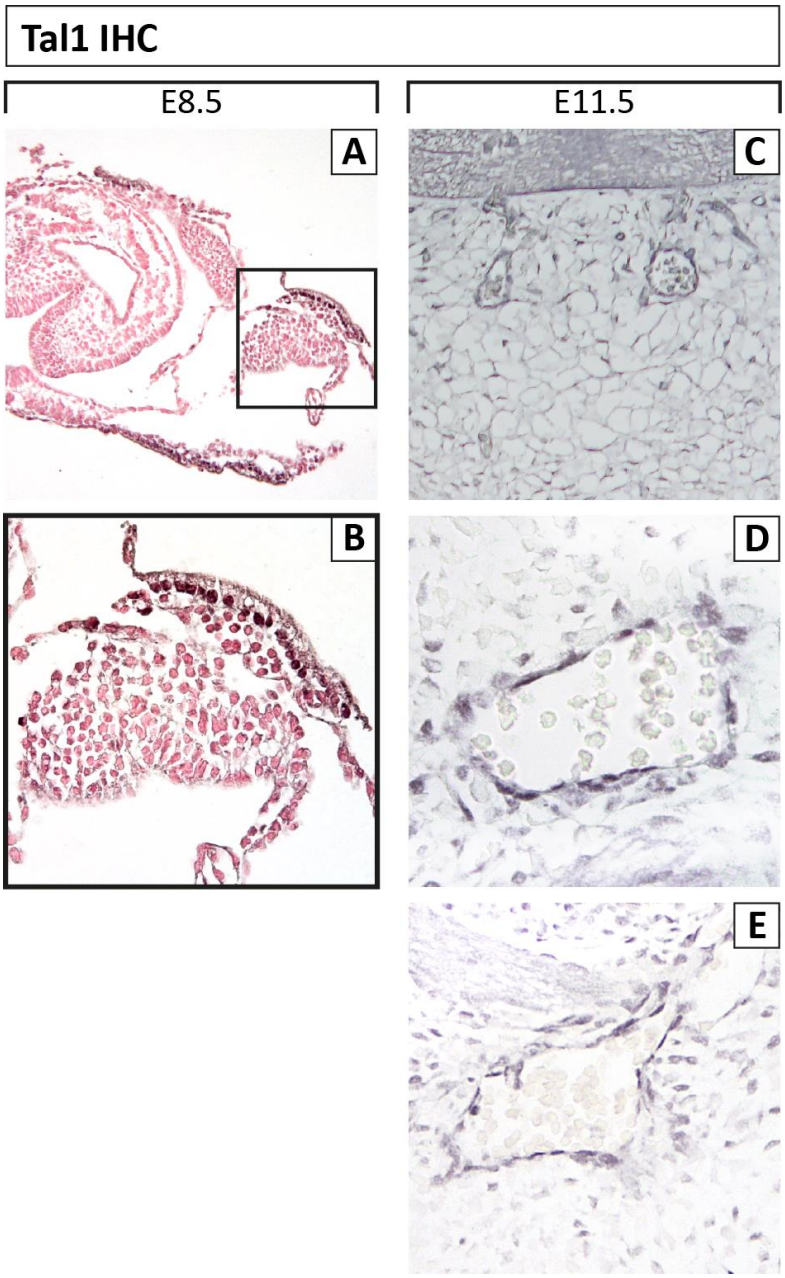

Figure 18 | Immunohistochemical staining for Tal1 in vasculature on E11.5 and E8.5 embryos

Transverse sections with Tal1 visualisation by peroxidase-labelled 2nd antibody and diaminobenzidine (DAB); counterstained by Nuclear Fast Red

A-B: Tal1 is present in peripheral endothelial cells of E8.5 embryos; (B) magnified view

C-E: ECs of major arteries and parts of microvasculature in E11.5 embryos seem to be positive for Tal1

vasculature, Tal1 could be detected only very weakly in microvascular ECs and stronger in the ECs of major arteries (Figure 18, C-E). Interestingly, venous ECs were almost absent of Tal1. Arteries and veins were distinguished by morphology.

Overall, it is important to note that the signal to noise ratio in all experiments was relatively low, impairing the significance and interpretability of the results. This problem was also present in other studies using IHC to determine Tal1 protein expression patterns.

4.3 Induced EC-Specific KO of Tal1 during Embryogenesis

After I could not find evidence for the involvement of Tal1 in postnatal angiogenesis, I focused my analysis on the vascularisation of the embryo and tried to elucidate if Tal1 might play a role within a confined developmental time-window. Previous reports of global (Robb et al., 1995; Shivdasani et al., 1995; Visvader et al., 1998) and Tie2-Cre mediated (Schlaeger et al., 2005) Tal1 deletion in the vasculature did not fully investigate vascular defects and were confounded by a loss of Tal1 in haematopoietic cells. Therefore, I decided to recapitulate and re-examine these experiments with a particular focus on vasculogenesis, angiogenesis, and, since IHC suggested a slightly increased expression of Tal1 in arteries, arterio-venous differentiation. Thereby I have used the inducible, EC-specific VE-CadherinCreERT2 mouse line and modern, whole-mount imaging techniques that were both not available when the role of Tal1 in the vasculature was first examined.

A schematic overview of the tamoxifen inductions and respective analysis of embryos at various developmental stages together with the observed phenotype is given in Figure 19.

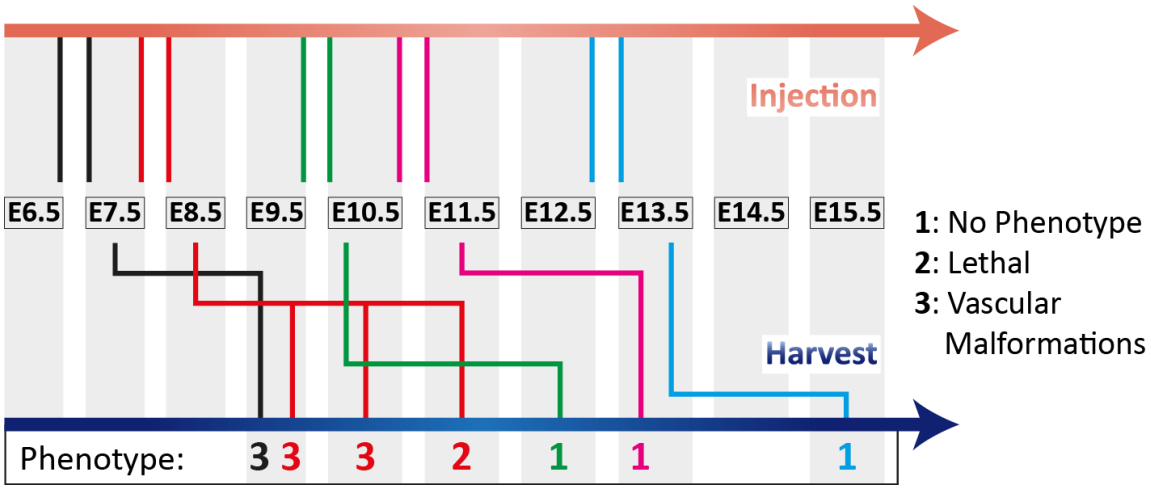

Figure 19 | Overview of tamoxifen injections and subsequent harvesting of VE-CadherinCreERT2;Tal1$^{flox/flox}$ embryos
Tamoxifen was administered on two consecutive days and embryos were harvested 2 – 4 days later; colour coded lines indicate days of injection (upper part) and respective day of harvest (lower part), as well as the observed phenotype (1: no phenotype, 2: lethal and in the process of re-absorption, 3: vascular malformations)

4.3.1 Positive Control for Inducible EC-Specific KO during Embryogenesis

In accordance with the previous KO experiments conducted in the mouse retina, I performed a positive-control experiment to monitor the Cre recombinase activity of the VE-CadherinCreERT2 line in mouse embryos before attempting the induced KO of Tal1. The VE-CadherinCreERT2 transgenic line has been successfully used before to knock-out genes in the endothelium of embryos (Turner et al., 2014) [*Injected E8.5/9.5/10.5 and embryos harvested E14.5*], and it has been demonstrated by lineage tracking [*Injected E8.5 and embryos harvested E10.5-E17.5*] that the line effectively drives Cre expression in embryonic ECs (Azzoni et al., 2014). However, most of the studies using that mouse line focussed on postnatal gene deletion and a detailed characterisation of the Cre expression pattern with special regard to the distribution in the embryonic vasculature has not yet been performed. Moreover, induction of CreERT2 lines at embryonic stages can be challenging due to the side-effects of tamoxifen (see 2.1.3.1). For that reason I had to ensure that my experimental set-up produces informative results.

As I originally planned to induce EC-specific Tal1 deletion at E9.5/E10.5 and to subsequently analyse the embryos at E12.5 (see 4.3.2), I have crossed the VE-CadherinCreERT2 line with the R26R-LacZ reporter line and performed the injection and analysis according to the aforementioned scheme. I could detect LacZ expression in the microvasculature of all parts of the embryo while expression in major arteries and veins was very faint (Figure 20, A-H). Surprisingly, I could observe a large spectrum of reporter gene expression strength between littermates harvested from one injected female. Transgenic embryos displayed X-Gal staining strength ranging from being barely visible (Figure 20, A-B) to robust staining across the whole embryo (Figure 20, G-H). When repeated, the experiment yielded similar results. I was not able to find a similar observation of intra-litter variation described in the literature. However, after correspondence with colleagues who faced similar problems, I changed the route of tamoxifen

administration from I.P. injection to oral gavage. Albeit the oral administration of tamoxifen induced detectable LacZ expression as well, the problem of variable expression strength persisted. Since the oral gavage procedure induces increased stress levels in mice, I ceased to employ this route of tamoxifen administration and resumed I.P. injections. On advice of a colleague, I have also tried to directly inject the active metabolite of tamoxifen, 4-OHT, into the pregnant mice. Again, although the induction of Cre recombinase was successful I still could observe variable LacZ expression.

I have noticed that the staining intensity seemed to be correlated to the position of the embryo within the uterine horn, since embryos with stronger LacZ expression were more likely to be found at the end of the uterine horns. Due to the bidirectional blood flow into the uterine artery from both ends of the uterine horn, embryos at the ends of the horn receive higher rates of placental blood flow (Even et al., 1994). It is possible that this affects the delivery of the active metabolite 4-OHT to the embryos as well. However, I did not analyse enough embryos to make a conclusive statement about this hypothesis.

After the first results of the induced EC-specific Tal1 KO experiments showed that E12.5 embryos display no vascular phenotype after injection at E9.5/E10.5, I decided to analyse earlier embryonic stages. Therefore, I performed an additional control experiment and injected pregnant females at E7.5/E8.5 and analysed VE-CadherinCreERT2; R26R-LacZ embryos at E10.5 (Figure 20, I-K). X-Gal staining could be detected in the microvasculature, intersomitic vessels and also in the heart and parts of the carotid artery. The problem of variable expression strength between littermates was still present but less bold, with most transgenic embryos displaying similar degrees of expression.

Overall it is important to note that, although the variable effectiveness of the Cre induction posed a problem, I could demonstrate that the VE-CadCreERT2 line was EC specific and active at different stages of embryonic development. For the interpretation of KO results it was important to clarify in which transgene embryo the Cre recombinase was actually active. I believe by analysing large numbers of injected embryos (see Table 14) and by having the well-

established yolk sac vasculature phenotype as a type of internal positive control (see 4.3.2), I established a way of verifying the deletion of Tal1.

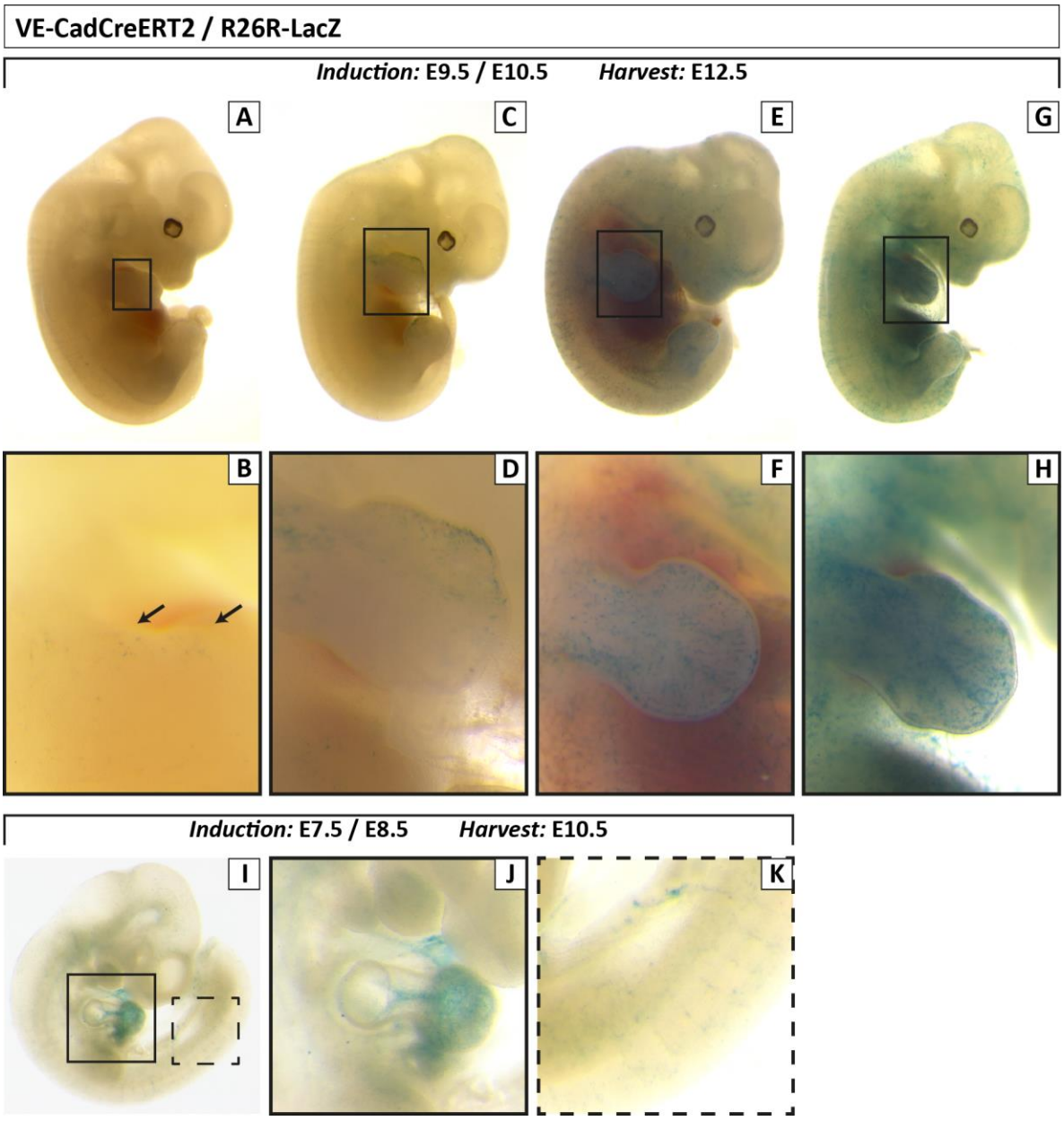

Figure 20 | Positive control for inducible, EC Specific KO during embryogenesis
X-Gal staining in whole-mount embryos, tested for two independent induction/harvest intervals
A-H: Representative overview of E12.5 littermates (injected E9.5/E10.5), displaying large variation in staining intensity; (B,D,F,H) magnified views on limbs showing variable X-Gal staining in microvasculature
I-K: Representative E10.5 embryo (injected E7.5/E8.5) showing LacZ expression in (J) the heart and parts of carotid artery and in (K) intersomitic vessels and parts of the microvasculature

4.3.2 Analysis of Induced EC-Specific Tal1 KO in Embryo

The previous publications reported an embryonic lethality at E9.5 for the global (Robb et al., 1995), and at ~E13.5 for the Tie2-Cre mediated (Schlaeger et al., 2005) deletion of Tal1. In spite of the previously discussed limitations of these studies, these time-points provided a good developmental timeframe to begin the analysis of the effects of induced, EC-specific KO of Tal1. I decided to inject tamoxifen at E9.5 and E10.5 in order to not interfere with the role of Tal1 as master regulator of early haematopoietic progenitor commitment. To compare the resulting phenotype with the Tie2-Cre mediated KO, which also deletes Tal1 from the hematopoietic lineage, embryos were harvested at E12.5, one day before the reported lethality. Considering that the *in vivo* half-life of TAL1 protein is only ~4 h (Lazrak et al., 2004) and Cre recombinase activity can be detected 8 h after tamoxifen injection (Nakamura et al., 2006), it is reasonable to assume that an interval of 72 h tamoxifen exposure is sufficient to induce developmental defects upon Tal1 depletion.

Through repeated analysis of E12.5 embryos I could not find morphological differences between VE-CadherinCreERT2(+);Tal1$^{flox/flox}$ and VE-CadherinCreERT2(-);Tal1$^{flox/flox}$ embryos. All analysed embryos appeared viable and displayed no intra- or extraembryonic vascular defects (data not shown). The same results were obtained for embryos in which deletion was induced at E10.5/E11.5 and analysed at E13.5, and embryos induced at E12.5/E13.5 and harvested at E15.5, see Table 14.

I concluded that endothelial specific Tal1 depletion after ~10.5 does not result in detectable vascular defects. Therefore, I shifted my focus to the vasculogenic processes earlier in development. When injected at E7.5/E9.5 and analysed at E11.5, embryos genotyped as VE-CadherinCreERT2(+);Tal1$^{flox/flox}$ displayed massive global defects and seemed to be in the process of re-absorption (Figure 21, A/B). The embryos were considerably smaller than WT littermates and appeared to display a developmental delay of around 1 day. However, due to the strength of the defects it was impossible to pinpoint specific vascular defects.

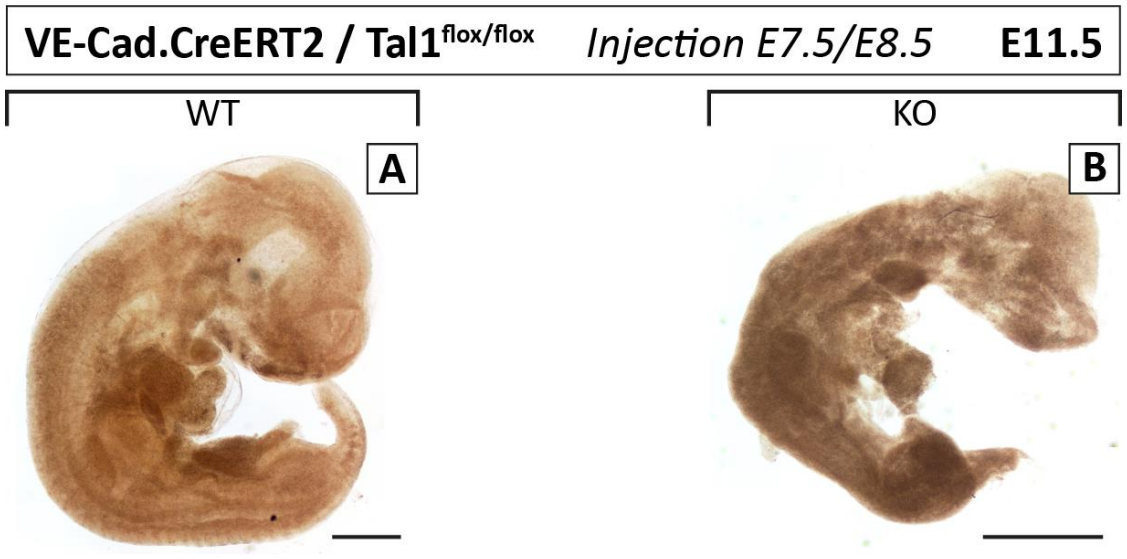

Figure 21 | Strong developmental defects in Tal1 KO embryos injected at E7.5/E8.5, harvested at E11.5
Representative images of whole-mount embryos, brown colour is due to anti-endomucin IHC staining
A: Healthy WT embryo
B: KO embryo in the process of re-absorption, displaying massive developmental defects and delay
Scale bars are 1 mm

Tamoxifen Injection	Embryo Harvest	No Defects	Vascular Defects	Lethal Defects
E6.5/E7.5	*E9.5*	10	6	2
E7.5/E8.5	*E9.5*	8	3	0
E7.5/E8.5	*E10.5*	7	3	2
E7.5/E8.5	*E11.5*	0	0	3
E9.5/E10.5	*E11.5*	3	0	0
E10.5/E11.5	*E13.5*	4	0	0
E12.5/E13.5	*E15.5*	2	0	0

Table 14 | Overview of injection schemes with respective numbers of observed phenotypes in KO embryos

E9.5 Embryo (Injected E6.5/E7.5)

Since early deletion of Tal1 resulted in lethality by E11.5, I decided to analyse the effects of tamoxifen injection at E6.5/E7.5 at the earlier time point of E9.5 embryos. Again, this resulted in global morphological abnormalities and a developmental delay in VE-CadherinCreERT2(+);Tal1$^{flox/flox}$ embryos. These embryos had turned, but formed only 19-21

somites and appeared smaller than their WT littermates that formed 23-26 somites (Figure 22, I).

Interconnected blood vessels were present in KO embryos but the vascular plexus appeared diminished and the vascular architecture distorted, indicating that initial vasculogenesis occurred but that subsequent remodelling was impaired. The intersomitic vessels were in the process of branching and anastomosis but appeared less regular compared to WT, suggesting angiogenic defects (Figure 22, C/G). Moreover, KO embryos displayed a dilated dorsal aorta, most prominently visible caudal to the pharyngeal arch arteries (Figure 22, B/F). I could also observe a distended pericardial sac, which is indicative of disrupted heart development. Despite of that beating hearts were observed shortly after dissection in KO animals.

In addition to the intraembryonic vasculature, also the vasculature of the yolk sac displayed abnormalities (Figure 22, D/H). This is reminiscent of what was reported for the global and Tie2-Cre mediated KO of Tal1. In contrast to these studies, I was able to identify the vitelline vessels and an interconnected network of ECs. However, the network appeared overgrown and immature, with almost no visible hierarchy between larger and smaller vessels.

Overall the observed phenotype of E9.5 VE-CadherinCreERT2(+);$Tal1^{flox/flox}$ mice that were induced at E6.5/E7.5 shared features with the global KO at the same developmental stage. An extended pericardial sac and lack of major vessels in the yolk sac were previously described in $Tal1^{LacZ/LacZ}$ embryos (Elefanty et al., 1999). However, the abnormalities appeared less severe compared to the global KO. Most importantly, I could detect blood inside the freshly dissected embryos, indicating that the total anaemia, that is characteristic for global Tal1 KOs, did not occur.

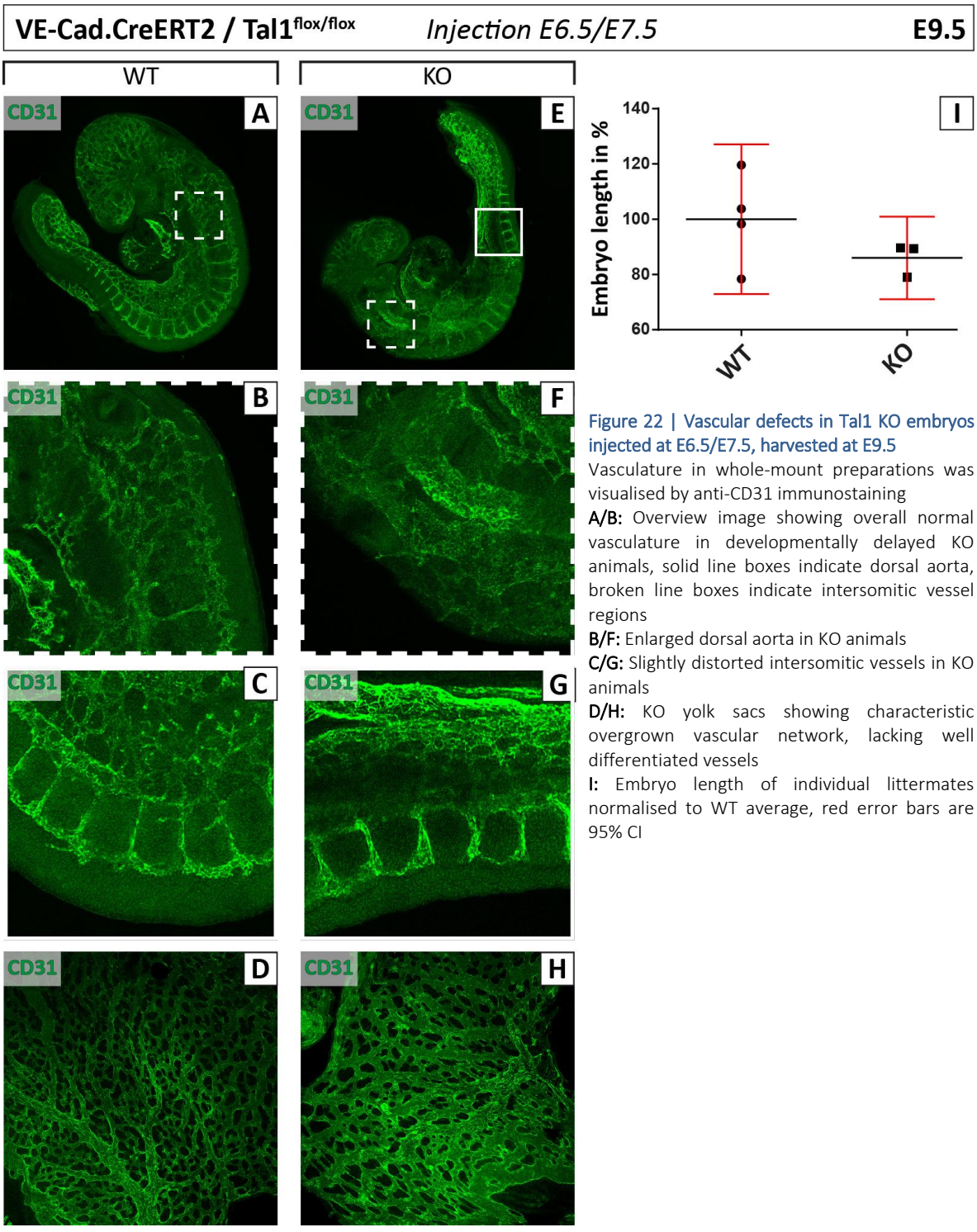

Figure 22 | Vascular defects in Tal1 KO embryos injected at E6.5/E7.5, harvested at E9.5

Vasculature in whole-mount preparations was visualised by anti-CD31 immunostaining

A/B: Overview image showing overall normal vasculature in developmentally delayed KO animals, solid line boxes indicate dorsal aorta, broken line boxes indicate intersomitic vessel regions

B/F: Enlarged dorsal aorta in KO animals

C/G: Slightly distorted intersomitic vessels in KO animals

D/H: KO yolk sacs showing characteristic overgrown vascular network, lacking well differentiated vessels

I: Embryo length of individual littermates normalised to WT average, red error bars are 95% CI

E10.5 Embryo (Injected E7.5/E8.5 and E8.5/E9.5)

To further investigate the vascular defects observed in E9.5 embryos, I continued and analysed embryos 24 h later at E10.5. In order to enable a concise interpretation of the KO phenotype I kept the short interval between tamoxifen induction and embryo harvest by injecting at E7.5/E8.5 and E8.5/E9.5, respectively.

E10.5 KO embryos injected at E7.5/8.5 displayed similar but much more severe defects then KO embryos at E9.5 (Figure 23, A/E). In particular, the cerebral vasculature architecture appeared distorted and was devoid of larger vessels like the primitive maxillary artery. In addition, large aggregations of CD31 (used as vascular marker) positive cells were visible in the posterior end of the embryo which did not form an interconnected network. Compared to E9.5 embryos, the pericardial sac was further extended and the heart seemed to be severely disorganised. No heartbeat could be detected in freshly dissected embryos.

Analysis of intersomitic vessels is especially informative as they are the first vessels in the developing embryo to form by sprouting angiogenesis (Walls et al., 2008). Similar to E9.5 KO embryos, the intersomitic vessels were present but only a subset had properly anastomosed, while the rest ended blindly (Figure 23, B/F). In particular, the anterior intersomitic vessels that surround the first somites displayed an abnormal morphology and were not properly connected to the dorsal aorta (Figure 23, C/G), indicating an early defect in vasculogenic patterning. The dorsal aorta was present but too distorted to verify if it appeared dilated, as observed in E9.5 KO embryos, or constricted compared to WT embryos.

The yolk sac vasculature was completely disorganised and lacked vitelline vessels. In contrast to previous studies that reported a reduction of ECs, I could observe a strong increase in the population of CD31 positive cells which covered almost the entire yolk sac (Figure 23, D/H). Three-dimensional reconstruction of confocal image stacks revealed that within the covered area, tubular structures were still present.

Next I investigated E10.5 embryos in which tamoxifen was injected one day later, at E8.5/E9.5. In these embryos, the vascular and developmental defects were still present but less pronounced (Figure 23, A'-H'). This could be explained either by the fact that an interval of 48 h is too short to efficiently reduce TAL1 protein levels or that the effects of Tal1 depletion are restricted to a specific developmental time window.

It is important to mention that only less than half of the embryos genotyped as KOs displayed visible defects. The most likely explanation is the variable effectiveness of the Cre recombinase induction described before. However, no embryo that did not carry the VE-CadherinCreERT2 allele showed defects that resembled the KOs. Together with the fact that I could observe the well described characteristic defects in the yolk sac vasculature of KO animals, this led me to the conclusion that the vascular aberrations observed in E9.5 and E10.5 KO animals were due to the endothelial specific depletion of Tal1.

It can therefore be concluded that induced, EC-specific deletion of Tal1 in embryos leads to intra- and extra-embryonic vascular defects. However, this effect is dependent on the time point of Cre induction, since Tal1 deletion later than ~E10.5 does not result in observable defects. Therefore, it is likely that the role of Tal1 in embryonic vascular patterning is restricted to a short developmental time window.

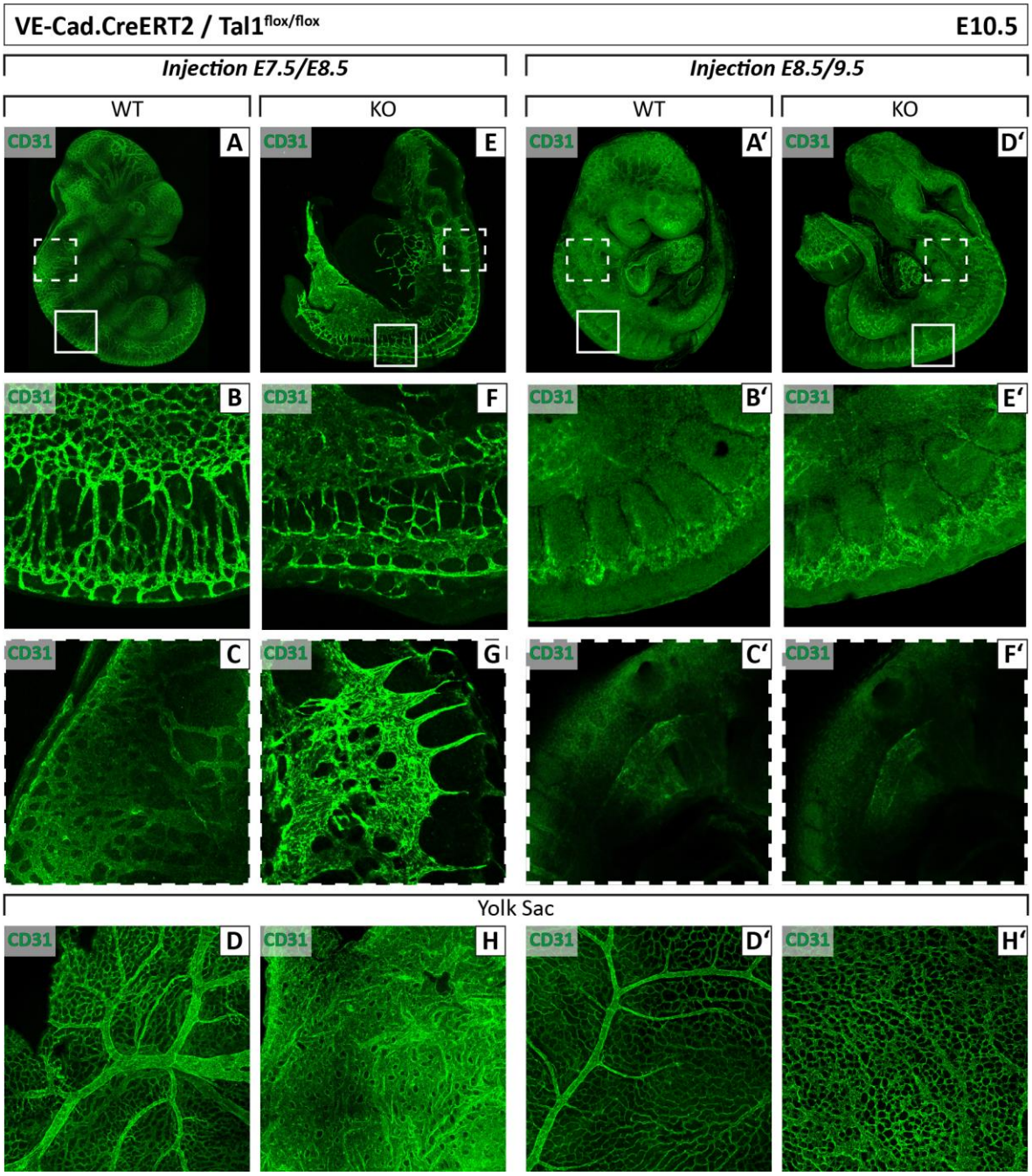

Figure 23 | Vascular defects in Tal1 KO embryos injected at E6.5/E7.5 and E7.5/E8.5, harvested at E9.5

Vasculature in whole-mount preparations was visualised by anti-CD31 immunostaining

A-H: E10.5 KO embryos that were induced at E6.5/E7.5 display more severe vascular defects compared to WT than (A'-H') E10.5 embryos induces at E7.5/E8.5

A/E: Overview image showing severely disrupted vasculature and bloated pericardial sac and (A'/E') slightly disrupted vasculature in KO embryos

B/F: Chaotic intersomitic vessels in KO embryos and (B'/F') slightly disorganised microvasculature in KO embryos

C/G: Blindly ending intersomitic vessels in KO animals and (C'/F') normal appearance of dorsal aorta in KO animals

D/H: KO yolk sacs showing characteristic sinus-like vascular network, lacking well differentiated vessels and (D'/H') less extensive yolk sac phenotype with some accounts

4.4 Immunostaining in Tal1 KO embryos

Shortly after the first identification of vascular defects in Tal1 KO embryos it has been suggested that Tal1 acts upstream of Vegfr-2, since overexpression of Tal1 leads to increased numbers of VEGFR-2 positive endothelial precursors (Gering et al., 1998). Later it has been shown by mutational analysis in reporter mice that a Vegfr-2 enhancer contains two functional Tal1 binding sites (Kappel et al., 2000). *Vice versa,* Tal1 expression is absent in Vegfr-2$^{-/-}$ embryos (Ema et al., 2003) and a mutual dependency of the two genes in specification of early haematopoietic and endothelial progenitors has been suggested (Chung et al., 2002).

Additionally, it was shown *in vitro* that Tal1 together with its binding partners E47 and Lmo2 can up-regulate VE-Cadherin in ECs (Deleuze et al., 2007) and that in zebrafish Tal1 regulates the formation of intercellular junctions, of which VE-Cadherin is a critical component (Schumacher et al., 2013).

To elucidate if these genes, which are essential for both angioblast and EC differentiation are affected the by the conditional KO of Tal1, I have investigated the expression of VEGFR-2 (Figure 24, A-D) and VE-Cadherin (Figure 24, E/F) in the vasculature of whole-mount specimens of E9.5 embryos. Although the vasculature of KO embryos displayed the previously described defects, I could detect VEGFR-2 and VE-Cadherin protein in ECs of both WT and KO animals. Faint anti-VEGFR-2 immunostaining was visible in foci within the dorsal aorta and parts of the head vasculature, whereas robust anti-VE-Cadherin staining was present in the vasculature of the whole embryo and labelled intercellular junctions of ECs.

I therefore conclude that the observed vascular defects in Tal1 KO embryos are not caused by VEGFR-2 or VE-Cadherin deficiency.

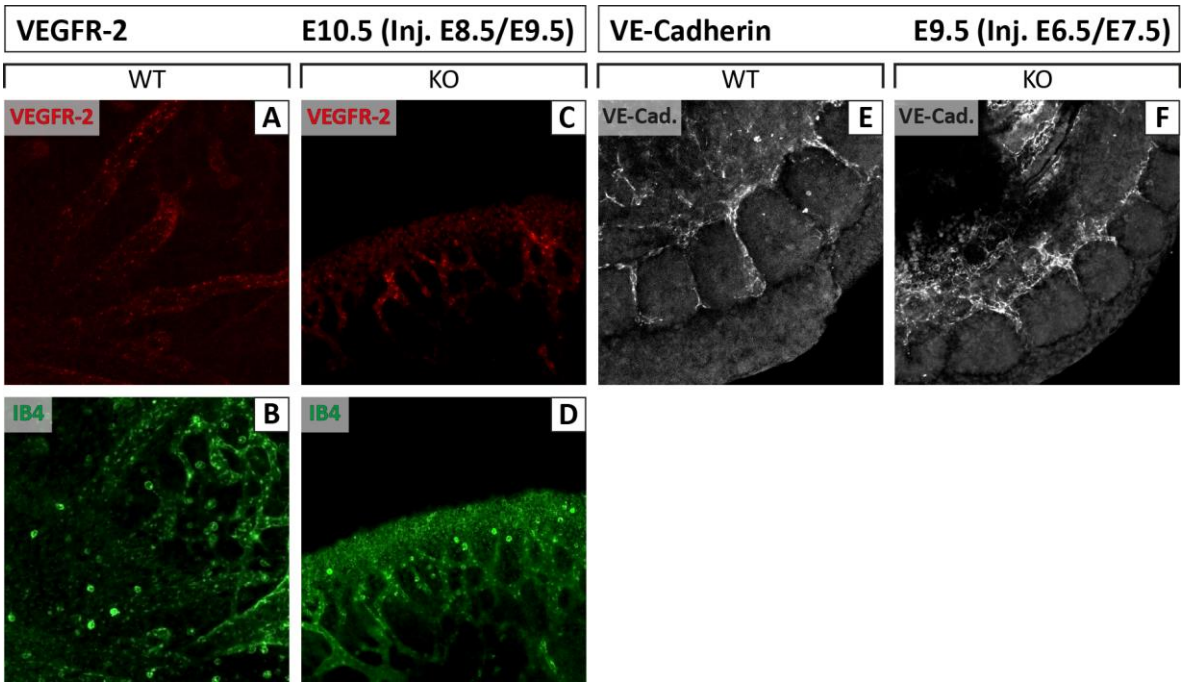

Figure 24 | Immunostaining for putative Tal1 targets VEGFR-2 and VE-Cadherin in E9.5 WT and KO embryos
A-D: Faint VEGFR-2 staining is detectable in the head vasculature of both WT (A/B) and KO (C/D) embryos, note that a slightly different frame is shown for KO and WT animals since major head vessels were absent in KO embryos
E/F: Robust VE-Cadherin staining is detectable in intersomitic vessels of both WT (E) and KO (F) animals, note the deformed intersomitic vessels in KO

4.5 Crossing of Dll4-i3smP-Cre with Tal1 $^{flox/flox}$

The newly developed Dll4-i3smP-Cre line has proved to drive Cre recombinase activity specifically in arterial ECs during embryonic development (see 5.1.4.1). Since the results from the previous conditional Tal1 KO experiments hinted towards a role of Tal1 in the formation of major vessels, with the dorsal aorta being affected, and Tal1 expression was reported to be increased in arterial endothelial cells (see 4.1), I decided to test whether arterial specific deletion of Tal1 results in a detectable phenotype. To achieve this, I crossed the Dll4-i3smP-Cre transgene into the Tal1$^{flox/flox}$ mouse line to generate Dll4-i3smP-Cre$^{+/-}$;Tal1$^{flox/WT}$ mice. As expected, those heterozygous mice were born in Mendelian ratios and showed no obvious defects. Then I set up breeding pairs of Dll4-in3smP-Cre$^{+/-}$;Tal1$^{flox/WT}$ mice and genotyped the offspring by PCR (see 2.1.5).

All 62 analysed mice were between 10 and 30 days old at the time of biopsy and displayed no obvious signs of impaired health. I expected approximately 12 mice of the Dll3-in3smP-Cre$^{+/WT}$;Tal1$^{flox/flox}$ (ratio of $^{3}/_{16}$). However, I only found two mice with that phenotype. A chi-square calculation showed with high significance ($p < 1e-8$) that the observed genotype frequencies were skewed and not within Mendelian ratios. This suggests that arterial specific KO of Tal1 may primarily be embryonically lethal. The two Dll4-in3smP-Cre$^{+/-}$;Tal1$^{flox/flox}$ animals that were observed could be explained by incomplete penetrance of the conditional KO, as previously described for the VE-CadherinCreERT line (see 4.3.1).

I have started to investigate at what developmental stage the lethality occurs and so far I could identify three phenotypically normal Dll4-in3smP-Cre$^{+/-}$;Tal1$^{flox/flox}$ embryos out of 12 embryos analysed at E13.5. This suggests that the lethality is occurring during the later phases of gestation.

The observed and expected genotype frequencies for the offspring of the Dll4-in3smP-Cre$^{+/WT}$;Tal1$^{flox/WT}$ x Dll4-in3smP-Cre$^{+/WT}$;Tal1$^{flox/WT}$ cross are shown in Figure 25.

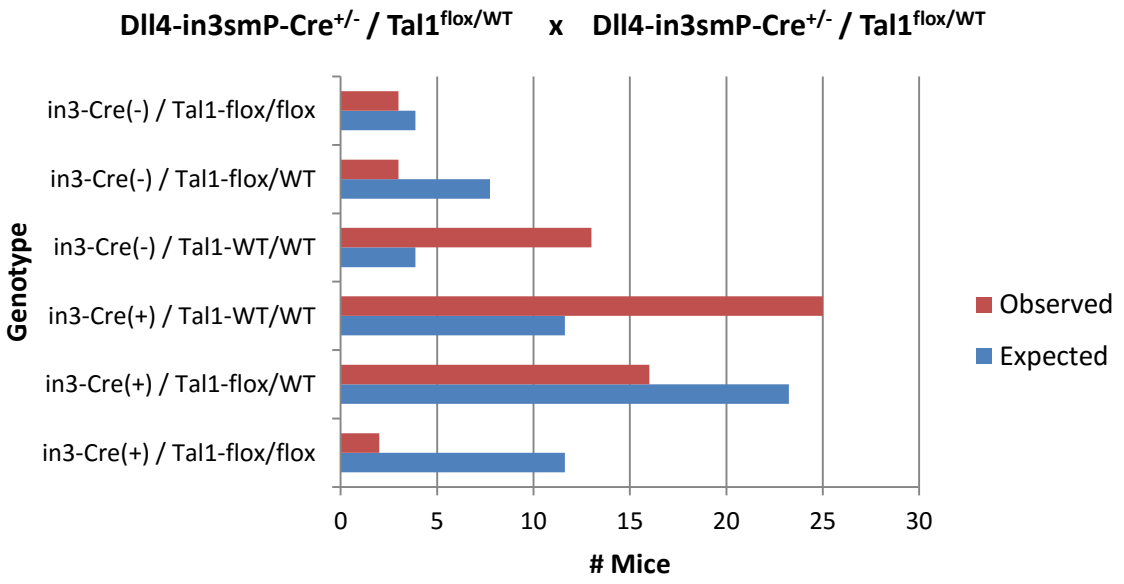

Figure 25 | Cross of Dll4-in3smP-Cre with Tal1$^{flox/flox}$ disrupts Mendelian distribution in offspring
All possible distinguishable genotypes in the offspring of the parental cross Dll4-in3smP-Cre$^{+/-}$ / Tal1$^{flox/WT}$ x Dll4-in3smP-Cre$^{+/-}$ / Tal1$^{flox/WT}$ are shown with their respective absolute observed and expected frequencies.
In total 62 mice were genotyped; Chi-square: 50.125, $p < 1e-8$

4.6 Conclusions

Similar to the analysis of a possible role of Tal1 in postnatal angiogenesis, I have also investigated Tal1 expression patterns and the effects of induced Tal1 deficiency in the endothelium of mouse embryos.

4.6.1 Tal1 Expression in the Embryonic Vasculature

Contrary to previous reports, I found very little evidence of Tal1 expression in the vasculature using the $Tal1^{LacZ/WT}$ reporter line. As discussed earlier in 3.4.1, this may be due the fact that the $Tal1^{LacZ/WT}$ mouse line may not accurately mimic endogenous Tal1 expression or that the single integrated transgenic allele produces a reporter signal too weak for detection. The fact that I found little expression of Tal1 in the hematopoietic system, where it fulfils well established roles, supports this hypothesis.

However, it should also be noted that previous studies using the $Tal1^{LacZ/+}$ line reports stronger staining than I could reproduce. Because I could generate strong whole-embryo X-Gal staining in other experiments, for example during the characterisation of the Dll4-in3smP-Cre line, I would exclude the possibility that this is due to technical shortcomings. Moreover, the staining intensity in other tissues such as the midbrain, resembled the previously published results. Considering that the original mouse line was created more than one decade ago, it is possible that LacZ expression levels in my mice are reduced due to genetic drift or mutation. Eventually, I do not have a satisfying explanation of the partial difference in expression strength.

The expression detected by immunostaining in putative peripheral ECs and haematopoietic cells in E8.5 embryos corroborates the widely accepted theory of Tal1 delineating the fate of hemangioblasts or hemogenic endothelium. The observation that Tal1 might be preferentially expressed in the endothelium of arteries is interesting considering the fact that Tal1 morpholino treated zebrafish lose arterial gene expression (Patterson et al., 2005). The authors

of this study argue that Tal1 might act upstream of VEGF and therefore a lack of Tal1 primarily affects arterial development. Together with my finding that Tal1 depleted E9.5 embryos display an abnormally formed dorsal aorta, this could hint to an additional, cell autonomous function of Tal1 in arterial development, rendering the arterial specific KO of Tal1 quite interesting. However, it has to be noted that the results from immunostaining were slightly compromised due to strong unspecific signals.

4.6.2 Effects of Tal1 Depletion on the Embryonic Vasculature

It has been reported that mouse embryos with a global deficiency for Tal1 die at ~E9.5 due to the effects of complete anaemia (Shivdasani et al., 1995), whereas Tie2-Cre/Tal1$^{flox/flox}$ mice die at ~E13.5 primarily from systemic oedema and haemorrhage (Schlaeger et al., 2005). Vascular defects have been reported in both studies but remained poorly described, largely because of the use of the dual lineage Tie2-Cre mouse line. I therefore hoped that by using the endothelial-specific inducible VE-CadherinCreERT2 line to delete Tal1 during different developmental stages, we would be able to re-investigate how EC specific Tal1 deficiency influences intra- and extraembryonic vascularisation. Using this system I have now demonstrated that tamoxifen-induced deletion of Tal1 in endothelial cells at time points later than E9.5 does not lead to observable embryonic defects, demonstrating that Tal1 is not required for later stages of embryonic vascular development.

Fascinatingly, tamoxifen induced deletion of Tal1 in endothelial cells starting from E7.5 resulted in lethal developmental defects in E11.5 embryo, so severe that they precluded a detailed analysis of the vasculature. Only by taking the embryos a day early, at E10.5, was I able to obtain sufficiently healthy embryos for analysis of the effects of Tal1 knockout. Some of the observed vascular defects, such as the aberrant dorsal aorta and disorganised yolk sac vasculature support a role of Tal1 in early vasculogenesis, while others, such as the misshaped and partially unconnected intersomitic vessels indicate a certain involvement in angiogenesis.

Moreover, the extension of the pericardial sac, ranging from moderate to severe, was observed in all KO embryos. This is indicative of disturbed heart function and has been previously described in Tal1 deficient E9.5 embryos (Elefanty et al., 1999).

Overall, I have demonstrated that VE-CadherinCreERT2 mediated induced EC-specific KO of Tal1 resulted in more severe defects than what was reported for Tal1 deletion mediated by the Tie2-Cre mouse line. I have already illustrated the possible shortcomings of the Kisanuki mouse line and hold the view that this mouse line is less than perfect for analysing vascular phenotypes. Nevertheless, the more severe phenotype of the induced Tal1 KO is an unexpected result, raising questions about the reproducibility and transferability of KO experiments. A plausible explanation to consider would be that side-effects of the tamoxifen injection itself add to the severity of the KO phenotype, potentially because of the anti-estrogenic properties of tamoxifen (Jordan and Murphy, 1990). However, due to the fact that I have injected progesterone in parallel (see 2.1.3.1) and only very rarely observed developmental defects in WT animals, I would exclude this possibility. Moreover, it is a well-known issue in the study of genetically engineered mice that genetic background onto which a modified allele is placed can cause considerable variation in the resulting phenotype (Doetschman, 2009). Therefore, a possible approach to validate my results would be to intercross the VE-CadherinCreERT2;$Tal^{flox/flox}$ mouse line with a mouse of different genetic background and partially repeat my experiments.

It must be noted that analysis of the effects of EC-specific deletion of Tal1 in the embryo is complicated by the severe developmental defects that accompany a lack of nourishment that is most likely induced by the defective yolk sac vasculature. It is therefore likely that the striking developmental delay I detect in E11.5 KO animals was primarily downstream of these defects. An additional explanation for the yolk sac phenotype is the possibility that lack of flow can lead to an over proliferation of yolk sac vasculature. Although it first seems counter-intuitive, it has been shown in avian and mouse yolk sacs that reduced shear stress, caused by lower cardiac output or reduced haematocrit content, leads to a failure of network remodelling and thereby

to an overgrown vascular network, reminiscent of what is observed in Tal1 deficient embryos (Chouinard-Pelletier et al., 2013; Lucitti et al., 2007). As suggested by the extended pericardial sac, it is likely that in the VE-CadherinCreERT2 mediated Tal1 KO the hemodynamic forces are reduced as well.

The fact that embryos that are double transgenic for both Dll4-in3smP-Cre and $Tal^{flox/flox}$ are not born in Mendelian ratios is an interesting observation that is worth following up. A likely explanation would be that, in contrast to absent primitive haematopoiesis observed in global $Tal1^{-/-}$, these embryos die due to defective definitive haematopoiesis caused by deletion of Tal1 in the arterial derived hemogenic endothelium. This hypothesis is supported by the observation that, when activated early enough, the Dll4-in3smP construct labels circulating cells (see 5.1.7.1). Moreover, it has been established in the literature that besides its role in differentiation of haematopoietic lineages from HSCs (Porcher et al., 1996; Robb et al., 1996), Tal1 is also essential for specifying the hemogenic endothelium from the haemangioblast in blast colony experiments (Van Handel et al., 2012; Lancrin et al., 2009). In addition, it has been demonstrated by *in vivo* imaging in zebrafish that loss of Tal1 results in impaired formation of the hemogenic endothelium (Zhen et al., 2013). However, to my knowledge the same has not yet been shown in mouse embryo, rendering the Dll4-in3smP-Cre mediated KO of Tal1 highly interesting.

The role of Tal1 in specification of the hemogenic endothelium also has implications for the short developmental interval in which the induced endothelial specific Tal1 deletion is embryonic lethal. Considering that when tamoxifen is injected at E9.5, the hemogenic endothelium can probably be specified before the KO becomes effective, whereas an early Tal1 deletion in arteries effects the hemogenic endothelium.

An alternative explanation for the embryonic lethality of Dll4-in3smP-Cre;$Tal^{flox/flox}$ mice would be that proper heart development is impaired, since the Dll4-in3smP-Cre line did label endothelial derived structures in the heart at E11.5 and Tal1 was shown to regulate the formation of endocardial intercellular junctions in zebrafish (Schumacher et al., 2013).

Finally, it should be stressed that the results of the Dll4-in3smP-Cre / $Tal^{flox/flox}$ cross are very preliminary and need further investigation. As discussed in the next section, the Cre mediated KO of Tal1 is probably not restricted to arteries and hemogenic endothelium but encompasses parts of the microvasculature and heart as well.

Chapter 5:

Development of Arterial Specific Cre Mouse Models

5.1 Development of Arterial Specific Cre Mouse Models

At the time when this project was conceived, no suitable transgenic mouse lines that direct pan-arterial EC specific gene inactivation from early on in development were available. One existing system is the Bmx(PAC)-CreERT2 mouse line which allows inducible conditional Cre expression in arterial ECs using the bone marrow x (Bmx) tyrosine kinase promoter (Ehling et al., 2013). One major drawback of this mouse line is that the detailed expression patterns and functions of Bmx in the vasculature are ill-defined. Bmx has been shown to be expressed in the endocardium and the endothelium of larger arteries (Ekman et al., 1997). Although there are three published studies using this mouse line, an initial study investigating the Bmx-LacZ expression pattern demonstrates the limitations of this mouse model (Rajantie et al., 2001). Bmx expression is only activated at E12.5, too late to study the formation of the first major arteries. Moreover, Bmx-LacZ expression is seen only in a few large arteries, and was not completely arterial specific, as β-Gal staining was detected in the thymus, the tongue, the heart, and the venae cavae. Indeed, a recent study using the Bmx-CreERT2 line revealed that it is not active in arterioles (Murphy et al., 2014).

The second existing mouse model, $Sox17^{iCre}$, uses a knock-in of Cre-recombinase at the locus of the transcription factor Sry-related HMG box 17 (Sox17) (Liao et al., 2009). A major disadvantage of this system is that one allele of Sox17 is lost, since Sox17 is essential for arterial development (Corada et al., 2013). Despite the fact that the $Sox17^{Cre/+}$ mice are phenotypically normal, the loss of one allele may have synergistic effects if the mouse line is used to delete other genes, masking the genuine underlying mechanisms of a phenotype. Further, since Sox17 is involved in specification of definitive endoderm, it is not surprising that Cre activity was also detected in organs of endodermal origin like the hindgut, thymus, and liver. Consequently the $Sox17^{Cre/+}$ mouse line has not yet been used for arterial specific knockout experiments.

Although recent research has revealed several arterial and venous specific molecular markers, many aspects of arterial-venous specification remain elusive. In particular, the plasticity of arterial and venous identity is relatively poorly understood but of great medical importance,

for example in scenarios like bypass operations and dialysis therapy, where vessels are surgically forced to adopt a new identity (Wallitt et al., 2007).

As the embryonic lethality of Tal1 deficient mice at E9.5 precludes further investigation of later angiogenic or vasculogenic defects, inducible KO strategies are required. Moreover, my initial results from induced Tal1 KO experiments in mouse embryo suggested a possible involvement of Tal1 in arteriogenesis. With the aim of performing an artery specific knock-out of Tal1 in embryos and to provide a valuable tool for the research community I have generated two novel arterial specific Cre recombinase mouse lines.

5.1.1 Identification of a Minimal Dll4 Promoter

To generate this arterial specific Cre lines, I utilised an enhancer that was found in the third intron of Notch ligand Dll4 (Dll4in3). It was identified recently by our lab and was shown to direct LacZ reporter gene expression very specifically to arterial ECs from early on in development at E9.0 (Sacilotto et al., 2013). However, the reporter constructs used in this study contain the heat shock protein 68 (hsp68) minimal promoter which is unsuitable for the generation of Cre mice, as it can lead to ectopic gene expression, primarily in the ventral neural tube (Kothary et al., 1987), and later in development also in other parts of the embryo (personal observation). It has recently been shown that the Dll4 5' region alone is not sufficient to drive arterial expression (Wythe et al., 2013). Therefore, I decided to use the endogenous mouse Dll4 promoter in place of the hsp68 minimal promoter, fused directly to the Dll4in3 enhancer to construct a transgene that mimics the highly arterial specific aspect of the Dll4 expression spectrum (Benedito and Duarte, 2005). Consequently, my first aim was to identify the endogenous Dll4 promoter, and to ensure that the resulting transgene construct was able to drive arterial endothelial specific expression of a reporter gene in transgenic mice, before creating constructs using the Cre recombinase.

A classical promoter fragment consists of around 100 - 1000 bp upstream and up to 200 bp downstream of the transcription start site (TSS). However, it is nontrivial to define a core minimal sequence that is necessary to drive the expression of a gene as recent publications suggest that most genes lack classical functional elements like TATA or CAAT boxes altogether (Yang et al., 2007). By combining a review of the literature with analysis of evolutionary conservation and the promoter prediction tool PromoterExplorer (Xie et al., 2006), I was able to identify two promising promoter sequences.

5.1.1.1 Literature Review

The mouse Dll4 promoter was not yet subject to intensive sequence characterisation. Therefore, I focused on studies about the human Dll4 promoter and transferred the results to the orthologous mouse sequence.

In a study of the transcriptional response of Dll4 towards hypoxia, with a special focus on endothelial activation of arterial cell fate, a 6 kb fragment upstream of the TSS was considered the full length promoter. Subsequently shorter fragments were created by restriction digest and tested with regard to their transcriptional induction by hypoxia. A 1.5 kb fragment containing several HRE and RBP-JK binding sites showed the strongest Dll4 induction (Diez et al., 2007).

A later study focused on the activation of Dll4 by VEGF-A and the feed-forward stabilisation of Dll4 expression by NICD1/NICD4 in ECs (Caolo et al., 2010). Their choice of possible promoters referred to the fragments already described by Diez *et al*. In their study a 2.6 kb fragment generated the strongest induction. Interestingly, this 2.6 kb fragment does not contain the Forkhead binding element (FBE) which other studies considered to be crucial for the VEGF-A mediated Dll4 transactivation through the Forkhead transcription factor FOXC2 (Hayashi and Kume, 2008). Moreover, it was shown that canonical Wnt/β-catenin signalling can upregulate Dll4 expression in ECs during vascular development (Corada et al., 2010). The binding site for

the TCF/LEF transcription factor that mediates Wnt signalling was contained in the 2.6 kb fragment.

An even smaller fragment capable of Dll4 induction was identified by another study which focused on the transcriptional regulation of endothelial sprouting. A 0.5 kb fragment with several ETS binding sites showed significant induction by VEGF-A, despite lacking all Forkhead and TCF/LEF binding sites (Roukens et al., 2010).

The promoter fragment for the generation of the arterial specific KO mouse line should be as small as possible to rule out any non-arterial expression, as Dll4 is also expressed in the gut and nervous system (Benedito and Duarte, 2005). However, it should also be long enough to include the minimal signals necessary for transcriptional induction. In order to find a compromise I chose one murine Dll4 promoter fragment homologous to the 2.6 kb fragment (hereafter referred to as "mP") that was first described Caolo *et al*. and a shorter one homologous to the 0.5 kb fragment (hereafter referred to as "smP") first described by Roukens *et al*. and decided to test them both.

5.1.1.2 Evolutionary Conservation of the Dll4 Promoter

To ensure that my fragment covers the important regulatory elements of the promoter and to find the appropriate mouse homologues to the human promoter fragments, I used the ECR browser (http://ecrbrowser.dcode.org) to perform a genome comparison. Deep evolutionary conservation has been shown to be a reliable indicator for identification of tissue-specific regulatory elements (Pennacchio et al., 2006).

I found that the shorter smP fragment covers a proximal deeply conserved region around the TSS and the longer mP fragment covers an additional, more distal, deeply conserved region. The threshold applied for sequence length (100 bp) and conservation level (77%) used to define an evolutionary conserved region (ECR) has been proven to be efficient for identifying functional elements (Ovcharenko et al., 2004). As both fragments appeared promising, I used both of them

to generate LacZ reporter constructs. An even more distal conserved region was recognised but not taken into consideration because the resulting promoter fragment would have been too large for effective transgene generation.

The position of the TSS provided by the RefSeq database (http://www.ncbi.nlm.nih.gov/refseq) was confirmed with help of the software PromoterExplorer (Xie et al., 2006), which utilises pentamer (sequence of 5 base pairs) distribution, CpG island features, and the local sequence features to predict promoter sites.

A schematic overview of the evolutionary conservation of the Dll4 promoter region and the position of the mP and smP fragments is given in Figure 26.

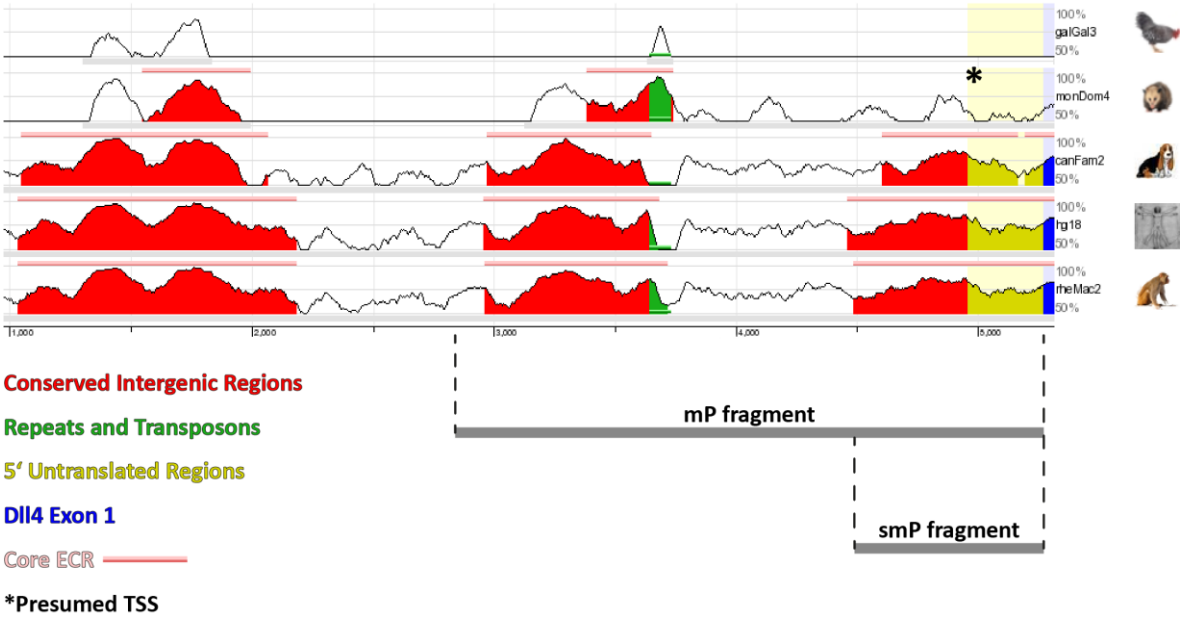

Figure 26 | Analysis of evolutionary conservation in Dll4 5' promoter region
Graphic generated with ECR browser; Core ECR: region of minimal 100 bp with a minimal conservation of 77 %; Positions of the long (mP) and short (smP) promoter fragments are indicated as grey bars; Asterisk indicates position of putative transcriptional start site (TSS); Mouse sequence was compared with chicken (galGal3), opossum (monDom4), dog (canFam2), human (hg18) and rhesus monkey (rheMac2) reference genomic sequences

5.1.2 Test of Dll4 Promoter/Enhancer Reporter Constructs

As the creation of stable mouse lines is a cost- and work-intensive process that can take up to one year, it is crucial to test the functionality of the transgene of interest in advance. Therefore, both putative Dll4 enhancer/promoter fragments were cloned upstream of the LacZ reporter gene and subsequently these reporter constructs were used to create transgenic mouse embryos by pronuclear injection, see 2.7 for a detailed cloning strategy.

In comparison with targeted transgenesis, pronuclear injection is an easier and faster technique as it does not need extensive pre-selection of transfected embryonic stem cells. In contrast to targeted approaches where genes are inserted, deleted or modified in a site-specific manner, pronuclear injection leads to integration of the transgene at random positions within the genome. A disadvantage of random integration of the transgene into the genome is that positional effects, integration number and orientation of integration are not controllable. Integration within heterochromatin or integration of large transgene concatemers can lead to completely silent transgenes (Ittner and Götz, 2007). Conversely, if the integration site is positioned in proximity to a strong regulatory element, undesired transgene expression can occur. Therefore, it was necessary to perform multiple injections to show the full expression spectrum of the reporter constructs.

5.1.2.1 X-Gal Staining of Embryo Whole-Mounts and Sections

Embryos resulting from pronuclear injections were euthanised at E15.5 and directly X-Gal stained and subsequently embedded in paraffin and sectioned. The transgenic status of the embryos was confirmed in parallel by genotyping PCR.

In total, five transgenic Dll4-in3mP-LacZ and four Dll4-in3smP-LacZ embryos were analysed. In non-transgenic embryos that served as negative controls no X-Gal staining could be observed. Dissection of X-Gal stained embryos revealed that both constructs direct highly arterial specific transgene expression at E15.5 with comparable efficiency. Staining was

detectable in ECs of both larger arteries like central tail artery and maxillary arteries and smaller arterioles throughout the whole embryo and within the yolk sac. Surprisingly, no X-Gal staining could be observed in the dorsal aorta although this is likely to be related to problems with X-Gal infiltration into the centre of the embryo. Arteries and veins could be distinguished by morphology, as arteries are enveloped in a thick sheet of smooth muscle cells which veins lack, and in certain cases, by location. In paraffin sections of both Dll4-in3mP-LacZ and Dll4-in3smP-LacZ transgene carrying embryos X-Gal staining was observable in a few circulating cells, mainly within veins.

The results from the injections of the in3mP-LacZ and in3-smP-LacZ reporter constructs are shown in Figure 27 and Figure 28.

Figure 27 | Expression of Dll4 in3mP-LacZ (long) construct in E15.5 embryos
X-gal staining of embryo and yolk sac whole mount preparations and X-Gal/Nuclear Fast Red co-stained 5 µm paraffin sections
I: Schematic representation of the transgene construct, Dll4 Intron 3 enhancer in3 was cloned in front of long Dll4 promoter fragment mP and the reporter gene LacZ
A-E: Representative overview images of embryo displaying the weakest (but not absent) staining strength
A'-E': Representative overview images of embryo displaying the strongest vascular specific staining strength
A/A': Embryo overview showing global arterial expression pattern
B/B': Yolk sac whole mounts, veins are naturally stained red due to remaining blood trapped in the vessel
C/C': Transverse section through embryo epithelium with positively stained arterioles and negative venules and few X-Gal positive circulating cells in C'
D/D': Magnification of head region with positive external maxillary arteries
E/E': Magnification of back region with positive arterial tree
A: arteries; V: veins, distinguished by morphology


Dll4 Intron 3 Enhancer Construct (i3)
End Intron2
Exon3
Intron 3
Beginning Exon 4
mP
LacZ reporter gene
I

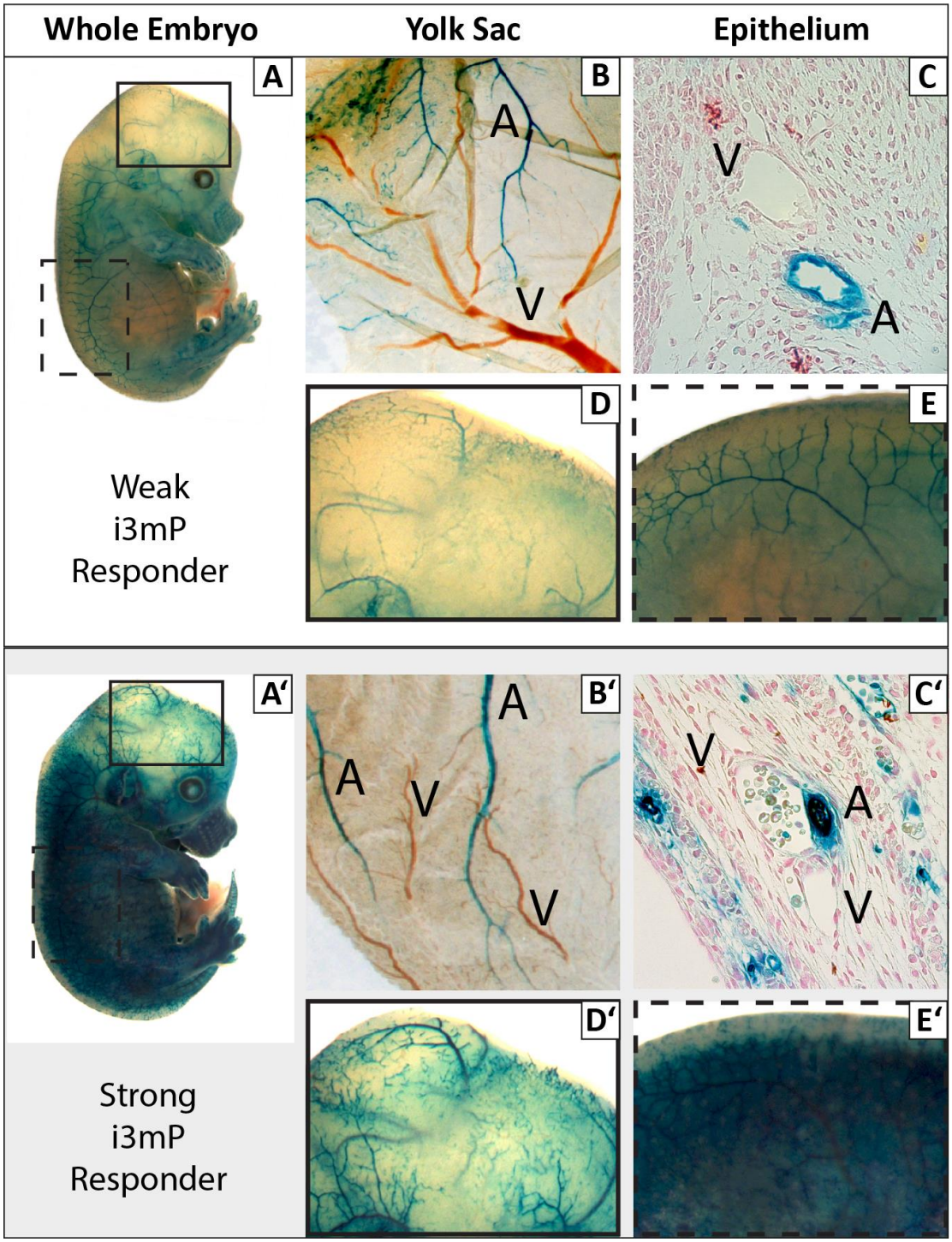
Whole Embryo
Yolk Sac
Epithelium
A
B
C
A
V
V
A
D
E
Weak
i3mP
Responder
A'
B'
C'
A
A
V
V
V
A
V
D'
E'
Strong
i3mP
Responder

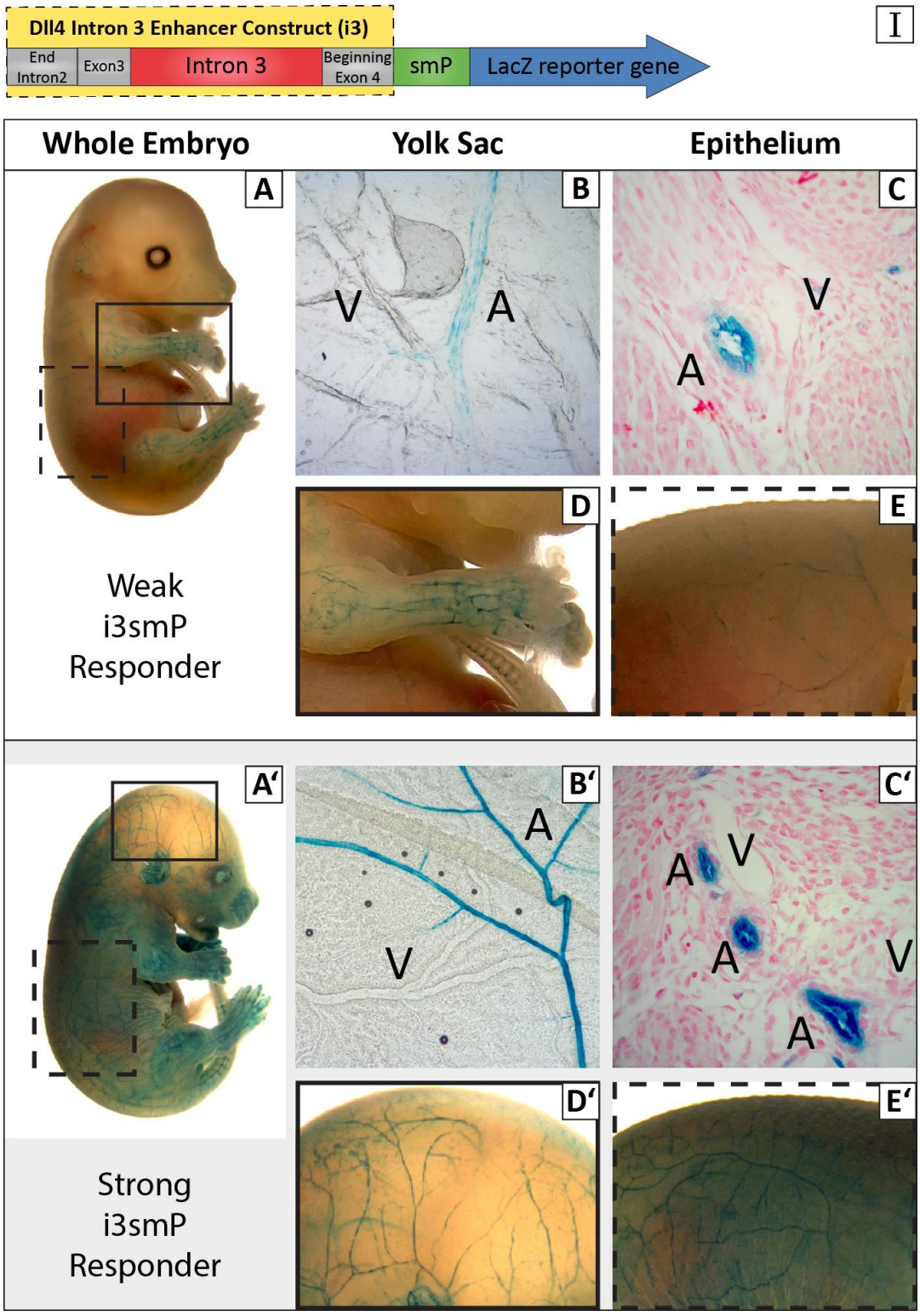

Figure 28 | Expression profile of Dll4 in3smP-LacZ (short) construct in E15.5 embryos
Labelling is analogous to Figure 27

5.1.2.2 IHC Analysis of Embryo Sections

In order to confirm that the reporter gene expression is restricted to arterial ECs, an immunohistochemical (IHC) analysis was performed. For that I have used the established molecular markers Nrp1 for arterial (Gu et al., 2003) and Endomucin for venous (Morgan et al., 1999) endothelial identity. Moreover, the X-Gal staining requires fully fixed tissue but the size of E15.5 embryos precludes the PFA from diffusing into the core tissues. This difficulty can be overcome by IHC staining on sections. However, the problem can arise that strong fixation which enables good X-Gal staining and fine histological analysis precludes specific IHC staining as the epitopes which are recognised by the molecular markers become masked.

Sections of all embryonic tissues were analysed thoroughly and the results mostly corroborated the conclusions from the X-Gal staining. Both constructs displayed a highly arterial specific expression pattern in all embryonic tissues. LacZ expression co-localised with the arterial marker Nrp1 and never overlapped with the venous marker Endomucin. The most intensive LacZ signals could be observed in the microvasculature of the epidermis, whereas the dorsal aorta did display very faint staining. An exception could be observed within the intestinal wall of embryos injected with in3mP-LacZ where lines of elliptic patches were visible. Co-staining with Nrp1 and the lack of a detectable vessel lumen suggested that these were not arterial structures. However, the same phenomenon could not be found in embryos injected with Dll4-in3smP-LacZ.

The results of the IHC experiments are summarised in Figure 29.

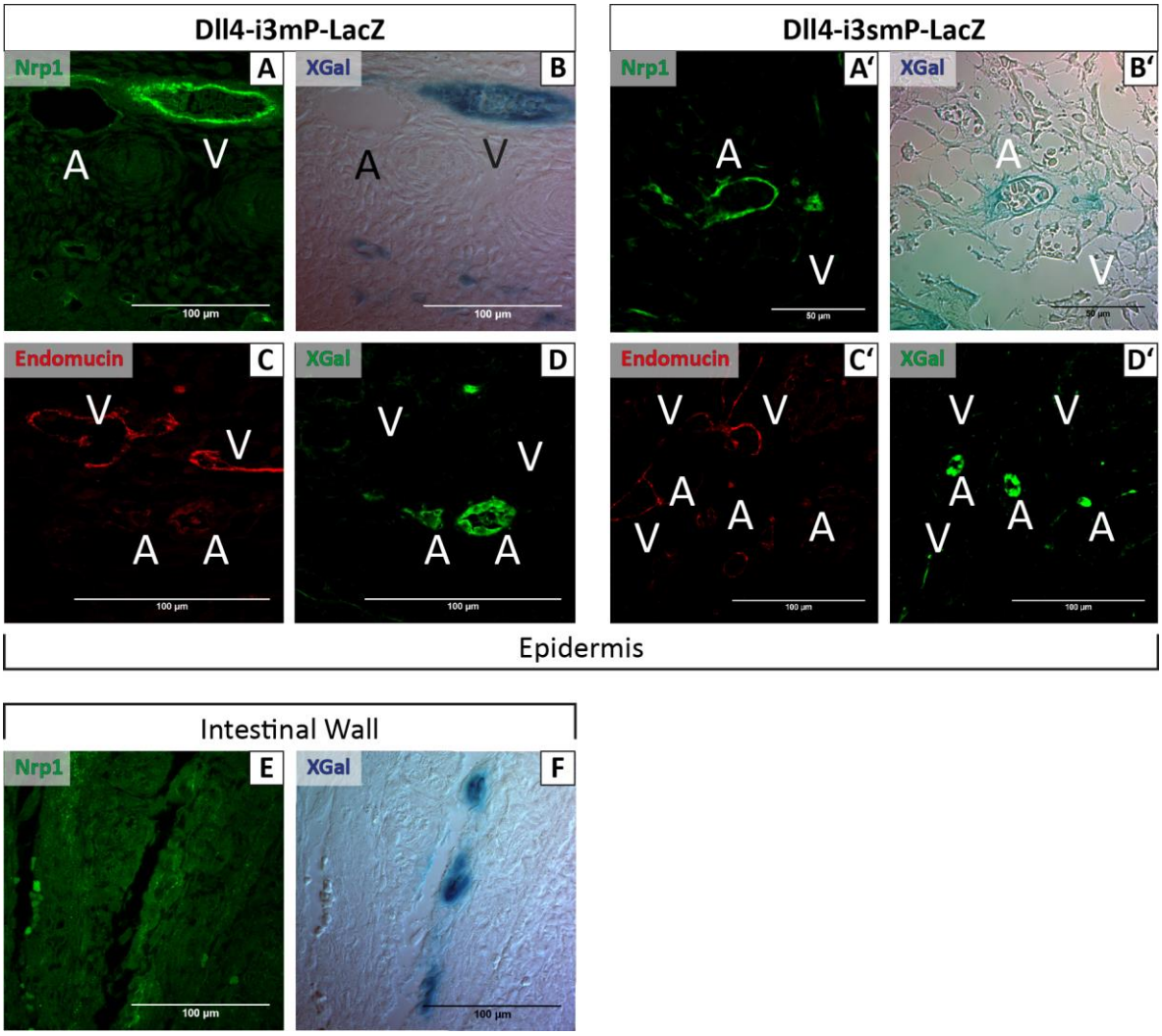

Figure 29 | IHC staining against arterial and venous markers on paraffin sections of E15.5 Dll4 in3 mP/smP-LacZ embryos
A/A'-B/B': Endogenous Nrp1 is positive in arterial ECs and co-localises with X-Gal pseudo-transmission staining
A'-D': Endomucin staining is venous-specific and does not overlap with Beta-Gal-IHC staining
E-F: In Dll4 in3mP-Lacz embryos X-Gal staining which did not co-localise with arterial markers could be observed in the intestinal wall

5.1.3 *In Vitro* Test of Dll4-in3smP-Cre and Dll4-in3smP-CreERT2

After the LacZ reporter experiments in mouse embryos demonstrated that both the longer in3mP and the shorter Dll4-in3smP construct drive highly specific expression within the arterial endothelium, I decided to continue the experiments with the shorter Dll4-in3smP. Shorter fragments are easier to handle in further cloning, transfection, and finally transgenesis experiments. Moreover, a smaller fragment simplifies further manipulations such as mutagenesis of the constructs and the Dll4-in3smP fragment also did not display the non-arterial expression pattern of in3mP within the intestinal wall.

Therefore, I cloned the i3smP construct upstream of the ORF of constitutively active Cre and Tamoxifen-inducible CreERT2 recombinase, followed by a β-Globin/SV40 termination sequence to avoid RNA polymerase read-through (see 2.7 for detailed cloning strategy).

Before stable transgenic mouse lines harbouring the i3smP-Cre/CreERT2 transgenes could be created, a final proof-of-principle test was required. To ensure that the promoter/enhancer construct efficiently drives expression of the Cre gene, I transfected it into primary mouse endothelial fibroblasts (MEFs) which carry the ROSA26R-LacZ (R26R-LacZ) reporter construct. The R26R construct contains a floxed stop cassette upstream of the LacZ gene. If the Cre-recombinase is active, the stop cassette is excised, which leads to subsequent expression of the LacZ gene (Soriano, 1999). Therefore, X-Gal staining on transfected R26R-LacZ MEFs enabled me to monitor the effectiveness of induced or constitutive Cre-recombinase expression.

Both constructs successfully drove expression of Cre which led to the activation of the LacZ gene resulting in positive XGal staining. No stained cells were detected within the negative controls, which included the addition of ddH_2O instead of vector DNA to the transfection mix and addition of ddH_2O instead of tamoxifen for induction. Note that the amount of stained cells transfected with inducible Dll4in3CreERT2 was significantly lower than in cells transfected with Dll4in3Cre. A possible explanation could be the fact that the pCRII-Dll4-in3smP-CreERT2 plasmid transfected with lower efficiency compared to the transfection-control plasmid

pSUPER-Tomato, probably due to its larger size (8.8 Kb vs. 4.6 Kb). Moreover, the tamoxifen induction may not yet have reached its peak after 48 h when the cells were fixed and the X-Gal staining was performed. Also, the lower overall cell number of the tamoxifen treated samples, which is probably due to toxic effects of tamoxifen and the prolonged culturing time of the primary cells after electroporation, has negatively influenced the staining efficiency.

A representative set of microscopy pictures and a schematic illustration of the transfected constructs are shown in Figure 30.

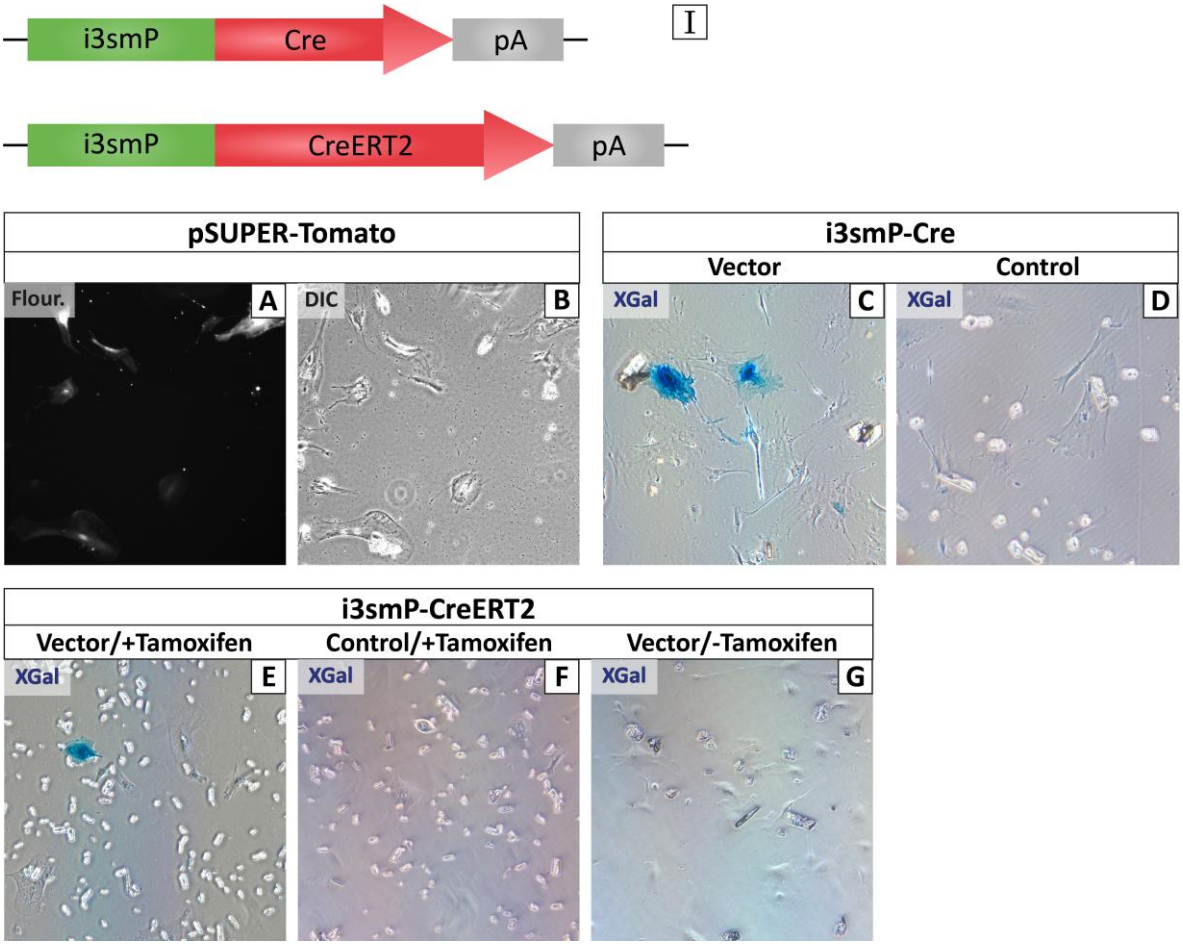

Figure 30 | *In vitro* activity test of in3smP-Cre and in3smP-CreERT2 constructs in R26R-LacZ MEFs
I: Schematic representation of the Cre and CreERT2 transgene constructs, Dll4 Intron 3 enhancer/promoter (in3smP) was cloned in front of the Cre/CreERT recombinase which is followed by the β-Globin / SV40 polyA termination sequence (pA)
A/B: Transfection control with pSUPER-Tomato; Fluorescence and DIC image, transfection efficiency was 20-30 %
C-G: DIC images of XGal staining on fixed cells, D, F and G are negative controls

5.1.4 Founder Line Identification and Characterisation

As the previously described experiments demonstrated that the Dll4 intron 3 enhancer/promoter constructs shows arterial specific expression patterns *in vivo* and proved to be capable of driving Cre and CreERT2 recombinase expression *in vitro*, I decided to continue and generate stable transgenic mouse lines.

Similar to the generation of reporter-lines described in 5.1.2, the transgenes were introduced into the mouse genome via pronuclear injection. However, this time the surrogate mothers were allowed to deliver the transgenic animals, which now represented transgenic line founders. As mentioned before, due to the random integration of transgenes through pronuclear injection, all founder animals have different expression patterns depending on the transgene locus. The offspring of a single founder animal will however all share the same transgene locus.

Therefore, male founders resulting from injection of Dll4-in3smP-Cre and Dll4-in3smP-CreERT2 constructs were directly bred with R26R-LacZ reporter mice and the embryos X-Gal stained and analysed at E13.5. Female founders were first crossed with WT mice to maintain the line and the resulting offspring subsequently were crossed with R26R-LacZ to analyse the embryos. For Dll4-in3smP-Cre three founders were analysed in total, from which one did not show any transgene expression and one displayed expression patterns that did not match the results of the previous experiments. For Dll4-in3smP-CreERT2 three founders were analysed in total, from which one did not show any transgene expression. I could identify one constitutively active Cre founder line (named L3) and two inducible CreERT2 founder lines (named L1 and L2) which showed arterial specific expression and decided to perform an in-depth analysis of their expression patterns. This was necessary in order to characterise them as future tools for arterial specific deletion, since exact information on the temporal and spatial distribution of Cre recombinase activity is crucial for meaningful KO experiments. The kinetics of tamoxifen, when administered at various developmental stages to induce Cre activity, add another factor that needs to be considered when interpreting KO phenotypes.

In addition to characterising the Cre lines, the analysis of the Dll4in3Cre and CreERT2 lines with the R26R-LacZ reporter line offers another opportunity of cell lineage tracing. All cells that activate the LacZ reporter gene upon tamoxifen induction keep the gene active and inherit the active gene to all daughter cells because the excision of the stop cassette is irreversible. As described in the introduction the two main processes, vasculogenesis and angiogenesis, by which the embryo is vascularised are heavily studied and a great amount of mechanistic details could be unveiled in recent years. However, the transition between both processes as well as ontogeny of arterial and venous endothelial cells is less well understood. With the ability to label ECs with arterial identity at a certain developmental stage and to track them and their progeny throughout embryonic and postnatal development, I decided to make additional use of the transgenic mouse lines and to elucidate the contribution of Dll4 positive arterial ECs to vascular and endocardial development.

5.1.4.1 Dll4-in3smP-Cre Expression in Embryo

Expression of Dll4 in the vascular system was reported to initiate at E8.0 in the cardiac crescent and the primordia of the dorsal aorta (Duarte et al., 2004). Moreover, Sacilotto *et al.* showed that the Dll4-in3-hsp68-LacZ transgene is active at E9.0 (Sacilotto et al., 2013). Therefore, I decided to choose E8.5 as the earliest developmental stages for a meaningful analysis. A slight delay in detectable expression was expected, since the process of Cre dependent R26R-LacZ transgene activation requires some time.

E8.5 Embryo

I could not detect any X-Gal staining in E8.5 embryos and moved on to E9.5 embryos as a next step in order to find the earliest point of detectable transgene activation.

E9.5 Embryo

X-Gal staining could be observed in E9.5 embryos but not in the yolk sac. The walls of the dorsal aorta and the pharyngeal arch arteries were X-Gal positive, with the staining within the dorsal aorta fad ing out towards the caudal aspect of the embryo. Moreover, a few patches of staining could be observed in the head which most likely correspond to parts of the internal carotid artery. Patchy staining could be observed in the ventral aspect of the heart.

The most intense staining was present within a tube-like structure in the anterior abdominal region of the embryo. This could either be the hindgut or the vitelline (omphalomesenteric) vessels which are located in close proximity and difficult to differentiate. Due to the large size

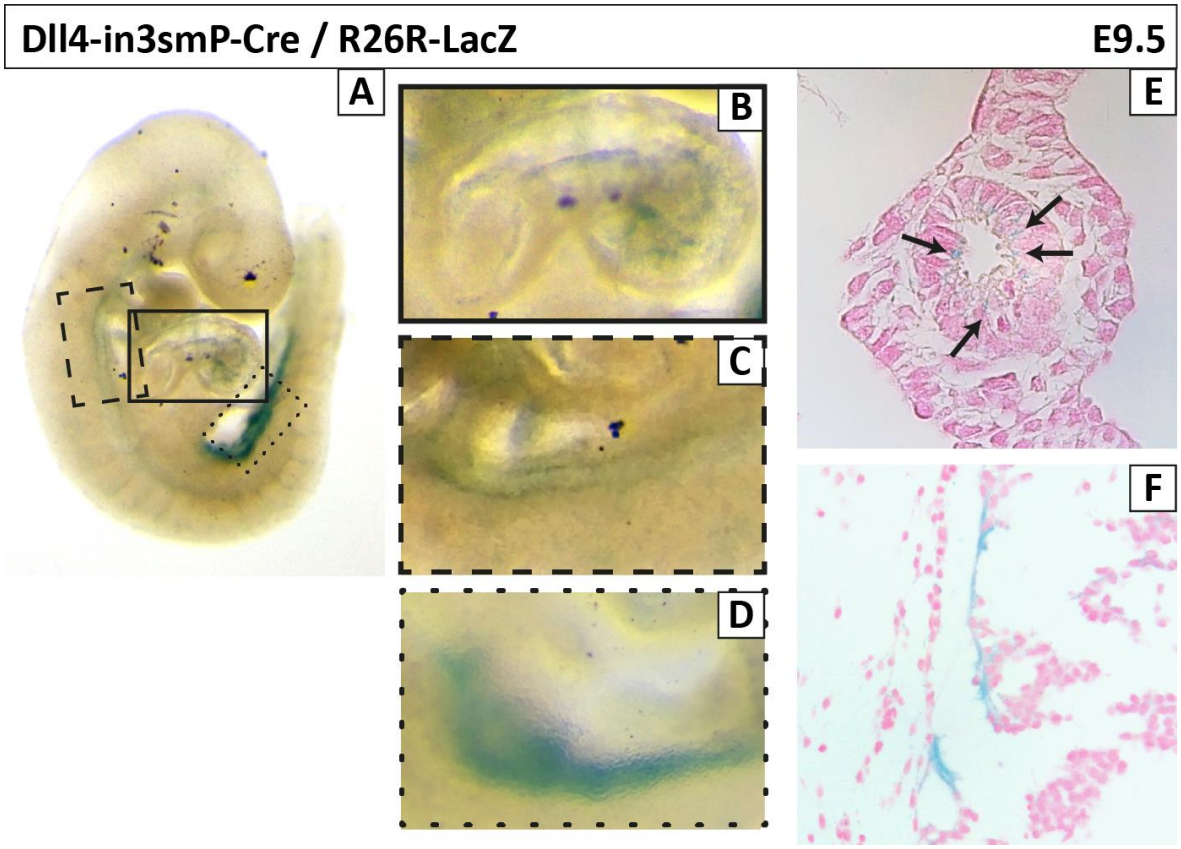

Figure 31 | LacZ expression in Dll4- in3smP-Cre / R26R-LacZ embryos at E9.5
X-Gal staining of whole-mount embryos and Nuclear Fast Red co-staining of paraffin sections
A: Representative overview image, X-Gal staining is visible in dorsal aorta, heart, gut or vitelline vessels and intersomitic vessels
B: Magnified view on heart with patchy X-Gal staining in ventral aspect
C: Magnified view on X-Gal staining in walls of dorsal aorta and two pharyngeal arch arteries
D: Magnified view on X-Gal positive gut tube or vitelline vessels
E: Transverse section through gut, arrows indicate small X-Gal positive cells at the luminal aspect of the gut
F: Transverse section through the trunk area revealed faint staining of the dorsal aorta

of the structure I assumed it is the vitelline artery or vein. Sectioning of the embryo revealed faint staining in the hindgut which is not sufficient to explain the intense staining observable in the whole-mount preparation. Unfortunately, the vitelline vessels were lost during paraffin embedding. The X-Gal staining in the heart that was visible in whole-mount preparations could not be found in paraffin sections, probably because of the weak staining intensity and too coarse sectioning. Overall, it was apparent that the staining intensity was much weaker than what was reported for the Dll4-in3hsp68-LacZ reporter mice at that developmental stage (Sacilotto et al., 2013). The results of X-Gal staining in E9.5 embryos are summarised in Figure 31.

E11.5 Embryo

Next, I analysed Dll4-in3smP-Cre embryos two days later at E11.5. The overall X-Gal staining appeared more intense compared to E9.5 and extended to wider areas of the embryo, including more intersomitic vessels, a larger part of the dorsal aorta, the vitelline artery and the maxillary arteries. In general, it became apparent that vascular expression was increasing in anterior to posterior direction with no expression in the top cranial parts of the brain vasculature and stronger expression in parts of the microvasculature and major arteries within the trunk. Again, the staining intensity was overall weaker compared to Dll4-in3hsp68-LacZ mice at E11.5.

In the vitelline artery of the yolk sac X-Gal positive ECs were distributed in a salt-and-pepper like distribution with expression gradually vanishing on the transition into smaller arterioles. The dot-like staining is most likely due to precipitation of the X-Gal dye as the dots are smaller than nuclei.

The previously described expression in the gut was more intense than observed at E9.5. In sections, staining could be detected in individual epithelial cells in the midgut, which gradually extended throughout the whole intestinal epithelium towards the region of the hindgut.

In the fetal liver, X-Gal staining could be detected in ECs of larger hepatic arteries as well as in ECs of the small sinusoidal capillaries. Also numerous X-Gal positive circulating cells were

visible in the strongly ramified hepatic vascular network. Some of those cells were seemingly di- and tri-nucleated which would indicate megakaryocytes. Although a histologist was consulted, this could not be conclusively clarified.

Intense staining could be observed in various tissues of the heart, particularly in the cushion tissues that give rise to the future valves, lining cells of the outflow tract, and the endocardium of the trabeculae.

Overall it can by summarised that reporter gene expression was largely artery-specific but was not present in all arterial ECs. An overview of the results of the analysis of E11.5 embryos can be found in Figure 32.

Figure 32 | LacZ expression in Dll4-in3smP-Cre / R26R-LacZ embryos at E11.5
X-Gal staining of whole-mount embryos and yolk sac and Nuclear Fast Red co-staining of transverse paraffin sections
A: Representative overview image, X-Gal staining is visible throughout the embryo
B/B': Magnified view on intersomitic vessels and co-staining with IB4 and false-coloured X-Gal in B'
C/D: Transverse sections through brain at (C) cranial level and at a (D) more apical level revealed increasing staining intensity in arteries and microvasculature in caudal direction
E/F: In the loops of the gut X-Gal positive non-ECs that can be detected individually in the (E) midgut and gradually extend through the whole intestinal epithelium in the (F) hindgut
G/H: In the fetal liver X-Gal positive ECs could be found in sinusoidal capillaries and larger hepatic arteries, magnified view in (H) with larger hepatic artery
I/J: X-Gal(+) cells could be detected in heart tissues with reported endothelial origin like cushion tissue, trabeculae, outflow tract of endocardium; (J) magnified view on endocardium within the left ventricle with stained trabeculae
K/L: In the yolk sac ECs of major vitelline vessel are X-Gal(+) with no detectable staining in smaller yolk sac capillaries; (L) magnified view
LA: left atrium; RA: right atrium; PLV: primitive left ventricle; PRV: primitive right ventricle; RCCV: right common cardinal vein; LCCV: left common cardinal vein; CT: cushion tissue; OFT: outflow tract

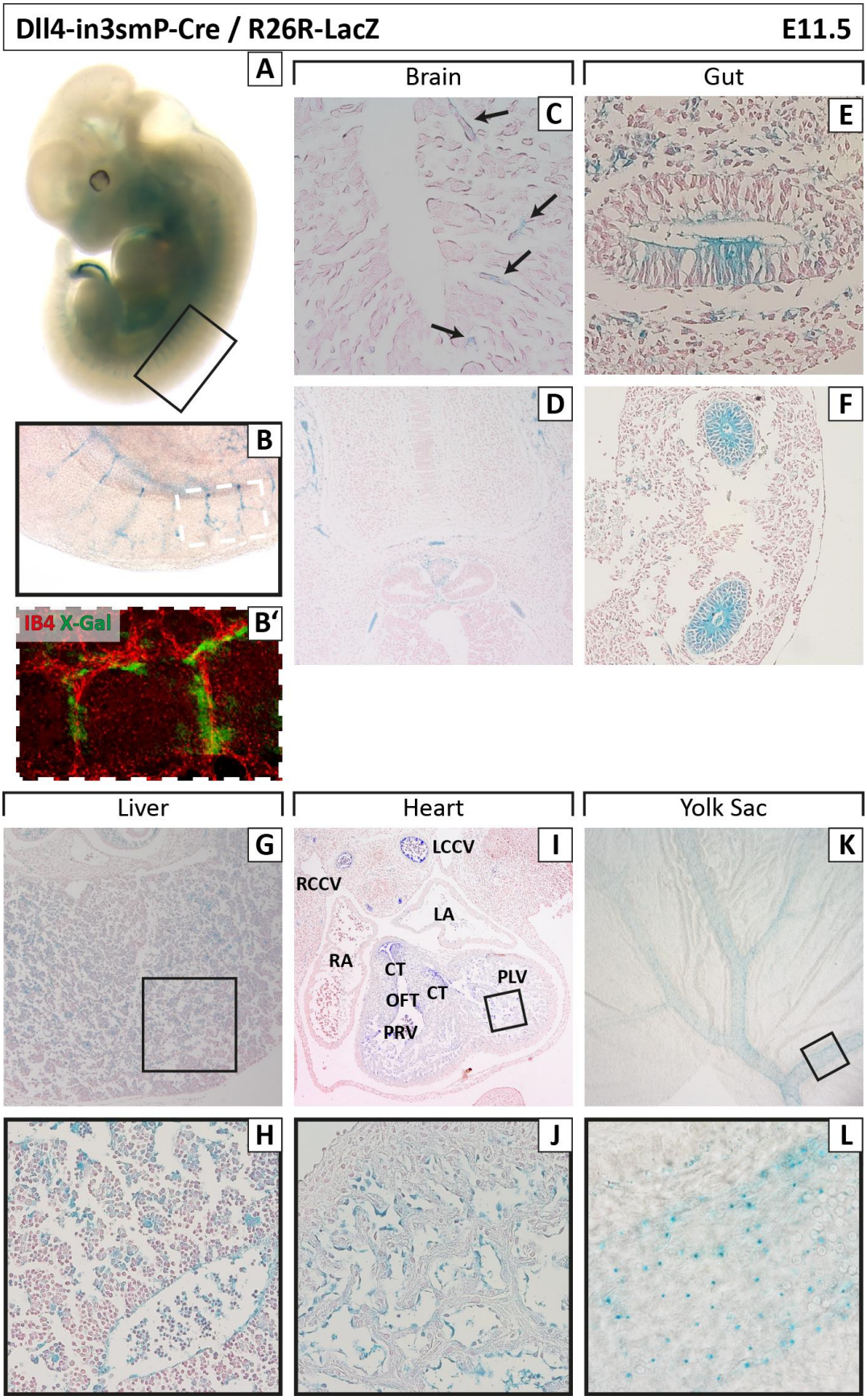
Dll4-in3smP-Cre / R26R-LacZ
E11.5
A
Brain
Gut
C
E
B
D
F
IB4 X-Gal
B'
Liver
Heart
Yolk Sac
G
I
K
LCCV
RCCV
LA
RA
CT
OFT
CT
PRV
PLV
H
J
L

E11.5/E12.5 Hindbrain

Although imaging of whole-mount preparations provides insight into the overall vascular expression pattern of the activated transgene in different anatomic regions, it does not allow analysis on the scale of individual ECs. Paraffin sections on the other hand enable to perform high resolution microscopy but generate a limited understanding of the three-dimensional nature of vascular anatomy. To visualise the transgene expression pattern with high resolution in the context of a fully recognisable vascular network, I decided to use the embryonic hindbrain.

The mouse hindbrain as a model for angiogenesis during embryonic development has been described in depth before (Fantin et al., 2013). At around E9.75 vessels from the underlying perineural vascular plexus start to enter the hindbrain and grow radially towards the ventricular surface. At around E10.0 these sprout laterally, extend beneath the ventricular surface, and begin to anastomose at around E10.5 and form the readily perfused subventricular plexus (SVP). Arteriovenous differentiation of the hindbrain capillary network begins later at around E14.5. Similar to the mouse retina, the embryonic hindbrain allows whole-mount high-resolution microscopy and the quantification of angiogenic processes. It is especially useful to study vascular KO phenotypes that are lethal in late embryonic or perinatal developmental stages.

X-Gal staining on E12.5 hindbrains revealed the surprising extent of LacZ expression in the microvasculature. Co-staining with IB4 demonstrated that around 40-50% of the visible vascular network was X-Gal positive. Staining appeared in random patches of adjacent ECs and did not seem to follow a particular pattern. Transmission images and transmission-like confocal images of X-Gal stained hindbrains have the disadvantage of not revealing the entire LacZ expression pattern of the three dimensional vascular network of the hindbrain. Due to the opaque nature of the hindbrain tissue, it is not possible to visualise the deeper layers of the vasculature. Therefore, I decided to repeat the experiment with the R26R-EYFP reporter line, which works on the same principle as the R26R-LacZ line but uses the enhanced yellow

fluorescent molecule (EYFP) as the reporter molecule. Thereby it was possible to perform high magnification confocal microscopy on the hindbrain and to use three-dimensional imaging to achieve a full-scale analysis of the vascular network.

Analysing the EYFP expression pattern showed that the previously described mosaic-like expression was present in both primary sprouts that emerge from perineural plexus and in the subventricular plexus. In addition, expression in individual ECs throughout the vascular network could be observed. Moreover, elevated EYFP expression could be detected in the tips of vascular sprouts close to the medial longitudinal fissure.

In order to get an impression of the temporal development of transgene expression in the hindbrain microvasculature, I investigated an earlier time point at E11.5. Staining intensity appeared weaker and less extensive compared to E12.5. However, similar to the later time point, reporter gene expression could be detected in both vertical sprouts and in the developing horizontal subventricular plexus. Thereby most of the stained vasculature localised close to the medial longitudinal fissure.

The results of the analysis of E12.5 and E11.5 hindbrains are summarised in Figure 33.

In order to see how the reporter gene activity compares to the endogenous expression of Dll4, I have performed IF staining on WT E12.5 hindbrains. This is especially informative because it allows to relate the snap shot-like characteristic of the immunostaining to the fate-mapping characteristic of the Cre dependent reporter gene.

As reported previously (Benedito and Duarte, 2005), DLL4 protein is not only present in the vasculature but also in the neurons of the hindbrain, which precluded the generation of overview images. On a higher magnification and by masking out the neuronal expression through optical sectioning, it became apparent that the endogenous DLL4 protein distribution is largely similar to the reporter gene expression patterns. DLL4 could be detected throughout the subventricular plexus in vertical sprouts from the perineuronal plexus and in most tip cells of the hindbrain vasculature. Thereby, the distribution of DLL4 throughout the vasculature was more widespread than what could be detected with the reporter gene. Moreover, it appeared

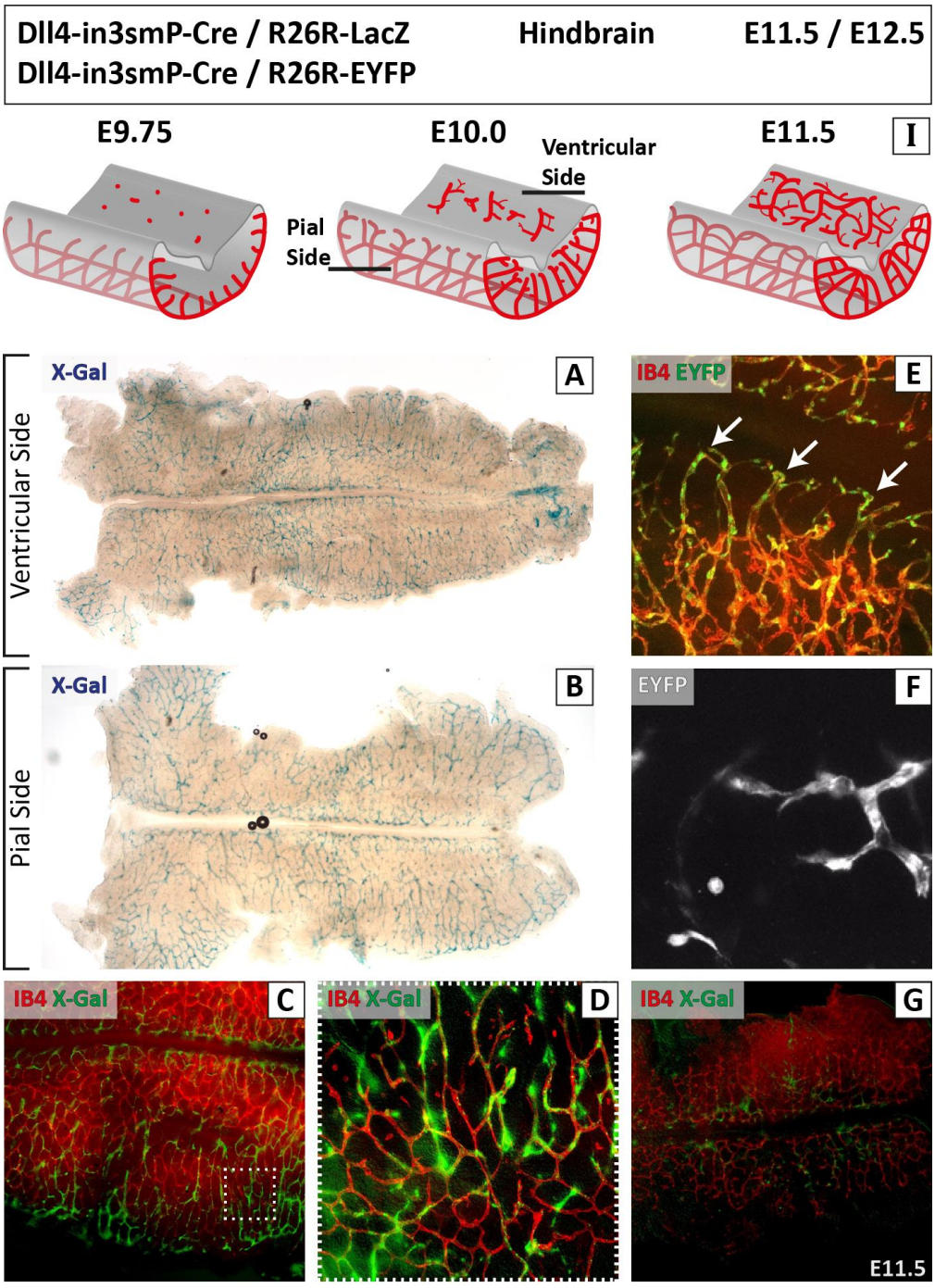

Figure 33 | LacZ/EYFP expression in Dll4-in3smP-Cre / R26R-LacZ / R26R-EYFP hindbrains at E12.5 and E11.5
X-Gal staining and IF staining of EYFP and IB4 on flat mounted E12.5 and E11.5 hinbrains
I: Schematic illustration of hindbrain vascularisation, vessels invade from the perineuronal plexus, grow radially towards the ventricular side and then sprout radially beneath the ventricular surface, adapted from *Fantin et al., 2013*
A/B: Representative overview images of (A) ventricular and (B) pial side of the hindbrain show extensive X-Gal staining in the microvasculature
C/D: False coloured X-Gal and IB4 IF co-staining in (C) one hemisphere shows that only parts of vascular network are X-Gal positive; (D) magnified view
E/F: IF co-staining of IB4 and EYFP shows transgene activity in tip of sprouts (white arrows) at microvascular front close to the medial longitudinal fissure, (F) magnified view on X-Gal(+)
G: Patchy staining in E11.5 hindbrains close to the medal longitudinal fissure

more continuous than the patchy reporter gene expression. Overall, it can be concluded that the Dll4 enhancer/promoter driven Cre transgene mimics the endogenous Dll4 expression but apparently only labels a subset of microvascular ECs.

The results of the DLL4 immunostaining on E12.5 hindbrains are summarised in Figure 34.

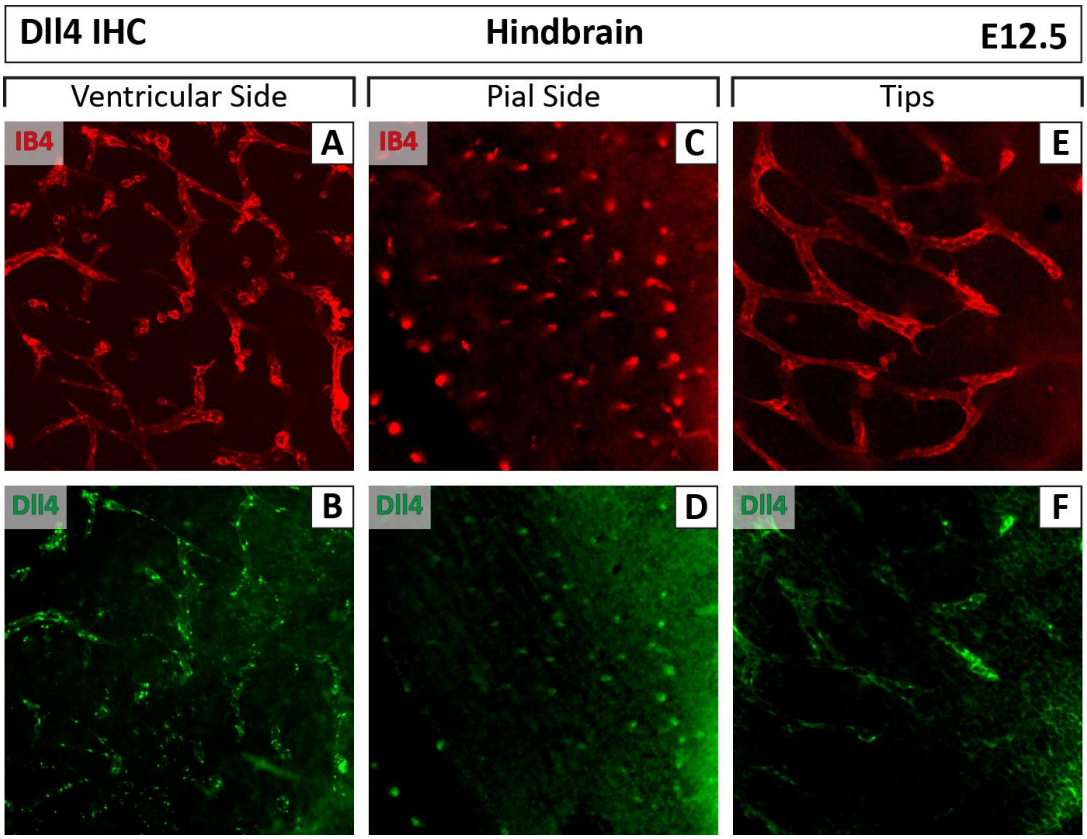

Figure 34 | Endogenous expression of DLL4 protein in E12.5 hindbrain
A/B: Extensive Dll4 expression throughout the ventricular plexus
C/D: Dll4(+) vascular sprouts that enter from the perineuronal plexus
E/F: Elevated Dll4 expression in tips of horizontal subventricular sprouts

E13.5 Embryo

At E13.5 the staining pattern was largely comparable to the pattern observed at E11.5, being arterial specific and visible in intersomitic vessels and maxillary arteries. However, there was more widespread expression in the microvasculature, especially within the developing limbs. In the yolk sac weak expression in the vitelline artery was present which gradually diminished in branching arterioles.

Surprisingly, the heart appeared to be stained less intensive compared to the E11.5 embryos. Expression was comparatively weak and restricted to the inner walls of the ventricles. Considering the lineage-tracing character of the Cre/R26R-LacZ labelling experiment, this difference can only be explained with inter-embryo variations as discussed in 4.3.1.

The previously observed non-EC expression in the wall of the gut appeared to be extended through most parts of the mid- and hindgut, showing irregular staining that gradually intensified in cranial to caudal direction.

The results of the analysis of E13.5 embryos are summarised in Figure 35.

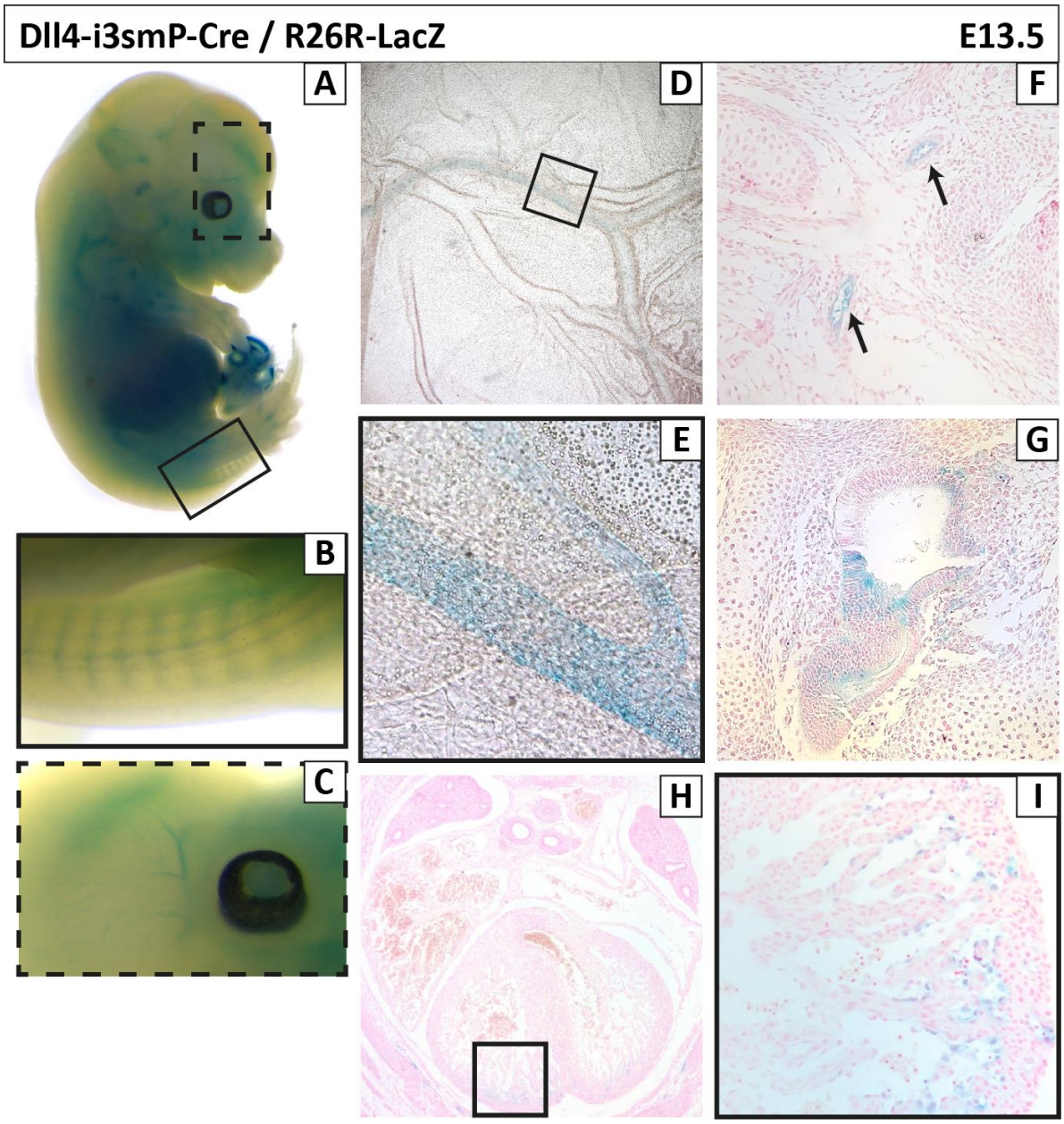

Figure 35 | LacZ expression in Dll4-in3smP-Cre / R26R-LacZ embryos at E13.5
X-Gal staining of whole-mount embryos and yolk sac and Nuclear Fast Red co-staining of transverse paraffin sections
A: Representative overview image with visible X-Gal staining in the whole embryo
B: Magnified view on X-Gal(+) intersomitic vessels in the tail
C: Magnified view on X-Gal(+) maxillary artery in the head
D/E: X-Gal(+) vitelline artery in yolk sac whole-mount; (H) magnified view shows gradually diminishing expression in branching arterioles
F: Consistent LacZ expression in arteries and absent expression in veins
G: Irregular staining in epithelial cells of the midgut
H/I: Overview over mostly negatively stained heart; (I) magnified view on X-Gal(+) wall of the right ventricle

E18.5 Embryo

E18.5 embryos displayed a global deep-blue X-Gal staining when imaged as whole-mounts. After sectioning it became clear that this was due to the fact that large parts of the microvasculature were stained. In addition a great number of circulating cells, found in vessels throughout the whole embryo, displayed strong X-Gal staining, which complicated the analysis of the vasculature. Especially in small vessels it was difficult to distinguish positive circulating cells and positive ECs. Therefore, I referred to the intercostal vessels, which are an easily identifiable anatomic structure, because they can be found in close proximity parallel to the ribs and display a stereotypic arrangement of one intercostal artery, vein and nerve. It could be found that all intercostal arteries showed X-Gal expression and the neighbouring veins and nerves remained negative.

Widespread expression could also be observed in various parts of the heart. Outflow tract, ascending artery, pulmonary and tricuspid valves as well as the trabeculae appeared X-Gal positive. In addition, some, but not all, coronary arteries showed LacZ expression.

The entire gut tube displayed very strong non-EC X-Gal staining.

An overview of the results of X-Gal staining in E18.5 embryos is given in Figure 36.

Figure 36 | LacZ expression in in3smP-Cre/R26R-LacZ embryos at E18.5
X-Gal staining of whole-mount hindgut and heart and Nuclear Fast Red co-staining of transverse paraffin sections
A/B: Intense X-Gal staining in microvasculature and arteries of the skin; (B) magnified view on X-Gal(+) capillaries
C/D: Rib and adjacent intercostal vessels; (D) magnified view on intercostal artery [A], vein [V] and nerve [N]
E/F: Intense X-Gal staining in hindgut whole-mount; (F) magnified transverse view
G/H: Faint positive vasculature and positive and circulating cells in atrium; (H) magnified view
I: X-Gal positive outflow tract (OT), ascending artery (AA) and pulmonary valves (PP)
J/K: Strong X-Gal staining in coronary vasculature in the periphery of the ventricle (left or right), (K) magnified view
L: X-Gal positive tricuspid valves (TV)
M: X-Gal positive trabeculae within ventricle
N: Whole-mount of heart, view of right ventricle with X-Gal positive coronary vasculature and vessels stained red due to remaining blood

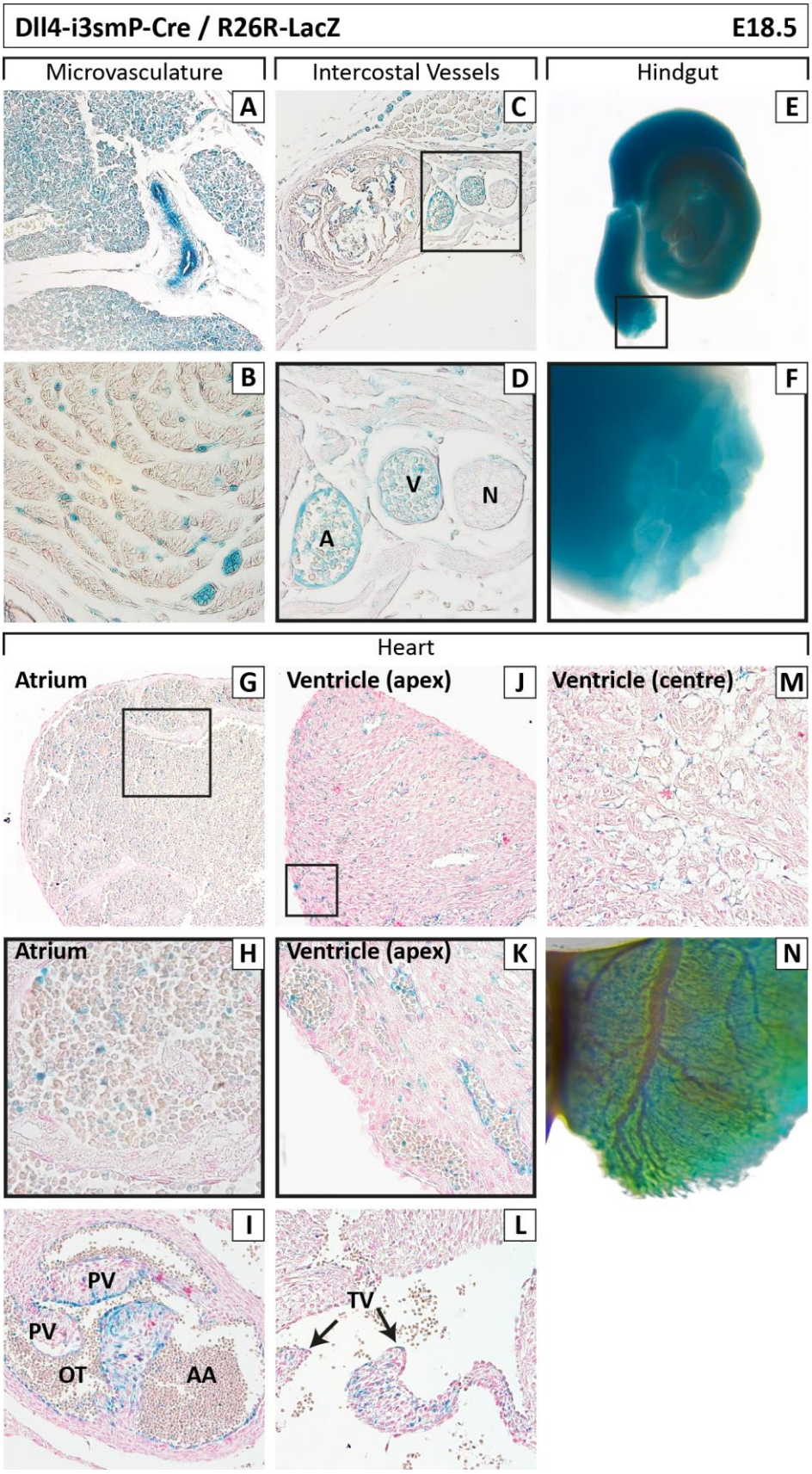
Dll4-i3smP-Cre / R26R-LacZ
E18.5
Microvasculature
Intercostal Vessels
Hindgut
A
C
E
B
D
F
V
N
A
Heart
Atrium
G
Ventricle (apex)
J
Ventricle (centre)
M
Atrium
H
Ventricle (apex)
K
N
I
L
PV
PV
OT
AA
TV

5.1.4.2 Dll4-in3smP-Cre Expression in Postnatal Development

After it could be established that the identified Dll4-in3smP-Cre founder line displays largely arterial specific transgene expression from E9.5 onwards, the analysis was extended to the postnatal vasculature.

For the analysis of postnatal Dll4-in3smP-Cre expression I focused on the mouse retina as a reliable model for vascular development. The advantages and disadvantages of the retina model, as well as its successive developmental stages, are outlined in 3.1.1. In order to investigate the transgene expression in the context of different angiogenic processes such as sprouting, remodelling, maturation and homeostasis, I decided to stain retinas at P3, P6, P9 and P30. Thereby I used both R26R-LacZ and R26R-EYFP reporter lines for the aforementioned reasons.

As described earlier, the retina model has some unique characteristics that are not present in other vascular beds and vice versa. Therefore, I chose the spinotrapezius muscle (Moraes et al., 2013) as an additional model for analysing transgene expression in adult mice.

The results of the analysis of the postnatal retinal vasculature at various developmental stages and of the spinotrapezius muscle in adult mice are summarised in Figure 37 and Figure 38.

P3 Retina

EYFP expression could be detected specifically in patches of adjacent ECs that were randomly distributed across the retinal vasculature. Also, individual EYFP positive ECs could be observed while no positive non-ECs were visible. Around 20-30% of the retinal vasculature appeared to be EYFP positive.

At P3 the retinal vasculature is not yet differentiated into morphologically distinguishable arteries and veins. However, close to the optical disc some larger, radially extending vessels displayed elevated EYFP expression and in context of the previous results it can be assumed that these are developing arteries.

Although most tip cells at the angiogenic front did not display reporter gene activity, individual positively stained tip cells could be observed. Expression was much more prominent in stalk cells.

P6 Retina

In P6 retinas the overall expression pattern observed at P3 appeared to be maintained. Moderate expression was visible at the angiogenic front with rare but detectable expression in tip cells and the major amount of expression to be found in an area around 5-6 cells behind the front. Overall the ratio of positive endothelium remained at around 20-30%.

Strong, but still patchy expression was observed in arteries which gradually faded in direction from the optical disc towards the angiogenic front. No expression could be detected in veins. The microvascular plexus displayed mosaic-like expression that originated from arteries and arterioles, especially in peripheral regions of the retina.

P9 Retina

At P9, transgene expression was more widespread with both arteries and micro-vasculature in the central areas around the optical disc appearing almost entirely LacZ positive. Interestingly, this was not true for the whole retinal vasculature. The staining appeared to be restricted to certain domains with completely stained areas bordering completely negative areas and abrupt transitions between the domains.

Weak LacZ expression was also visible as individual diffuse patches within veins. In contrast to arteries the venous expression was homogenous across the retina and partly prolonged into the microvasculature of the otherwise negative areas. Therefore, it is likely that this staining is not endothelial and can be explained by LacZ positive circulating cells that remained within the retinal veins.

P30 Retina and Adult Organs

At P30 strong widespread expression in non-vascular cells could be detected across the retina. These cells appeared to lie between the tertiary and superficial vascular plexus and therefore probably are a kind of amacrine or bipolar neuronal cell type.

Arteries were entirely positive for LacZ across the retina with expression prolonging into arterioles. Surprisingly, although present in all three vascular layers, the expression in the microvasculature appeared weaker compared to earlier stages. However, the domain-like distribution of staining had disappeared. No expression in veins could be detected any more.

In addition to the P30 retina, also vascular beds in different organs of six month old transgenic mice were analysed to gain a more complete overview of the transgene expression. The vasculature of the spinotrapezius muscle showed robust and arterial specific transgene expression. X-Gal staining could be detected in major arteries and extended into arterioles and was mostly absent from capillaries. Veins and lymphatic vessels appeared negative. X-Gal staining on whole-mounts of heart and bladder revealed that LacZ was present in the pulmonary artery, the aorta and parts of the coronary vasculature, as well as extensively in the microvasculature of the bladder. The results of the analysis of various adult organs are summarised in Figure 38.

In summary, it can be concluded that the labelling of arterial and microvascular ECs, which was observed in previous developmental stages, continues into adulthood without becoming truly pan-vascular. Moreover, the endothelial specificity is partially lost as also other cell types display transgene expression.

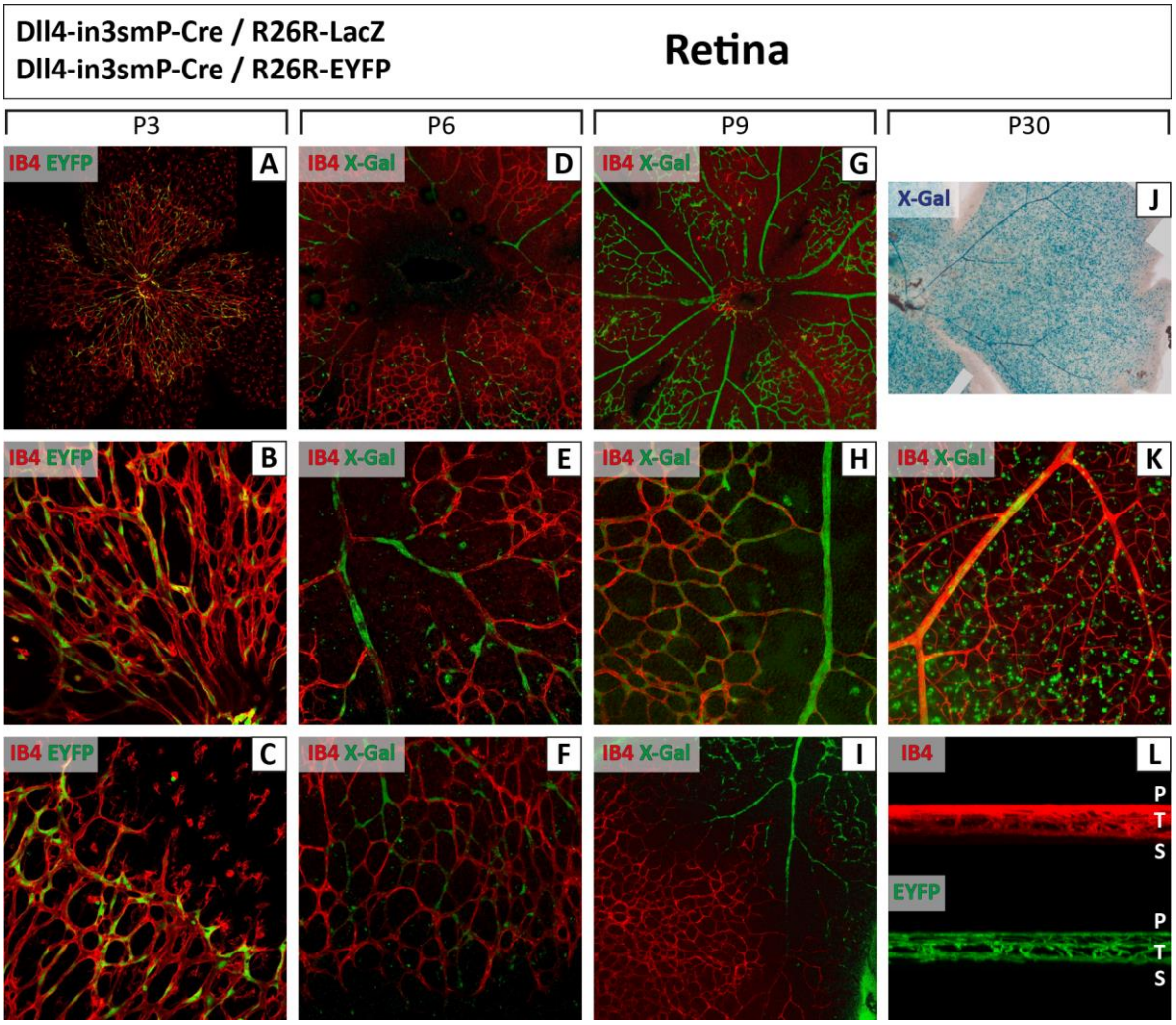

Figure 37 | LacZ/EYFP expression in Dll4-in3smP-Cre / R26R-LacZ / R26R-EYFP retinas at various stages
False-coloured X-Gal and IB4 IF staining on whole-mount retinas
A/B/C: P3 retina, overview over (A) entire retinal vasculature; (B) central vasculature and (C) angiogenic front
D/E/F: P6 retina, overview over (D) central vasculature; (E) artery and arterioles and (F) angiogenic front
G/H/I: P9 retina, overview over (G) central vasculature; (H) artery and arterioles, (I) transition zone between X-Gal positive and negative areas
J/K/L: P30 retina, (A) overview image with two positive arteries and positive non-ECs; (K) magnified view on positive artery and positive non-ECs and underlying secondary and tertiary plexuses; (L) orthogonal views of z-stack maximum intensity projections showing positive primary [P], secondary [S] and interconnecting tertiary plexus [T]

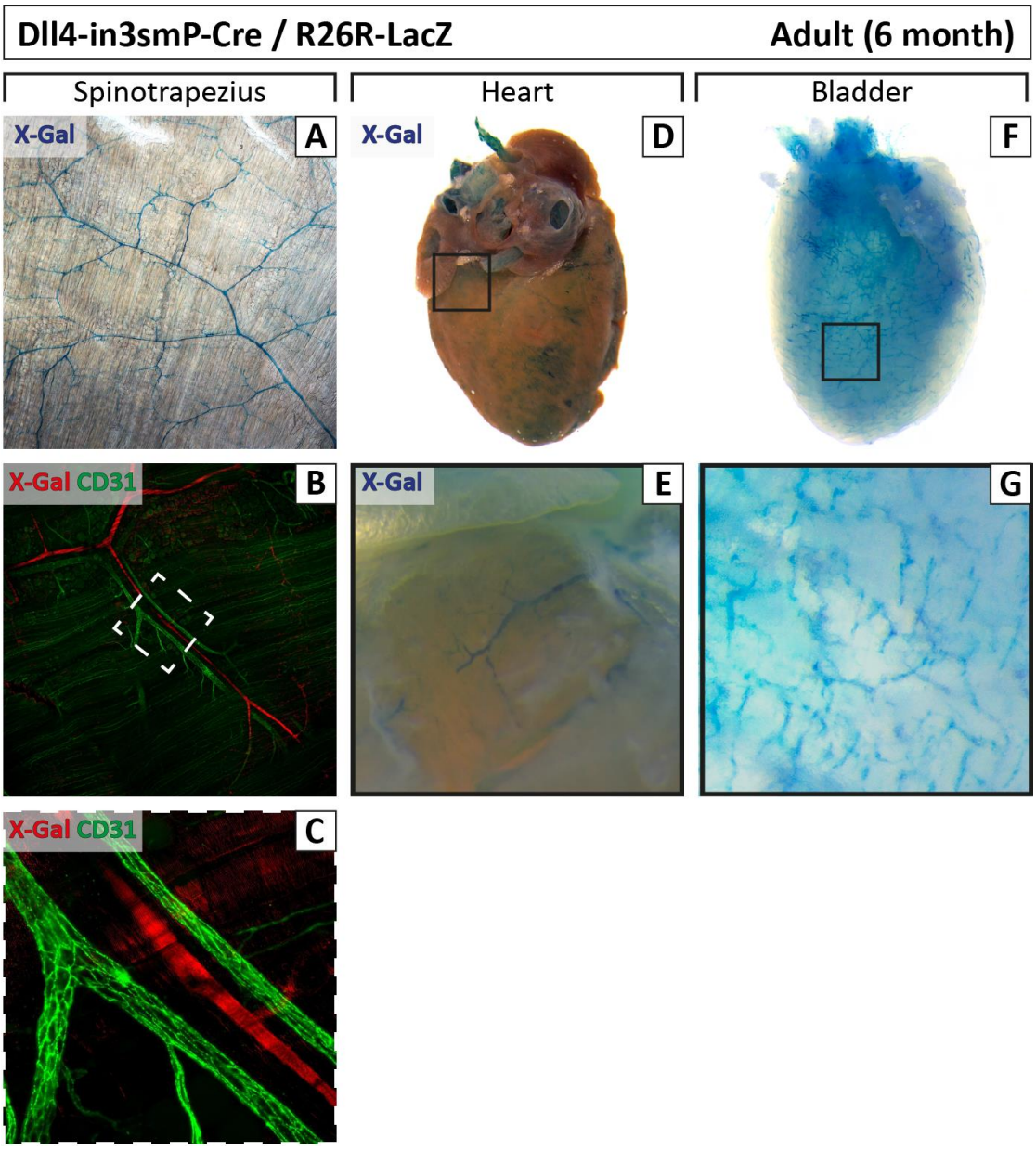

Figure 38 | LacZ expression in various organs of 6 month old Dll4-in3smP-Cre / R26R-LacZ mice
X-Gal and false-coloured X-Gal and CD31-564 IF staining on whole-mounts
A: Overview of spinotrapezius muscle with X-Gal(+) major vessels and capillaries
B/C: X-Gal/CD31co-staining showing parallel running artery, vein and lymphatic vessel; (C) magnified view
D/E: Overview of heart whole-mount with X-Gal(+) coronary vessels and pulmonary artery; (E) magnified view on coronary vessels
F/G: Overview of bladder whole-mount with extensive X-Gal staining in microvasculature; (G) magnified view

5.1.5 Dll4-in3smP-CreERT2 Expression in Embryo

As mentioned previously, two inducible CreERT2 founder lines (L1 and L2) were initially identified. Unfortunately, the line which I decided to base my initial experiments on (L1) failed to pass an active copy of the transgene into its descendants, possibly due to epigenetic inactivation of the transgene or the loss of the active allele. After I performed the initial experiments to identify the founder male, I continued by breeding it with wild-type females in order to expand the lines. The ensuing F1 generation was then crossed again with reporter mice. However, when I analysed animals from the F2 generation that carried both the Dll4-in3smP-CreERT2 and the R26R-LacZ/EYFP reporter transgenes, I could not reproduce the initial results. Therefore, I abandoned analysing this line and focused on L2 instead. A schematic overview of the tamoxifen inductions and respective analysis of embryos at various developmental stages is given in Figure 39.

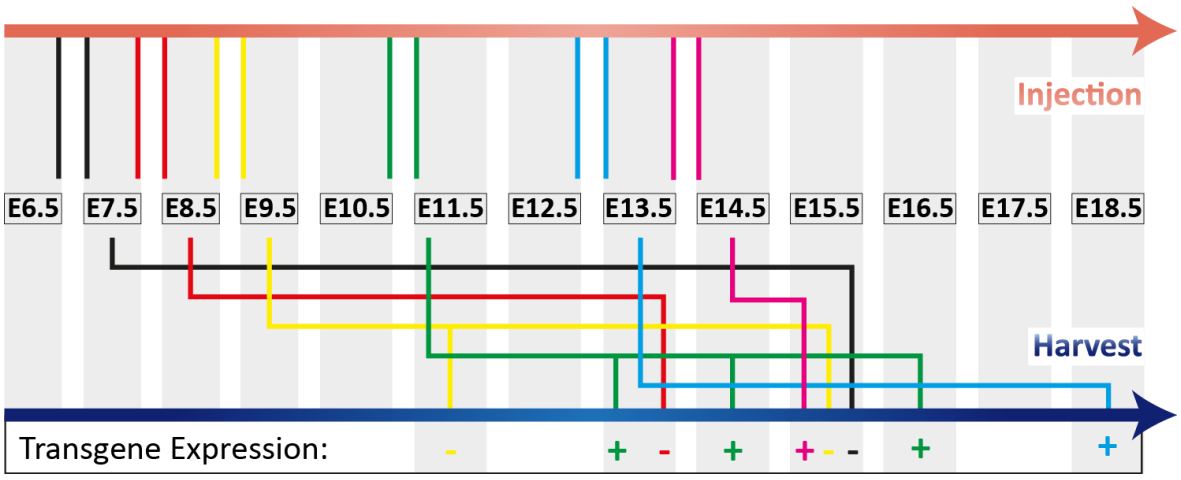

Figure 39 | Overview of tamoxifen injections and subsequent harvesting in Dll4-in3smP-CreERT2 embryos
Tamoxifen was administered on two consecutive days and embryos were harvested 1 – 8 days later; colour coded lines indicate days of injection (upper part) and respective day of harvest (lower part), as well as the observed positive (+) or negative (-) transgene expression

The earliest time point at which I could detect reporter gene expression in Dll4-in3smP-Cre / R26R-LacZ mice was at E9.5. As discussed in 5.1.4, the kinetics of tamoxifen induced Cre recombinase activation in mouse embryo are relatively poorly described. However, considering that the *in vivo* half-life of 4-OHT after I.P. injection in mice is around 16 h (Robinson et al., 1991) and that plateauing Cre-dependent LacZ reporter gene activity has been described 24 h post injection (Nakamura et al., 2006), I decided that two consecutive I.P. injections at E6.5 and E7.5 should be sufficient to achieve cell labelling from E9.5 onwards, in case the promoter/enhancer construct is active. A simplified estimation of tamoxifen levels was conducted as follows:

Estimated plasma concentration at E6.5 after first injection of 2 mg tamoxifen:

2 mg (for simplicity initial clearance is ignored)

Estimated plasma concentration at E7.5 after second injection of 2 mg tamoxifen:

2.7 mg ($C_t = C_0 e^{-(\frac{\ln 2}{t_{1/2}})\,t} \rightarrow C_{24\,h} = 2\ mg * e^{-\left(\frac{\ln 2}{16\,h}\right) * 24\,h} = 0.7\ mg;\ 0.7\ mg + 2\ mg = 2.7\ mg$)

Estimated plasma concentration at E8.5:

0.95 mg ($C_{24\,h} = 2.7\ mg * e^{-\left(\frac{\ln 2}{16\,h}\right) * 24\,h} = 0.95\ mg$)

As suggested by (Wilson et al., 2014), I.P. doses of 0.8 mg tamoxifen already saturate CreERT2 activity.

The embryos were harvested at E15.5, as I expected the R26R-LacZ cell labelling to remain stable throughout development. However, I could not detect any reporter gene expression at E15.5.

As a next step I shortened the interval between tamoxifen administration and embryo analysis by injecting at E7.5/E8.5 and harvesting at E13.5 Again, no reporter gene expression was detectable. Similarly, tamoxifen injection at E8.5/E9.5 and embryo analysis at E11.5 and E15.5 did not result in detectable LacZ expression, suggesting that the Dll4-in3smP-CreERT2 line is not active during early gestation.

E13.5 Embryo (Tamoxifen Injected E10.5/E11.5)

The earliest time point at which I could observe reporter gene expression was E13.5 after tamoxifen injection at E10.5 and E11.5. Embryonic expression were confined to the microvasculature of the epithelium of the limbs. No expression in larger intraembryonic vessels could be detected (Figure 40, A-B). Speckled LacZ expression was present in the vitelline artery but quickly faded out in the yolk sac (Figure 40, C-D).

Due to the fact that the X-Gal staining was so faint, I have performed an analysis of the hindbrain vasculature as well, using the R26R-EYFP reporter line. Although very faint, I could detect EYFP in randomly distributed parts of the subventricular vasculature (Figure 40, E-F). At E13.5 the hindbrain is already fully vascularised, therefore no angiogenic front exists and I could not elucidate if reporter gene expression was present in tip cells.

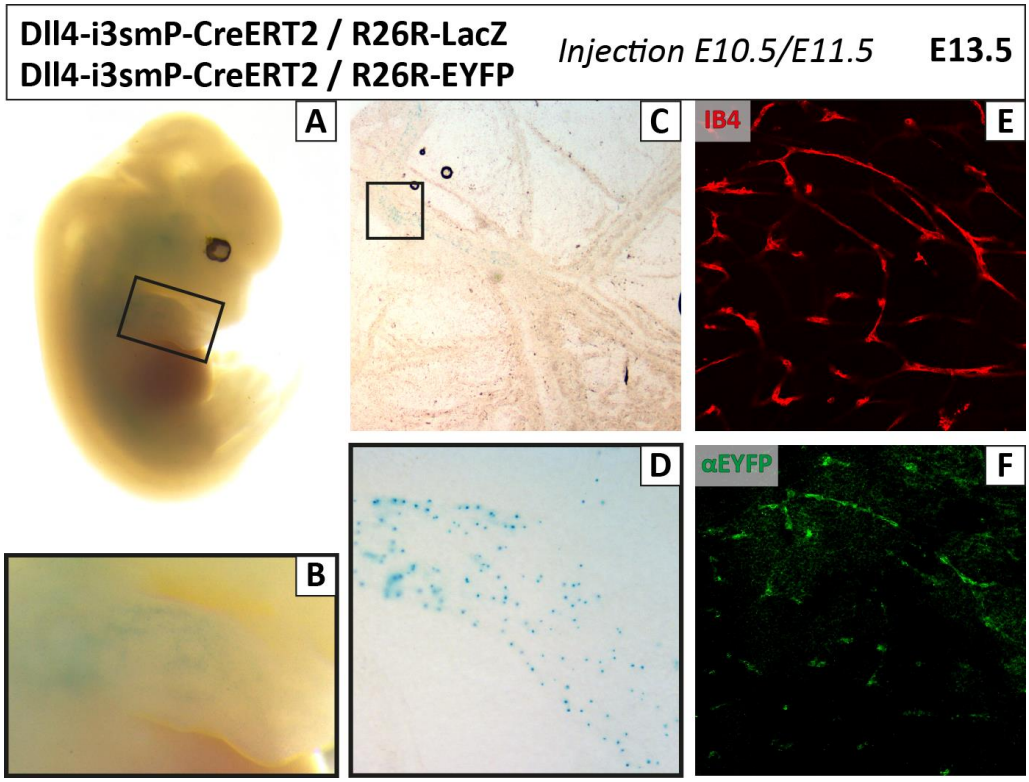

Figure 40 | LacZ expression in in3smP-CreERT2/R26R-LacZ/R26R-EYFP embryos injected at E10.5/E11.5, harvested at E13.5
X-Gal staining of whole-mount embryos yolk sacs and hindbrains; anti-EYFP/IB4 immunostaining in hindbrain
A/B: Representative overview image with faint and diffuse vascular X-Gal staining in parts of the embryo; (B) magnified view on X-Gal(+) microvasculature of limb
C/D: Faint salt-and-pepper like staining in vitelline artery; (D) magnified view on individual speckles
E/F: Faint EYFP expression (visualised through anti-EYFP immunostaining) in horizontal subventricular sprouts of the hindbrain

E14.5 Embryo (Tamoxifen Injected E10.5/E11.5)

Since very early tamoxifen induction failed to achieve any expression, and to aid my aim of lineage tracing arterial ECs, I decided to continue tamoxifen induction at E10.5/E11.5, but to extend the interval between induction and analysis. At E14.5, LacZ expression was much more widespread compared to E13.5 and could be detected specifically in arteries and microvasculature, especially in the epithelium and inside the mesonephric tissue (Figure 41, A, B, F). Overall, the staining patterns resembled what could be observed in the Dll4-in3smP-Cre line but appeared weaker. Most notably, X-Gal staining was present in many major arteries, including the common carotid artery, aortic arches, descending aorta, abdominal aorta, and common iliac artery, and to a lesser degree, the vitelline artery (Figure 41, B, C, E, I). In some of the largest arteries, such as the aortic arches, X-Gal positive cells from the arterial walls were protruding into the vessel lumen (Figure 41, D). These protrusions morphologically resemble intra-aortic clusters in which endothelial cells can undergo a transition to haematopoietic cells (see 1.3.3). However, intra-aortic clusters are usually more characteristic for earlier embryonic stages from E9.5 – E11.5, since generation of haematopoietic precursors then moves to the fetal liver (Mizuochi et al., 2012).

No X-Gal staining was detected in the inner tissues of the heart and only faint staining was present in the coronary vasculature. This is a marked contrast to the constitutively active Cre in which X-Gal staining could be observed in heart tissues of endothelial origin. In contrast to the results from the analysis of the constitutively active Cre line, no LacZ expression could be detected in the gut, circulating cells, or any other non-endothelial cell type.

To confirm the expression pattern in detail, I repeated the experiment with EYFP as a reporter and analysed skin whole-mounts. Thereby I could confirm reporter gene expression in arteries and microvasculature but not veins (Figure 41, G, H, J). Microvascular expression was most intense in the region of the developing digits and absent in the back of the embryo. Close examination of positively stained arteries revealed that EYFP expression appeared continuous in larger arteries and was spread out to individual ECs in smaller arterioles.

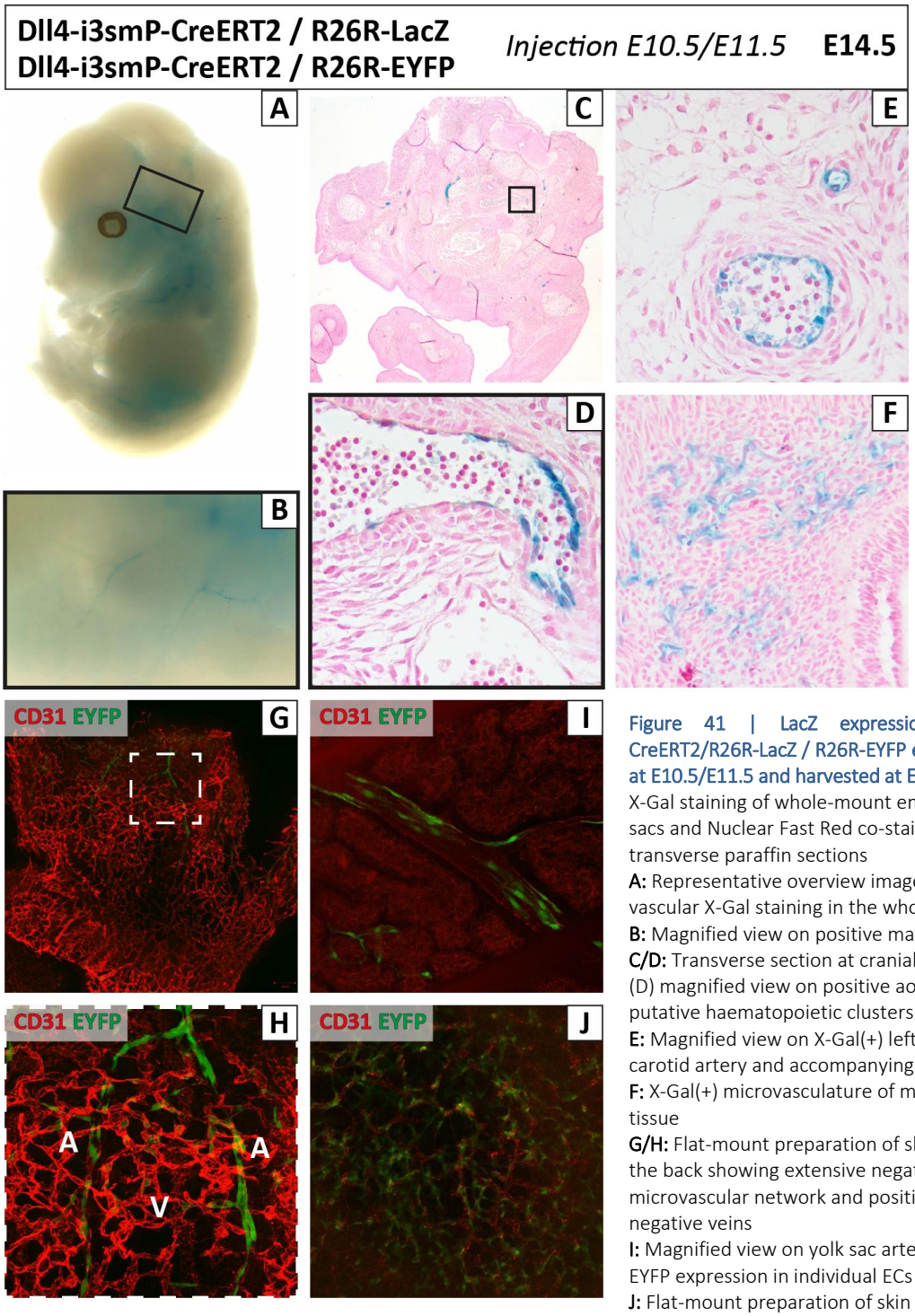

Figure 41 | LacZ expression in in3smP-CreERT2/R26R-LacZ / R26R-EYFP embryos injected at E10.5/E11.5 and harvested at E14.5

X-Gal staining of whole-mount embryos and yolk sacs and Nuclear Fast Red co-staining of transverse paraffin sections

A: Representative overview image with diffuse vascular X-Gal staining in the whole embryo

B: Magnified view on positive maxillary arteries

C/D: Transverse section at cranial aspect of heart; (D) magnified view on positive aortic arches with putative haematopoietic clusters

E: Magnified view on X-Gal(+) left common carotid artery and accompanying smaller artery

F: X-Gal(+) microvasculature of mesonephric tissue

G/H: Flat-mount preparation of skin patch from the back showing extensive negative microvascular network and positive arteries and negative veins

I: Magnified view on yolk sac artery with patchy EYFP expression in individual ECs

J: Flat-mount preparation of skin patch from the developing limbs showing EYFP(+) microvasculature

E16.5 Embryo (Tamoxifen Injected E10.5/E10.5)

E16.5 embryos displayed widespread reporter gene expression in ECs lining major vessels and inside large parts of the microvasculature (Figure 43, A-C). Since the increased size and reduced translucence of E16.5 embryos impaired visibility of structures inside the body, one positive embryo was cleared to more easily visualise reporter gene expression patterns throughout the whole embryo (see 2.2.3). X-Gal staining was present continuously in large vessels including the tail arteries, intersomitic arteries, intercostal arteries and many smaller arteries of the skin. In addition to the major arteries, intense X-Gal staining was also found in large, but isolated parts of the microvasculature, especially around the nasal cavity, the pulmonary vasculature, the choroid plexus, and inside the developing digits (Figure 43, B, E, L). None of the larger veins, which I could clearly identify through their morphology, displayed detectable X-Gal staining.

With the exception of a subset of vessels in the coronary vasculature, no X-Gal staining could be detected in the heart or the aorta and pulmonary artery (Figure 43, F, J, K). Again, this is in stark contrast to the staining pattern of the Dll4-in3smP-Cre line where expression could be found in valves and trabeculae. Also some larger vessels in the centre of the embryo like the thoracic artery were not stained. This might be due to incomplete penetration of X-Gal dye.

Interestingly, no reporter gene expression was detected in the yolk sac and within circulating cells, indicating a transient activity of the Dll4 enhancer/promoter construct in HSCs. Intense staining could also be found inside the epithelium of the mid- and hindgut and in the gut vasculature (Figure 43, G-H). This is a somewhat surprising result, because no expression could be found in E14.5 embryos when injected at E10.5/E11.5.

Figure 42 | LacZ expression in E15.5 Dll4-in3smP-CreERT2/R26R-LacZ embryos injected at E13.5/E14.5
X-Gal staining of whole-mount embryos and yolk sacs and Nuclear Fast Red co-staining of transverse paraffin sections
A: Representative overview image with X-Gal staining in major vessels
B: Magnified view on positive maxillary arteries
C: Magnified view on positive tail artery and intersomitic vessels
D/E: Overview of section through head at the level of the bulbus oculi displaying almost no staining and (E) magnified view on positive left internal carotid artery
F/G: Overview of section through midsection at the level of the heart showing positive larger and smaller arteries and negative veins; (G) magnified view on positive arteries and negative veins
H: Overview of section through tail showing the tail artery being the only positive vessel inside the tail
I: Individual X-Gal(+) cells could be found in the walls of major yolk sac arteries and branching arterioles

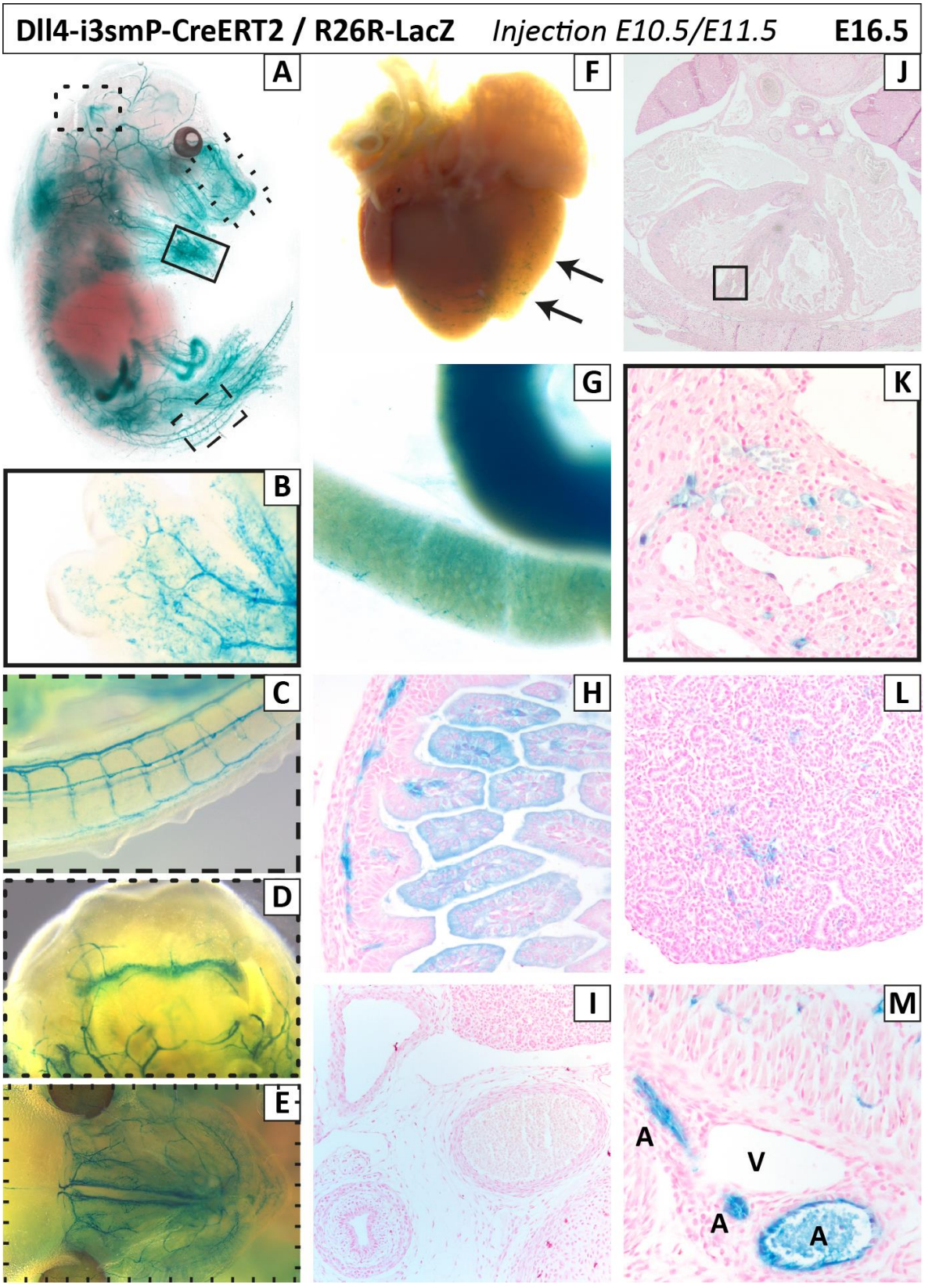
Dll4-i3smP-CreERT2 / R26R-LacZ
Injection E10.5/E11.5
E16.5
A
B
C
D
E
F
G
H
I
J
K
L
M
A
V
A
A

E15.5 Embryo (Tamoxifen Injected E13.5/E14.5)

In addition to the previously analysed intervals in which the induction was started at E10.5, I also analysed E15.5 embryos, injected at E13.5/E14.5, in order to investigate which expression pattern a short interval produces in later stages of gestation.

In E15.5 embryos that were under tamoxifen induction for only 48 h reporter gene expression was endothelial specific and mainly restricted to major arteries, while only very weak expression could be detected in the microvasculature (Figure 42, A-C). As noted before in the constitutively active Cre line, a cranial to caudal gradient in staining intensity could be observed, with the head and upper trunk region remaining largely X-Gal negative with the exception of large arteries like the internal carotid artery and maxillary arteries and few individual smaller mesenchymal head arteries. In the lower segments of the embryo staining could be found prominently in the tail artery and in the intersomitic vessels and in many smaller arteries within the epithelium of the skin, especially in the area of the developing limbs (Figure 42, H-G).

No expression could be detected in the heart or in the coronary vasculature. Also the main arteries that feed into the heart and the dorsal aorta remained negative. Similarly, no expression could be found in circulating cells or in the gut walls. In the yolk sac faint staining could be detected in individual cells of the major vitelline artery (Figure 42, I).

In summary it can be said that a short interval between tamoxifen induction and analysis at 15.5 results in transgene expression that is mainly restricted to larger arteries and, in comparison to the previous experiments, quite weak in the microvasculature.

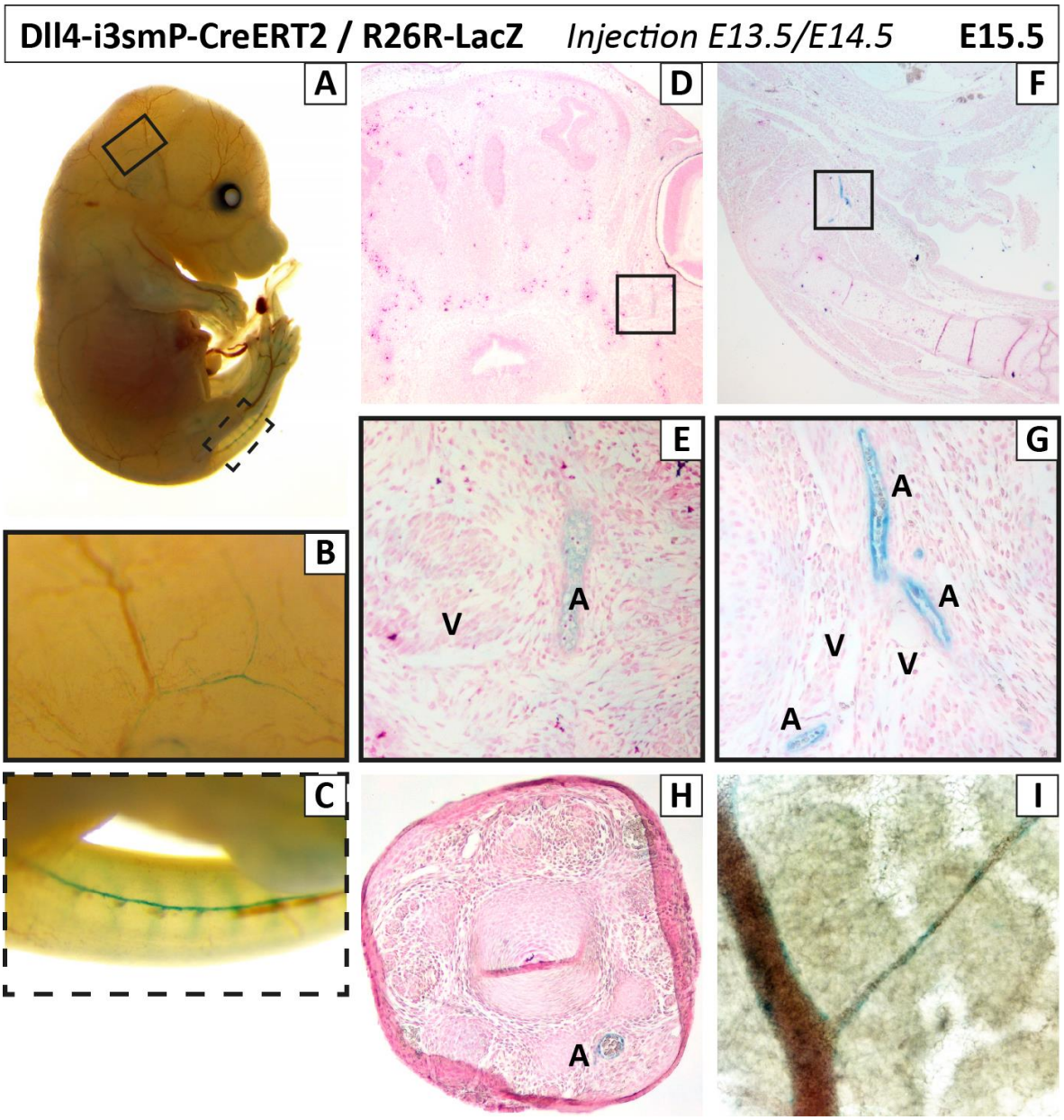

Figure 43 | LacZ expression in E16.5 Dll4-in3smP-CreERT2/R26R-LacZ embryos injected at E10.5/E11.5
X-Gal staining of whole-mount embryos and organs and Nuclear Fast Red co-staining of transverse paraffin sections
A-E: Representative overview image of cleared embryo**;** (B) magnified view on digits with X-Gal(+) microvasculature and major vessels; (C) magnified view on tail with four X-Gal(+) tail arteries and intersomitic vessels; (D) dorsal view on back of the head with X-Gal(+) choroid plexus and vertebral arteries; (E) cranial view on snout with intense X-Gal staining in the microvasculature of tongue and around the nasal cavity
F: Overview of heart whole-mount with X-Gal staining in coronary vessels of various sizes
G: Magnified view on loops of X-Gal(+) mid- and hindgut with positive gut vasculature
H: Section through hindgut loop with X-Gal(+) epithelium and gut vasculature
I: Negative pulmonary artery and aorta
J/K: Overview of section through mostly negative heart; (K) magnified view on X-Gal(+) coronary vasculature
L: Section through lung with positive pulmonary microvasculature
M: Magnified view on positive arteries and microvasculature and negative veins

5.1.6 Dll4-in3smP-CreERT2 Expression in Postnatal Development

After the evaluation of induced Cre recombinase activity throughout embryonic development demonstrated that the Dll4-in3smP-CreERT2 line is specific to the arterial and microvascular endothelium, I continued my analysis in the postnatal retina to verify my observations and to gain additional insight on a cellular scale. The tamoxifen injection scheme was largely adopted from Pitulescu *et al.*, 2010 and adapted for the purposes of my analysis. I tried to balance the need to have short intervals between injection and harvest, thereby permitting investigation into the fate of CreERT2 expressing ECs during different angiogenic processes like sprouting or vessel maturation, with the requirements to induce a robust activation of the reporter gene and to overcome mosaicism, which had been described for several Cre lines (Heffner et al., 2012). Due to the fact that I observed increased mortality of pups that received tamoxifen injections at P1, I used P2 as the earliest time point for injection.

The results of the analysis of the postnatal retinal vasculature at various developmental stages are summarised in Figure 44.

P6 Retina (Tamoxifen injected P2-P4)

Analysis of P6 retinas revealed that the CreERT2 transgene activity is specific to ECs in arteries and parts of the capillary system. Reporter gene expression, which gradually faded out towards the periphery, could be detected in major arteries and arterioles that branched away from positive arteries. Patchy X-Gal staining was visible in capillaries but appeared to be less prominent than in the respective experiment with the constitutively active Cre line. At the angiogenic front reporter gene activity could be detected in a few isolated patches which consisted mostly of stalk cells and a minority of tip cells. In rare cases, isolated positive ECs could be detected as well. No expression in veins or non-ECs could be observed.

P10 Retina (Tamoxifen Injected P6 – P8)

At P10 I could detect robust and continuous staining in all major arteries that gradually faded out towards the periphery of the retina. While staining was present in all three vascular layers, no staining could be observed in veins or non-ECs. Similar to the previously described expression patterns in the constitutively active Cre line, reporter gene activity expanded into the artery derived microvasculature, while being mostly absent in venous derived microvasculature and sinuses. Again, this distinction led to the formation of large X-Gal positive and X-Gal negative vascular domains. However, the transitions appeared less abrupt compared to the constitutively active Cre line.

P20 Retina (Tamoxifen Injected P12 – P15)

Comparatively weak reporter gene activity could be detected in P20 retinas. Staining was present in capillaries of all three vascular layers and in major arteries but appeared patchier compared to previous experiments. In order to gain additional insight into the reporter gene expression patterns, I also X-Gal stained whole-mounts of the peritoneum. Although the vascular network of the peritoneum is less stereotypical than the vasculature of the retina or the spinotrapezius muscle (which I could not analyse due to the small size of the mice), it is still a useful model as it is very accessible to staining and whole-mount microscopy. I could detect X-Gal staining in major vessels of the peritoneum that appeared stronger compared to the retina.

Adult Retina and Spinotrapezius Muscle

In contrast to the previous results, tamoxifen administration in adult mice (~3 month) induced only a weak reporter gene response in retinas. Although EYFP expression could be detected in parts of the microvasculature, which were scattered randomly across the retina, and major arteries, staining intensity was very faint. Therefore, an anti-EYFP antibody IHC strategy in

conjunction with signal amplification had to be used for detection, resulting in more unspecific staining. The same was true for the analysis of spinotrapezius muscle, which was rendered inconclusive due to strong unspecific staining next to the blood vessels.

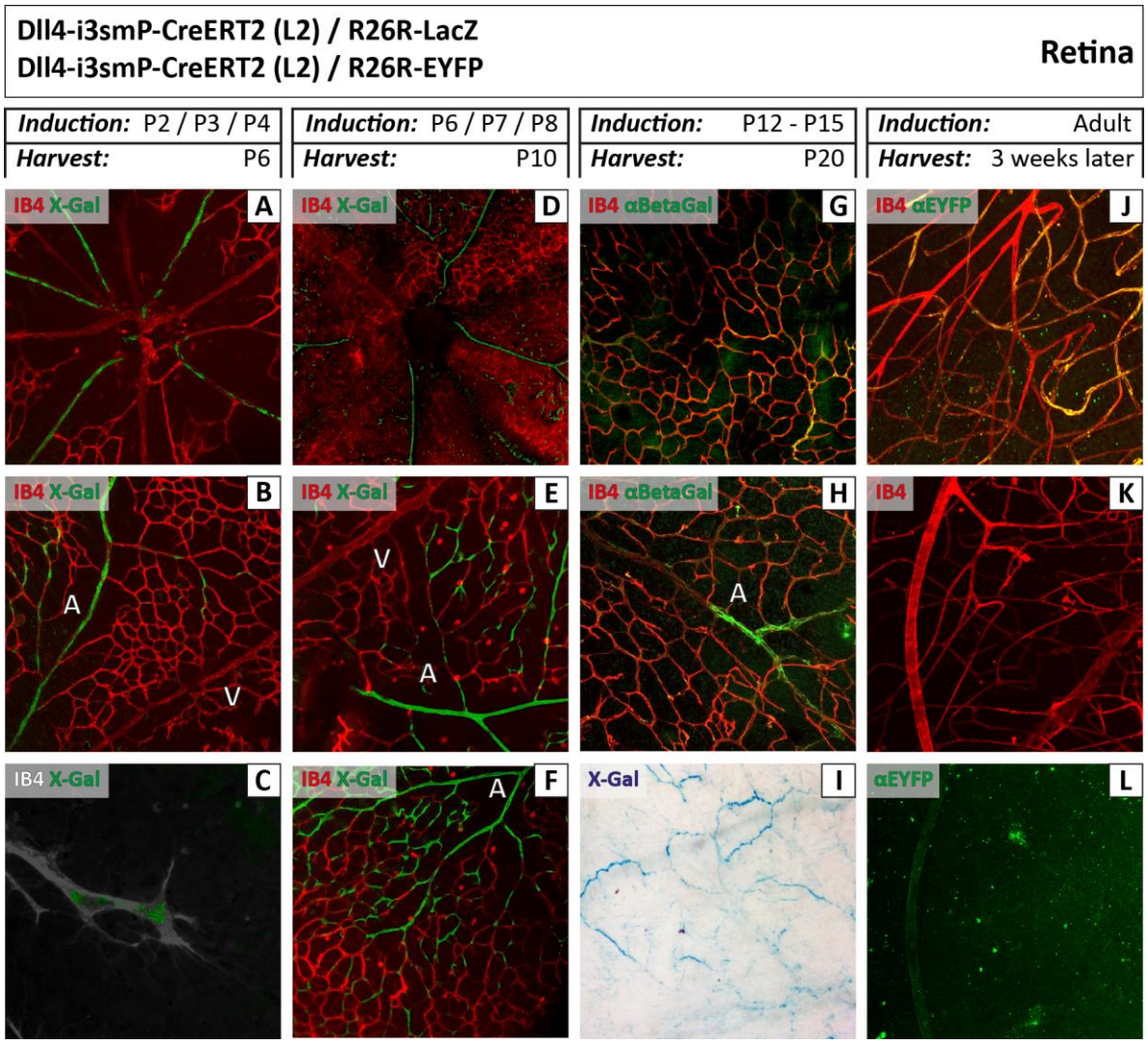

Figure 44 | LacZ in in3smP-CreERT2 / R26R-LacZ / R26R-EYFP retinas at various stages
A/B/C: P6 retina; (A) overview over central vasculature; (B) X-Gal staining in arteries extending into capillaries; (C) positive tip cell at angiogenic front,
D/E/F: P10 retina; (A) overview over central vasculature; (B) X-Gal staining in arteries extending into capillaries; (C) X-Gal(+) capillaries derive from arteries in peripheral areas
G/H/I: P20 retina; (G) patchy staining in primary plexus; (H) patchy staining in major artery; (I) X-Gal staining on whole-mount preparation of the peritoneum showing positive major vessels
J/K/L: Adult retina; (J) weak, irregular EYFP expression in capillary system; (K/L) weak staining in artery, channels separated for better visibility, speckles are most likely due to unspecific staining since very high photomultiplier gain settings had to be used
A: Artery; V: Vein

5.1.6.1 Expression of Endogenous Dll4 in P6 Retina

Similar to the experiments in the embryonic hindbrain, a comparison of Dll4-in3CreERT2 dependent reporter gene and endogenous Dll4 expression was performed. It allowed to determine which part of the Dll4 expression spectrum is covered by the Dll4-in3smP construct and if once labelled ECs continue to follow the endogenous Dll4 expression pattern. Therefore, I have performed IHC staining on the vasculature of P6 retinas. As expected Dll4 expression was detectable in arteries and arterioles. However, it is absent in virtually all arterial ECs as observed in the Dll4-in3smP-CreERT2 experiment. Moreover, it became apparent, that endogenous Dll4 was detectable in a larger portion of the capillary system and the previously observed distinction between positively and negatively stained regions was not present. Albeit, in increased staining intensity could be observed at the transition zone between arterioles and capillaries. At the angiogenic front Dll4 expression was much more prominent in tip cell than the reporter gene and showed a speckle-like distribution.

The results of the Dll4 IHC staining in the P6 retina are shown in Figure 45.

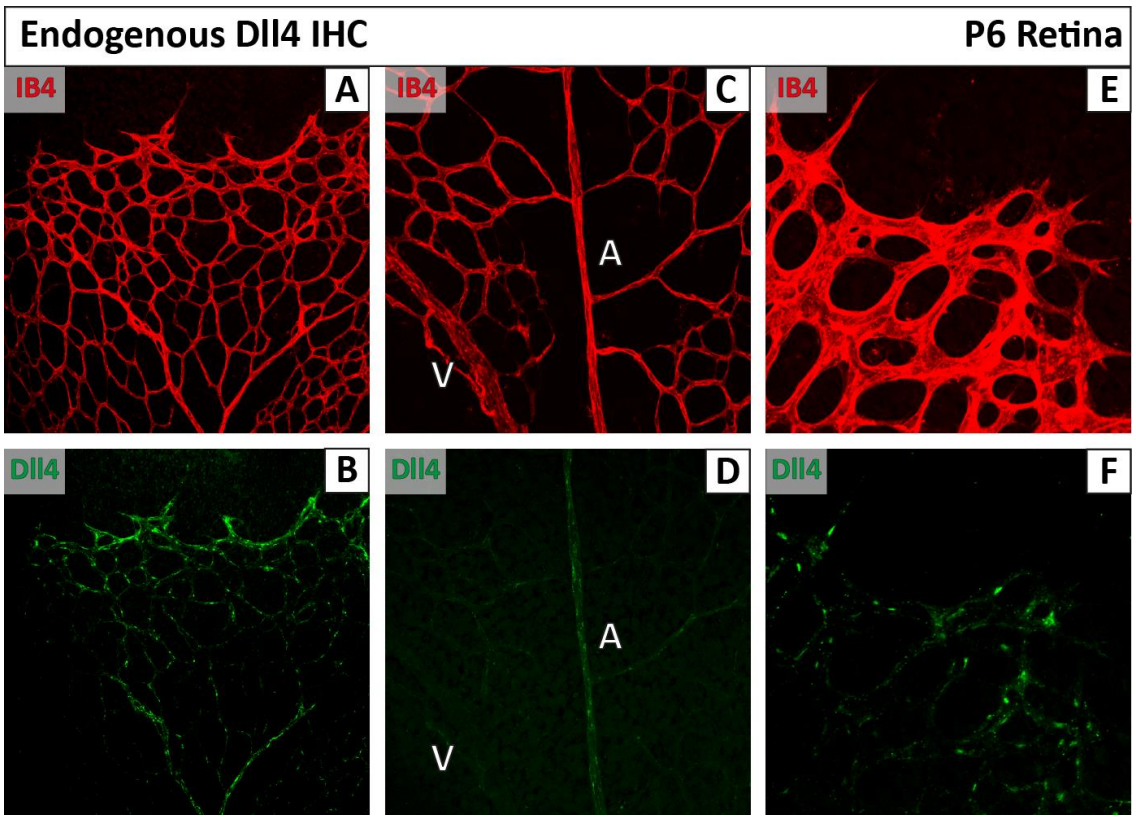

Figure 45 | Expression of endogenous Dll4 in P6 retina
A/B: Overview of capillary system shows speckled Dll4 expression that intensifies at angiogenic front
C/D: Magnified view on Dll4(+) artery and arteriole and negative vein
E/F: Magnified view on angiogenic front with speckle-like Dll4 expression in tip and stalk cells
A: Artery; V: Vein

5.1.7 Conclusions

In order to generate novel transgenic mouse lines that direct constitutively active and inducible Cre recombinase activity to the arterial endothelium, I have combined an enhancer element, found in the third intron of Notch ligand Dll4, with the endogenous minimal Dll4 promoter to drive Cre and Cre-ERT2 expression. After proving *in vitro* and *in vivo* that the Dll4-in3smP construct is inducible and specifically active in arteries, I performed a fate map analysis of arterial ECs.

5.1.7.1 Lineage Tracing of Arterial ECs in Vascular Development

For the constitutively active Cre line, I was able to detect reporter gene expression from E9.5 onwards and for the CreERT2 line the earliest time point with detectable reporter gene expression was E13.5 after tamoxifen injection at E10.5 and E11.5. In both lines expression could first be detected in almost all major arteries throughout the whole embryo and with increasing length of transgene activity expression extended into parts of the microvasculature. Remarkably, even at E18.5 only a part of the microvasculature displayed reporter gene expression, usually at sites of increased proliferation and morphological change, such as within the developing limbs and pulmonary vasculature. This expression pattern remained stable in postnatal development as well. I could detect widespread arterial expression and partially microvascular expression in 6 month old mice.

Reporter gene expression in the tissues of the heart showed some interesting patterns. After the cardiac mesoderm has been specified and the primitive heart tube has been formed, Notch signalling has a crucial role in cardiac development (Niessen and Karsan, 2008). In the constitutively active Cre line, reporter gene activity was present at E11.5 in the cushion tissues that give rise to the future valves, lining cells of the outflow tract, and the endocardium of the trabeculae. Consequently, at E16.5 expression was detectable in aortic arch arteries, in pulmonary and tricuspid valves, which derive from the cushion tissue, and within the

trabeculae. All these findings are in line with the well-established expression of Dll4 at E9.5 in the atrioventricular (AV) canal endocardium that gives rise to the mentioned structures. Interestingly, when induced at E10.5 and E11.5 the time window for activation in AV canal derived tissues seemed to be closed since no expression, with the exception of the coronary vasculature, could be detected in E16.5 hearts of Dll4-in3smP-CreERT2 mice. The ontogeny of the coronary vasculature is subject of current research and such diverse tissues as the proepicardium (Lavine and Ornitz, 2009) and the sinus venosus (Red-Horse et al., 2010) have been proposed as developmental origins for the ECs of coronary vessels. My observation that Dll4-in3smP-CreERT2 labels the coronary vasculature supports the latter, as Red-Horse *et al.* reported Dll4 expression in angiogenic sprouts extending from the sinus venosus, whereas Lavine and Ornitz suggest that epithelial cells transdifferentiate into endothelial progenitors that then form the coronary vasculature through vasculogenesis.

Neuronal expression, characteristic for endogenous Dll4, especially prior to E14.5 (Benedito and Duarte, 2005), was not observed in any reporter experiment, proving that the enhancer/reporter construct does not cover this aspect of the Dll4 expression spectrum.

Intriguingly, I was able to detect reporter gene activity in individual circulating cells, possibly erythrocytes and megakaryocytes, although these cells do not express endogenous Dll4 during embryonic development. However, I could observe Dll4-in3smP expression in the arteries during the formation of the hemogenic endothelium from the ventral wall of the dorsal aorta (Kim et al., 2013). Therefore, I assume that these cells derive from haematopoietic precursors that were labelled by the Dll4-in3smP reporter gene. This is supported by the observation that no positive circulating cells were found in the inducible Cre line, which is probably due to the fact that Cre activity was induced after definitive haematopoiesis had been established in the fetal liver. It is noteworthy that in the constitutively active Cre line, labelled circulating cells were present in neonatal mice at P9, since this supports the hypothesis that AGM derived HSCs contribute to adult haematopoiesis (Ueno and Weissman, 2007).

In both Cre and CreERT2 lines, X-gal stained non-ECs could be found in the wall of the gut, possibly related to previous reports that found endogenous Dll4 expression after E15.5 in the epithelial cells of the villi projections of the gut and in adult mice in the crypts (Benedito and Duarte, 2005). I could detect gut Dll4 expression at the onset of reporter gene expression at E9.5 and show that through the course of development, expression in the mid- and hindgut gradually increases from anterior to posterior direction. Interestingly, when Cre recombinase was induced at E10.5, expression in the gut was not yet present at E14.5 but had begun by E16.5. Dll4 mediated Notch signalling was shown to be required for homeostasis of intestinal stem cells (Pellegrinet et al., 2011) but very little is known about its role in embryonic gut development.

In summary, it becomes apparent that, although the Dll4-i3smP enhancer/promoter construct is expressed in the arterial endothelium from early on in development, its expression is fairly limited in E16.5 embryos, with only parts of the microvasculature being labelled and labelling being absent in veins. This suggests that arterial ECs constitute a distinct lineage that rarely trans-differentiates into microvascular or venous cells. It has been shown that arterial cells can trans-differentiate into venous tissue during the formation of intersomitic vessels in zebrafish (Quillien et al., 2014). However, this capability is likely to be restricted to early embryonic development. The limited transition between arteries, arterioles and capillaries constitutes a fascinating observation and is discussed in the next section.

While analysis of embryos allowed a global view on reporter gene expression in the vasculature, the embryonic hindbrain and postnatal retina permitted me to trace the fate of individual ECs, in particular those at the angiogenic front, particularly tip and stalk cells. Detailed analysis of both vascular beds demonstrated that Cre recombinase was active in tip cells, although most expression in the capillaries was primarily distributed among the stalk cells, unlike endogenous Dll4, which showed stronger expression in tip cells. It is important to be aware of the fact that, although the mouse retina has many invaluable advantages as a model system, it only provides a static snapshot of the dynamic processes in angiogenesis. Individual ECs are thought to

remain in the tip cell position on average for less than 4 h (Jakobsson et al., 2010). Therefore, due to the temporal lag between Cre activation and sufficient reporter gene levels and the fact that β-Galactosidase and EYFP both have half-lives of ~30 h, it is inevitable that the visible reporter gene expression does not exactly mirror expression pattern of the Dll4 regulatory elements.

As outlined in the introduction, Dll4/Notch signalling is involved in several aspects of angiogenesis. Dll4 is expressed in tip cells and suppresses the tip cell phenotype in adjacent, Notch signal receiving ECs, and thereby induces stalk cell behaviour (Hellström et al., 2007; Leslie et al., 2007; Siekmann and Lawson, 2007). In addition, Dll4 is also a molecular marker of arterial endothelium (Shutter et al., 2000; Villa et al., 2001) and loss of just one Dll4 allele leads to failed arterial lineage specification (Duarte et al., 2004; Gale et al., 2004; Krebs et al., 2004). Overall, the results from the lineage tracing experiments, where I characterised the inducible and constitutively active Dll4-in3smP-Cre lines, suggest that the Dll4-in3smP enhancer/promoter construct mimics both the tip cell and arterial aspect of the Dll4 expression pattern. This raises the intriguing question how it is possible that even after constant Cre activation from E9.5 onwards, a relatively small portion of the vasculature is positive for the reporter gene later on in development? Due to the nature of the R26R-LacZ and R26R-EYFP lines, once the reporter gene is activated in a certain cell, it stays active and is transmitted in active state to its daughter cells, even if the controlling regulatory elements have been switched off in the meantime. In the standard model of angiogenesis, sprouts from pre-existing vascular beds invade avascular tissues and form a primitive plexus that later is remodelled into a highly hierarchical network with arteries and veins. Hence, it would be obvious to assume that most, if not all ECs, originate from cells, which at one point in time during development had occupied tip cell position. Nevertheless, this simplistic view is not consistent with my observations. Of particular note, at no time was reporter gene expression detectable in the venous endothelium. It is a known characteristic of the inducible Cre-loxP system that gene inactivation does not occur abruptly but in a gradual fashion. Different cells activate the Cre gene at slightly different time points and with different efficiencies. This leads to the phenomenon that after induction

the organism contains a mosaic of cells with active and non-active Cre recombinase. This can explain the patchwork-like distribution of positively and negatively stained regions in the retinal vasculature. However, even if Cre mosaicism is taken into account, the observation that reporter gene expression can be traced over extended periods in both tip cells and arteries, but remains exclusive from veins, is surprising and raises questions concerning the balance of tip and stalk cell incorporation into the vascular tree.

Chapter 6:

Discussion and Future Directions

6.1 Possible Role of Tal1 in Postnatal Vasculogenesis

Through analysis of Tal1 reporter gene and protein expression in the vasculature of the murine retina, I found no solid evidence for Tal1 being present in sprouting, remodelling, or quiescent blood vessels. Additionally, I have investigated the effects of induced, endothelial specific Tal1 deletion on the retinal and spinotrapezius vasculature and concluded that Tal1 does not play a critical role in postnatal sprouting angiogenesis or vascular homeostasis.

These results contradict the conclusions drawn by previous studies that relied on *in vitro* models (Deleuze et al., 2007, 2012; Lazrak et al., 2004). However, the findings could be explained by the developmental origin of the retinal vasculature. Being part of the central nervous system, the retina has some unique features concerning the vasculature, including a lack of resident angioblasts (Fruttiger, 2002). Considering that the vasculogenic function of Tal1 might be linked to endothelial precursor formation, it would be possible that it is not involved in retinal vascularisation, which occurs entirely due to angiogenesis. Indeed, in the study that reported Tal1 expression in the non-resting vasculature, TAL1 protein could only be detected in ECs and endothelial progenitors at sites of neovascularisation, such as wound healing and tumour vascularisation (Tang et al., 2006). This would be indicative for a role in vasculogenesis. Moreover, both the collective weight of the published studies on the defects in $Tal^{-/-}$ embryos, as well as my own results (see 4.6.2), suggest an involvement of Tal1 in vasculogenesis, at least during embryogenesis.

6.1.1 Outlook

Since my results suggest that Tal1 is not relevant in postnatal sprouting angiogenesis, while allowing the possibility of an involvement in other forms of blood vessel development, an interesting option for a follow up experiment is to study the influence of Tal1 depletion in a tumour mouse model.

It has been shown that besides angiogenesis, tumours can meet their high metabolic demands by developing new blood vessels via vasculogenesis or vasculogenesis-like mechanisms, especially when treated with anti-angiogenic drugs or radiotherapy (Ahn and Brown, 2008). Although the exact mechanisms seem to vary between different types of tumours, it is generally assumed that the incorporation of circulating putative endothelial progenitors plays a central role in tumour vasculogenesis (Brown, 2014). Besides its expression in tumour vasculature (Tang et al., 2006), Tal1 has also been reported to be expressed in haemangioblast-like cells that contribute to Hippel-Lindau disease associated haemangioblastomas (Zhuang et al., 2014).

Tumours can be induced in mice by radiation, carcinogen treatment, or by allograft or xenograft transplantation. Tal1 could be targeted by conditional KO either *in vitro* in the transplanted cancer cells or via tamoxifen induction in the transplant-receiving mouse.

Tumour vasculature often appears highly disorganised with heavily vascularised areas neighbouring vessel-poor regions and vessels displaying irregular and tortuous morphologies (Potente et al., 2011), thereby especially complicating analysis on sectioned tissues. Therefore, recently developed imaging techniques like optical coherence tomography (OCT) or intravital microscopy, which allow three-dimensional, deep-tissue imaging (Fukumura and Jain, 2008; Reif and Wang, 2012), could be utilised to investigate the impact of global or endothelial specific Tal1 deficiency on the organisation and function of tumour vasculature.

In order to follow the hypothesis of a role for Tal1 in vasculogenesis, it would also be worth considering if the induced, EC-specific KO of Tal1 could be analysed in an oxygen-induced retinopathy (OIR) experiment. This experimental approach uses exposure of mouse pups to hyperoxia, which leads to retinal capillary depletion. When the animals are returned to normoxia this results in retinal ischaemia and aberrant neovascularisation (Scott and Fruttiger, 2010). The mechanisms of neovascularisation differ from normal angiogenesis and have strong implications for blinding eye diseases and cancer, rendering a possible role of Tal1 in these conditions highly relevant.

6.2 Tal1 in between Angiogenesis and Vasculogenesis

Through investigation of vascular Tal1 expression patterns and the effects of VE-CadherinCreERT mediated Tal1 deficiency in the endothelium of mouse embryos, I found evidence for an involvement in both embryonic angiogenesis and vasculogenesis. Tamoxifen induced deletion of Tal1 in ECs at time points later than E9.5 did not lead to observable embryonic defects, whereas deletion of Tal1 in ECs starting from E7.5 resulted in lethal developmental defects at E11.5, which precluded a detailed analysis of the vasculature. Only by choosing an intermediate interval for tamoxifen induction and embryo harvest, I could perform an analysis of the effects of the Tal1 KO. Thereby, some of the observed vascular defects suggest a role of Tal1 in early vasculogenesis, while others indicate a certain involvement in angiogenesis. Moreover, the observation that Dll4-in3smP-Cre(+);Tal1$^{flox/flox}$ are not born in Mendelian ratios together with the fact that Dll4-in3smP constructs labels circulating cells when activated early on in development, indicate that the observed defects are due to defective definitive haematopoiesis caused by deletion of Tal1 in the arterial derived hemogenic endothelium.

For the interpretation of my results it is important to mention that in 2012, after this project was initiated, it was reported that Tal1$^{-/-}$ embryos display aberrant conversion of hemogenic endothelium within the yolk sac and placenta into cardiac fate, suggesting a role of Tal1 in endothelial plasticity (Van Handel et al., 2012). In this paper, the authors demonstrate that Tal1 inhibits activation of cardiomyocyte differentiation in the yolk sac and placenta, as well as in the endocardium, by repressing a broad range of cardiac transcription factors as well as canonical Wnt antagonists. The authors suggest that this finding could provide a possible explanation for the vascular phenotype of Tal1 deficient embryos, since a partial conversion of ECs into misplaced cardiomyocytes could explain the failure of Tal1$^{-/-}$ yolk sacs to develop organised vasculature that exceeds the primary plexus derived from fused blood islands. Their findings were corroborated by a more recent study that used ChIP-Seq on VEGFR-2 positive mesodermal cells differentiated *in vitro* from mouse ES cells (Org et al., 2015). The observed

endothelial plasticity is restricted to a developmental window, since deletion of Tal1 later than E9.5 does not induce cardiac conversion. This is reminiscent of the time window I observed, where embryos induced at E9.5 did not display an observable vascular phenotype anymore, leading to the possible conclusion that Tal1 does not fulfil a role in later vascular development.

However, the question remains how the vascular defects that I have observed in the non-hemogenic endothelium like the intersomitic vessels or head vasculature can be explained. Also the down-regulation of several vascular genes, such as Kdr, Flk1 and Esam1 in Tal1 depleted ECs hints to a more general function of Tal1 in angiogenesis (Org et al., 2015). Another unresolved issue is that the Tie2-Cre mediated KO does not show signs of a dedifferentiated hemogenic endothelium, since markers of definitive haematopoiesis are present, but still displays vascular defects (Schlaeger et al., 2005). Therefore, I assume that aberrant trans-differentiation of hemogenic endothelium may contribute to the observed developmental defects, but is not sufficient to explain the overall vascular phenotype resulting from Tal1 deficiency.

At the very basis of our current understanding of how vertebrate organisms form the complex vascular network that penetrates almost every part of their bodies, lies the distinction between vasculogenesis - the *de novo* formation of blood vessels, and angiogenesis – the formation of blood vessels from existing ones. Already in 1854 the growth of new capillaries from pre-existing vessels was described by Mejer (Mejer, 1852) and in 1917 Sabin described the formation of blood vessels by angioblasts (Sabin, 2002). In some cases, this binary view on blood vessel development might be an over-simplification, since during development both types of vessel formation occur in conjunction and a clear distinction is often not possible. In my opinion, the developmental transition between genetically "hard wired" vascular structures like the major vessels, and the self-organising vascular network of arterioles, venules and capillaries is a subject that still remains poorly understood. At E10.5, the vascular defects observed in the Tal1 conditional KO experiment fall into that grey area of development were both angiogenesis and vasculogenesis act in parallel to form the still stereotypic, but already

highly complex embryonic vasculature. Although the physiological role of Tal1 might be restricted to vasculogenesis until midgestation, tumour vasculature was shown to rely on vasculogenesis and vasculogenesis-like processes (Brown, 2014; Zhuang et al., 2014). Therefore, the aforementioned investigation of Tal1 in a tumour environment appears even more intriguing.

6.2.1 Outlook

In order to prove the hypothesis that the embryonic defects caused by the VE-CadherinCreERT2 mediated KO of Tal1 are related to a failed specification of the hemogenic endothelium, it is imperative to perform a detailed analysis of the present haematopoietic precursor cells.

The focus of this thesis lay on hole-mount immunostaining experiments in order to visualise the vasculature on an embryonic scale. Although this approach allowed novel insight into developmental defects of Tal1 deficient embryos, it is not suitable for investigating the emergence and differentiation of haematopoitic lineages. For future experiments I would therefore consider cell sorting strategies to isolate ECs and HSCs from WT and EC-specific Tal1 KO embryos that were tamoxifen induced at various time points. Related to the experiments performed by Van Handel *et al.*, a possible strategy would involve first to isolate CD31(+) endothelial cells and then to correlate the expression of the well-established haematopoietic marker CD45 with the presence of Tal1, since co-expression of CD31 and CD45 is a putative indicator for endothelium derived haematopoietic cells (Hirschi, 2012). Additionally, it would be interesting to investigate how differentially regulated genes that were enriched for the GO term “blood vessel development” in the microarray experiment performed by Van Handel *et al.* are affected by induced Tal1 KO.

6.3 Lineage Tracing of Arterial ECs

In the course of my investigation of the function of Tal1 in embryonic and postnatal vascularisation, a possible involvement of Tal1 in arterial development began to emerge. Since no transgenic Cre mouse line that sufficiently ablates gene expression in arterial ECs was available to investigate this hypothesis, I aimed to create a constitutive Cre and an inducible Cre pan-arterial specific mouse line. Therefore, I have combined a Dll4 enhancer element with the endogenous minimal Dll4 promoter to drive Cre and CreERT2 expression. After demonstrating that the Dll4-in3smP construct is inducible and specifically active in arteries and parts of the microvasculature, I performed a fate map analysis of arterial ECs. Although I could confirm a widely arterial expression pattern of the Dll4-in3smP construct from early on in development, it became apparent that during development its expression remained fairly limited, with only parts of the microvasculature being labelled and no expression detectable in veins. Moreover, I could show that the transgenic Cre lines also label tip cells in parts of the sprouting microvasculature. The resulting conclusion that arterial ECs constitute a distinct lineage, rarely trans-differentiating into microvascular or venous cells, raises questions concerning the variable commitment of ECs to different parts of the vascular system during development.

During the last decade, a tremendous amount of insight has been gained into the fundamental mechanics of vessel branching, leading to the model of EC sub-differentiation, in which motile tip cells, which lead new sprouts by sensing guidance cues, are followed by dividing stalk cells that form the vessel lumen. Since this model offered a solid framework for investigation of blood vessel development on cellular and molecular level, it was swiftly adapted and confirmed by countless studies. Thereby, only limited attention was given to the migratory behaviour of ECs within the developing vascular plexus. However, these processes are of critical importance for understanding how the vascular network becomes functional and how complex hierarchies among vessels are established. In recent years newly available techniques like *in vivo* time-lapse microscopy and the study of mosaic transgenic mouse lines generated insight into the dynamic movements of ECs within the developing vascular plexus.

It was found that EC proliferation during retinal vascular plexus formation differs between cells of arterial and venous origin. Endothelial proliferation seemed to be persistent in veins, the surrounding peri-venous vessel plexus and capillaries of the deeper layers, while being largely absent from arteries and surrounding vessels (Ehling et al., 2013). More recently Xe *et al*. corroborated this finding and additionally reported, by using cell tracking in the mouse retina and regenerating zebrafish fin, that endothelial tip cells contribute mainly to forming arteries, and only marginally contribute to veins (Xu et al., 2014). Together these findings have the potential to partially explain the observed expression pattern of the EC fate mapping experiments. Considering that new ECs originate from venous domains, subsequently assume tip cell positions, where they activate reporter gene, and finally contribute to forming arteries, this could lead to the formation of the observed distinct reporter gene positive and negative vascular domains. This hypothesis is supported by the finding that endogenous Dll4 expression in ECs of major arteries and capillaries significantly overlaps with reporter gene expression.

The question remains how venous-derived capillaries initially sprout without activating the transgene in the tip cells. I speculate that venous-derived ECs display a transcriptional and signalling profile that inherently differs from arterial-derived ECs, possibly is not dependent on Dll4, and therefore the Dll4-in3smP transgene is not activated. This would also explain the finding that the complete microvasculature in embryonic hindbrains was positively stained. At the analysed developmental stages no arteriovenous differentiation had yet occurred in the hindbrain. In the regenerating zebrafish fin it was shown that venous derived tip cells perform highly stereotypic “turning” migratory movements to contribute to regenerating arteries, indicating a sophisticated transcriptional program in venous ECs (Xu et al., 2014). However, one should keep in mind that the zebrafish fin with its ray bifurcating arteries constitutes a very special vascular bed and similar experiments in other vascular beds should be awaited.

6.3.1 Outlook

Due to their expression in parts of the microvasculature, I have to state that the Dll4-in3smP-Cre and Dll4-in3smP-CreERT2 mouse lines might not be perfectly suited for their originally intended purpose of analysing the effects of gene deletion in arteries only. However, in the light of the recent developments in the research area of intra-network EC motility, I believe that insightful use of these transgenic lines is possible. For example, it was reported that the secreted molecule Endothelial cell–specific molecule 1 (Esm1) is specifically expressed in tip cells and influences sprouting by regulating VEGF-A bioavailability (Rocha et al., 2014). A specific KO of Esm1 in the arterial domain of the retinal vasculature could further deepen the understanding of the organisational principles that underlie the sprouting and remodelling vasculature.

The lineage tracing experiments performed with the Dll4-in3smP-Cre and Dll4-in3smP-CreERT2 mouse lines raised intriguing questions about the behaviour of arterial derived ECs during embryonic and postnatal vascularisation. Therefore, I suggest that it would be a promising option to further investigate the detailed migration patterns of ECs that were labelled by the Dll4-in3smP transgene. One possible approach is to simply repeat the lineage tracing experiments in the retina but with a series of increasing time intervals (around 12 h per step) between tamoxifen induction and analysis of the retinal vasculature. However, it has to be considered that shorter intervals might not result in detectable reporter gene activation.

As already discussed, the inherent disadvantage of the retina as a model system for angiogenesis is its inability to reveal the highly dynamic processes of blood vessel sprouting and remodelling. It is restricted to snapshots and does not allow real-time observation of angiogenic processes. In contrast, *ex vivo* assays like the aortic ring assay or the embryonic body assay offer the possibilities of live imaging and tracing of individual ECs. However, a disadvantage of these systems is the lack of real network maturation and the absence of arteriovenous differentiation. An ideal model system would combine the advantages of

both model systems. Although the procedure is technically challenging, it is possible to culture neonatal mouse retinas *ex vivo* for approximately 10 h (Sawamiphak et al., 2010b). This assay has mainly been used to evaluate the EC responses at the vascular front upon pharmacological manipulation. Although the hyperoxic conditions and lack of circulation have so far prevented extended cultivation of retinal explants, I think it is worth considering to use this model for time-lapse microscopy since this would allow unique insight into the migration patterns of labelled ECs during network formation.

Bibliography

Abedin, M.J., Nguyen, A., Jiang, N., Perry, C.E., Shelton, J.M., Watson, D.K., and Ferdous, A. (2014). Fli1 acts downstream of etv2 to govern cell survival and vascular homeostasis via positive autoregulation. Circ. Res. *114*, 1690–1699.

Adams, R.H., and Alitalo, K. (2007). Molecular regulation of angiogenesis and lymphangiogenesis. Nat. Rev. Mol. Cell Biol. *8*, 464–478.

Ahn, G.-O., and Brown, J.M. (2008). Matrix metalloproteinase-9 is required for tumor vasculogenesis but not for angiogenesis: role of bone marrow-derived myelomonocytic cells. Cancer Cell *13*, 193–205.

Antas, V.I., Al-Drees, M.A., Prudence, A.J.A., Sugiyama, D., and Fraser, S.T. (2013). Hemogenic endothelium: A vessel for blood production. Int. J. Biochem. Cell Biol. *45*, 692–695.

Armulik, A., Genové, G., Mäe, M., Nisancioglu, M.H., Wallgard, E., Niaudet, C., He, L., Norlin, J., Lindblom, P., Strittmatter, K., et al. (2010). Pericytes regulate the blood-brain barrier. Nature *468*, 557–561.

Arnold, C.D., Gerlach, D., Stelzer, C., Boryń, Ł.M., Rath, M., and Stark, A. (2013). Genome-wide quantitative enhancer activity maps identified by STARR-seq. Science *339*, 1074–1077.

Arroyo, A.G., and Iruela-Arispe, M.L. (2010). Extracellular matrix, inflammation, and the angiogenic response. Cardiovasc. Res. *86*, 226–235.

Asahara, T., Murohara, T., Sullivan, A., Silver, M., van der Zee, R., Li, T., Witzenbichler, B., Schatteman, G., and Isner, J.M. (1997). Isolation of putative progenitor endothelial cells for angiogenesis. Science *275*, 964–967.

Aspalter, I.M., Gordon, E., Dubrac, A., Ragab, A., Narloch, J., Vizán, P., Geudens, I., Collins, R.T., Franco, C.A., Abrahams, C.L., et al. (2015). Alk1 and Alk5 inhibition by Nrp1 controls vascular sprouting downstream of Notch. Nat. Commun. *6*, 7264.

Atkins, G.B., Jain, M.K., and Hamik, A. (2011). Endothelial differentiation: Molecular mechanisms of specification and heterogeneity. Arterioscler. Thromb. Vasc. Biol. *31*, 1476–1484.

Ausprunk, D.H., and Folkman, J. (1977). Migration and proliferation of endothelial cells in preformed and newly formed blood vessels during tumor angiogenesis. Microvasc. Res. *14*, 53–65.

Azzoni, E., Conti, V., Campana, L., Dellavalle, A., Adams, R.H., Cossu, G., and Brunelli, S. (2014). Hemogenic endothelium generates mesoangioblasts that contribute to several mesodermal lineages in vivo. Development *141*, 1821–1834.

Baluk, P., Morikawa, S., Haskell, A., Mancuso, M., and McDonald, D.M. (2003). Abnormalities of basement membrane on blood vessels and endothelial sprouts in tumors. Am. J. Pathol. *163*, 1801–1815.

Banerji, J., Rusconi, S., and Schaffner, W. (1981). Expression of a beta-globin gene is enhanced by remote SV40 DNA sequences. Cell *27*, 299–308.

Bannister, A.J., and Kouzarides, T. (2011). Regulation of chromatin by histone modifications. Cell Res. *21*, 381–395.

Beck, M., Schmidt, A., Malmstroem, J., Claassen, M., Ori, A., Szymborska, A., Herzog, F., Rinner, O., Ellenberg, J., and Aebersold, R. (2014). The quantitative proteome of a human cell line. Mol. Syst. Biol. *7*, 549–549.

Begley, C.G., Aplan, P.D., Davey, M.P., Nakahara, K., Tchorz, K., Kurtzberg, J., Hershfield, M.S., Haynes, B.F.,

Cohen, D.I., and Waldmann, T.A. (1989). Chromosomal translocation in a human leukemic stem-cell line disrupts the T-cell antigen receptor delta-chain diversity region and results in a previously unreported fusion transcript. Proc. Natl. Acad. Sci. U. S. A. *86*, 2031–2035.

Benedito, R., and Duarte, A. (2005). Expression of Dll4 during mouse embryogenesis suggests multiple developmental roles. Gene Expr. Patterns *5*, 750–755.

Benedito, R., Roca, C., Sörensen, I., Adams, S., Gossler, A., Fruttiger, M., and Adams, R.H. (2009). The Notch Ligands Dll4 and Jagged1 Have Opposing Effects on Angiogenesis. Cell *137*, 1124–1135.

Benedito, R., Rocha, S.F., Woeste, M., Zamykal, M., Radtke, F., Casanovas, O., Duarte, A., Pytowski, B., and Adams, R.H. (2012). Notch-dependent VEGFR3 upregulation allows angiogenesis without VEGF–VEGFR2 signalling. Nature *484*, 110–114.

Berthod, F., Symes, J., Tremblay, N., Medin, J.A., and Auger, F.A. (2012). Spontaneous fibroblast-derived pericyte recruitment in a human tissue-engineered angiogenesis model in vitro. J. Cell. Physiol. *227*, 2130–2137.

Bi, W., Drake, C.J., and Schwarz, J.J. (1999). The transcription factor MEF2C-null mouse exhibits complex vascular malformations and reduced cardiac expression of angiopoietin 1 and VEGF. Dev. Biol. *211*, 255–267.

Biggin, M.D. (2011). Animal Transcription Networks as Highly Connected, Quantitative Continua. Dev. Cell *21*, 611–626.

Birdsey, G.M., Shah, A. V, Dufton, N., Reynolds, L.E., Almagro, L.O., Yang, Y., Hodivala-dilke, K., Aspalter, I.M., Khan, S.T., Mason, J.C., et al. (2015). The Endothelial Transcription Factor ERG Promotes Vascular Stability and Growth through Wnt / b -Catenin Signaling. Dev. Cell *32*, 82–96.

Boeger, H., Bushnell, D.A., Davis, R., Griesenbeck, J., Lorch, Y., Strattan, J.S., Westover, K.D., and Kornberg, R.D. (2005). Structural basis of eukaryotic gene transcription. In FEBS Letters, pp. 899–903.

Boisset, J.-C., van Cappellen, W., Andrieu-Soler, C., Galjart, N., Dzierzak, E., and Robin, C. (2010). In vivo imaging of haematopoietic cells emerging from the mouse aortic endothelium. Nature *464*, 116–120.

Bonn, S., Zinzen, R.P., Girardot, C., Gustafson, E.H., Perez-Gonzalez, A., Delhomme, N., Ghavi-Helm, Y., Wilczyński, B., Riddell, A., and Furlong, E.E.M. (2012). Tissue-specific analysis of chromatin state identifies temporal signatures of enhancer activity during embryonic development. Nat. Genet. *44*, 148–156.

Bradley, C.K., Takano, E. a., Hall, M. a., Gothert, J.R., Harvey, A.R., Begley, C.G., and van Eekelen, J.A. (2006). The essential haematopoietic transcription factor Scl is also critical for neuronal development. Eur J Neurosci *23*, 1677–1689.

Brown, J.M. (2014). Vasculogenesis: a crucial player in the resistance of solid tumours to radiotherapy. Br. J. Radiol. *87*, 20130686.

Butler, J.M., Kobayashi, H., and Rafii, S. (2010). Instructive role of the vascular niche in promoting tumour growth and tissue repair by angiocrine factors. Nat. Rev. Cancer *10*, 138–146.

Caolo, V., Van Den Akker, N.M.S., Verbruggen, S., Donners, M.M.P.C., Swennen, G., Schulten, H., Waltenberger, J., Post, M.J., and Molin, D.G.M. (2010). Feed-forward signaling by membrane-bound ligand receptor circuit: The case of notch delta-like 4 ligand in endothelial cells. J. Biol. Chem. *285*, 40681–40689.

Capelson, M., and Corces, V.G. (2004). Boundary elements and nuclear organization. Biol. Cell *96*, 617–629.

Carmeliet, P., and Jain, R. (2011). Molecular mechanisms and clinical applications of angiogenesis. Nature *473*, 298–307.

Carmeliet, P., Ferreira, V., Breier, G., Pollefeyt, S., Kieckens, L., Gertsenstein, M., Fahrig, M., Vandenhoeck, A., Harpal, K., Eberhardt, C., et al. (1996). Abnormal blood vessel development and lethality in embryos lacking a single VEGF allele. Nature *380*, 435–439.

Castañares, C., Redondo-Horcajo, M., Magán-Marchal, N., ten Dijke, P., Lamas, S., and Rodríguez-Pascual, F. (2007). Signaling by ALK5 mediates TGF-beta-induced ET-1 expression in endothelial cells: a role for migration and proliferation. J. Cell Sci. *120*, 1256–1266.

Cermenati, S., Moleri, S., Cimbro, S., Corti, P., Giacco, L. Del, Amodeo, R., Dejana, E., Koopman, P., Cotelli, F., and Beltrame, M. (2008). Sox 18 and Sox7 play redundant roles in vascular development. Blood *111*, 2657–2666.

Chagraoui, H., Kassouf, M., Banerjee, S., Goardon, N., Clark, K., Atzberger, A., Pearce, A.C., Skoda, R.C., Ferguson, D.J.P., Watson, S.P., et al. (2011). SCL-mediated regulation of the cell-cycle regulator p21 is critical for murine megakaryopoiesis. Blood *118*, 723–735.

Chiang, C., Litingtung, Y., Lee, E., Young, K.E., Corden, J.L., Westphal, H., and Beachy, P. a (1996). Cyclopia and defective axial patterning in mice lacking Sonic hedgehog gene function. Nature *383*, 407–413.

Choi, K., Kennedy, M., Kazarov, A., Papadimitriou, J.C., and Keller, G. (1998). A common precursor for hematopoietic and endothelial cells. Development *125*, 725–732.

Chong, D.C., Koo, Y., Xu, K., Fu, S., and Cleaver, O. (2011). Stepwise arteriovenous fate acquisition during mammalian vasculogenesis. Dev. Dyn. *240*, 2153–2165.

Chouinard-Pelletier, G., Jahnsen, E.D., and Jones, E.A. V (2013). Increased shear stress inhibits angiogenesis in veins and not arteries during vascular development. Angiogenesis *16*, 71–83.

Chung, Y.S., Zhang, W.J., Arentson, E., Kingsley, P.D., Palis, J., and Choi, K. (2002). Lineage analysis of the hemangioblast as defined by FLK1 and SCL expression. Development *129*, 5511–5520.

Claxton, S., and Fruttiger, M. (2003). Role of arteries in oxygen induced vaso-obliteration. Exp. Eye Res. *77*, 305–311.

Claxton, S., and Fruttiger, M. (2005). Oxygen modifies artery differentiation and network morphogenesis in the retinal vasculature. Dev. Dyn. *233*, 822–828.

Corada, M., Nyqvist, D., Orsenigo, F., Caprini, A., Giampietro, C., Taketo, M.M., Iruela-Arispe, M.L., Adams, R.H., and Dejana, E. (2010). The Wnt/β-catenin pathway modulates vascular remodeling and specification by upregulating Dll4/notch signaling. Dev. Cell *18*, 938–949.

Corada, M., Orsenigo, F., Morini, M.F., Pitulescu, M.E., Bhat, G., Nyqvist, D., Breviario, F., Conti, V., Briot, A., Iruela-Arispe, M.L., et al. (2013). Sox17 is indispensable for acquisition and maintenance of arterial identity. Nat. Commun. *4*, 2609.

Cortegano, I., Melgar-Rojas, P., Luna-Zurita, L., Siguero-Álvarez, M., Marcos, M.A., Gaspar, M.L., and de la Pompa, J.L. (2014). Notch1 regulates progenitor cell proliferation and differentiation during mouse yolk sac hematopoiesis. Cell Death Differ. 1–14.

Cromey, D.W. (2010). Avoiding Twisted Pixels: Ethical Guidelines for the Appropriate Use and Manipulation of Scientific Digital Images. Sci. Eng. Ethics *16*, 639–667.

Curtis, D.J., Hall, M. a., Van Stekelenburg, L.J., Robb, L., Jane, S.M., and Begley, C.G. (2004). SCL is required for normal function of short-term repopulating hematopoietic stem cells. Blood *103*, 3342–3348.

D'Souza, B., Meloty-Kapella, L., and Weinmaster, G. (2010). Canonical and non-canonical notch ligands.

D'Souza, S.L., Elefanty, A.G., and Keller, G. (2005). SCL/Tal-1 is essential for hematopoietic commitment of the hemangioblast but not for its development. Blood *105*, 3862–3870.

Daly, C., Eichten, A., Castanaro, C., Pasnikowski, E., Adler, A., Lalani, A.S., Papadopoulos, N., Kyle, A.H., Minchinton, A.I., Yancopoulos, G.D., et al. (2013). Angiopoietin-2 functions as a Tie2 agonist in tumor models, where it limits the effects of VEGF inhibition. Cancer Res. *73*, 108–118.

Dejana, E. (2010). The role of wnt signaling in physiological and pathological angiogenesis. Circ. Res. *107*, 943–952.

Deleuze, V., Chalhoub, E., El-Hajj, R., Dohet, C., Le Clech, M., Couraud, P.-O., Huber, P., and Mathieu, D. (2007). TAL-1/SCL and its partners E47 and LMO2 up-regulate VE-cadherin expression in endothelial cells. Mol. Cell. Biol. *27*, 2687–2697.

Deleuze, V., El-Hajj, R., Chalhoub, E., Dohet, C., Pinet, V., Couttet, P., and Mathieu, D. (2012). Angiopoietin-2 is a direct transcriptional target of tal1, lyl1 and lmo2 in endothelial cells. PLoS One *7*, e40484.

Diez, H., Fischer, A., Winkler, A., Hu, C.J., Hatzopoulos, A.K., Breier, G., and Gessler, M. (2007). Hypoxia-mediated activation of Dll4-Notch-Hey2 signaling in endothelial progenitor cells and adoption of arterial cell fate. Exp. Cell Res. *313*, 1–9.

Doetschman, T. (2009). Influence of genetic background on genetically engineered mouse phenotypes. Methods Mol. Biol. *530*, 423–433.

Dooley, K.A., Davidson, A.J., and Zon, L.I. (2005). Zebrafish scl functions independently in hematopoietic and endothelial development. Dev. Biol. *277*, 522–536.

Doolittle, W.F. (2013). Is junk DNA bunk? A critique of ENCODE. Proc. Natl. Acad. Sci. U. S. A. *110*, 5294–5300.

Drake, C.J., and Fleming, P.A. (2000). Vasculogenesis in the day 6.5 to 9.5 mouse embryo. Blood *95*, 1671–1679.

Drake, C.J., Brandt, S.J., Trusk, T.C., and Little, C.D. (1997). TAL1/SCL is expressed in endothelial progenitor cells/angioblasts and defines a dorsal-to-ventral gradient of vasculogenesis. Dev. Biol. *192*, 17–30.

Duarte, A., Hirashima, M., Benedito, R., Trindade, A., Diniz, P., Bekman, E., Costa, L., Henrique, D., and Rossant, J. (2004). Dosage-sensitive requirement for mouse Dll4 in artery development. Genes Dev. *18*, 2474–2478.

Ehling, M., Adams, S., Benedito, R., and Adams, R.H. (2013). Notch controls retinal blood vessel maturation and quiescence. Development *140*, 3051–3061.

Eilken, H.M., Nishikawa, S.-I., and Schroeder, T. (2009). Continuous single-cell imaging of blood generation from haemogenic endothelium. Nature *457*, 896–900.

Eklund, L., and Saharinen, P. (2013). Angiopoietin signaling in the vasculature. Exp. Cell Res. *319*, 1271–1280.

Ekman, N., Lymboussaki, A., Västrik, I., Sarvas, K., Kaipainen, A., and Alitalo, K. (1997). Bmx tyrosine kinase is specifically expressed in the endocardium and the endothelium of large arteries. Circulation *96*, 1729–1732.

Elefanty, a G., Begley, C.G., Metcalf, D., Barnett, L., Köntgen, F., and Robb, L. (1998). Characterization of

hematopoietic progenitor cells that express the transcription factor SCL, using a lacZ "knock-in" strategy. Proc. Natl. Acad. Sci. U. S. A. *95*, 11897–11902.

Elefanty, A.G., Begley, C.G., Hartley, L., Papaevangeliou, B., and Robb, L. (1999). SCL expression in the mouse embryo detected with a targeted lacZ reporter gene demonstrates its localization to hematopoietic, vascular, and neural tissues. Blood *94*, 3754–3763.

Ema, M., Faloon, P., Zhang, W.J., Hirashima, M., Reid, T., Stanford, W.L., Orkin, S., Choi, K., and Rossant, J. (2003). Combinatorial effects of Flk1 and Tal1 on vascular and hematopoietic development in the mouse. Genes Dev. *17*, 380–393.

Even, M.D., Laughlin, M.H., Krause, G.F., and vom Saal, F.S. (1994). Differences in blood flow to uterine segments and placentae in relation to sex, intrauterine location and side in pregnant rats. J Reprod Fertil *102*, 245–252.

Fantin, A., Vieira, J.M., Gestri, G., Denti, L., Schwarz, Q., Prykhozhij, S., Peri, F., Wilson, S.W., and Ruhrberg, C. (2010). Tissue macrophages act as cellular chaperones for vascular anastomosis downstream of VEGF-mediated endothelial tip cell induction. Blood *116*, 829–840.

Fantin, A., Vieira, J.M., Plein, A., Maden, C.H., and Ruhrberg, C. (2013). The embryonic mouse hindbrain as a qualitative and quantitative model for studying the molecular and cellular mechanisms of angiogenesis. Nat. Protoc. *8*, 418–429.

Faul, F., Erdfelder, E., Buchner, A., and Lang, A.-G. (2009). Statistical power analyses using G*Power 3.1: tests for correlation and regression analyses. Behav. Res. Methods *41*, 1149–1160.

Feil, R., Brocard, J., Mascrez, B., LeMeur, M., Metzger, D., and Chambon, P. (1996). Ligand-activated site-specific recombination in mice. Proc. Natl. Acad. Sci. U. S. A. *93*, 10887–10890.

Feil, S., Valtcheva, N., and Feil, R. (2009). Inducible cre mice. Methods Mol. Biol. *530*, 343–363.

Ferdous, A., Caprioli, A., Iacovino, M., Martin, C.M., Morris, J., Richardson, J.A., Latif, S., Hammer, R.E., Harvey, R.P., Olson, E.N., et al. (2009). Nkx2-5 transactivates the Ets-related protein 71 gene and specifies an endothelial/endocardial fate in the developing embryo. Proc. Natl. Acad. Sci. U. S. A. *106*, 814–819.

Ferguson, J.E., Kelley, R.W., and Patterson, C. (2005). Mechanisms of endothelial differentiation in embryonic vasculogenesis. Arterioscler. Thromb. Vasc. Biol. *25*, 2246–2254.

Ferrando, A.A., Neuberg, D.S., Staunton, J., Loh, M.L., Huard, C., Raimondi, S.C., Behm, F.G., Pui, C.H., Downing, J.R., Gilliland, D.G., et al. (2002). Gene expression signatures define novel oncogenic pathways in T cell acute lymphoblastic leukemia. Cancer Cell *1*, 75–87.

Fischer, A., Schumacher, N., Maier, M., Sendtner, M., and Gessler, M. (2004). The Notch target genes Hey1 and Hey2 are required for embryonic vascular development. Genes Dev. *18*, 901–911.

Fruttiger, M. (2002). Development of the mouse retinal vasculature: Angiogenesis versus vasculogenesis. Investig. Ophthalmol. Vis. Sci. *43*, 522–527.

Fukumura, D., and Jain, R.K. (2008). Imaging angiogenesis and the microenvironment. Apmis *116*, 695–715.

Furuyama, T., Kitayama, K., Shimoda, Y., Ogawa, M., Sone, K., Yoshida-Araki, K., Hisatsune, H., Nishikawa, S.I., Nakayama, K., Nakayama, K., et al. (2004). Abnormal angiogenesis in Foxo1 (Fkhr)-deficient mice. J. Biol. Chem. *279*, 34741–34749.

Gaengel, K., Genové, G., Armulik, A., and Betsholtz, C. (2009). Endothelial-mural cell signaling in vascular development and angiogenesis. Arterioscler. Thromb. Vasc. Biol. *29*, 630–638.

Gale, N.W., Thurston, G., Hackett, S.F., Renard, R., Wang, Q., McClain, J., Martin, C., Witte, C., Witte, M.H., Jackson, D., et al. (2002). Angiopoietin-2 is required for postnatal angiogenesis and lymphatic patterning, and only the latter role is rescued by angiopoietin-1. Dev. Cell *3*, 411–423.

Gale, N.W., Dominguez, M.G., Noguera, I., Pan, L., Hughes, V., Valenzuela, D.M., Murphy, A.J., Adams, N.C., Lin, H.C., Holash, J., et al. (2004). Haploinsufficiency of delta-like 4 ligand results in embryonic lethality due to major defects in arterial and vascular development. Proc. Natl. Acad. Sci. U. S. A. *101*, 15949–15954.

Galie, P. a, Nguyen, D.-H.T., Choi, C.K., Cohen, D.M., Janmey, P. a, and Chen, C.S. (2014). Fluid shear stress threshold regulates angiogenic sprouting. Proc. Natl. Acad. Sci. U. S. A. *111*, 7968–7973.

Gekas, C., Dieterlen-Lièvre, F., Orkin, S.H., and Mikkola, H.K.A. (2005). The placenta is a niche for hematopoietic stem cells. Dev. Cell *8*, 365–375.

Gerety, S.S., Wang, H.U., Chen, Z.F., and Anderson, D.J. (1999). Symmetrical mutant phenotypes of the receptor EphB4 and its specific transmembrane ligand ephrin-B2 in cardiovascular development. Mol. Cell *4*, 403–414.

Gerhardt, H. (2008). VEGF and endothelial guidance in angiogenic sprouting. Organogenesis *4*, 241–246.

Gering, M., and Patient, R. (2005). Hedgehog signaling is required for adult blood stem cell formation in zebrafish embryos. Dev. Cell *8*, 389–400.

Gering, M., Rodaway, A.R.F., Göttgens, B., Patient, R.K., and Green, A.R. (1998). The SCL gene specifies haemangioblast development from early mesoderm. EMBO J. *17*, 4029–4045.

Gering, M., Yamada, Y., Rabbitts, T.H., and Patient, R.K. (2003). Lmo2 and Scl/Tal1 convert non-axial mesoderm into haemangioblasts which differentiate into endothelial cells in the absence of Gata1. Development *130*, 6187–6199.

Giroux, S., Kaushik, A.L., Capron, C., Jalil, A., Kelaidi, C., Sablitzky, F., Dumenil, D., Albagli, O., and Godin, I. (2007). lyl-1 and tal-1/scl, two genes encoding closely related bHLH transcription factors, display highly overlapping expression patterns during cardiovascular and hematopoietic ontogeny. Gene Expr. Patterns *7*, 215–226.

Goardon, N., Lambert, J. a, Rodriguez, P., Nissaire, P., Herblot, S., Thibault, P., Dumenil, D., Strouboulis, J., Romeo, P.-H., and Hoang, T. (2006). ETO2 coordinates cellular proliferation and differentiation during erythropoiesis. EMBO J. *25*, 357–366.

Goldie, L.C., Lucitti, J.L., Dickinson, M.E., and Hirschi, K.K. (2008). Cell signaling directing the formation and function of hemogenic endothelium during murine embryogenesis. Blood *112*, 3194–3204.

Golub, R., and Cumano, A. (2013). Embryonic hematopoiesis. Blood Cells, Mol. Dis. *51*, 226–231.

Goodwin, A.M., Sullivan, K.M., and D'Amore, P.A. (2006). Cultured endothelial cells display endogenous activation of the canonical Wnt signaling pathway and express multiple ligands, receptors, and secreted modulators of Wnt signaling. Dev. Dyn. *235*, 3110–3120.

Göttgens, B., Ferreira, R., Sanchez, M.-J., Ishibashi, S., Li, J., Spensberger, D., Lefevre, P., Ottersbach, K., Chapman, M., Kinston, S., et al. (2010). cis-Regulatory remodeling of the SCL locus during vertebrate evolution. Mol. Cell. Biol. *30*, 5741–5751.

Goumans, M.-J., Valdimarsdottir, G., Itoh, S., Rosendahl, A., Sideras, P., and ten Dijke, P. (2002). Balancing the activation state of the endothelium via two distinct TGF-beta type I receptors. EMBO J. *21*, 1743–1753.

Graur, D., Zheng, Y., Price, N., Azevedo, R.B.R., Zufall, R.A., and Elhaik, E. (2013). On the immortality of

television sets: "Function" in the human genome according to the evolution-free gospel of encode. Genome Biol. Evol. *5*, 578–590.

Grego-Bessa, J., Luna-Zurita, L., del Monte, G., Bolós, V., Melgar, P., Arandilla, A., Garratt, A.N., Zang, H., Mukouyama, Y. suke, Chen, H., et al. (2007). Notch Signaling Is Essential for Ventricular Chamber Development. Dev. Cell *12*, 415–429.

Grosveld, F., van Assendelft, G.B., Greaves, D.R., and Kollias, G. (1987). Position-independent, high-level expression of the human β-globin gene in transgenic mice. Cell *51*, 975–985.

Gu, C., Rodriguez, E.R., Reimert, D. V., Shu, T., Fritzsch, B., Richards, L.J., Kolodkin, A.L., and Ginty, D.D. (2003). Neuropilin-1 conveys semaphorin and VEGF signaling during neural and cardiovascular development. Dev. Cell *5*, 45–57.

Guruharsha, K.G., Kankel, M.W., and Artavanis-Tsakonas, S. (2012). The Notch signalling system: recent insights into the complexity of a conserved pathway. Nat. Rev. Genet. *13*, 654–666.

Hahn, C., and Schwartz, M.A. (2009). Mechanotransduction in vascular physiology and atherogenesis. Nat. Rev. Mol. Cell Biol. *10*, 53–62.

Hall, M.A., Slater, N.J., Begley, C.G., Salmon, J.M., Van Stekelenburg, L.J., McCormack, M.P., Jane, S.M., and Curtis, D.J. (2005). Functional but abnormal adult erythropoiesis in the absence of the stem cell leukemia gene. Mol. Cell. Biol. *25*, 6355–6362.

Hammes, H.P., Lin, J., Wagner, P., Feng, Y., Vom Hagen, F., Krzizok, T., Renner, O., Breier, G., Brownlee, M., and Deutsch, U. (2004). Angiopoietin-2 Causes Pericyte Dropout in the Normal Retina: Evidence for Involvement in Diabetic Retinopathy. Diabetes *53*, 1104–1110.

Han, X., Boyd, P.J., Colgan, S., Madri, J.A., and Haas, T.L. (2003). Transcriptional Up-regulation of Endothelial Cell Matrix Metalloproteinase-2 in Response to Extracellular Cues Involves GATA-2. J. Biol. Chem. *278*, 47785–47791.

Van Handel, B., Montel-Hagen, A., Sasidharan, R., Nakano, H., Ferrari, R., Boogerd, C.J., Schredelseker, J., Wang, Y., Hunter, S., Org, T., et al. (2012). Scl represses cardiomyogenesis in prospective hemogenic endothelium and endocardium. Cell *150*, 590–605.

Harrison, D.E., Astle, C.M., and Delaittre, J.A. (1978). Loss of proliferative capacity in immunohemopoietic stem cells caused by serial transplantation rather than aging. J. Exp. Med. *147*, 1526–1531.

Hayashi, H., and Kume, T. (2008). Foxc transcription factors directly regulate DII4 and hey2 expression by interacting with the VEGF-notch signaling pathways in endothelial cells. PLoS One *3*.

Heffner, C.S., Herbert Pratt, C., Babiuk, R.P., Sharma, Y., Rockwood, S.F., Donahue, L.R., Eppig, J.T., and Murray, S.A. (2012). Supporting conditional mouse mutagenesis with a comprehensive cre characterization resource. Nat. Commun. *3*, 1218.

Hellström, M., Gerhardt, H., Kalén, M., Li, X., Eriksson, U., Wolburg, H., and Betsholtz, C. (2001). Lack of pericytes leads to endothelial hyperplasia and abnormal vascular morphogenesis. J. Cell Biol. *152*, 543–553.

Hellström, M., Phng, L.-K., Hofmann, J.J., Wallgard, E., Coultas, L., Lindblom, P., Alva, J., Nilsson, A.-K., Karlsson, L., Gaiano, N., et al. (2007). Dll4 signalling through Notch1 regulates formation of tip cells during angiogenesis. Nature *445*, 776–780.

Herbert, S.P., Huisken, J., Kim, T.N., Feldman, M.E., Houseman, B.T., Wang, R.A., Shokat, K.M., and Stainier, D.Y.R. (2009). Arterial-venous segregation by selective cell sprouting: an alternative mode of blood vessel formation. Science *326*, 294–298.

Herpers, R., Van De Kamp, E., Duckers, H.J., and Schulte-Merker, S. (2008). Redundant roles for sox7 and sox18 in arteriovenous specification in Zebrafish. Circ. Res. *102*, 12–15.

Herzlinger, D., and Hurtado, R. (2014). Patterning the renal vascular bed. Semin. Cell Dev. Biol. *36*, 1–7.

Hicks, C., Johnston, S.H., diSibio, G., Collazo, A., Vogt, T.F., and Weinmaster, G. (2000). Fringe differentially modulates Jagged1 and Delta1 signalling through Notch1 and Notch2. Nat. Cell Biol. *2*, 515–520.

High, F.A., Lu, M.M., Pear, W.S., Loomes, K.M., Kaestner, K.H., and Epstein, J.A. (2008). Endothelial expression of the Notch ligand Jagged1 is required for vascular smooth muscle development. Proc. Natl. Acad. Sci. U. S. A. *105*, 1955–1959.

Hiratsuka, S., Minowa, O., Kuno, J., Noda, T., and Shibuya, M. (1998). Flt-1 lacking the tyrosine kinase domain is sufficient for normal development and angiogenesis in mice. Proc. Natl. Acad. Sci. U. S. A. *95*, 9349–9354.

Hirschi, K.K. (2012). Hemogenic endothelium during development and beyond. Blood *119*, 4823–4837.

Hollenhorst, P.C., Jones, D.A., and Graves, B.J. (2004). Expression profiles frame the promoter specificity dilemma of the ETS family of transcription factors. Nucleic Acids Res. *32*, 5693–5702.

Hong, J.-W., Hendrix, D.A., and Levine, M.S. (2008). Shadow enhancers as a source of evolutionary novelty. Science *321*, 1314.

Hsu, H.C., Ema, H., Osawa, M., Nakamura, Y., Suda, T., and Nakauchi, H. (2000). Hematopoietic stem cells express Tie-2 receptor in the murine fetal liver. Blood *96*, 3757–3762.

Huber, T.L., Kouskoff, V., Fehling, H.J., Palis, J., and Keller, G. (2004). Haemangioblast commitment is initiated in the primitive streak of the mouse embryo. Nature *432*, 625–630.

Indra, A.K., Warot, X., Brocard, J., Bornert, J.M., Xiao, J.H., Chambon, P., and Metzger, D. (1999). Temporally-controlled site-specific mutagenesis in the basal layer of the epidermis: Comparison of the recombinase activity of the tamoxifen-inducible Cre-ER(T) and Cre-ER(T2) recombinases. Nucleic Acids Res. *27*, 4324–4327.

Ingham, P.W., Nakano, Y., and Seger, C. (2011). Mechanisms and functions of Hedgehog signalling across the metazoa. Nat. Rev. Genet. *12*, 393–406.

Ittner, L.M., and Götz, J. (2007). Pronuclear injection for the production of transgenic mice. Nat. Protoc. *2*, 1206–1215.

Jabbari, K., and Bernardi, G. (2004). Cytosine methylation and CpG, TpG (CpA) and TpA frequencies. Gene *333*, 143–149.

Jahnsen, E.D., Trindade, A., Zaun, H.C., Lehoux, S., Duarte, A., and Jones, E.A. V (2015). Notch1 Is pan-endothelial at the onset of flow and regulated by flow. PLoS One *10*, e0122622.

Jakobsson, L., Franco, C. a, Bentley, K., Collins, R.T., Ponsioen, B., Aspalter, I.M., Rosewell, I., Busse, M., Thurston, G., Medvinsky, A., et al. (2010). Endothelial cells dynamically compete for the tip cell position during angiogenic sprouting. Nat. Cell Biol. *12*, 943–953.

Jordan, H.E. (1917). Aortic Cell Clusters in Vertebrate Embryos. Proc. Natl. Acad. Sci. U. S. A. *3*, 149–156.

Jordan, V.C., and Murphy, C.S. (1990). Endocrine pharmacology of antiestrogens as antitumor agents. Endocr. Rev. *11*, 578–610.

Juven-Gershon, T., and Kadonaga, J.T. (2010). Regulation of gene expression via the core promoter and

the basal transcriptional machinery. Dev. Biol. *339*, 225–229.

Kallianpur, A.R., Jordan, J.E., and Brandt, S.J. (1994). The SCL/TAL-1 gene is expressed in progenitors of both the hematopoietic and vascular systems during embryogenesis. Blood *83*, 1200–1208.

Kamachi, Y., and Kondoh, H. (2013). Sox proteins: regulators of cell fate specification and differentiation. Development *140*, 4129–4144.

Kamath, B.M., Bauer, R.C., Loomes, K.M., Chao, G., Gerfen, J., Hutchinson, A., Hardikar, W., Hirschfield, G., Jara, P., Krantz, I.D., et al. (2012). NOTCH2 mutations in Alagille syndrome. J. Med. Genet. *49*, 138–144.

Kamei, M., Saunders, W.B., Bayless, K.J., Dye, L., Davis, G.E., and Weinstein, B.M. (2006). Endothelial tubes assemble from intracellular vacuoles in vivo. Nature *442*, 453–456.

Kanki, Y., Kohro, T., Jiang, S., Tsutsumi, S., Mimura, I., Suehiro, J.-I., Wada, Y., Ohta, Y., Ihara, S., Iwanari, H., et al. (2011). Epigenetically coordinated GATA2 binding is necessary for endothelium-specific endomucin expression. EMBO J. *30*, 2582–2595.

Kano, A., Wolfgang, M.J., Gao, Q., Jacoby, J., Chai, G.-X., Hansen, W., Iwamoto, Y., Pober, J.S., Flavell, R.A., and Fu, X.-Y. (2003). Endothelial cells require STAT3 for protection against endotoxin-induced inflammation. J. Exp. Med. *198*, 1517–1525.

Kappel, a, Schlaeger, T.M., Flamme, I., Orkin, S.H., Risau, W., and Breier, G. (2000). Role of SCL/Tal-1, GATA, and ets transcription factor binding sites for the regulation of flk-1 expression during murine vascular development. Blood *96*, 3078–3085.

Karkkainen, M.J., Haiko, P., Sainio, K., Partanen, J., Taipale, J., Petrova, T. V, Jeltsch, M., Jackson, D.G., Talikka, M., Rauvala, H., et al. (2004). Vascular endothelial growth factor C is required for sprouting of the first lymphatic vessels from embryonic veins. Nat. Immunol. *5*, 74–80.

Kassouf, M.T., Chagraoui, H., Vyas, P., and Porcher, C. (2008). Differential use of SCL/TAL-1 DNA-binding domain in developmental hematopoiesis. Blood *112*, 1056–1067.

Kauffman, S.A. (1969). Metabolic stability and epigenesis in randomly constructed genetic nets. J. Theor. Biol. *22*, 437–467.

Kearney, J.B., Kappas, N.C., Ellerstrom, C., DiPaola, F.W., and Bautch, V.L. (2004). The VEGF receptor flt-1 (VEGFR-1) is a positive modulator of vascular sprout formation and branching morphogenesis. Blood *103*, 4527–4535.

Kennedy, M., Firpo, M., Choi, K., Wall, C., Robertson, S., Kabrun, N., and Keller, G. (1997). A common precursor for primitive erythropoiesis and definitive haematopoiesis. Nature *386*, 488–493.

Kiel, M.J., Yilmaz, Ö.H., Iwashita, T., Yilmaz, O.H., Terhorst, C., and Morrison, S.J. (2005). SLAM family receptors distinguish hematopoietic stem and progenitor cells and reveal endothelial niches for stem cells. Cell *121*, 1109–1121.

Kim, P.G., Albacker, C.E., Lu, Y., Jang, I., Lim, Y., Heffner, G.C., Arora, N., Bowman, T. V, Lin, M.I., Lensch, M.W., et al. (2013). Signaling axis involving Hedgehog, Notch, and Scl promotes the embryonic endothelial-to-hematopoietic transition. Proc. Natl. Acad. Sci. U. S. A. *110*, E141–E150.

King, C.G. (2006). On the Parts of Animals (review). Class. World *99*, 188–189.

Kisanuki, Y.Y., Hammer, R.E., Miyazaki, J., Williams, S.C., Richardson, J. a, and Yanagisawa, M. (2001). Tie2-Cre transgenic mice: a new model for endothelial cell-lineage analysis in vivo. Dev. Biol. *230*, 230–242.

Ko, L.J., and Engel, J.D. (1993). DNA-binding specificities of the GATA transcription factor family. Mol. Cell.

Biol. *13*, 4011–4022.

Koni, P.A., Joshi, S.K., Temann, U.A., Olson, D., Burkly, L., and Flavell, R.A. (2001). Conditional vascular cell adhesion molecule 1 deletion in mice: impaired lymphocyte migration to bone marrow. J. Exp. Med. *193*, 741–754.

Kothary, R., Perry, M.D., Moran, L. a, and Rossant, J. (1987). Cell-lineage-specific expression of the mouse hsp68 gene during embryogenesis. Dev. Biol. *121*, 342–348.

Krebs, L.T., Shutter, J.R., Tanigaki, K., Honjo, T., Stark, K.L., and Gridley, T. (2004). Haploinsufficient lethality and formation of arteriovenous malformations in Notch pathway mutants. Genes Dev. *18*, 2469–2473.

Krebs, L.T., Starling, C., Chervonsky, A. V., and Gridley, T. (2010). Notch1 activation in mice causes arteriovenous malformations phenocopied by EphrinB2 and EphB4 mutants. Genesis *48*, 146–150.

Kudo, F.A., Muto, A., Maloney, S.P., Pimiento, J.M., Bergaya, S., Fitzgerald, T.N., Westvik, T.S., Frattini, J.C., Breuer, C.K., Cha, C.H., et al. (2007). Venous identity is lost but arterial identity is not gained during vein graft adaptation. Arterioscler. Thromb. Vasc. Biol. *27*, 1562–1571.

Kume, T., Jiang, H., Topczewska, J.M., and Hogan, B.L.M. (2001). The murine winged helix transcription factors, Foxc1 and Foxc2, are both required for cardiovascular development and somitogenesis. Genes Dev. *15*, 2470–2482.

de Laat, W., and Duboule, D. (2013). Topology of mammalian developmental enhancers and their regulatory landscapes. Nature *502*, 499–506.

Laitinen, L. (1987). Griffonia simplicifolia lectins bind specifically to endothelial cells and some epithelial cells in mouse tissues. Histochem. J. *19*, 225–234.

Lancrin, C., Sroczynska, P., Stephenson, C., Allen, T., Kouskoff, V., and Lacaud, G. (2009). The haemangioblast generates haematopoietic cells through a haemogenic endothelium stage. Nature *457*, 892–895.

Landry, J.-R., Bonadies, N., Kinston, S., Knezevic, K., Wilson, N.K., Oram, S.H., Janes, M., Piltz, S., Hammett, M., Carter, J., et al. (2009). Expression of the leukemia oncogene Lmo2 is controlled by an array of tissue-specific elements dispersed over 100 kb and bound by Tal1/Lmo2, Ets, and Gata factors. Blood *113*, 5783–5792.

Lanner, F., Sohl, M., and Farnebo, F. (2007). Functional arterial and venous fate is determined by graded VEGF signaling and notch status during embryonic stem cell differentiation. Arterioscler. Thromb. Vasc. Biol. *27*, 487–493.

Lavine, K.J., and Ornitz, D.M. (2009). Shared circuitry: developmental signaling cascades regulate both embryonic and adult coronary vasculature. Circ. Res. *104*, 159–169.

Lavine, K.J., White, A.C., Park, C., Smith, C.S., Choi, K., Long, F., Hui, C.C., and Ornitz, D.M. (2006). Fibroblast growth factor signals regulate a wave of Hedgehog activation that is essential for coronary vascular development. Genes Dev. *20*, 1651–1666.

Lawson, N.D., Scheer, N., Pham, V.N., Kim, C.H., Chitnis, A.B., Campos-Ortega, J.A., and Weinstein, B.M. (2001). Notch signaling is required for arterial-venous differentiation during embryonic vascular development. Development *128*, 3675–3683.

Lawson, N.D., Vogel, A.M., and Weinstein, B.M. (2002). Sonic hedgehog and vascular endothelial growth factor act upstream of the Notch pathway during arterial endothelial differentiation. Dev. Cell *3*, 127–136.

Lawson, N.D., Mugford, J.W., Diamond, B.A., and Weinstein, B.M. (2003). Phospholipase C gamma-1 is required downstream of vascular endothelial growth factor during arterial development. Genes Dev. *17*, 1346–1351.

Lazrak, M., Deleuze, V., Noel, D., Haouzi, D., Chalhoub, E., Dohet, C., Robbins, I., and Mathieu, D. (2004). The bHLH TAL-1/SCL regulates endothelial cell migration and morphogenesis. J. Cell Sci. *117*, 1161–1171.

Lee, D., Park, C., Lee, H., Lugus, J.J., Kim, S.H., Arentson, E., Chung, Y.S., Gomez, G., Kyba, M., Lin, S., et al. (2008). ER71 Acts Downstream of BMP, Notch, and Wnt Signaling in Blood and Vessel Progenitor Specification. Cell Stem Cell *2*, 497–507.

Lee, M.E., Temizer, D.H., Clifford, J.A., and Quertermous, T. (1991). Cloning of the GATA-binding protein that regulates endothelin-1 gene expression in endothelial cells. J. Biol. Chem. *266*, 16188–16192.

Lee, S., Kang, J., Yoo, J., Ganesan, S.K., Cook, S.C., Aguilar, B., Ramu, S., Lee, J., and Hong, Y.K. (2009). Prox1 physically and functionally interacts with COUP-TFII to specify lymphatic endothelial cell fate. Blood *113*, 1856–1859.

Leslie, J.D., Ariza-McNaughton, L., Bermange, A.L., McAdow, R., Johnson, S.L., and Lewis, J. (2007). Endothelial signalling by the Notch ligand Delta-like 4 restricts angiogenesis. Development *134*, 839–844.

Liao, E.C., Paw, B.H., Oates, A.C., Pratt, S.J., Postlethwait, J.H., and Zon, L.I. (1998). SCL/Tal-1 transcription factor acts downstream of cloche to specify hematopoietic and vascular progenitors in zebrafish. Genes Dev. *12*, 621–626.

Liao, W.P., Uetzmann, L., Burtscher, I., and Lickert, H. (2009). Generation of a mouse line expressing Sox17-driven Cre recombinase with specific activity in arteries. Genesis *47*, 476–483.

Lim, K.C., Hosoya, T., Brandt, W., Ku, C.J., Hosoya-Ohmura, S., Camper, S.A., Yamamoto, M., and Engel, J.D. (2012). Conditional Gata2 inactivation results in HSC loss and lymphatic mispatterning. J. Clin. Invest. *122*, 3705–3717.

Lin, Q., Lu, J., Yanagisawa, H., Webb, R., Lyons, G.E., Richardson, J.A., and Olson, E.N. (1998). Requirement of the MADS-box transcription factor MEF2C for vascular development. Development *125*, 4565–4574.

Lindahl, P., Johansson, B.R., Levéen, P., and Betsholtz, C. (1997). Pericyte loss and microaneurysm formation in PDGF-B-deficient mice. Science *277*, 242–245.

Liu, F., and Patient, R. (2008). Genome-wide analysis of the zebrafish ets family identifies three genes required for hemangioblast differentiation or angiogenesis. Circ. Res. *103*, 1147–1154.

Liu, F., Walmsley, M., Rodaway, A., and Patient, R. (2008). Fli1 Acts at the Top of the Transcriptional Network Driving Blood and Endothelial Development. Curr. Biol. *18*, 1234–1240.

Lodish, H., Berk, A., Matsudaira, P., Kaiser, C.A., Krieger, M., Scott, M.P., Zipursky, L., and Darnell, J. (2008). Molecular Cell Biology.

Loonstra, A., Vooijs, M., Beverloo, H.B., Allak, B.A., van Drunen, E., Kanaar, R., Berns, A., and Jonkers, J. (2001). Growth inhibition and DNA damage induced by Cre recombinase in mammalian cells. Proc Natl Acad Sci U S A *98*, 9209–9214.

Lu, S.-J., Lu, S.-J., Feng, Q., Feng, Q., Caballero, S., Caballero, S., Chen, Y., Chen, Y., Moore, M.A.S., Moore, M.A.S., et al. (2007). Generation of functional hemangioblasts from human embryonic stem cells. Nat. Methods *4*, 501–509.

Lucitti, J.L., Jones, E.A. V, Huang, C., Chen, J., Fraser, S.E., and Dickinson, M.E. (2007). Vascular remodeling

of the mouse yolk sac requires hemodynamic force. Development *134*, 3317–3326.

Magrane, M., and Consortium, U.P. (2011). UniProt Knowledgebase: A hub of integrated protein data. Database *2011*.

Maisonpierre, P.C., Suri, C., Jones, P.F., Bartunkova, S., Wiegand, S.J., Radziejewski, C., Compton, D., McClain, J., Aldrich, T.H., Papadopoulos, N., et al. (1997). Angiopoietin-2, a natural antagonist for Tie2 that disrupts in vivo angiogenesis. Science *277*, 55–60.

Maiti, D., Xu, Z., and Duh, E.J. (2008). Vascular endothelial growth factor induces MEF2C and MEF2-dependent activity in endothelial cells. Invest. Ophthalmol. Vis. Sci. *49*, 3640–3648.

Majesky, M.W., Dong, X.R., Regan, J.N., and Hoglund, V.J. (2011). Vascular smooth muscle progenitor cells: Building and repairing blood vessels. Circ. Res. *108*, 365–377.

Makanya, A.N., Hlushchuk, R., and Djonov, V.G. (2009). Intussusceptive angiogenesis and its role in vascular morphogenesis, patterning, and remodeling. Angiogenesis *12*, 113–123.

Massagué, J. (2012). TGFβ signalling in context. Nat. Rev. Mol. Cell Biol. *13*, 616–630.

Maston, G.A., Evans, S.K., and Green, M.R. (2006). Transcriptional regulatory elements in the human genome. Annu. Rev. Genomics Hum. Genet. *7*, 29–59.

Mato, M., and Ookawara, S. (1982). Ultrastructural observation on the tips of growing vascular cords in the rat cerebral cortex. Experientia *38*, 499–501.

Matsui, T., Kanai-Azuma, M., Hara, K., Matoba, S., Hiramatsu, R., Kawakami, H., Kurohmaru, M., Koopman, P., and Kanai, Y. (2006). Redundant roles of Sox17 and Sox18 in postnatal angiogenesis in mice. J. Cell Sci. *119*, 3513–3526.

Mattila, P.K., and Lappalainen, P. (2008). Filopodia: molecular architecture and cellular functions. Nat. Rev. Mol. Cell Biol. *9*, 446–454.

Maximow, A. (1924). Relation of blood cells to connective tissues and endothelium. Physiol. Rev. *IV*, 533–563.

McGrath, K.E., Koniski, A.D., Malik, J., and Palis, J. (2003). Circulation is established in a stepwise pattern in the mammalian embryo. Blood *101*, 1669–1676.

Mead, P.E., Kelley, C.M., Hahn, P.S., Piedad, O., and Zon, L.I. (1998). SCL specifies hematopoietic mesoderm in Xenopus embryos. Development *125*, 2611–2620.

Mead, P.E., Deconinck, A.E., Huber, T.L., Orkin, S.H., and Zon, L.I. (2001). Primitive erythropoiesis in the Xenopus embryo: the synergistic role of LMO-2, SCL and GATA-binding proteins. Development *128*, 2301–2308.

Meeson, A., Palmer, M., Calfon, M., and Lang, R. (1996). A relationship between apoptosis and flow during programmed capillary regression is revealed by vital analysis. Development *122*, 3929–3938.

Mejer, J. (1852). Über die Neubildung von Blutgefäßen in plastischen Exudaten serösen Membranen und in Hautwunden.

Mentzer, S.J., and Konerding, M.A. (2014). Intussusceptive angiogenesis: Expansion and remodeling of microvascular networks. In Angiogenesis, pp. 499–509.

Metzger, R.J., and Krasnow, M.A. (1999). Genetic control of branching morphogenesis. Science *284*, 1635–1639.

Mishiro, T., Ishihara, K., Hino, S., Tsutsumi, S., Aburatani, H., Shirahige, K., Kinoshita, Y., and Nakao, M. (2009). Architectural roles of multiple chromatin insulators at the human apolipoprotein gene cluster. EMBO J. *28*, 1234–1245.

Mizuochi, C., Fraser, S.T., Biasch, K., Horio, Y., Kikushige, Y., Tani, K., Akashi, K., Tavian, M., and Sugiyama, D. (2012). Intra-aortic clusters undergo endothelial to hematopoietic phenotypic transition during early embryogenesis. PLoS One *7*, e35763.

Moens, S., Goveia, J., Stapor, P.C., Cantelmo, A.R., and Carmeliet, P. (2014). The multifaceted activity of VEGF in angiogenesis - Implications for therapy responses. Cytokine Growth Factor Rev. *25*, 473–0482.

Moraes, F., Paye, J., Gabhann, F. Mac, Zhuang, Z.W., Zhang, J., Lanahan, A. a., and Simons, M. (2013). Endothelial cell-dependent regulation of arteriogenesis. Circ. Res. *113*, 1076–1086.

Morgan, S.M., Samulowitz, U., Darley, L., Simmons, D.L., and Vestweber, D. (1999). Biochemical characterization and molecular cloning of a novel endothelial-specific sialomucin. Blood *93*, 165–175.

Morikawa, M., Koinuma, D., Tsutsumi, S., Vasilaki, E., Kanki, Y., Heldin, C.H., Aburatani, H., and Miyazono, K. (2011). ChIP-seq reveals cell type-specific binding patterns of BMP-specific Smads and a novel binding motif. Nucleic Acids Res. *39*, 8712–8727.

Müller, A.M., Medvinsky, A., Strouboulis, J., Grosveld, F., and Dzierzakt, E. (1994). Development of hematopoietic stem cell activity in the mouse embryo. Immunity *1*, 291–301.

Murphy, P.A., Kim, T.N., Huang, L., Nielsen, C.M., Lawton, M.T., Adams, R.H., Schaffer, C.B., and Wang, R.A. (2014). Constitutively active Notch4 receptor elicits brain arteriovenous malformations through enlargement of capillary-like vessels. Proc. Natl. Acad. Sci. *111*, 18007–18012.

Murray, P.D.. (1932). The development in vitro of the blood of early chick embryo. Proc. R. Soc. London *111*, 497–521.

Nagase, M., Nagase, T., Koshima, I., and Fujita, T. (2006). Critical time window of hedgehog-dependent angiogenesis in murine yolk sac. Microvasc. Res. *71*, 85–90.

Nagase, T., Nagase, M., Machida, M., and Fujita, T. (2008). Hedgehog signalling in vascular development. Angiogenesis *11*, 71–77.

Nakamura, E., Nguyen, M.T., and Mackem, S. (2006). Kinetics of tamoxifen-regulated Cre activity in mice using a cartilage-specific CreERT to assay temporal activity windows along the proximodistal limb skeleton. Dev. Dyn. *235*, 2603–2612.

Nicoli, S., Standley, C., Walker, P., Hurlstone, A., Fogarty, K.E., and Lawson, N.D. (2010). MicroRNA-mediated integration of haemodynamics and Vegf signalling during angiogenesis. Nature *464*, 1196–1200.

Niessen, K., and Karsan, A. (2008). Notch signaling in cardiac development. Circ. Res. *102*, 1169–1181.

le Noble, F., Moyon, D., Pardanaud, L., Yuan, L., Djonov, V., Matthijsen, R., Bréant, C., Fleury, V., and Eichmann, A. (2004). Flow regulates arterial-venous differentiation in the chick embryo yolk sac. Development *131*, 361–375.

Nolan, D., Ginsberg, M., Israely, E., Palikuqi, B., Poulos, M.G., James, D., Ding, B. Sen, Schachterle, W., Liu, Y., Rosenwaks, Z., et al. (2013). Molecular Signatures of Tissue-Specific Microvascular Endothelial Cell Heterogeneity in Organ Maintenance and Regeneration. Dev. Cell *26*, 204–219.

Nolan, D.J., Ciarrocchi, A., Mellick, A.S., Jaggi, J.S., Bambino, K., Gupta, S., Heikamp, E., McDevitt, M.R., Scheinberg, D.A., Benezra, R., et al. (2007). Bone marrow-derived endothelial progenitor cells are a major

determinant of nascent tumor neovascularization. Genes Dev. *21*, 1546–1558.

Noordermeer, D., de Wit, E., Klous, P., van de Werken, H., Simonis, M., Lopez-Jones, M., Eussen, B., de Klein, A., Singer, R.H., and de Laat, W. (2011). Variegated gene expression caused by cell-specific long-range DNA interactions. Nat. Cell Biol. *13*, 944–951.

O'Neil, J., Shank, J., Cusson, N., Murre, C., and Kelliher, M. (2004). TAL1/SCL induces leukemia by inhibiting the transcriptional activity of E47/HEB. Cancer Cell *5*, 587–596.

Org, T., Duan, D., Ferrari, R., Montel-Hagen, A., Van Handel, B., Kerényi, M.A., Sasidharan, R., Rubbi, L., Fujiwara, Y., Pellegrini, M., et al. (2015). Scl binds to primed enhancers in mesoderm to regulate hematopoietic and cardiac fate divergence. EMBO J. *34*, 1–20.

Ovcharenko, I., Stubbs, L., and Loots, G.G. (2004). Interpreting mammalian evolution using Fugu genome comparisons. Genomics *84*, 890–895.

Pardali, E., Goumans, M.J., and ten Dijke, P. (2010). Signaling by members of the TGF-β family in vascular morphogenesis and disease. Trends Cell Biol. *20*, 556–567.

Park, C., Kim, T.M., and Malik, A.B. (2013). Transcriptional regulation of endothelial cell and vascular development. Circ. Res. *112*, 1380–1400.

Park, J.E., Chen, H.H., Winer, J., Houck, K.A., and Ferrara, N. (1994). Placenta growth factor: Potentiation of vascular endothelial growth factor bioactivity, in vitro and in vivo, and high affinity binding to Flt-1 but not to Flk-1/KDR. J. Biol. Chem. *269*, 25646–25654.

Patterson, L.J., Gering, M., and Patient, R. (2005). Scl is required for dorsal aorta as well as blood formation in zebrafish embryos. Blood *105*, 3502–3511.

Pellegrinet, L., Rodilla, V., Liu, Z., Chen, S., Koch, U., Espinosa, L., Kaestner, K.H., Kopan, R., Lewis, J., and Radtke, F. (2011). Dll1- and Dll4-mediated notch signaling are required for homeostasis of intestinal stem cells. Gastroenterology *140*, 1230–1240.

Pelton, J.C., Wright, C.E., Leitges, M., and Bautch, V.L. (2014). Multiple endothelial cells constitute the tip of developing blood vessels and polarize to promote lumen formation. Development *141*, 4121–4126.

Pendeville, H., Winandy, M., Manfroid, I., Nivelles, O., Motte, P., Pasque, V., Peers, B., Struman, I., Martial, J.A., and Voz, M.L. (2008). Zebrafish Sox7 and Sox18 function together to control arterial-venous identity. Dev. Biol. *317*, 405–416.

Pennacchio, L.A., Ahituv, N., Moses, A.M., Prabhakar, S., Nobrega, M.A., Shoukry, M., Minovitsky, S., Dubchak, I., Holt, A., Lewis, K.D., et al. (2006). In vivo enhancer analysis of human conserved non-coding sequences. Nature *444*, 499–502.

Pereira, F.A., Yuhong, Q., Zhou, G., Tsai, M.J., and Tsai, S.Y. (1999). The orphan nuclear receptor COUP-TFII is required for angiogenesis and heart development. Genes Dev. *13*, 1037–1049.

Phng, L.K., Potente, M., Leslie, J.D., Babbage, J., Nyqvist, D., Lobov, I., Ondr, J.K., Rao, S., Lang, R. a., Thurston, G., et al. (2009). Nrarp Coordinates Endothelial Notch and Wnt Signaling to Control Vessel Density in Angiogenesis. Dev. Cell *16*, 70–82.

Phng, L.-K., Stanchi, F., and Gerhardt, H. (2013). Filopodia are dispensable for endothelial tip cell guidance. Development *140*, 4031–4040.

Pirot, N., Deleuze, V., El-Hajj, R., Dohet, C., Sablitzky, F., Couttet, P., Mathieu, D., and Pinet, V. (2010). LYL1 activity is required for the maturation of newly formed blood vessels in adulthood. Blood *115*, 5270–5279.

Pitulescu, M.E., Schmidt, I., Benedito, R., and Adams, R.H. (2010). Inducible gene targeting in the neonatal vasculature and analysis of retinal angiogenesis in mice. Nat. Protoc. *5*, 1518–1534.

Pola, R., Ling, L.E., Silver, M., Corbley, M.J., Kearney, M., Blake Pepinsky, R., Shapiro, R., Taylor, F.R., Baker, D.P., Asahara, T., et al. (2001). The morphogen Sonic hedgehog is an indirect angiogenic agent upregulating two families of angiogenic growth factors. Nat. Med. *7*, 706–711.

Porcher, C., Swat, W., Rockwell, K., Fujiwara, Y., Alt, F.W., and Orkin, S.H. (1996). The T cell leukemia oncoprotein SCL/tal-1 is essential for development of all hematopoietic lineages. Cell *86*, 47–57.

Porcher, C., Liao, E.C., Fujiwara, Y., Zon, L.I., and Orkin, S.H. (1999). Specification of hematopoietic and vascular development by the bHLH transcription factor SCL without direct DNA binding. Development *126*, 4603–4615.

Potente, M., Gerhardt, H., and Carmeliet, P. (2011). Basic and therapeutic aspects of angiogenesis. Cell *146*, 873–887.

Pott, S., and Lieb, J.D. (2015). What are super-enhancers ? Nat. Publ. Gr. *47*, 8–12.

Proctor, J.M., Zang, K., Wang, D., Wang, R., and Reichardt, L.F. (2005). Vascular development of the brain requires beta8 integrin expression in the neuroepithelium. J. Neurosci. *25*, 9940–9948.

Pulford, K., Lecointe, N., Leroy-Viard, K., Jones, M., Mathieu-Mahul, D., and Mason, D.Y. (1995). Expression of TAL-1 proteins in human tissues. Blood *85*, 675–684.

Quillien, A., Moore, J.C., Shin, M., Siekmann, A.F., Smith, T., Pan, L.Y., Moens, C.B., Parsons, M.J., and Lawson, N.D. (2014). Distinct Notch signaling outputs pattern the developing arterial system. Development *141*, 1544–1552.

Rada-Iglesias, A., Bajpai, R., Swigut, T., Brugmann, S.A., Flynn, R.A., and Wysocka, J. (2011). A unique chromatin signature uncovers early developmental enhancers in humans. Nature *470*, 279–283.

Rajantie, I., Ekman, N., Iljin, K., Arighi, E., Gunji, Y., Kaukonen, J., Palotie, A., Dewerchin, M., Carmeliet, P., and Alitalo, K. (2001). Bmx tyrosine kinase has a redundant function downstream of angiopoietin and vascular endothelial growth factor receptors in arterial endothelium. Mol. Cell. Biol. *21*, 4647–4655.

Ramasamy, S.K., Kusumbe, A.P., Wang, L., and Adams, R.H. (2014). Endothelial Notch activity promotes angiogenesis and osteogenesis in bone. Nature *507*, 376–380.

Randi, A.M., Sperone, A., Dryden, N.H., and Birdsey, G.M. (2009). Regulation of angiogenesis by ETS transcription factors. Biochem. Soc. Trans. *37*, 1248–1253.

Red-Horse, K., Ueno, H., Weissman, I.L., and Krasnow, M.A. (2010). Coronary arteries form by developmental reprogramming of venous cells. Nature *464*, 549–553.

Reif, R., and Wang, R.K. (2012). Label-free imaging of blood vessel morphology with capillary resolution using optical microangiography. Quant. Imaging Med. Surg. *2*, 207–212.

Robb, L., Lyons, I., Li, R., Hartley, L., Köntgen, F., Harvey, R.P., Metcalf, D., and Begley, C.G. (1995). Absence of yolk sac hematopoiesis from mice with a targeted disruption of the scl gene. Proc. Natl. Acad. Sci. U. S. A. *92*, 7075–7079.

Robb, L., Elwood, N.J., Elefanty, A.G., Köntgen, F., Li, R., Barnett, L.D., and Begley, C.G. (1996). The scl gene product is required for the generation of all hematopoietic lineages in the adult mouse. EMBO J. *15*, 4123–4129.

Robinson, S.P., Langan-Fahey, S.M., Johnson, D.A., and Jordan, V.C. (1991). Metabolites,

pharmacodynamics, and pharmacokinetics of tamoxifen in rats and mice compared to the breast cancer patient. Drug Metab. Dispos. *19*, 36–43.

Rocha, S.F., Schiller, M., Jing, D., Li, H., Butz, S., Vestweber, D., Biljes, D., Drexler, H.C.A., Nieminen-Kelhä, M., Vajkoczy, P., et al. (2014). Esm1 modulates endothelial tip cell behavior and vascular permeability by enhancing VEGF bioavailability. Circ. Res. *115*, 581–590.

Roukens, M.G., Alloul-Ramdhani, M., Baan, B., Kobayashi, K., Peterson-Maduro, J., van Dam, H., Schulte-Merker, S., and Baker, D. a (2010). Control of endothelial sprouting by a Tel-CtBP complex. Nat. Cell Biol. *12*, 933–942.

Sabin, F.R. (2002). Preliminary note on the differentiation of angioblasts and the method by which they produce blood-vessels, blood-plasma and red blood-cells as seen in the living chick. 1917. J. Hematother. Stem Cell Res. *11*, 5–7.

Sabine, F.R. (1920). Studies On The Origin Of Blood-Vessels And Of Red Blood-Corpuscles As Seen In The Living Blastoderm Of Chicks During The Second Day Of Incubation. Contrib. to Embryol. - Carnegie Inst. Washingt. *36*, 215–262.

Sacilotto, N., Monteiro, R., Fritzsche, M., Becker, P.W., Sanchez-Del-Campo, L., Liu, K., Pinheiro, P., Ratnayaka, I., Davies, B., Goding, C.R., et al. (2013). Analysis of Dll4 regulation reveals a combinatorial role for Sox and Notch in arterial development. Proc. Natl. Acad. Sci. U. S. A. *110*, 11893–11898.

Saharinen, P., Eklund, L., Miettinen, J., Wirkkala, R., Anisimov, A., Winderlich, M., Nottebaum, A., Vestweber, D., Deutsch, U., Koh, G.Y., et al. (2008). Angiopoietins assemble distinct Tie2 signalling complexes in endothelial cell-cell and cell-matrix contacts. Nat. Cell Biol. *10*, 527–537.

Samokhvalov, I.M., Samokhvalova, N.I., and Nishikawa, S. (2007). Cell tracing shows the contribution of the yolk sac to adult haematopoiesis. Nature *446*, 1056–1061.

Sanyal, A., Lajoie, B.R., Jain, G., and Dekker, J. (2012). The long-range interaction landscape of gene promoters. Nature *489*, 109–113.

Sawamiphak, S., Seidel, S., Essmann, C.L., Wilkinson, G.A., Pitulescu, M.E., Acker, T., and Acker-Palmer, A. (2010a). Ephrin-B2 regulates VEGFR2 function in developmental and tumour angiogenesis. Nature *465*, 487–491.

Sawamiphak, S., Ritter, M., and Acker-Palmer, A. (2010b). Preparation of retinal explant cultures to study ex vivo tip endothelial cell responses. Nat. Protoc. *5*, 1659–1665.

Schachterle, W., Rojas, A., Xu, S.M., and Black, B.L. (2012). ETS-dependent regulation of a distal Gata4 cardiac enhancer. Dev. Biol. *361*, 439–449.

Schatz, O., Golenser, E., and Ben-Arie, N. (2005). Clearing and photography of whole mount X-gal stained mouse embryos. Biotechniques *39*, 650–653.

Schlaeger, T.M., Mikkola, H.K. a, Gekas, C., Helgadottir, H.B., and Orkin, S.H. (2005). Tie2Cre-mediated gene ablation defines the stem-cell leukemia gene (SCL/tal1)-dependent window during hematopoietic stem-cell development. Blood *105*, 3871–3874.

Schmidt, A., Brixius, K., and Bloch, W. (2007). Endothelial precursor cell migration during vasculogenesis. Circ. Res. *101*, 125–136.

Schoenfelder, S., Clay, I., and Fraser, P. (2010). The transcriptional interactome: Gene expression in 3D. Curr. Opin. Genet. Dev. *20*, 127–133.

Schumacher, J.A., Bloomekatz, J., Garavito-Aguilar, Z. V., and Yelon, D. (2013). Tal1 regulates the formation

of intercellular junctions and the maintenance of identity in the endocardium. Dev. Biol. *383*, 214–226.

Schwanhäusser, B., Busse, D., Li, N., Dittmar, G., Schuchhardt, J., Wolf, J., Chen, W., and Selbach, M. (2011). Global quantification of mammalian gene expression control. Nature *473*, 337–342.

Scott, a, and Fruttiger, M. (2010). Oxygen-induced retinopathy: a model for vascular pathology in the retina. Eye (Lond). *24*, 416–421.

Seo, S., Fujita, H., Nakano, A., Kang, M., Duarte, A., and Kume, T. (2006). The forkhead transcription factors, Foxc1 and Foxc2, are required for arterial specification and lymphatic sprouting during vascular development. Dev. Biol. *294*, 458–470.

Shalaby, F., Rossant, J., Yamaguchi, T.P., Gertsenstein, M., Wu, X.F., Breitman, M.L., and Schuh, A.C. (1995). Failure of blood-island formation and vasculogenesis in Flk-1-deficient mice. Nature *376*, 62–66.

Shi, Q., Rafii, S., Wu, M.H., Wijelath, E.S., Yu, C., Ishida, A., Fujita, Y., Kothari, S., Mohle, R., Sauvage, L.R., et al. (1998). Evidence for circulating bone marrow-derived endothelial cells. Blood *92*, 362–367.

Shi, X., Richard, J., Zirbes, K.M., Gong, W., Lin, G., Kyba, M., Thomson, J.A., Koyano-Nakagawa, N., and Garry, D.J. (2014). Cooperative interaction of Etv2 and Gata2 regulates the development of endothelial and hematopoietic lineages. Dev. Biol. *389*, 208–218.

Shivdasani, R.A., Mayer, E.L., and Orkin, S.H. (1995). Absence of blood formation in mice lacking the T-cell leukaemia oncoprotein tal-1/SCL. Nature *373*, 432–434.

Shlyueva, D., Stampfel, G., and Stark, A. (2014). Transcriptional enhancers: from properties to genome-wide predictions. Nat. Rev. Genet. *15*, 272–286.

Shutter, J.R., Scully, S., Fan, W., Richards, W.G., Kitajewski, J., Deblandre, G.A., Kintner, C.R., and Stark, K.L. (2000). Dll4, a novel Notch ligand expressed in arterial endothelium. Genes Dev. *14*, 1313–1318.

Siekmann, A.F., and Lawson, N.D. (2007). Notch signalling limits angiogenic cell behaviour in developing zebrafish arteries. Nature *445*, 781–784.

Sinclair, A.M., Gottgens, B., Barton, L.M., Stanley, M.L., Pardanaud, L., Klaine, M., Gering, M., Bahn, S., Sanchez, M., Bench, A.J., et al. (1999). Distinct 5' SCL enhancers direct transcription to developing brain, spinal cord, and endothelium: neural expression is mediated by GATA factor binding sites. Dev. Biol. *209*, 128–142.

Soker, S., Takashima, S., Miao, H.Q., Neufeld, G., and Klagsbrun, M. (1998). Neuropilin-1 is expressed by endothelial and tumor cells as an isoform-specific receptor for vascular endothelial growth factor. Cell *92*, 735–745.

Song, H., Suehiro, J.I., Kanki, Y., Kawai, Y., Inoue, K., Daida, H., Yano, K., Ohhashi, T., Oettgen, P., Aird, W.C., et al. (2009). Critical role for GATA3 in mediating Tie2 expression and function in large vessel endothelial cells. J. Biol. Chem. *284*, 29109–29124.

Sörensen, I., Adams, R.H., and Gossler, A. (2009). DLL1-mediated Notch activation regulates endothelial identity in mouse fetal arteries. Blood *113*, 5680–5688.

Soriano, P. (1999). Generalized lacZ expression with the ROSA26 Cre reporter strain. Nat. Genet. *21*, 70–71.

Spyropoulos, D.D., Pharr, P.N., Lavenburg, K.R., Jackers, P., Papas, T.S., Ogawa, M., and Watson, D.K. (2000). Hemorrhage, impaired hematopoiesis, and lethality in mouse embryos carrying a targeted disruption of the Fli1 transcription factor. Mol. Cell. Biol. *20*, 5643–5652.

Srinivas, S., Watanabe, T., Lin, C.S., William, C.M., Tanabe, Y., Jessell, T.M., and Costantini, F. (2001). Cre reporter strains produced by targeted insertion of EYFP and ECFP into the ROSA26 locus. BMC Dev. Biol. *1*, 4.

Srinivasan, R.S., Geng, X., Yang, Y., Wang, Y., Mukatira, S., Studer, M., Porto, M.P.R., Lagutin, O., and Oliver, G. (2010). The nuclear hormone receptor Coup-TFII is required for the initiation and early maintenance of Prox1 expression in lymphatic endothelial cells. Genes Dev. *24*, 696–707.

Stahl, A., Connor, K.M., Sapieha, P., Chen, J., Dennison, R.J., Krah, N.M., Seaward, M.R., Willett, K.L., Aderman, C.M., Guerin, K.I., et al. (2010). The mouse retina as an angiogenesis model. Investig. Ophthalmol. Vis. Sci. *51*, 2813–2826.

Di Stefano, I., Koopmans, D.R., and Langille, B.L. (1998). Modulation of arterial growth of the rabbit carotid artery associated with experimental elevation of blood flow. J. Vasc. Res. *35*, 1–7.

Stefater, J.A., Lewkowich, I., Rao, S., Mariggi, G., Carpenter, A.C., Burr, A.R., Fan, J., Ajima, R., Molkentin, J.D., Williams, B.O., et al. (2011). Regulation of angiogenesis by a non-canonical Wnt-Flt1 pathway in myeloid cells. Nature *474*, 511–515.

Strilić, B., Kučera, T., Eglinger, J., Hughes, M.R., McNagny, K.M., Tsukita, S., Dejana, E., Ferrara, N., and Lammert, E. (2009). The Molecular Basis of Vascular Lumen Formation in the Developing Mouse Aorta. Dev. Cell *17*, 505–515.

Sturtzel, C., Testori, J., Schweighofer, B., Bilban, M., and Hofer, E. (2014). The transcription factor MEF2C negatively controls angiogenic sprouting of endothelial cells depending on oxygen. PLoS One *9*.

Sumanas, S., and Lin, S. (2006). Ets1-related protein is a key regulator of vasculogenesis in zebrafish. PLoS Biol. *4*, 60–69.

Surace, E.M., Balaggan, K.S., Tessitore, A., Mussolino, C., Cotugno, G., Bonetti, C., Vitale, A., Ali, R.R., and Auricchio, A. (2006). Inhibition of ocular neovascularization by Hedgehog blockade. Mol. Ther. *13*, 573–579.

Tammela, T., Zarkada, G., Wallgard, E., Murtomäki, A., Suchting, S., Wirzenius, M., Waltari, M., Hellström, M., Schomber, T., Peltonen, R., et al. (2008). Blocking VEGFR-3 suppresses angiogenic sprouting and vascular network formation. Nature *454*, 656–660.

Tammela, T., Zarkada, G., Nurmi, H., Jakobsson, L., Heinolainen, K., Tvorogov, D., Zheng, W., Franco, C. a., Murtomäki, A., Aranda, E., et al. (2011). VEGFR-3 controls tip to stalk conversion at vessel fusion sites by reinforcing Notch signalling. Nat. Cell Biol. *13*, 1202–1213.

Tanaka, A., Itoh, F., Itoh, S., and Kato, M. (2009). TAL1/SCL relieves the E2-2-mediated repression of VEGFR2 promoter activity. J. Biochem. *145*, 129–135.

Tanaka, A., Itoh, F., Nishiyama, K., Takezawa, T., Kurihara, H., Itoh, S., and Kato, M. (2010). Inhibition of endothelial cell activation by bHLH protein E2-2 and its impairment of angiogenesis. Blood *115*, 4138–4147.

Tang, T., Shi, Y., Opalenik, S.R., Brantley-Sieders, D.M., Chen, J., Davidson, J.M., and Brandt, S.J. (2006). Expression of the TAL1/SCL transcription factor in physiological and pathological vascular processes. J. Pathol. *210*, 121–129.

The ENCODE Project Consortium (2012). An integrated encyclopedia of DNA elements in the human genome. Nature *489*, 57–74.

Theis, M., De Wit, C., Schlaeger, T.M., Eckardt, D., Krger, O., Dring, B., Risau, W., Deutsch, U., Pohl, U., and Willecke, K. (2001). Endothelium-specific replacement of the connexin43 coding region by a lacZ

reporter gene. Genesis *29*, 1–13.

Tsai, F.Y., and Orkin, S.H. (1997). Transcription factor GATA-2 is required for proliferation/survival of early hematopoietic cells and mast cell formation, but not for erythroid and myeloid terminal differentiation. Blood *89*, 3636–3643.

Tsai, F.Y., Keller, G., Kuo, F.C., Weiss, M., Chen, J., Rosenblatt, M., Alt, F.W., and Orkin, S.H. (1994). An early haematopoietic defect in mice lacking the transcription factor GATA-2. Nature *371*, 221–226.

Tsunoda, T., Takashima, Y., Tanaka, Y., Fujimoto, T., Doi, K., Hirose, Y., Koyanagi, M., Yoshida, Y., Okamura, T., Kuroki, M., et al. (2010). Immune-related zinc finger gene ZFAT is an essential transcriptional regulator for hematopoietic differentiation in blood islands. Proc. Natl. Acad. Sci. U. S. A. *107*, 14199–14204.

Turner, C.J., Badu-Nkansah, K., Crowley, D., van der Flier, A., and Hynes, R.O. (2014). Integrin-α5β1 is not required for mural cell functions during development of blood vessels but is required for lymphatic-blood vessel separation and lymphovenous valve formation. Dev. Biol. *392*, 381–392.

Ueno, H., and Weissman, I.L. (2007). Stem cells: blood lines from embryo to adult. Nature *446*, 996–997.

De Val, S. (2011). Key transcriptional regulators of early vascular development. Arterioscler. Thromb. Vasc. Biol. *31*, 1469–1475.

De Val, S., and Black, B.L. (2009). Transcriptional Control of Endothelial Cell Development. Dev. Cell *16*, 180–195.

De Val, S., Chi, N.C., Meadows, S.M., Minovitsky, S., Anderson, J.P., Harris, I.S., Ehlers, M.L., Agarwal, P., Visel, A., Xu, S.M., et al. (2008). Combinatorial Regulation of Endothelial Gene Expression by Ets and Forkhead Transcription Factors. Cell *135*, 1053–1064.

Venter, J.C., Adams, M.D., Myers, E.W., Li, P.W., Mural, R.J., Sutton, G.G., Smith, H.O., Yandell, M., Evans, C.A., Holt, R.A., et al. (2001). The sequence of the human genome. Science *291*, 1304–1351.

Villa, N., Walker, L., Lindsell, C.E., Gasson, J., Iruela-Arispe, M.L., and Weinmaster, G. (2001). Vascular expression of Notch pathway receptors and ligands is restricted to arterial vessels. Mech. Dev. *108*, 161–164.

Visvader, J.E., Fujiwara, Y., and Orkin, S.H. (1998). Unsuspected role for the T-cell leukemia protein SCL/tal-1 in vascular development. Genes Dev. *12*, 473–479.

Vogeli, K.M., Jin, S.-W., Martin, G.R., and Stainier, D.Y.R. (2006). A common progenitor for haematopoietic and endothelial lineages in the zebrafish gastrula. Nature *443*, 337–339.

Vokes, S.A., Yatskievych, T.A., Heimark, R.L., McMahon, J., McMahon, A.P., Antin, P.B., and Krieg, P.A. (2004). Hedgehog signaling is essential for endothelial tube formation during vasculogenesis. Development *131*, 4371–4380.

Wadman, I.A., Osada, H., Grütz, G.G., Agulnick, A.D., Westphal, H., Forster, A., and Rabbitts, T.H. (1997). The LIM-only protein Lmo2 is a bridging molecule assembling an erythroid, DNA-binding complex which includes the TAL1, E47, GATA-1 and Ldb1/NLI proteins. EMBO J. *16*, 3145–3157.

Wallitt, E.J.W., Jevon, M., and Hornick, P.I. (2007). Therapeutics of Vein Graft Intimal Hyperplasia: 100 Years On. Ann. Thorac. Surg. *84*, 317–323.

Walls, J.R., Coultas, L., Rossant, J., and Henkelman, R.M. (2008). Three-dimensional analysis of vascular development in the mouse embryo. PLoS One *3*.

Wang, H.U., Chen, Z.F., and Anderson, D.J. (1998). Molecular distinction and angiogenic interaction between embryonic arteries and veins revealed by ephrin-B2 and its receptor Eph-B4. Cell *93*, 741–753.

Wang, R., Chadalavada, K., Wilshire, J., Kowalik, U., Hovinga, K.E., Geber, A., Fligelman, B., Leversha, M., Brennan, C., and Tabar, V. (2010a). Glioblastoma stem-like cells give rise to tumour endothelium. Nature *468*, 829–833.

Wang, Y., Nakayama, M., Pitulescu, M.E., Schmidt, T.S., Bochenek, M.L., Sakakibara, A., Adams, S., Davy, A., Deutsch, U., Lüthi, U., et al. (2010b). Ephrin-B2 controls VEGF-induced angiogenesis and lymphangiogenesis. Nature *465*, 483–486.

Warburg, O. (1927). Über die Klassifizierung tierischer Gewebe nach ihrem Stoffwechsel. Biochem Z *184*, 484–488.

Warren, A.J., Colledge, W.H., Carlton, M.B.L., Evans, M.J., Smith, A.J.H., and Rabbitts, T.H. (1994). The oncogenic cysteine-rich LIM domain protein rbtn2 is essential for erythroid development. Cell *78*, 45–57.

Weiss, M.J., Keller, G., and Orkin, S.H. (1994). Novel insights into erythroid development revealed through in vitro differentiation of GATA-1- embryonic stem cells. Genes Dev. *8*, 1184–1197.

Whyte, W.A., Orlando, D.A., Hnisz, D., Abraham, B.J., Lin, C.Y., Kagey, M.H., Rahl, P.B., Lee, T.I., and Young, R.A. (2013). Master transcription factors and mediator establish super-enhancers at key cell identity genes. Cell *153*, 307–319.

Wiley, D.M., Kim, J.-D., Hao, J., Hong, C.C., Bautch, V.L., and Jin, S.-W. (2011). Distinct signalling pathways regulate sprouting angiogenesis from the dorsal aorta and the axial vein. Nat. Cell Biol. *13*, 686–692.

Williams, C., Kim, S.-H., Ni, T.T., Mitchell, L., Ro, H., Penn, J.S., Baldwin, S.H., Solnica-Krezel, L., and Zhong, T.P. (2010). Hedgehog signaling induces arterial endothelial cell formation by repressing venous cell fate. Dev. Biol. *341*, 196–204.

Wilson, C.H., Gamper, I., Perfetto, A., Auw, J., Littlewood, T.D., and Evan, G.I. (2014). The kinetics of ER fusion protein activation in vivo. Oncogene *33*, 4877–4880.

Wythe, J., Dang, L.H., Devine, W.P., Boudreau, E., Artap, S., He, D., Schachterle, W., Stainier, D.R., Oettgen, P., Black, B., et al. (2013). ETS factors regulate Vegf-dependent arterial specification. Dev. Cell *26*, 45–58.

Xie, X., Wu, S., Lam, K.M., and Yan, H. (2006). PromoterExplorer: An effective promoter identification method based on the AdaBoost algorithm. Bioinformatics *22*, 2722–2728.

Xiong, J.W. (2008). Molecular and developmental biology of the hemangioblast. Dev. Dyn. *237*, 1218–1231.

Xu, C., Hasan, S.S., Schmidt, I., Rocha, S.F., Pitulescu, M.E., Bussmann, J., Meyen, D., Raz, E., Adams, R.H., and Siekmann, A.F. (2014). Arteries are formed by vein-derived endothelial tip cells. Nat. Commun. *5*, 5758.

Xue, Y., Gao, X., Lindsell, C.E., Norton, C.R., Chang, B., Hicks, C., Gendron-Maguire, M., Rand, E.B., Weinmaster, G., and Gridley, T. (1999). Embryonic lethality and vascular defects in mice lacking the Notch ligand Jagged1. Hum. Mol. Genet. *8*, 723–730.

Yamada, Y., Pannell, R., Forster, A., and Rabbitts, T.H. (2002). The LIM-domain protein Lmo2 is a key regulator of tumour angiogenesis: a new anti-angiogenesis drug target. Oncogene *21*, 1309–1315.

Yamamizu, K., Matsunaga, T., Uosaki, H., Fukushima, H., Katayama, S., Hiraoka-Kanie, M., Mitani, K., and Yamashita, J.K. (2010). Convergence of Notch and β-catenin signaling induces arterial fate in vascular progenitors. J. Cell Biol. *189*, 325–338.

Yang, C., Bolotin, E., Jiang, T., Sladek, F.M., and Martinez, E. (2007). Prevalence of the initiator over the TATA box in human and yeast genes and identification of DNA motifs enriched in human TATA-less core promoters. Gene *389*, 52–65.

Ye, X., Wang, Y., Cahill, H., Yu, M., Badea, T.C., Smallwood, P.M., Peachey, N.S., and Nathans, J. (2009). Norrin, Frizzled-4, and Lrp5 Signaling in Endothelial Cells Controls a Genetic Program for Retinal Vascularization. Cell *139*, 285–298.

Ye, X., Wang, Y., and Nathans, J. (2010). The Norrin / Frizzled4 signaling pathway in retinal vascular development and disease. Trends Mol. Med. *16*, 417–425.

Yoder, M.C., and Ingram, D.A. (2009). Endothelial progenitor cell: ongoing controversy for defining these cells and their role in neoangiogenesis in the murine system. Curr. Opin. Hematol. *16*, 269–273.

Yokomizo, T., and Dzierzak, E. (2010). Three-dimensional cartography of hematopoietic clusters in the vasculature of whole mouse embryos. Development *137*, 3651–3661.

You, L.-R., Lin, F.-J., Lee, C.T., DeMayo, F.J., Tsai, M.-J., and Tsai, S.Y. (2005). Suppression of Notch signalling by the COUP-TFII transcription factor regulates vein identity. Nature *435*, 98–104.

Zarkada, G., Heinolainen, K., Makinen, T., Kubota, Y., and Alitalo, K. (2015). VEGFR3 does not sustain retinal angiogenesis without VEGFR2. Proc. Natl. Acad. Sci. *112*, 201423278.

Zhang, X.Y., and Rodaway, A.R.F. (2007). SCL-GFP transgenic zebrafish: In vivo imaging of blood and endothelial development and identification of the initial site of definitive hematopoiesis. Dev. Biol. *307*, 179–194.

Zhen, F., Lan, Y., Yan, B., Zhang, W., Wen, Z., Bernard, O., Azogui, O., Lecointe, N., Mugneret, F., Berger, R., et al. (2013). Hemogenic endothelium specification and hematopoietic stem cell maintenance employ distinct Scl isoforms. Development *140*, 3977–3985.

Zheng, R., and Blobel, G.A. (2010). GATA Transcription Factors and Cancer. Genes Cancer *1*, 1178–1188.

Zhong, T.P., Childs, S., Leu, J.P., and Fishman, M.C. (2001). Gridlock signalling pathway fashions the first embryonic artery. Nature *414*, 216–220.

Zhuang, Z., Frerich, J.M., Huntoon, K., Yang, C., Merrill, M.J., Abdullaev, Z., Pack, S.D., Shively, S.B., Stamp, G., and Lonser, R.R. (2014). Tumor derived vasculogenesis in von Hippel-Lindau disease-associated tumors. Sci. Rep. *4*, 4102.

Zovein, A.C., Hofmann, J.J., Lynch, M., French, W.J., Turlo, K.A., Yang, Y., Becker, M.S., Zanetta, L., Dejana, E., Gasson, J.C., et al. (2008). Fate Tracing Reveals the Endothelial Origin of Hematopoietic Stem Cells. Cell Stem Cell *3*, 625–636.

Zudaire, E., Gambardella, L., Kurcz, C., and Vermeren, S. (2011). A computational tool for quantitative analysis of vascular networks. PLoS One *6*.

Zuercher, J., Fritzsche, M., Feil, S., Mohn, L., and Berger, W. (2012). Norrin stimulates cell proliferation in the superficial retinal vascular plexus and is pivotal for the recruitment of mural cells. Hum. Mol. Genet. *21*, 2619–2630.